Characterization of a mammalian neural-specific poly(A) binding protein with unique properties

By
Sahil Sharma

Department of Medicine
Division of Experimental Medicine
McGill University, Montreal, QC, Canada

August 2023

A thesis submitted to McGill University in partial fulfillment of the requirements of the degree of Doctor of Philosophy

TABLE OF CONTENTS

ABSTRACT

Almost all eukaryotic mRNAs maintain a 3' poly(A) tail that is bound by the cytoplasmic poly(A) binding protein (PABPC). PABPC can regulate mRNA translation and turnover by interacting with translation initiation factors and mRNA decay machineries. PABPC is highly conserved in eukaryotes, from yeast to humans, with the prototypical PABPC (PABPC1) being ubiquitously expressed in most mammalian tissues, albeit at different levels. PABPC1 binds the translation initiation factor 4G (eIF4G), an interaction that stimulates translation in certain contexts. Here, we uncover a new mammalian-specific PABPC that is coded by the X-linked ampliconic gene *Pabpc1l2a/b*. PABPC1L2 is predominantly expressed in neural tissues in neurons, which we have subsequently named neural PABP (neuPABP) and is a bona fide poly(A) binding protein. neuPABP expression is temporally regulated, with its expression peaking during neuronal maturation in synaptogenesis. neuPABP localizes in neurons to the soma and to postsynaptic densities. In contrast to PABPC1, neuPABP contains only the first two RNA recognition motifs (RRMs) and maintains a unique N-terminal domain of unknown function (DUF) not found in other PABPCs. RNA-immunoprecipitation-Seq analyses indicate that neuPABP interacts with select RNA populations, namely brain-specific non-coding RNAs (BC1 and BC200) and nuclear-derived mRNAs coding for ribosomal and mitochondrial proteins. In contrast to PABPC1, which associates with actively translated mRNAs, neuPABP associated mRNAs are translationally dormant. In support of this, our data suggest that while neuPABP has maintained functional RRMs for poly(A) RNA binding, it has evolutionarily diverged to not bind eIF4G, and as a consequence, inhibits protein synthesis *in vitro*.

These seminal findings presented in my thesis provide evidence that mammals have expanded their repertoire of PABPCs in the brain by coding for a predominantly neuronal protein, neuPABP. The ability of neuPABP to localize to the postsynaptic terminals, and associate with translationally inactive mRNA subpopulation, suggests a function of neuPABP in regulating local mRNA translation in neurons. In support of this, we demonstrate neuPABP is a protein that does not stimulate translation initiation. Moreover, the classes of mRNAs that we identify as neuPABP targets, are of utmost importance, as their protein products are required for ribosomal and mitochondrial biogenesis and repair in neurites, as many studies suggest. Our data also highlights lncRNA BC1 as a top neuPABP interactor, which intriguingly mirrors the developmental expression pattern of neuPABP, and is previously suggested to inhibit local mRNA translation in dendrites. These data have revealed a new PABPC in the mammalian brain, which may function to regulate local protein synthesis, a prerequisite for synaptic plasticity in learning and memory.

RÉSUMÉ

Presque tous les ARNm eucaryotes ont une queue poly(A) en 3' qui est liée par la protéine cytoplasmique de liaison poly(A) (PABPC). La PABPC peut réguler la traduction et le renouvellement des ARNm en interagissant avec les facteurs d'initiation de la traduction et les mécanismes de décroissance des ARNm. La PABPC est très conservée chez les eucaryotes, de la levure à l'homme, la PABPC prototypique (PABPC1) étant exprimée de manière ubiquitaire dans la plupart des tissus des mammifères, bien qu'à des niveaux différents. PABPC1 lie le facteur d'initiation de la traduction 4G (eIF4G), une interaction qui stimule la traduction dans certains contextes. Nous découvrons ici un nouveau PABPC spécifique aux mammifères, codé par le gène ampliconique lié à l'X Pabpc1l2a/b. La PABPC1L2 est principalement exprimée dans les tissus neuronaux, dans les neurones, que nous avons par la suite nommée PABP neuronale (neuPABP) et qui est une véritable protéine de liaison poly(A). L'expression de la neuPABP est régulée temporellement, avec un pic d'expression pendant la maturation neuronale dans la synaptogenèse. La neuPABP se localise dans les neurones au niveau du soma et des densités postsynaptiques. Contrairement à PABPC1, neuPABP ne contient que les deux premiers motifs de reconnaissance de l'ARN (RRM) et conserve un domaine N-terminal unique de fonction inconnue (DUF) que l'on ne retrouve pas dans les autres PABPC. Les analyses d'immunoprécipitation-Seq de l'ARN indiquent que la neuPABP interagit avec certaines populations d'ARN, à savoir les ARN non codants spécifiques du cerveau (BC1 et BC200) et les ARNm d'origine nucléaire codant pour des protéines ribosomiques et mitochondriales. Contrairement à PABPC1, qui s'associe à des ARNm activement traduits, les ARNm associés à neuPABP sont dormants sur le plan de la traduction. A l'appui de ce constat, nos données suggèrent que si le neuPABP a conservé des RRM fonctionnels

pour la liaison à l'ARN poly(A), il a divergé au cours de l'évolution pour ne pas lier l'eIF4G et, par conséquent, inhibe la synthèse protéique in vitro.

Les résultats fondamentaux présentés dans ma thèse prouvent que les mammifères ont élargi leur répertoire de PABPC dans le cerveau en codant pour une protéine essentiellement neuronale, la neuPABP. La capacité de la neuPABP à se localiser dans les terminaux postsynaptiques et à s'associer à une sous-population d'ARNm inactive sur le plan de la traduction suggère une fonction de la neuPABP dans la régulation de la traduction locale de l'ARNm dans les neurones. À l'appui de cette hypothèse, nous démontrons que la neuPABP est une protéine qui ne stimule pas l'initiation de la traduction. De plus, les classes d'ARNm que nous identifions comme cibles de neuPABP sont de la plus haute importance, car leurs produits protéiques sont nécessaires à la biogenèse et à la réparation des ribosomes et des mitochondries dans les neurites, comme le suggèrent de nombreuses études. Nos données mettent également en évidence l'ARNnc BC1 en tant qu'interacteur principal du neuPABP, qui reflète de manière intrigante le modèle d'expression développementale du neuPABP, et qui a déjà été suggéré pour inhiber la traduction locale de l'ARNm dans les dendrites. Ces données ont révélé l'existence d'un nouveau PABPC dans le cerveau des mammifères, dont la fonction pourrait être de réguler la synthèse locale des protéines, une condition préalable à la plasticité synaptique dans l'apprentissage et la mémoire.

I. ACKNOWLEDGEMENTS

First and foremost, I would like to start by acknowledging my supervisor Dr. Marc Fabian for his exceptional mentorship and tremendous support during my time as a PhD candidate in his lab. My academic journey in his lab commenced with the inception of a project which was still in its embryonic stages and was inevitably accompanied by many complexities. Nevertheless, his patience and wisdom helped me to keep looking forward and without his guidance this work would not have been possible. I met Marc in OIST, Okinawa, Japan where he was giving a guest talk to my previous research group. He eventually gave me the opportunity to pursue my scientific career as a PhD student in his lab, for which I will forever be grateful. Thank you, Marc for your steadfast mentorship in facilitating the progression of my scientific endeavors.

I would also like to extend my sincere thanks to my thesis committee members Drs. Wayne Sossin, Michael Witcher, Colin Crist, and Alexandre Orthwein for their extremely valuable feedback and insights into my research work. In particular, I would like to thank my academic advisor Michael for his help in organizing my annual committee meetings and Wayne for imparting his invaluable wisdom in neuroscience that helped me in propelling this project.

Additionally, I would like to thank my collaborators, Dr. Claudia Kleinman for single cell RNA-seq data analyses of *Pabpc1l2,* Dr. Debashish Ray for RNACompete analysis, Isabelle Carrier for help with FISH analysis, and Vincent Richard for help with proteomics.

I have all my past and present lab members to thank for inspiring me to keep doing science and making it a memorable experience. Thank you, Tamiko, Hana, Zineb, Benedeta, Sam, Will, Zane, Victoria, Zara, and Allen. In particular, I would like to thank Zineb, Sam and Benedeta who worked with me on this project, and especially thank you Sam and Victoria for all your help and our long scientific discussions. A special thanks to Hana and Tamiko for their support, guidance and enthusiasm.

I have my pillars of strength, my parents, to thank for the countless sacrifices they have made to ensure my higher education. Your selflessness and dedication have shaped not only my academic

path, but also the person I am becoming. I am truly fortunate to have parents like you. A special thanks to my sisters, Deepika and Monika, for their unconditional love and support.

Last but not least, I would like to thank everyone who touched my life in a positive way during my time at McGill. Thank you, Stephanie, for always encouraging me and making me feel at home in this foreign country, you have left an indelible mark on my life. My cousins Aishwarya and Bhartesh, for always being there for me, and my dear friend Ezhil for your support and friendship. Finally, how can I forget my little four-legged buddy, my dog Teddy, who supported me in writing this thesis in his own ways.

II. MANUSCRIPTS INCLUDED IN THESIS

My thesis was written as a monograph format, which includes my first authored manuscript which is now published in *Genes and Development*. Further, this thesis includes additional research findings from a manuscript that is under preparation.

Published manuscript included in this thesis:

1. **Authors: Sahil Sharma***, Sam Kajjo, Zineb Harra, Benedeta Hasaj, Victoria Delisle, Debashish Ray, Rodrigo L Gutierrez, Isabelle Carrier, Claudia Kleinman, Quaid Morris, Timothy R. Hughes, Roderick McInnes, and Marc R. Fabian
Title: Uncovering a mammalian neural-specific poly(A) binding protein with unique properties.
Journal: *Genes and Development* (Impact factor: 12.89) *first author

Published/submitted manuscripts NOT included in this thesis:

2. Kajjo S, **Sharma S**, Chen S, Brothers WR, Cott M, Hasaj B, Jovanovic P, Larsson O, Fabian MR. PABP prevents the untimely decay of select mRNA populations in human cells. *EMBO J.* 2022 Mar 15;41(6):e108650. (Impact factor: 13.783)

3. Rivera B, Nadaf J, Fahiminiya S, Apellaniz-Ruiz M, Saskin A, Chong AS, **Sharma S,** Wagener R, Revil T, Condello V, Harra Z, Hamel N, Sabbaghian N, Muchantef K, Thomas C, de Kock L, Hébert-Blouin MN, Bassenden AV, Rabenstein H, Mete O, Paschke R, Pusztaszeri MP, Paulus W, Berghuis A, Ragoussis J, Nikiforov YE, Siebert R, Albrecht S, Turcotte R, Hasselblatt M, Fabian MR, Foulkes WD. DGCR8 microprocessor defect characterizes familial multinodular goiter with schwannomatosis. *J Clin Invest.* 2020 Mar 2;130(3):1479-1490. (Impact factor: 19.477)

4. **Authors:** Sam Kajjo, **Sahil Sharma**, William R. Brothers, Victoria Delisle, Shan Chen, Ola Larsson and Marc R. Fabian
Title: PABPC plays a critical role in mTOR-mediated translational control of TOP mRNAs.
Journal: In review at *Cell Reports* (Impact factor: 8.8)

III. CONTRIBUTION TO ORIGINAL KNOWLEDGE

1. I characterized the neural-specific expression of *Pabpc1l2* ampliconic gene.

2. I characterized neuPABP as a temporally upregulated protein in mature neurons that localizes in postsynaptic densities.

3. I identified the correct N-term sequence of neuPABP and classified neuPABP as a GUG codon-initiated protein.

4. I characterized neuPABP as a poly(A) RNA binding protein.

5. I identified the endogenous mRNA targets of neuPABP.

6. I identified brain-specific non-coding BC1 RNA as the top target of neuPABP.

7. I classified neuPABP as a putative translation repressor that associates with untranslated RNAs.

8. I identified neuPABP as a component of translationally repressed RNPs and neuronal RNA transport granules.

9. I identified the association of neuPABP to non-translating RNAs in synapses, which contrasts PABPC1 association with translating RNAs.

IV. CONTRIBUTIONS OF AUTHORS

Chapter 1 and 2: Introduction, Rationale and Hypotheses

S.S. wrote and edited the entire chapters.

M.R.F. helped with proof reading and editing.

Chapter 3: Results

The results sections 3.1 to 3.5 are from the published manuscript:

1. **Authors: Sahil Sharma***, Sam Kajjo, Zineb Harra, Benedeta Hasaj, Victoria Delisle, Debashish Ray, Rodrigo L Gutierrez, Isabelle Carrier, Claudia Kleinman, Quaid Morris, Timothy R. Hughes, Roderick McInnes, and Marc R. Fabian

Title: Uncovering a mammalian neural-specific poly(A) binding protein with unique properties.

Journal: *Genes and Development*

Contributions: M.R.F and S.S. designed research; S.S., Z.H., S.K., D.R. and R.G. carried out experiments. All authors contributed to writing and/or editing the manuscript.

My specific contributions:

S.S. cowrote the original draft with M.R.F. and helped with editing and reviewing the subsequent drafts.

S.S. performed experiments for thesis figures 11, 13, 17, 18, 19, 22, 23B, 23C, 24, 25, 26, 27, 28, 29, 30, 31, and 32. These figures are named figures 1, S2, S6, S7, S8, 2, 3B, 3C, 4, S10, 5, S11, S13, 6, 7, S12, and 8, respectively, in the manuscript.

For the results sections 3.6 to 3.8:

S.S. wrote these results sections and M.R.F. helped with reviewing and editing.
S.S., S.K. and B.H. performed experiments for the validation of neuPABP^{KO} mouse in figures 38A and 38B.
S.K. helped with making the sucrose gradients for RNA granule isolation in Figure 36A and performed polysome fractionation of brain tissue lysates in figures 35D and 38F.

S.S. performed the remaining experiments for figures 34, 35, 36, 37, 38, and 39.

Bioinformatics analyses throughout the results chapter were performed by S.S. and M.R.F.

Chapter 4: Comprehensive Discussion

S.S. wrote and edited the entire chapter.

M.R.F. reviewed and helped with editing.

Chapter 5: Methods

D.R. wrote the RNAcompete methodology.

R.G. wrote the Single-nuclei RNA-seq data processing method.

S.S. wrote the remaining methods sections 5.1 and 5.2, and M.R.F. helped with reviewing and editing.

V. ABBREVIATIONS LIST

AGO: argonaute
AMPA: α-amino-3-hydroxy-5-methyl-4-isoxazole propionic acid
AMPAR: AMPA-receptor
APA: alternative polyadenylation
ARE: A-rich element
ASD: autism spectrum disorder
ATP5J2 : ATP Synthase Membrane Subunit F
BC RNA: brain cytoplasmic RNA
BDNF: brain-derived neurotrophic factor
CASP2: caspase 2 protease
CBP20: cap binding protein 20
CDS: coding sequence
CLIP: formaldehyde cross-linking and immunoprecipitation
CPE: cytoplasmic polyadenylation element
CPEB: cytoplasmic polyadenylation element binding
CPSF: cleavage and polyadenylation specificity factor
CRISPR: clustered regularly interspaced short palindromic repeats
cryo-EM: cryo-electron microscopy
CTD: c-terminal domain
CTIF: CBP80/20-dependent translation initiation factor
DAPI: 4′,6-diamidino-2-phenylindole
DCP1: decapping protein 1
DEDD: death effector domain containing
DHX34: DExH-Box Helicase 34
DIV: days in vitro
DRG: dorsal Root Ganglia
DUF: domain of unknown function
EDC4: enhancer of decapping 4
eEF1: eukaryotic elongation factor 1
eIF: eukaryotic initiation factor
eIF4G: eukaryotic initiation factor 4G
EJC: exon junction complex
EMSA: electrophoretic mobility shift assay
EPSP: excitatory postsynaptic potentials
eRF1: eukaryotic release factor 1
ERK: extracellular signal-regulated kinase
FL: firefly luciferase
FMRP: fragile X protein
GFAP: glial fibrillary acidic protein
GPCR: G protein-coupled receptor
GST: glutathione-S-transferase
HCV: hepatitis C virus
HNRNPA1: heterogeneous nuclear ribonucleoprotein A1

HNRNPQ: heterogeneous nuclear ribonucleoprotein Q
HRV-3C: human rhinovirus 3C protease
IF: immunofluorescence
IP: immunoprecipitation
IPTG: isopropyl-β-D-Thiogalactopyranoside
IRES: internal ribosome entry site
IVT: in vitro translation
JNK: c-Jun N-terminal Kinase
KH1: K-homology 1
KIF5: kinesin Family Member 5
LSM1: like Sm1
LTD: long-term depression
LTP: long-term potentiation
MAGUK: membrane-associated guanylate kinases
MAP2: microtubule associated protein 2
MAPK: mitogen activated serine/threonine protein kinase
MBP: maltose binding protein
MIF4G: middle-domain of eIF4G
miRISC: miRNA-induced silencing complex
MLLE: mademoiselle' domain
mt.ND1: mitochondrial NADH dehydrogenase 1
mTORC1: mammalian target of rapamycin complex 1
NDUFA2: NADH:ubiquinone oxidoreductase subunit A2
neuPABP: neural PABP
NLS: nuclear localization signal
NMD: non-sense mediated decay
NMDA: N-methyl-D-aspartate
NMDAR: NMDA receptor
NPC: neural progenitor cells
ORF: open reading frame
PABP: poly(A) binding protein
PABPC: cytoplasmic Poly(A) binding protein
PABPC1L2: cytoplasmic Poly(A) binding protein 1-like-2
PAIP2: PABP-interacting protein-2
PAM2: PABP interacting motif 2
PAP: poly(A) polymerase
PARN: poly(A) ribonuclease
PAS: poly(A) signal
PKB: protein kinase B
PLA: proximity ligation assay
PSD: postsynaptic density
PSD95: postsynaptic density-95
PTC: premature termination codon
PURα: purine-rich element binding protein α
RACE: rapid amplification of cDNA ends
RAN: repeat associated non-AUG

RBD: RNA binding domain
RBP: RNA binding protein
RG: RNA granule
RHEB: Ras homolog enriched in brain
RIP: RNA immunoprecipitation
RL: Renilla luciferase
RNP: ribonucleoprotein
RPLP0 : ribosomal protein lateral stalk subunit P0
RPS6: ribosomal protein S6
RRM: RNA recognition motif
S6K: protein S6 kinase
SLBP: stem-loop binding protein
SLIP1: stem-loop interacting protein
SMG1: serine/threonine protein kinase 1
SMN: survival of motor neuron
SRE: staufen response elements
SYNCRIP: synaptotagmin Binding Cytoplasmic RNA Interacting Protein
TCA: trichloroacetic acid
TDP43 : TAR DNA-binding protein 43
TNRC6: trinucleotide repeat containing 6
TOB: transducer of ErbB2
TOP: terminal oligo pyrimidine tract
TREX: transcription-export complex
TTP: tristetraprolin
TUT4: terminal uridylyltransferase
UPF1: up frameshift 1
XAR: X-chromosome added region
XCR: X-chromosome conserved region
XRN1: 5'-3' exoribonuclease 1
ZBP1: zipcode-binding protein 1

VI. LIST OF FIGURES

1. INTRODUCTION

Earliest microfossils provide evidence that first single cell eukaryotes appeared around 1.5 billion years ago (1). During the course of evolution, eukaryotic single cell organisms formed symbiotic associations for survival in the ever-changing environment, which gave rise to the complex multicellular lifeforms of today. Multicellular organisms have acquired complex, yet efficient mechanisms to respond and adapt to their environment through intricately modulating the gene expression programs in different cell types.

1.1. GENE EXPRESSION IN EUKARYOTES

The gene expression programs in eukaryotes differ greatly from prokaryotes. Unlike prokaryotes, where transcription and translation can occur concurrently in the cytoplasm (2-5), eukaryotes have ingeniously compartmentalized different steps of gene expression. Genes are first transcribed into precursor-mRNAs (pre-mRNAs) in the nucleus, and after several steps of post-transcriptional processing, mature mRNAs are exported into the cytoplasm for translation. This decoupling of translation from transcription may have imparted eukaryotes with a superior multi-dimensional gene expression control. Indeed, eukaryotic gene expression can be regulated at both transcription and translation level by complex molecular machines. Of importance are the mRNA stability complexes, which can greatly influence the spatiotemporal gene expression, especially when protein synthesis rates are tightly regulated, thus providing eukaryotes with the “third axis” of gene expression control. In both the nucleus and cytoplasm, several post-transcriptional modifications are added onto an mRNA molecule. These modifications on an mRNA molecule are absolute requirements for efficient nuclear export, translation, and stability by preventing its untimely

demise in the cytoplasm. Therefore, mRNA has emerged as a central molecule that carries genetic codes for the synthesis of a functional protein in the cytoplasm.

Overview: A complex life of mRNA

The life-cycle of mRNA begins with its transcription from the DNA, followed by translation using ribosomes, and finally degradation by RNA decay machines. Since its inception, mRNA is decorated by an array of RNA binding proteins (RBPs) that regulate every aspect of gene expression control. RBPs associate with mRNAs via RNA-binding domains (RBD), and influence mRNA export, transport/localization, translation, and stability.

Gene expression begins in the nucleus where a DNA template is transcribed into a precursor mRNA copy (pre-mRNA) by the coordinated action of RNA polymerase II and other DNA binding proteins like transcription factors, and coactivators [(6-8), (**Figure 1**)]. During the process of transcription, a 5' m7G-cap structure is added to the pre-mRNA as soon as it reaches 20-30 nucleotides in length (9). The 5' end capping is carried out by a series of enzymatic steps, which include removal of a phosphate group, addition of a GMP group, and finally transfer of a methyl group to the guanine (10). The cap structure is bound by a heterodimer of cap binding proteins (CBP), CBP20 and CBP80 (11-14). Most pre-mRNAs contain exons that are alternated by introns. A multi-megadalton pre-mRNA splicing machinery called spliceosome removes the intronic regions and joins the exons, thus forming exon-exon junctions (15-18). After splicing, a complex called exon-junction complex (EJC) is deposited some ~20-25 nucleotides upstream of the exon-exon junctions, which has a major implication for translation "go ahead", and nonsense mRNA mediated decay (NMD) (19, 20). The 3' end of the mRNA is finally processed by a cleavage event

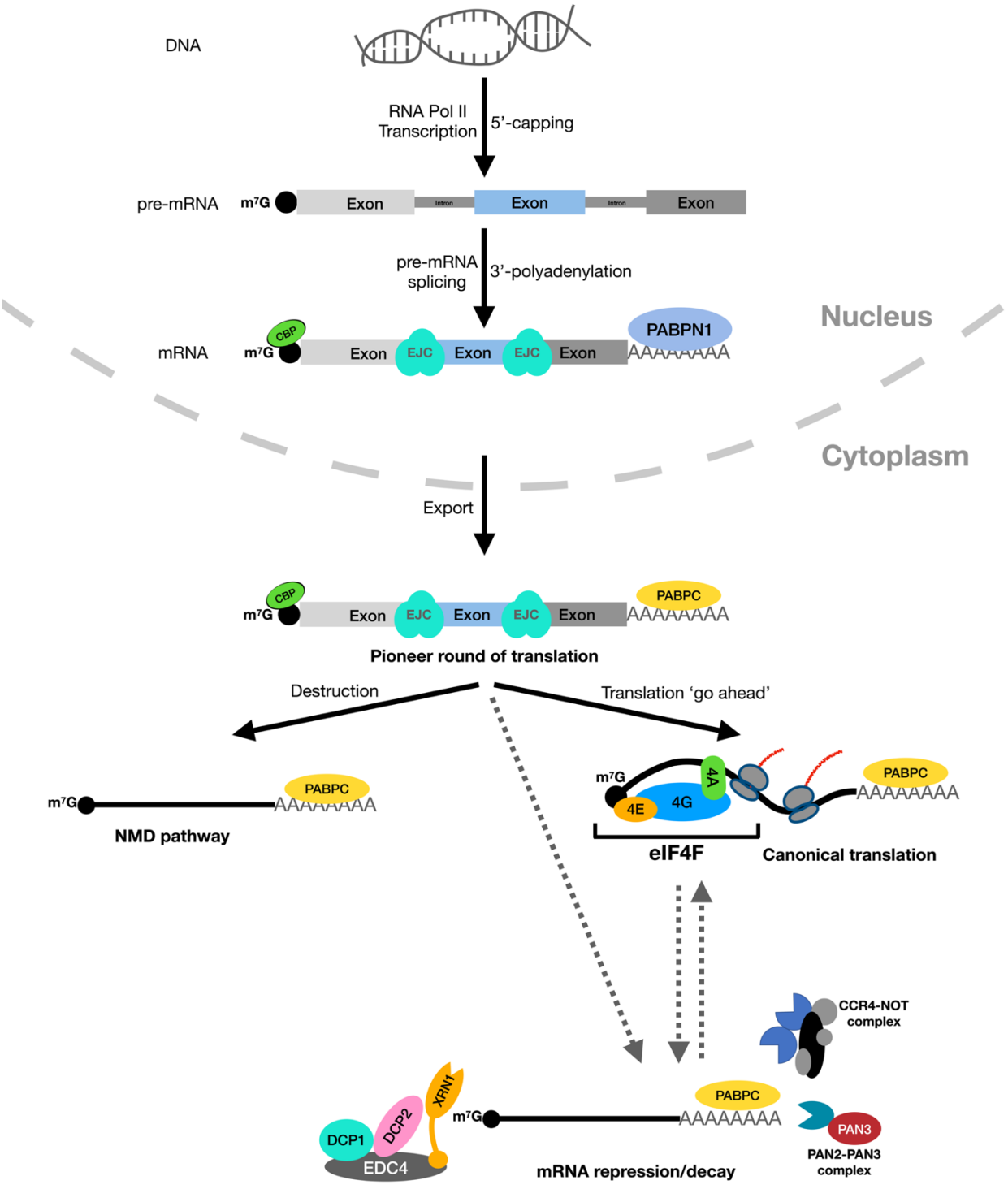

Figure 1. mRNA life cycle. In the nucleus, DNA template is transcribed into pre-mRNA containing exons and exons. Introns are spliced-out and mRNAs are decorated with terminal modifications: 5' cap and 3' poly(A) tails. After splicing, exon-exon junctions are deposited with

exon junction complexes (EJCs), and mRNA cap and poly(A) tail is bound by cap-binding proteins (CBPs) and nuclear poly(A) binding protein (PABPN1), respectively. mRNA is exported into the cytoplasm where it undergoes “pioneer-round of translation” to determine the quality of transcript by checking for premature termination codons (PTCs). In which case, the nonsense mRNA mediated decay (NMD) pathway is triggered. EJCs are removed by the ribosomes in the pioneer round of translation. A transcript can either serve as a template for protein synthesis by canonical translation or undergo reversible translation repression or ultimate decay.

followed by the addition of a poly(A) tail (~200-250 nucleotides) by the poly(A) polymerase enzyme (PAP) (21). The newly synthesized poly(A) tail is coated by the nuclear poly(A) binding protein (PABPN1) (21). Finally, the mature RNA is exported into the cytoplasm by a protein complex called the transcription-export complex (TREX) via the nucleopore complex (NPC) (22-24). The export of mRNA is facilitated by various factors, including CBP80 and PABPN1 that are bound to the 5'cap structure and poly(A) tail, respectively (13, 14, 25). Moreover, the cytoplasmic poly(A) binding protein (PABPC) has been suggested to shuttle into the nucleus and replace PABPN1 prior to mRNA export (26, 27).

The 5' cap structure of mRNAs undergoing their first, or pioneering, round of translation upon export to the cytoplasm are bound by the CBP20/80 heterodimer rather than the eukaryotic initiation factor (eIF), eIF4E (28, 29). Briefly, during this process the CBP20/80 heterodimer binds to a non-canonical translation initiation factor called middle-domain of eIF4G (MIF4G)-containing protein, CTIF (CBP20/80-dependent translation initiation factor). CTIF interacts with CBP80 and ribosome-bound eIF3, thus recruiting the ribosomes (29). During the pioneering round of translation, ribosomes normally encounter EJCs upstream of the stop codon and remove them; however, EJCs deposited downstream of a premature stop codon would trigger an NMD response to decay the mRNA (13, 30-32). After an mRNA has passed the "quality check" of NMD in the pioneer round of translation, eIF4E replaces CBP20/80 heterodimer from the 5' cap, which assembles the canonical translation factors, including the eIF4F complex for subsequent rounds of translation (28).

mRNAs are vulnerable to deadenylation and decay in the cytoplasm and poly(A) tails are trimmed to an average poly(A) tail length of 50-100 nucleotides, as opposed to ~250 in the nucleus (21, 33-35). Several major deadenylase machineries, including the PAN2-PAN3 and CCR4-NOT complexes, trim the mRNA poly(A) tails, and can instigate an mRNA decay regime by the mRNA decapping complexes (DCP1-DCP2) and exoribonucleases (XRN1) (36-41).

mRNA 5' Capping

All eukaryotic mRNAs contain a specialized "cap" structure at their 5' end. This structure is composed of a N7-methylguanosine residue (m^7G) linked to the first nucleotide of an mRNA. A majority of the mRNAs utilize the m^7G-cap for their translation by recruiting several translation initiation factors (41-43). Moreover, the m^7G-cap plays important roles in: stabilizing the mRNAs against exonucleases, pre-mRNA splicing, polyadenylation, and mature mRNA export from the nucleus (44-50). 5' end capping is the first cotranscriptional modification on an RNA polymerase II transcribed transcript and generally occurs when the pre-mRNA reaches 20-30 nucleotides in length (9, 51). Capping requires three enzymatic steps for its addition. The first step is carried out by the enzyme called RNA triphosphatase (TPase), which involves the removal of ɣ-phosphate from the 5' triphosphate end of the nascent transcript to generate a 5' diphosphate end. The second step involves the activity of an enzyme called RNA guanylyltransferase (GTase), which transfers a GMP group derived from the hydrolysis of a GTP molecule onto the 5' diphosphate RNA. Thus, forming a 5'-5' triphosphate linkage between the first base of the nascent RNA and the guanosine capping base of GMP. The final step requires the activity of yet another enzyme called guanine-N^7-methytransferase (MTase), which adds a methyl group to an amine group at the 7^{th} position (N^7) of the guanine cap, which forms the "cap 0" structure (10). Further, other methyltransferases

can add a methyl group to the 2'O of +1 ribose to generate "cap 1" structure (52). Interestingly, while in yeast each enzymatic activity of capping is carried out by one enzyme, in metazoans, an enzyme called capping enzyme is responsible for both triphosphatase and guanylyltransferase functions (53-56). The capping enzyme complex is recruited to the transcribing pre-mRNA during the elongation step via its interaction with the phosphorylated C-terminal domain (CTD) of RNA polymerase II (57, 58). The CTD also stimulates pre-mRNA splicing by interacting with the spliceosome machinery (59), and 3' end processing by interfacing with the cleavage stimulation factor (CstF) and cleavage and polyadenylation specific factor (CPSF) (60).

3' Poly(A) tail synthesis

Most Eukaryotic mRNAs contain a homopolymeric polyadenylated sequence at their 3' end, with the exception being the replication-dependent histone proteins coding mRNAs (61). Poly(A) tail is added to the pre-mRNA co-transcriptionally during 3' end processing (62), and plays an important role in mRNA export to the cytoplasm (63-66). Eukaryotic mRNAs maintain an average poly(A) tail length of ~200 nucleotide (67). However, in yeast, the average mRNA poly(A) tail length is ~50 nucleotide (68). The length of poly(A) tail is determined by several sequence elements in the 3'UTR region of mRNAs. In the nucleus, unprocessed pre-mRNAs undergo cleavage at poly(A) cleavage site which is 10-30 nucleotide downstream of the poly(A) signal (PAS) hexamer sequence "A[A/U]UAAA" (69-71). PAS provides binding platform to CPSF complex, and its catalytic subunit CPSF73 carries out the cleavage in coordination with the subunit CPSF100 (72-76). Additionally, CstF complex is recruited to a GU-rich sequence present downstream of the cleavage site and is required for stimulation of the cleavage event (77, 78). After cleavage, the cleavage/polyadenylation machinery recruits the poly(A) polymerase (PAP)

enzyme to mRNAs in a close proximity to their 3' ends (79, 80). PAP adds the initial poly(A) tail, which is bound by the nuclear poly(A) binding protein PABPN1 (81). PAP binds CPSF and PABPN1 simultaneously, which in turn synergistically enhances its poly(A) polymerase activity (82). Interaction of PAP with either of these factors alone imparts only a modest polymerase activity (82). Therefore, both "AAUAAA" hexamer for CPSF binding, and initial oligo(A) tail for PABPN1 binding are necessary for a cooperative addition of a long poly(A) tail. However, as the poly(A) tail length reaches ~200-250 nucleotide and gets coated by multiple PABPN1 molecules, this leads to a disruption of the binding between CPSF and PAP. As a consequence, the polyadenylation reaction stops, and PAP dissociates from the mRNAs (21).

Alternative polyadenylation

Many mRNAs contain more than one PAS-hexamer sequence in their 3' UTRs, and alternative usage of these sequences can generate mRNA isoforms with diverse 3' ends, a phenomenon named alternative polyadenylation (APA) (83). The 3' UTR length is an important factor in determining mRNA translation, stability, and subcellular localization (84). The process of cleavage and polyadenylation by the multi-subunit CPSF complex is tightly regulated and the availability of each member protein can affect the pre-mRNA 3'end processing, which can generate alternative 3' UTR-length isoforms (84-87). These isoforms can include or exclude various cis-regulatory elements in their 3' UTRs like microRNA binding sites, RNA binding proteins (RBPs) binding sites, and RNA secondary structures. This can directly influence the mRNA stability, steady states, translation efficiency, as well as mRNA transport (88-93). APA isoforms can be generated by two methods. In first method, multiple PAS sites are present in tandem in the terminal exon, therefore, alternate usage of these sites gives rise to isoforms with variable 3' UTR lengths, although coding

identical proteins (94). In second method, PASs can be present in the introns, and their usage gives rise to truncated protein coding isoforms (95, 96). In neurons, dendritic delivery of mRNAs is prerequisite for efficient local translation and synaptic plasticity (97). Indeed, APA isoforms of genes like *Impa1*, *BDNF, CaMKIIα*, and *Importin-β1* are differentially localized in neuronal compartments, where isoforms generated from distal PASs are preferentially localized into the neurites (84, 98, 99). The current evidence also suggests that many mRNAs, including *PSD-95* and *CaMKIIα* use *cis*-acting elements in the 3' UTRs for their dendritic delivery (93). This highlights the role of APA in differential subcellular localization of mRNA isoforms. The use of distal PASs for APA leads to the generation of mRNA isoforms with longer 3' UTRs, which may harbour miRNA targeting sites. This leaves certain mRNA isoforms more susceptible for miRNA-mediated silencing, whereas short 3' UTR isoforms are resistant (90). The role of APA in translation is best described for *BDNF* mRNA. BDNF protein is encoded by two 3' UTR isoforms. At rest, BDNF protein output is mainly contributed by the short 3' UTR isoform, while the long 3' UTR isoform is translationally supressed. However, after neuronal activation, the long 3' UTR isoform in contrast to the short 3' UTR isoform, associates rapidly with polyribosomes for translation (100). In cancer cells, mRNA isoforms with short 3' UTRs are often accumulated (90). These isoforms typically exhibit longer RNA half-lives and overexpress proteins, for example, the expression of a short 3' UTR isoform of the protooncogene *IGF2BP1/IMP1* leads to oncogenic transformation of cell lines (90).

Cytoplasmic polyadenylation

Some mRNAs can also undergo polyadenylation in the cytoplasm, but require the PAS as well as

a U-rich cytoplasmic polyadenylation sequence element (CPE, 'UUUUA$_{1-3}$U') in their 3' UTRs (101, 102), which is usually within 20-100 nucleotide upstream of the PAS sequence (102-105). It is estimated that approximately 30-40% of mRNAs in vertebrate species harbour CPEs that may be subjected to CPE-mediated translational control (106). Cytoplasmic polyadenylation and its role in translation regulation was first described in Sea Urchin and *Xenopus* oocytes (107-110). Similarly, CPE-mediated polyadenylation and translational control has been suggested in mouse oocytes (111). In early oocytes, the mRNAs are stored in dormant states containing short poly(A) tails; however, as the oocytes mature the mRNA poly(A) tails get elongated, which facilitate their efficient translation (112-115). In *Xenopus* oocytes, a distinct cytoplasmic polyadenylation element binding protein (CPEB) binds the CPE and facilitates mRNA polyadenylation in the cytoplasm (116). In the nucleus, CPSF and CPEB bind the mRNA PAS and CPE sequences, respectively, and are exported into the cytoplasm. A scaffold protein called symplekin contacts both CPSF and CPEB, and helps CPEB to recruit a non-canonical poly(A) polymerase called germline development 2 (Gld2) and a poly(A) ribonuclease (PARN) (117). A balance between the antagonist activity of these two proteins maintains short poly(A) tails on mRNAs (117). CPEB ribonucleoprotein complex also contacts a protein called maskin, which binds the 5' cap-bound translation initiation factor (eIF4E), and prevents the assembly of eIF4F translation initiation complex (118). However, after progesterone hormone stimulation, CPEB gets phosphorylated by a kinase called aurora A (119), which causes the release of PARN from the CPEB-RNP complex (117), promotes a strong CPSF-CPEB interaction (120), and enhances Gld2 mediated polyadenylation of mRNAs (117).

Exceptions to the rule: mRNAs lacking poly(A) tails

Interestingly, not all capped mRNAs undergo polyadenylation, for example, replication-dependent histone mRNAs do not contain a poly(A) tail and are transcriptionally upregulated only during the S-phase of cell cycle by a transcription factor called NPAT, to provide abundant supply of histone proteins necessary for the packaging of newly replicated DNA (121, 122). Histone pre-mRNAs contain a unique and highly conserved stem-loop structure in their 3' UTR (123). An RNA-protein complex called U7-snRNP-complex, which consists of a 60 nucleotide U7-snRNA, a cleavage factor called CFSF73, which is the same cleavage factor utilized by the canonical cleavage-polyadenylation machinery, and several other proteins including the histone stem-loop binding protein (SLBP), binds the histone pre-mRNAs by base-pairing (124). The U7-snRNP-complex once recruited to the histone pre-mRNAs, cleaves immediately downstream of the stem-loop structure, leaving only a 4-5 nucleotide long tail (124). In contrast to other mRNAs, replication-dependent histone mRNAs do not undergo polyadenylation after the cleavage event. The SLBP remains bound to the stem-loop of mature histone RNAs, and accompanies them during translation and decay (125-127). Importantly, this highlights the conservation of CPSF73 cleavage factor between two functionally distinct mRNA 3' end processing machineries.

Mature polyadenylated mRNAs are ultimately exported to the cytoplasm where 5' cap and poly(A) tails are thought to play an important role in mRNA fate determination. Poly(A) tail length is highly regulated in the cytoplasm by a number of RNA binding proteins whose binding can either stabilize the mRNA or accelerate its decay (37, 128, 129). One such class of protein is the cytoplasmic poly(A) binding protein (PABPC). Although PABPC lacks nuclear localization signal (NLS), it can still shuttle between nucleus and cytoplasm and bind mRNA poly(A) tails in the nucleus (26).

After nuclear localization, although not well understood, PABPC may displace PABPN1 from mRNA poly(A) tails and facilitate their export to the cytoplasm (26). In the cytoplasm, mRNA poly(A) tails are bound by PABPC, which plays a critical role in mRNA fate determination, including mRNA translation, stability and turnover.

1.2. TRANSLATION INITIATION

Canonical mode of translation initiation

mRNA translation initiation is a crucial step in protein synthesis orchestrated by numerous eukaryotic initiation factors (eIFs). Several of these initiation factors assemble at the 5' end of an mRNA to facilitate ribosome recruitment (**Figure 2**). One such initiation factor is a scaffold protein eIF4G, which simultaneously binds the mRNA cap binding protein eIF4E and an ATP-dependent RNA dead-box helicase protein eIF4A (130-132). This forms the eIF4F complex bound to the mRNA 5' cap structure (132, 133). eIF4G further interacts with eIF3 to recruit the 43S-preinitiation complex. The 43S-preinitiation complex consists of a 40S small ribosomal subunit bound by eIF3, eIF1A, and eIF2-GTP-Met-tRNAi ternary complex (132, 134). Once the 43S-preinitiation complex is assembled on the mRNA 5' end, a step requiring ATP hydrolysis, it then traverses the mRNA 5' UTR to scan for a canonical AUG start codon in a favourable Kozak sequence context "(A/G)CCAUGG" (135-137). This leads to the formation of a 48S-preinitiation complex at the start codon (132, 138). To facilitate the joining of a 60S ribosomal subunit and form a functional 80S ribosome, initiation factors are released from the preinitiation complex by the GTP-hydrolysis activity of eIF2. This activity of eIF2 is promoted by eIF5, a GTPase-activating protein (GAP) (139-141). The functional 80S ribosome once assembled begins polypeptide synthesis in the elongation step of translation.

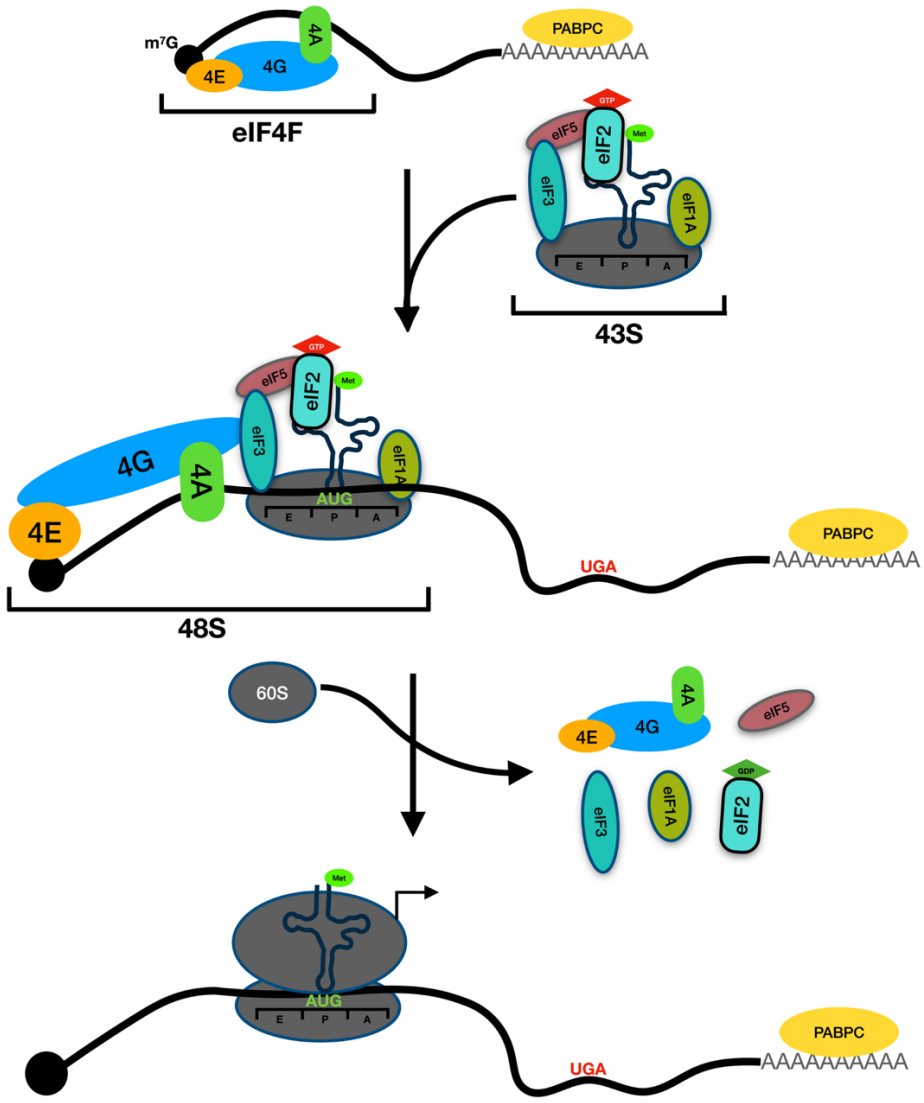

Figure 2. Canonical 5' cap dependent translation initiation. Several initiation factors (eIFs) orchestrate translation initiation process. The cap-binding protein eIF4E is bound on the 5' cap structure and recruits a scaffold protein eIF4G, which simultaneously binds the RNA helicase, eIF4A, this forms the eIF4F complex. The eIF4F complex recruits the 40S ribosomal subunit and eIF2-GTP-Met-tRNAi ternary complex containing 43S-preinitiation complex via eIF4G-eIF3 interactions, which leads to the formation of 48S-preinitiation complex. The 48S complex scans the 5' UTR for a suitable AUG codon. Finally, the 60S ribosomal subunit is recruited to form a functional 80S ribosome for translation.

Role of PABPC in translation initiation

PABPC is characterized as a translation initiation factor important for stimulating translation (142). PABPC favours translation initiation by simultaneously binding the mRNA poly(A) tail and scaffold protein eIF4G [(142, 143), (**Figure 3A**)]. This interaction bridges the 5' and 3' ends and allows for the mRNA to attain a circular conformation (144, 145). This circular model of mRNA is believed to be energetically favourable for ribosome subunit recycling and initiation of multiple round of translation from the same mRNA molecule (145, 146). PABPC interacts with the N-terminus of eIF4G through RRM2 (143), and disrupting this interaction by a mutation (M161A) in PABPC RRM2, has implications for translation initiation complex assembly and protein synthesis (142, 147). As PABPC-eIF4G contact stimulates translation in *in vitro* cell free systems like Krebs extracts (142), in *in vivo* systems like *Xenopus* oocytes this contact is important for their maturation (148). Expressing a mutant eIF4G that cannot interface with PABPC RRM2, leads to the inhibition of progesterone-induced oocyte maturation (148). This effect comes from the reduced translation efficiency of polyadenylated RNAs.

In oocytes and early embryos, PABPC levels are low (149, 150), transcriptional programs are shut down due to a highly condensed chromatin configuration (151-156), and maternal mRNAs are stored as short poly(A) tailed transcripts in stable cytoplasmic granules (157, 158). Cytoplasmic polyadenylation during early embryogenesis translationally activates these mRNAs and plays an important role in maternal to zygotic transition (101, 109, 110, 158, 159). The low levels of PABPC in these early developmental systems, therefore, confers the poly(A) tail length as a major determinant of translation efficiency as mRNAs with longer poly(A) tails can compete better for the limited quantity of PABPC to stimulate their translation (160). While this poly(A) tail length

bias disappears after overexpression of PABPC in *Xenopus* oocytes, overexpression of PABPC (M161A) mutant diminished the translation of both short and long poly(A)-tailed RNAs (160). This highlights the importance of poly(A) tail length in PABPC limiting systems, and that in conjunction, PABPC-eIF4G interaction is required to achieve a greater translation efficiency in early developmental systems.

In postembryonic systems, like *Drosophila* S2 cells and human cells, the PABPC and eIF4G cooccupancy on mRNAs is strongly correlated; however, poly(A) tail length does not influence PABPC occupancy (161). In HeLa cells, PABPCs are not limited (162), and they contain two PABPC paralogs namely, PABPC1 and PABPC4 (163). PABPC1 is the major PABPC in these cells, and surprisingly, PABPC1 protein amounts are in three-fold excess over the cytoplasmic poly(A) RNAs (162). In HeLa cells the poly(A) tail length and translation efficiency are weakly correlated with the strongest correlation observed only for mRNAs with tail length of <20nucleotides (164). Since, majority of mRNAs maintain tail lengths longer than 20 nucleotides, the poly(A) tail length and translation efficiency are not correlated globally in HeLa cells (164). Additionally, although PABPC occupancy on mRNAs corelates positively with translation efficiency, the correlation is weak when compared with mRNA stability (161). Interestingly, the depletion of PABPC from HeLa cells only establishes a weak correlation between poly(A) tail length and translation efficiency, thus indicating that factors other than excess PABPC are responsible for this diminished correlation (160). Even though depletion of PABPC does not appear to strongly impact translation, the effects are significant on global protein synthesis, and the depletion strongly impacts the stability of short-tailed abundant cytoplasmic mRNAs that are

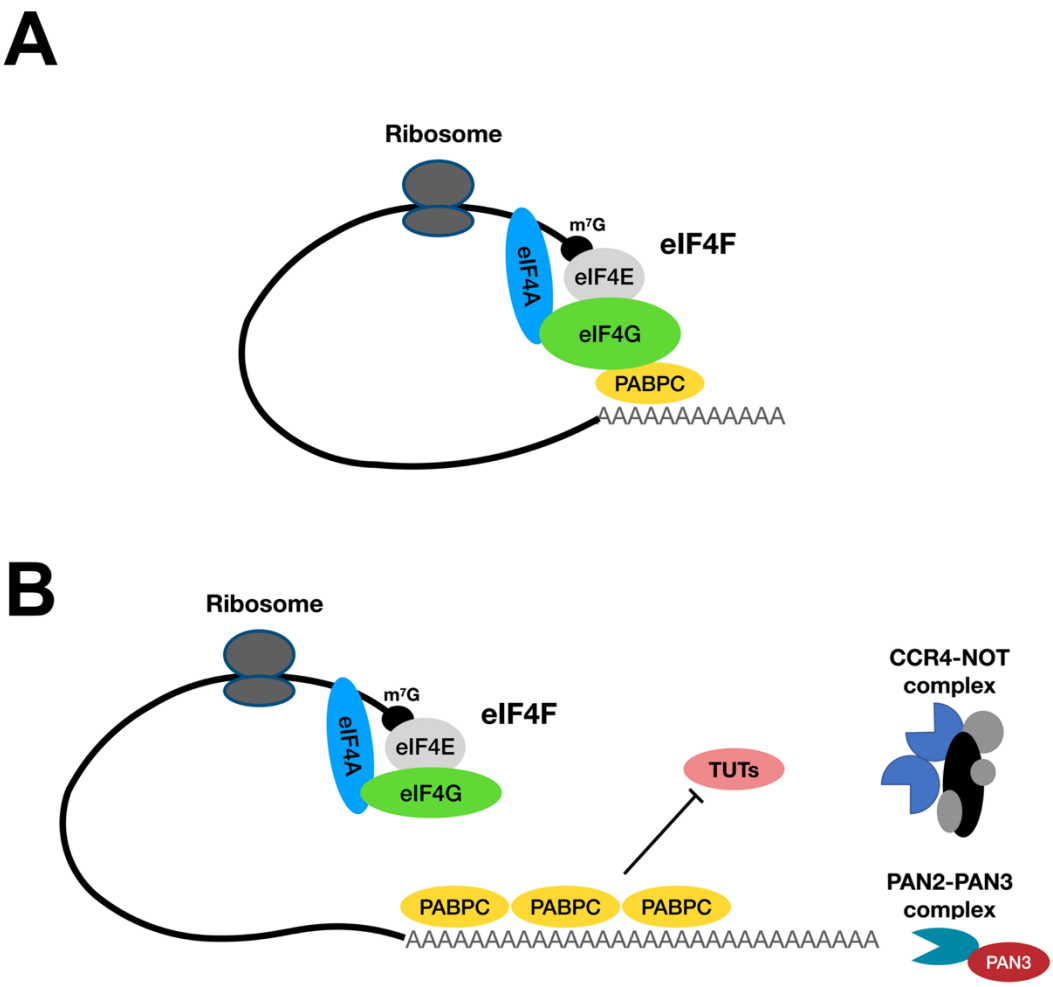

Figure 3. Role of PABPC in translation initiation. (A) The eIF4F complex is recruited to the 5'capped and PABPC-bound polyadenylated mRNA. The interaction between eIF4G and PABPC bridges mRNA 5'- and 3'-ends which stimulates translation in *in vitro* and several early developmental systems. (B) In postembryonic system, PABPC does not appear to stimulate translation, however, promotes poly(A) trimming by PAN2-PAN3 and CCR4-NOT deadenylase complexes, and prevents further mRNA decay by blocking uridylation by TUT4/TU7.

generally stable namely, nucleus encoded ribosomal and mitochondrial proteins coding transcripts (128, 160). Interestingly, these classes of mRNAs are previously shown to have higher occupancies of PABPC, eIF4E, and eIF4G (161). As a consequence of their reduced stability, PABPC depletion in HeLa cells leads to an increase in the median poly(A) tail length of mRNAs as they are not efficiently destabilized i.e., their decay rates are slower (128, 160). Poly(A) tail lengths of mRNAs that are destabilized after PABPC depletion ranges from 10-135 nucleotides, with mRNAs having tail length around 25 nucleotides showing the strongest destabilization effects (160). It is unclear as to why mRNAs with longer poly(A) tails are degraded inefficiently in PABPC limited system; however, one possibility is deadenylation impairment in PABPC depleted systems. PABPC can promote deadenylation in cooperation with a major deadenylation complex called CCR4-NOT complex [(37), (**Figure 3B**)]. Even though PABPC promotes deadenylation of a transcript, it prevents 3' terminal uridylation by terminal uridylyl transferases, TUT4 and TUT7, which marks mRNAs for decay by recruiting mRNA decay factors (37). Interestingly, in PABPC depleted system, mRNAs with short poly(A) tails are destabilized by terminal uridylation and in a deadenylation independent manner through decapping and 5' to 3' decay (128, 160). Therefore, in post-embryonic HeLa cells, establishing a strong correlation between poly(A) tail length and translation efficiency is challenging, as limiting PABPC leads to mRNAs destabilization of short-tailed mRNAs rather than their inefficient translation. The impact of PABPC on translation is suggested to be a context dependent phenomenon, where in actively dividing cell lines where PABPC is abundant, it plays a role in maintaining the stability of transcripts (128, 160), while in PABPC-limited systems, like oocytes, PABPC has a greater influence on mRNA translation (148, 160).

Whether PABPC directly influences translation in terminally differentiated cells, like neurons, is not clear. A recent study suggests that there is only a modest correlation between poly(A) tail length and translation efficiency in neurons and vast majority of translational changes are comparable to other post-embryonic cells (165). This study highlights that only a subset of mRNAs undergoes cytoplasmic polyadenylation to enhance their translation after neuronal stimulation. A bulk majority of the RNA did not get their poly(A) tails elongated for efficient translation. However, as neurons respond to external stimuli through local protein synthesis in the synaptic terminals (166), away from the cell bodies, a more rigorous analysis is needed to investigate the correlation between poly(A) tail length and translation efficiency in the synaptic compartments (165).

Poly(A) tail-independent mRNA translation

In metazoans, the majority of histone proteins are coded for by replication-dependent histone genes. Importantly, the mRNAs coded by these genes are a unique class of RNA polymerase II transcripts, which are unadenylated (167). These mRNAs code for all core histone proteins, including H2A, H2B, H3 and H4. The 3' end of replication-dependent histone mRNAs is formed by endonucleolytic cleavage of their pre-mRNAs (123). The replication-dependent histone mRNAs, unlike other mRNAs, end in a conserved 26-nucleotide sequence which forms a 16-nucleotide stem-loop structure (123). A protein called the stem-loop binding protein (SLBP) recognizes this stem-loop and plays important roles in regulating histone pre-mRNA processing, mRNA translation, and degradation (125, 126, 168, 169). SLBP stimulates the translation of capped and histone stem-loop containing artificial mRNAs in *Xenopus* oocytes and its stimulatory effect increases during oocyte maturation (125, 169, 170). SLBP can interact with eIF3 and PAIP1 directly; however, it stimulates translation by playing a role in 40S ribosomal subunit recruitment,

and physically associating with eIF3 and eIF4G in mammalian cells (169, 171). SLBP works in coordination with a protein called SLBP-interacting protein (SLIP1) to stimulate translation [(172), (**Figure 4A**)]. SLBP simultaneously binds SLIP1 and the stem-loop structure, and SLIP1 in turn interacts with eIF4G. This facilitates bridging of the 5' and 3' ends, which stimulates translation in the absence of PABPC-eIF4G interaction on non-polyadenylated histone mRNAs (172).

IRES-mediated translation initiation

The recruitment of preinitiation complex on mRNA is a rate limiting step in translation (173-176). While all cellular mRNAs are expected to be capped, and therefore, are capable of binding eIF4F complex to initiate their translation, some mRNAs with highly complex 5' UTRs and high GC content do not conform to the canonical cap-dependent scanning mode of translation initiation (177, 178). To overcome this limitation, especially under stress conditions, several cellular mRNAs (like viral RNAs) are capable of utilizing the complex structural elements in their 5' UTRs called IRES (Internal ribosome entry sites) to initiate translation (177, 179, 180). Some IRESes can directly interact with the ribosome bound initiation factors like eIF3, therefore, reducing the requirement of 5' end bound eIF4F complex for ribosome recruitment [(181), (**Figure 4B**)]. IRESes can also directly recruit ribosomal subunits, therefore negating the requirement of initiation factors altogether (182-184).

In neuronal dendrites, several RNAs have been identified to utilize IRES elements for their translation (180). Specifically, *Arc, Map2, Dendrin, Neurogranin,* and *CaMKIIα* contain complex IRES elements in their 5' leader sequences that have the potential to initiate translation in dendrites. Interestingly, these RNAs have the ability to utilize both 5' cap-dependent and IRES-mediated

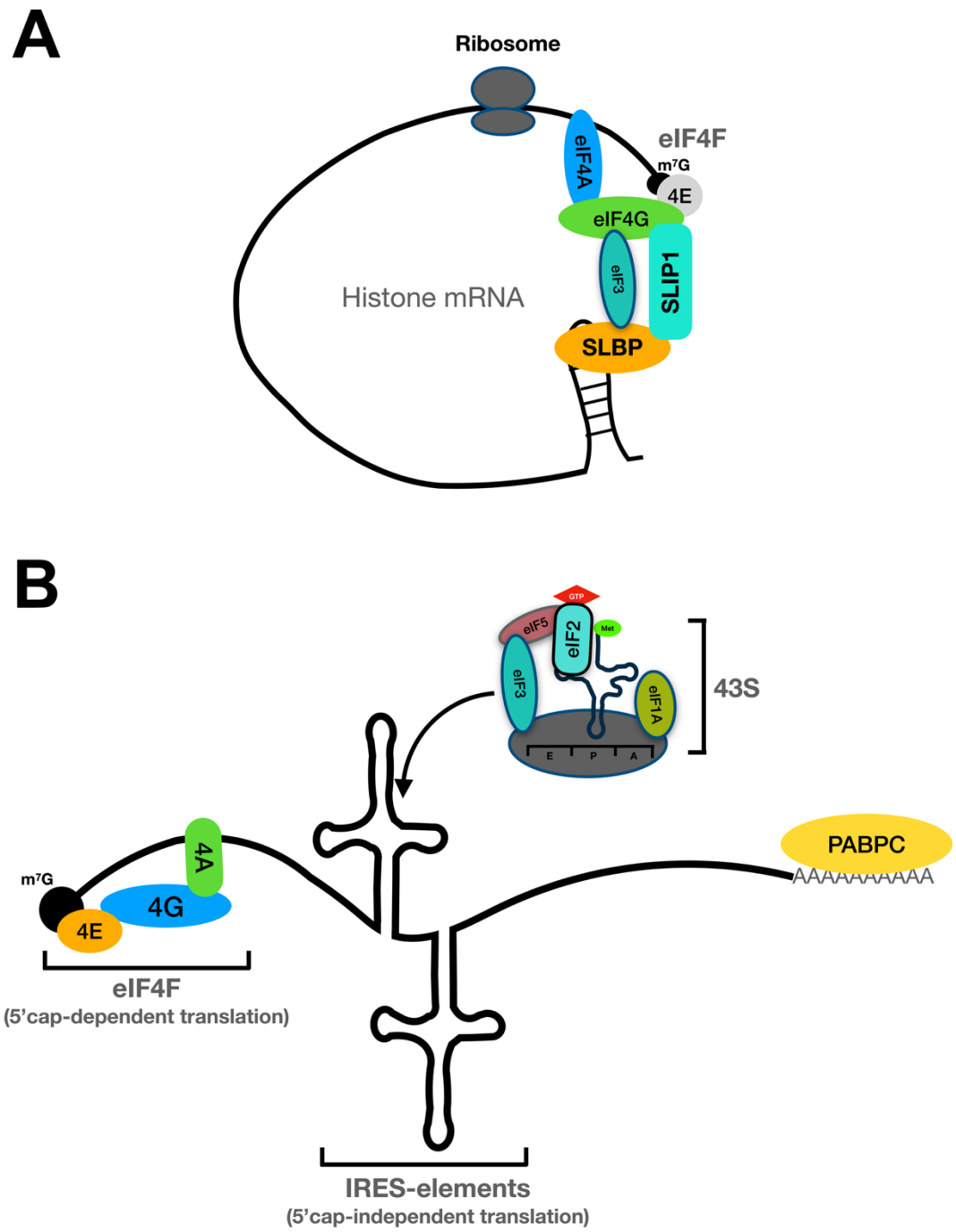

Figure 4. Replication-dependent histone mRNA and IRES-mediated translation. (A) Histone mRNAs contain a stem-loop structure in their 3' UTRs, and are not polyadenylated. A stem-loop binding protein (SLBP) binds this structure, and binds eIF3 and SLBP-interacting protein (SLIP1). SLIP1 interacts with eIF4G subunit of eIF4F complex to promote translation. (B) Shows an example of IRES-mediated translation initiation. eIF3 can directly interact with IRES-elements in several mRNAs to recruit 43S-preinitiation complex, therefore, bypassing the 5'cap dependency.

mechanisms for their translation (180). Therefore, mRNA sequence characteristics can play an important role in determining their translation fate.

non-AUG codon mediated translation initiation

The majority of cytoplasmic mRNAs that conform to the canonical mode of translation initiation utilize the AUG triplet codon in a Kozak context "(A/G)CCAUGG" (135-137), which is recognized by the initiator tRNA bound to the eIF2-GTP-Met-tRNAi ternary complex, which codes for the first methionine amino acid (132, 134). A pioneer work by Kozak utilizing 153 eukaryotic transcripts suggests that for an efficient utilization of AUG as a start codon, it must contain a purines "A/G" at -3 position and "G" at +4 position (135). Some mRNAs however, do not contain the AUG codon, and therefore, rely on other less-efficient codons like "GUG", "CUG", or "UUG" (185-188). Non-canonical start codons are rarely used in eukaryotes and are less efficient than AUG (188), even when present in favourable consensus Kozak sequence (136). The efficient utilization is these codons is dictated by important factors like, sequence context of their embedment, GC-rich leader sequence, and downstream secondary structures (189). The presence of a downstream secondary structure favours the usage of a non-canonical start codon like GUG (189), probably by slowing down the scanning 40S ribosomal subunit (189). A good example of a non-AUG codon-initiated translation event is NAT1 (or eIF4G2). *NAT1* mRNA translation is initiated from a GUG codon present in Kozak context, with a predicted hairpin structure downstream (190). The *c-Myc* oncogene is a unique example where the gene contains three exons and codes for two highly related proteins (191). These proteins differ only at the N-terminus, where the smaller form is initiated by a canonical AUG codon in exon-2, while the longer form is CUG-

initiated in exon-1 (192). The presence of an alternate translation initiation site is suggested to contribute to the oncogenic properties of *c-myc* (192).

In neurons, non-AUG translation is linked to neurological disorders associated with microsatellite expansion (193). Several genes accumulate abnormally long stretches of nucleotide repeats, which triggers repeat associated non-AUG (RAN) translation of their mRNAs. The translation of these mRNAs leads to the accumulation of homopolymeric protein products in the brain as toxic aggregates, which causes neuron cell death (193-196). For example, expansion of CAG-repeats in *Htt* and *Atxn1* genes, leads to the synthesis of poly-glutamine stretch containing proteins, which causes huntingtin disease and spinocerebellar ataxia, respectively (195, 197). Similarly, expansion of CGG-repeats in the 5' leader sequence of fragile X protein (FMRP) coding gene *Fmr1*, leads to neurodegeneration triggered by a loss of FMRP. A normal CGG-repeat length in *Fmr1* mRNA is around 30 repeats; however, the repeats can get expanded to more than 200, which leads to transcriptional silencing of *Fmr1* gene by a widespread cytosine methylation (198, 199). In contrast, if the CGG-repeats are in between 55-200, the gene transcription remains active, but codes for a toxic homopolymeric protein product (200). The expanded CGG-repeats lead to a non-AUG translation initiation upstream of the repeats, and leading to the synthesis of a poly-glycine stretch containing protein (201). The poly-glycine stretch containing protein accumulates in neuronal inclusions in the brain, thus leading to a neurodegenerative disorder Fragile X-associated tremor/ataxia syndrome (FXTAS) (200). Therefore, there is a plethora of nucleotide-repeat disorders in which RAN translation occurs and induces toxicity by various means: RNA gain of function and protein loss/or gain of function.

Mechanistically how a non-AUG codon is recognized by the Met-tRNAi can be explained by the fact that during the elongation phase codon-anticodon interactions take place in the A-site of a traversing ribosome; however, for the start codon recognition, the Met-tRNAi base pairs in the P-site, where the Watson-Crick base pairing is not enforced as strictly, therefore, allowing codons other than AUG to be used, albeit less efficiently (202, 203).

1.3. MAJOR mRNA DECAY MACHINERIES

Deadenylation

In the nucleus, most mRNAs acquire long poly(A) tails reaching a length of 200-250 nucleotides (21, 204, 205). However, mRNA poly(A) tails are subjected to extensive shortening in the cytoplasm, and most mRNAs maintain a median poly(A) tail length of 50-100 nucleotides (33-35). mRNA deadenylation is the first and often a rate-limiting step in mRNA decay, making it an important regulatory step in translation silencing [(206) (**Figure 5**)]. In the cytoplasm, mRNA deadenylation is mainly carried out by two deadenylation complexes, namely PAN2-PAN3 and CCR4-NOT (36, 37, 207, 208). However, CCR4-NOT serves as the predominant deadenylase complex in the cytoplasm, as its depletion causes major deadenylation defects (37, 207, 209, 210). mRNA deadenylation occurs in two steps where, PAN2-PAN3 trims excessively long poly(A) tails to a length of ~110-150 nucleotides, at which point CCR4-CNOT complex takes over and rapidly deadenylates the poly(A) tails (37, 211). Interestingly, the depletion of PAN2-PAN3 from cells, leads to an accumulation of very long poly(A) tails (>150 nucleotides), whereas depletion of a catalytic subunit of CCR4-NOT complex, leads to a strong accumulation of poly(A) tails of ~150 nucleotides in length (37).

PAN2-PAN3 deadenylase complex is conserved from yeast to mammals. PAN2-PAN3 is a heterotrimeric complex consisting of a PAN3 dimer and a PAN2 monomer (212, 213). The catalytic activity of PAN2-PAN3 complex resides in the exonuclease subunit PAN2 (214). The PAN2 subunit belongs to a DEDD class of hydrolytic 3' exonucleases (208, 215). The N-terminus of PAN3 subunit contains a PAM2-motif for PABPC-binding (213, 216), and a zinc finger domain for RNA binding (213). Therefore, PAN3 plays a role in the recruitment of PAN2-exonuclease to the mRNAs. The PAN3-PABPC interaction is stimulatory for PAN2-PAN3 deadenylase activity in yeast and humans (217, 218). A study analysed the cryoEM structure of PAN2-PAN3 in complex with poly(A_{90}) RNP and Pab1 (36). The structure shows that PAN2-PAN3 recognizes the oligomerization interface between two Pab1 molecules (2^{nd} and 3^{rd} Pab1 protomers) via PAN2-WD40 domain, and therefore, can sense the poly(A) tail length. Interestingly, deleting the WD40 domain of PAN2, severely impacts the deadenylase activity of the PAN2mutant-PAN3 complex (36). Notably, PAN3 directly interacts with GW182, therefore, the deadenylase complex can be recruited to miRNA (microRNA) targets (219). In mammalian CCR4-NOT complex, CNOT7/CNOT8 (or yeast CAF1) and CNOT6/CNOT6L (or yeast CCR4) subunits are the exonucleases. CNOT7/CNOT8 catalytic subunit is a member of DEDD class of exonucleases, which requires a divalent ion for its activity (220), whereas the CNOT6/CNOT6L catalytic subunit belongs to the exonuclease-endonuclease-phosphatase (EEP) family of proteins, which requires Mg^{2+} ions for its activity (221). A study demonstrated that CAF1/CNOT7 trims poly(A) sequence not bound by PABPC, while CCR4/CNOT6 deadenylates PABPC-protected poly(A) tails, thereby releasing PABPC (37). The CCR4-NOT complex also contains other non-catalytic subunits namely, CNOT1, CNOT2, CNOT3, CNOT4, CNOT9, CNOT10, and CNOT11 (222, 223). The largest among these, CNOT1, is a scaffold protein which contacts most other subunits (224). The

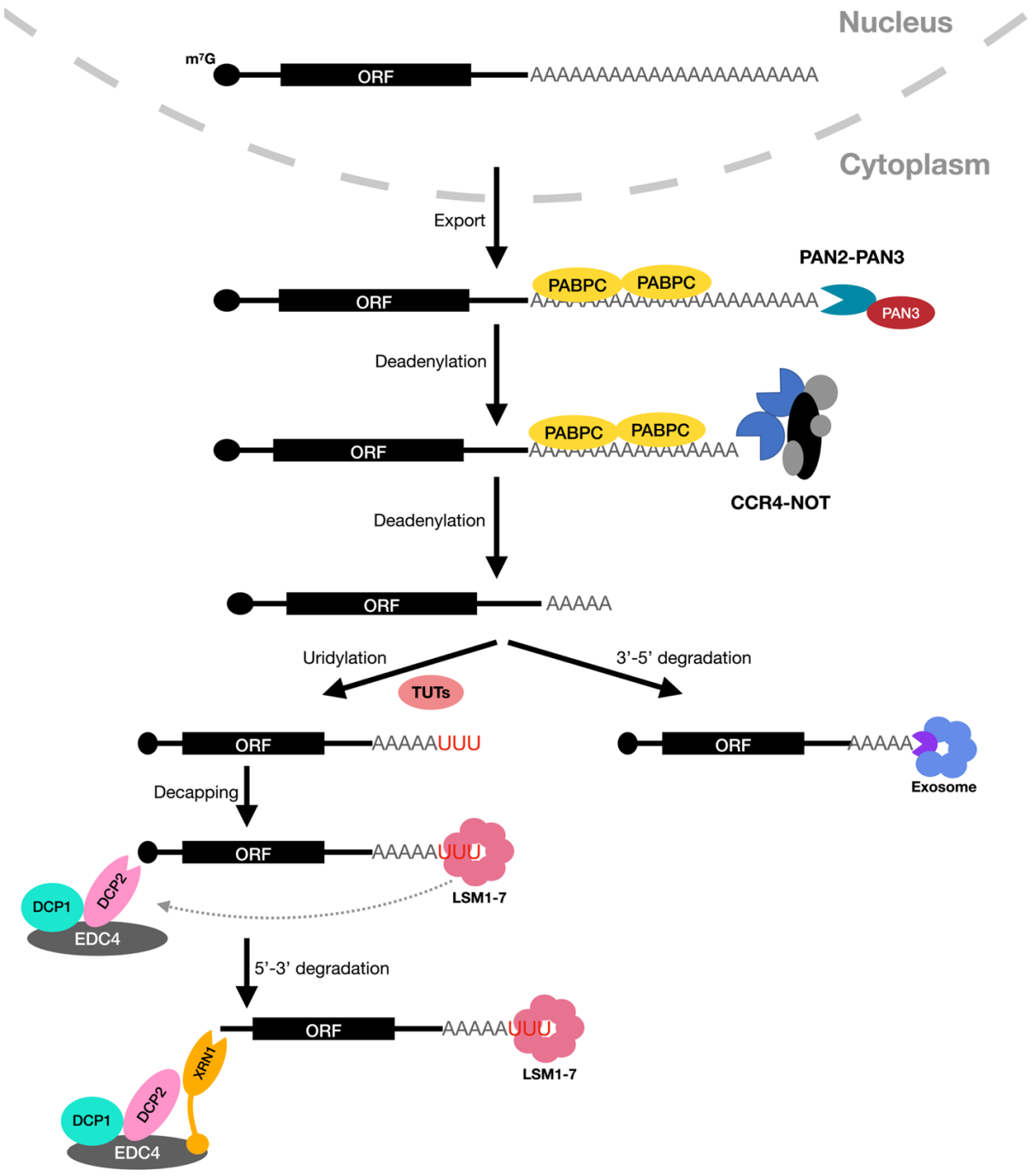

Figure 5. mRNA turnover pathways. A mature mRNA containing long poly(A) tails is exported into the cytoplasm where it is bound by PABPC. The mRNA poly(A) tails undergo trimming first by PAN2-PAN3 deadenylase complex and then by CCR4-NOT complex. mRNAs poly(A) tails are trimmed such that it can no longer accommodate a PABPC molecule (<25 adenosines). At this point, mRNA can be degraded by 3'-5' exonucleases of exosome complex. Alternatively, 3'end are uridylated by TUT4/TU7. Uridylated 3'ends are bound by LSM1-7 complex which assembles the mRNA decapping complex (DCP1-DCP2). Decapping is enhanced by decapping enhancers like EDC4. The decapped mRNAs are susceptible to degradation by 5'-3' exonuclease XRN1.

middle domain in CNOT1, named MIF4G (middle domain of eukaryotic initiation factor eIF4G), binds CAF1/CNOT7, which in turn binds CCR4/CNOT6 (225). CNOT1 depletion destabilizes the CCR4-NOT complex and leads to the degradation of most of its subunits, and cell death by apoptosis (226). CCR4-NOT complex also interacts with several other proteins, including TOB family, GW182 of miRISC mRNA silencing complex, RNA binding proteins like A-rich element (ARE) binding protein Tristetraprolin (TTP), and Pumilio response element (PRE; 'UGUANAUA', 'N' is any nucleotide) binding protein Pumilio (129, 227-232). TOB proteins contain a PABPC-interacting PAM2 motif, and interact with CCR4-NOT complex through CNOT1 scaffold (227, 233). Therefore, TOB can recruit the CCR4-NOT complex to PABPC-containing mRNAs. Moreover, TOB proteins also interact with CPEB and can recruit the CCR4-NOT complex to CPE-containing mRNAs (234, 235). The interaction between GW182-CNOT1 and GW182-CONT9 recruits CCR4-NOT complex to miRNA targets (219, 228, 236). CCR4-NOT complex directly interacts with RNA binding proteins TTP and Pumilio via CNOT1 and CNOT1-CNOT2-CNOT3 subunits, respectively (129, 229). These studies highlight a vast protein interaction network involved in CCR4-NOT complex recruitment to regulate deadenylation and ultimately the decay of distinct mRNA populations.

Decapping

Generally, mRNA deadenylation is followed by mRNA decapping (237). The 5' m^7G-cap structure protects the mRNA from decay by blocking the 5'-3' exonucleases (41). To initiate decapping, the deadenylated 3' end of an mRNA gets uridylated (oligoU-track), which stimulates decapping [(238), (**Figure 5**)]. Terminal uridylation was first observed in miRNA-directed cleavage products in plants as well as in mammalian cells (239). Interestingly, replication-dependent histone mRNAs

that lack poly(A) tails, also get uridylated (240). Terminal uridylyl transferase enzymes TUT4/TUT7 uridylate mRNAs that have short poly(A) tails (<25 nucleotides) (241), which can no longer accommodate a PABPC molecule (242, 243). Therefore, PABPC protects mRNAs from uridylation by TUT4/TUT7 (37, 241). After uridylation, a multi-subunit complex called "LSM1-7 complex" binds the terminal "oligoU" track of the mRNA (244-247). LSM1-7 complex contains seven "Sm-like" folds containing proteins that are related to small-nuclear RNA (snRNA) binding "Sm-complexes" (248). Sm folds are domains with high affinity for U-rich sequences (249). Next, the LSM1-7 complex recruits the DCP1-DCP2 decapping enzyme via its interaction with Pat1 (250-253). DCP2 catalytic subunit belongs to the Nudix-family of pyrophosphatases, which hydrolyzes the removal of 5' m^7G-cap, by releasing a m^7GDP and leaving the terminal 5' monophosphate end vulnerable to decay by 5'-3' exoribonuclease, XRN1 (39-41, 254). Interestingly, RNA polymerase I and III transcripts that lack 5' m^7G-cap, usually maintain 5' tri- or diphosphate, which would prevent their decay by XRN1 (255, 256). While in yeast, DCP1 and DCP2 can interact directly, in metazoans, DCP2 requires a scaffold protein called enhancer of decapping (EDC4) to enhance its enzymatic activity (38). EDC4 binds DCP1, DCP2, and XRN1, and plays an important role in the assembly of decapping complex (38). Alternatively, mRNAs are also degraded from 3'-5' direction by exonucleolytic RNA exosome machinery (257).

miRNA-mediated mRNA decay

microRNAs (miRNAs) are highly abundant small non-coding RNAs (~22 nucleotides) encoded by most eukaryotic genomes (258). miRNAs post-transcriptionally regulate the gene expression by mainly repressing the protein synthesis (259-261). miRNAs base-pair with the target site in partial complementarity (259, 260); however, require perfect Watson-crick base pairing centered

on nucleotides numbered 2 to 8 in the 5' region of miRNAs called "miRNA seed" sequence (262, 263). Several mRNAs harbour miRNA-target sites in their 3' UTRs and occasionally the CDS region (258, 264). miRNAs induce gene silencing via formation of a miRNA-induced silencing complex (miRISC). The miRISC consists of a miRNA as a core component, which is bound by Argonaute protein and glycine (G)-tryptophan (W) repeats containing 182 kDa protein GW182 [(258), (**Figure 6A**)]. The miRNA-Ago2 complex recognizes the target mRNA by base pairing, and Ago2 then recruits GW182 via direct interactions to form miRISC (265). One of the first studies in miRNA target recognition was done in *C. elegans* (266, 267), where a small RNA encoded by *lin-4* gene was found to be complementary to *lin-14* mRNA (267). It was found that *lin-4* coded small RNA negatively regulates the LIN-14 protein levels. Similarly, *let-7* RNA was found to have complementarity to the 3' UTRs of several heterochronic genes l*in-14, lin-28, lin-41, lin-42*, and *daf-12* (268). miRISC can destabilize the mRNA by triggering its deadenylation by directly recruiting the CCR4-NOT complex via GW182-CNOT1 and GW182-CNOT9 interactions (219, 228, 236). It can also recruit PAN2-PAN3 deadenylase complex via GW182-PAN3 interactions (219). Additionally, the GW182 protein can interact with PABPC as it contain a PAM2-motif in its C-terminus (269). In *Drosophila* and human cell lines, the GW182-PABPC interaction is demonstrated to be a requirement in miRNA mediated translation repression and mRNA deadenylation (269, 270).

Nonsense mediated decay (NMD)

The NMD pathway was first described as a surveillance pathway in yeast (271), and thereafter in other eukaryotes. In humans, it was first described for *β-globulin* mRNA expression in β-o-thalassemia. They found that when *β-globulin* mRNA was carrying nonsense mutations, its levels

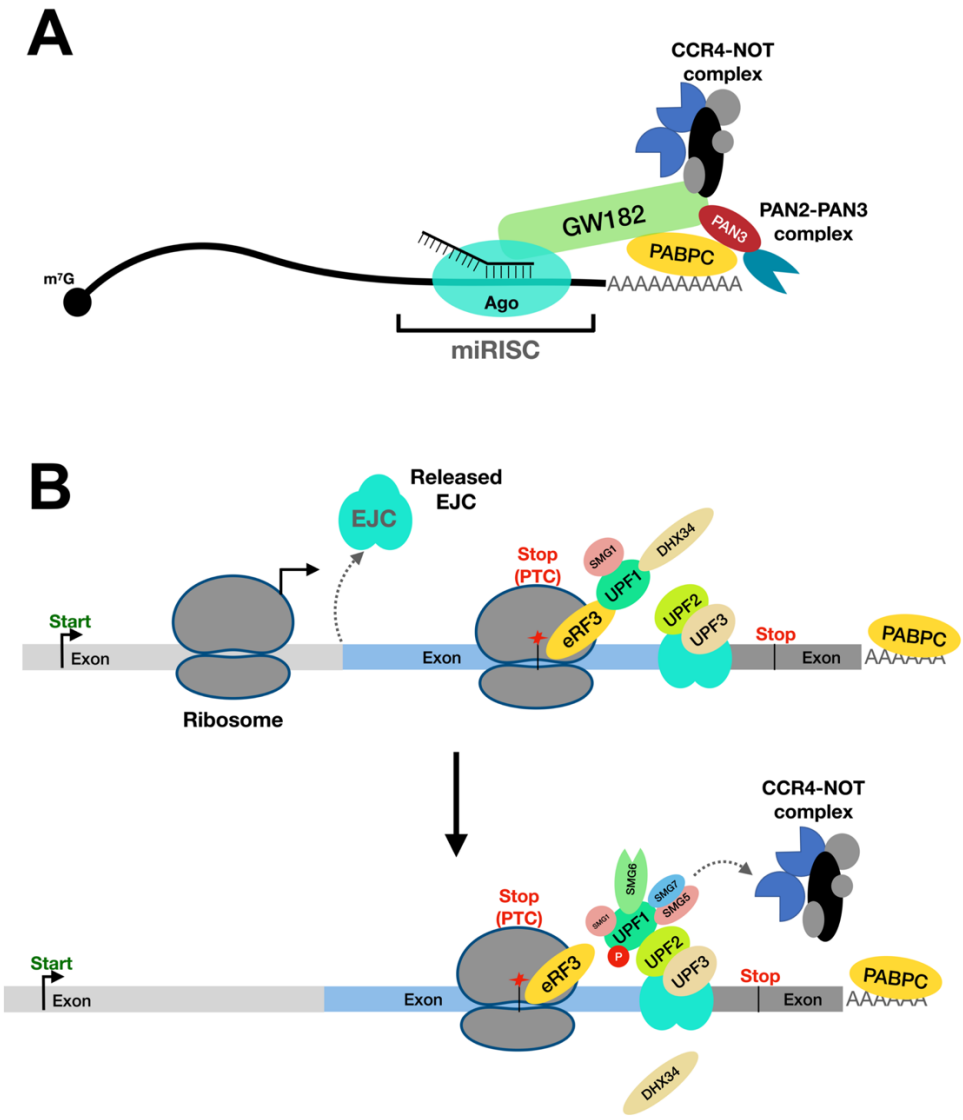

Figure 6. miRNA-mediated decay and NMD pathways. (A) Shows an mRNA containing microRNA (miRNA) targeting site in its 3'UTR. A miRNA-Argonaute (Ago) complex base-pairs with the target site, and recruits GW182 protein to form "miRNA induced silencing complex" (miRISC). The GW182 protein interacts with PABPC and can recruit deadenylase complexes PAN2-PAN3 and CCR4-NOT to decay mRNAs. (B) Shows a normal scenario where a ribosome engaged in translation elongation causing the release of an exon-exon junction complex (EJC) upstream of the stop-codon. However, interruption of the ORF by a premature-termination codon (PTC), leads to the assembly of NMD factors (UPF1, UPF2, UPF3), on the downstream EJC and terminating ribosome. This recruits endonuclease SMG6 and CCR4-NOT complex to decay abnormal transcripts.

were rapidly reduced by degradation (272). The responsibility of NMD pathway is to safeguard against the abnormal transcriptional products which could generate toxic proteins. The transcription machinery can occasionally make errors during alternative splicing or by randomly inserting mutations, and as a result, produce mRNAs harbouring premature-termination codons (PTC) (273). Intriguingly, it is estimated that NMD targets alternative splicing isoforms of as much as 30% of the expressed genes (274-276). This reflects the probability of errors committed during transcription and the importance of NMD pathway in cellular quality control. In humans, the premature termination of translation at a PTC leads to the assembly of a multiprotein complex, which carries out the degradation of an mRNA (276). The core NMD factor involved in orchestrating the degradation process is an ATP-dependent RNA-helicase, up frameshift 1 (UPF1) (277, 278). The ATP-dependent helicase activity of UPF1 is essential for the NMD (279). UPF1 forms the UPF1-3 complex with two other proteins namely, UPF2 and UPF3 (276). UPF1 interacts with eRF3 on terminating ribosomes when a PTC is encountered, which prevents the canonical eRF3-PABPC interaction required during normal translation termination [(280, 281), (**Figure 6B**)]. NMD activation also depends on the presence of one or more exon junction complexes (EJC), which are deposited ~20-25 nucleotides upstream of the exon-exon junctions after introns are spliced out (19). The presence of a PTC approximately 30 or more nucleotides upstream of an EJC is suggested to trigger NMD activation (282). While traditionally NMD was suggested to target aberrant mRNAs harbouring PTCs during the pioneer round of translation (30), many studies have now suggested that NMD can also destabilize mRNAs during canonical translation (283). Importantly, NMD can target specific mRNAs lacking PTCs, but contain long 3'UTRs and may harbour an EJC downstream of the physiological stop codon(284, 285).

For example, *Arc* mRNA contains two conserved introns in its long 3'UTR and is rapidly regulated by EJC-dependent NMD (286).

When a ribosome encounter a PTC, UPF2 and UPF3 assemble on the downstream EJC (287, 288), UPF1 binds eRF1-eRF3 complex on the terminating ribosome (280), and simultaneously binds the ATP-dependent RNA helicase DHX34 and serine/threonine protein kinase SMG1 (289). SMG1 phosphorylates UPF1, which leads to its dissociation from eRF3 and DHX34, and association with EJC-UPF2-UPF3 complex to form the decay inducing complex (289, 290). Phosphorylated UPF1 binds other NMD factors like SMG5, SMG7, and SMG6 (276). SMG5-SMG7 dimerize and recruit mRNA decay complex CCR4-NOT (291), while endoribonuclease SMG6 carries out endonucleolytic cleavage of the mRNA (292). Other than the mRNAs harbouring PTC in the coding region, mRNAs with extended 3'UTRs are also targets of NMD (293). NMD plays a critical role in embryonic development in animals. For example, in zebra fish and mice, knocking down NMD factors like Upf1, Upf2, Smg1, Smg5, and Smg6 is embryonic lethal (274, 294-298). Moreover, in humans, NMD defects are linked to neurodevelopmental disorders (299).

1.4. CYTOPLASMIC POLY(A) BINDING PROTEINS

Expanded repertory of cytoplasmic poly(A) binding proteins

Cytoplasmic PABPs (PABPCs) are evolutionarily well conserved from yeast to humans. While yeast and *Drosophila* genomes encode one PABP each: Pab1 and pAbp, respectively (300-302), *C. elegans* contain two PABP genes namely, Pab-1 and Pab-2 (303). In higher order metazoans, like mammals, several cytoplasmic PABPs have been identified, which include (i) a well characterized and ubiquitously expressed PABPC called PABPC1 (304), (ii) testis-specific PABP

(tPABP) expressed in round spermatids (305), (iii) inducible PABP (iPABP) expressed in activated T-cells (306), (iv) ovary-specific PABPC5 (307), and (v) embryonic PABP (ePABP) expressed in oocytes and early embryos [(149), (**Figure 7**)].

Mammalian PABPCs

PABPC1

PABPC1 is an extensively studied gene that is evolutionarily well conserved and is ubiquitously expressed among various mammalian tissues (304). PABPC1 contains four RNA Recognition Motifs (RRMs), a proline-rich linker domain, and a C-terminal 'MLLE' domain (302). RRMs 1 and 2 preferably bind poly(A) sequences, while RRMs 3 and 4 bind both poly(A) and A/U rich sequences equally well (243, 308). A single PABPC1 covers ~23-27 adenosines (242, 243), and multiple PABPC1 molecules can oligomerize on poly(A) sequences via interactions between the linker domain of one PABPC1 and RRM2 of an adjacent molecule (36, 309-311). PABPC1 utilizes RRM2 to directly interact with eIF4G (143), an interaction that stimulates mRNA translation *in vitro* and in *Xenopus* oocytes (142, 148), contexts where mRNA poly(A) tail length correlates with translational efficiency (142, 148, 312). Notwithstanding that PABPC1 stimulates mRNA translation stimulation in certain systems (148, 160), recent reports have shown that PABPC1 plays a negligible role in enhancing the translation efficiency of the transcriptome in post-embryonic mammalian cell lines (128, 160).

PABPC1 uses its C-terminal "MLLE" domain to directly bind PABPC-interacting proteins, including PAIP1, PAIP2, and eRF3 (313-317). Interestingly, PAIP2 inhibits mRNA translation by binding to PABPC1 and displacing it from mRNA poly(A) tails. Moreover, PABPC1-PAIP2

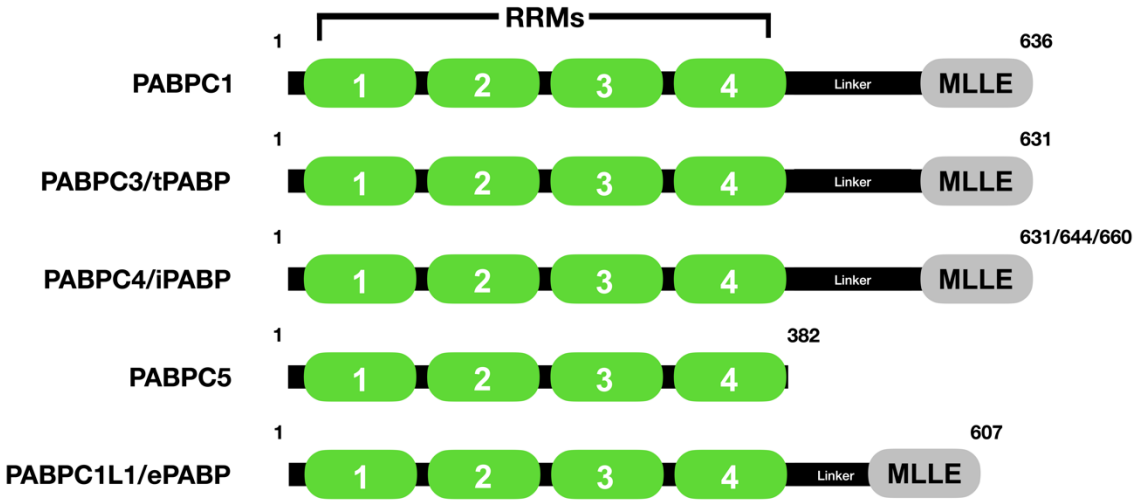

Figure 7. Mammalian PABPC family. Several mammalian PABPC family members are shown. Like PABPC1, tPABP, iPABP, and ePABP contain a proline-rich linker region and MLLE-domain. All PABPCs, including PABPC5 contain RNA-recognition motifs (RRMs).

interaction protects PAIP2 from E3 ubiquitin ligase-mediated ubiquitination and subsequent degradation (313, 318). The PABPC MLLE domain also interacts with several other proteins that play important roles in regulating mRNA decay. These include the PAN2-PAN3 deadenylase complex, which trims excessively long poly(A) tails (36), as well as proteins that recruit the CCR4-NOT deadenylase complex (i.e., Tob proteins and the miRNA-associated protein GW182/TNRC6). PABPC has been shown to promote poly(A) tail trimming by CCR4-NOT complex, but prevents premature 3' terminal uridylation (37), and blocks deadenylation-independent decay of transcripts coding for proteins with constitutive functions (128).

Testis-specific PABPC (tPABP) or PABPC3

PABPC3 mRNA expression is first detected when germ cells (spermatogonia) enter meiosis, with its expression peaking in early postmeiotic stages in round spermatids (319, 320). The expression further decreases significantly at the end of spermatogenesis (319, 320). In mammalian testis, PABPC3 binds mRNAs in both translated and non-translated states (319). This suggests a role of PABPC3 in both mRNA storage and translational regulation during development (319). The stabilization of mRNA during spermatogenesis is very crucial where transcription is mainly active during the early stages of meiosis (321-323). Therefore, the mRNAs are stored as RNPs and are translated in later stages (319, 324). PABPC3 protein expression peaks during this time in round spermatids (305), and therefore, may play a role in storing the mRNAs as RNPs and regulating their translation (305, 319, 325). Similar to PABPC1, PABPC3 contains four RRMs and a C-terminal MLLE-domain (305, 326). Human PABPC3 shares ~92% sequence identity with PABPC1, and binds poly(A) sequences with affinity similar to PABPC1 (305, 320).

Inducible PABP (iPABP) or PABPC4

PABPC4 expression was first described in activated T-cells, where its expression is rapidly upregulated after T-cell activation, with a very low expression in resting human T cells (306). This contrasts PABPC1, which is expressed in both resting and activated T-cells at comparative levels (306). PABPC4 has been suggested to play an important role in erythroid differentiation by stabilizing a subset of mRNAs that contain AU-rich elements in their 3' UTRs and short poly(A) tails (327). PABPC4 depletion in mouse erythroleukemia cells alters the ratio of long versus short poly(A) tails of PABPC4-target mRNAs, for example, *α-globin and Samd9l* mRNA isoforms containing short poly(A) tails (<30 adenosines) are selectively lost after PABPC4 depletion, while the long poly(A) tail containing mRNA isoforms remain unaffected (327). Additionally, the depletion of PABPC4 from an erythroblast cell line inhibits erythroid maturation, thereby indicating a role of PABPC4 in this developmental context (327). Moreover, multiple PABPCs can cooperate to support their function. For example, in HeLa cells, although PABPC4 is relatively less abundant than PABPC1 (162, 163, 328), it can still compensate for the loss of PABPC1 to support cell viability (128).

PABPC4 mRNA levels in skeletal muscles are highly upregulated compared to other tissues, where PABPC1 levels are low (306). This suggests a compensatory role of PABPC4 in skeletal muscles, where it may contribute to maintain a repertoire of PABPC. However, at protein level, PABPC4 levels are downregulated after differentiation of mouse C2C12 cells (329), similar to PABPC1 (304). In this context, PABPC4 has been shown to directly contact nuclear receptor corepressor 1 (NCoR1) (329). In mice, muscle-specific deletion of NCoR1 improves glucose and fatty acid metabolism (330). Downregulation of PABPC4 after C2C12 differentiation leads to NCoR1

ubiquitination and degradation, and artificially maintaining PABPC4 levels lead to a stabilization of NCoR1 levels (329). Therefore, downregulation of PABPC4 after C2C12 differentiation suggests an adaptive response to maintain healthy mitochondrial function in skeletal muscles by promoting the degradation of NCoR1 (329). Similar to PABPC1, PABPC4 contains four RRMs and a C-terminal MLLE-domain (306, 326). Human PABPC4 shares ~79% sequence identity with PABPC1 and binds both poly(A) and poly(U) sequences, and its affinity to poly(A) sequences is similar to PABPC1 (306).

PABPC5

Pabpc5 is an X-linked gene coding for a protein with four RRMs, but unlike other PABPCs lacks the linker region and C-term MLLE-domain entirely (307, 326). *Pabpc5* mRNA is expressed in fetal brain and several adult tissues (307). The location of *Pabpc5* on X-chromosome is in proximity to translocation breakpoint defects linked with premature ovarian failures, therefore, making *Pabpc5* a potential gene for this phenotype (307). Human PABPC5 shares ~64% identity with both PABPC1 and PABPC4.

ePABP or PABPC1L1

ePABP was first identified in *Xenopus* oocytes as an ARE-elements binding protein (150). *Xenopus* ePABP shares 72% identity with both frog and human PABPC1 (150). ePABP is the predominant PABPC expressed in oocytes and early embryos (150). ePABP protein can be detected in stage I-VI oocytes, mature oocytes, and throughout the early embryonic development stages, but is absent in mature tissues (150, 331). In contrast, PABPC1 is barely detected in oocytes, but its expression is turned on after the onset of zygotic transcription (149, 150, 155, 332, 333). In oocytes, poly(A) tail length is an important determinant of translation efficiency, where mRNAs with longer poly(A)

tails are efficiently translated (102, 110, 334). ePABP has been demonstrated to protect poly(A) tails from deadenylation, similar to PABPC1 (150). ePABP stimulates translation of reporter mRNAs injected into oocytes and associates with endogenous mRNAs in polysomes (331). ePABP was initially identified as *Xenopus* specific protein that is not conserved in other vertebrates (150); however, now it has been identified in various mammals and is present in the genomes of other vertebrates (149, 331, 335, 336). ePABP contains four RNA recognition motifs and a C-terminal MLLE domain (150, 331), and maintains interactions with PABPC1-interacting proteins like eRF3, eIF4G, and PAIP1 (331). Therefore, ePABP is suggested to play an important role in regulating mRNA translation and stability during early development.

1.5. NEUROGENESIS AND NEURON MATURATION

Neurons are arguably the most complex of all the cells in vertebrates, in both structural and functional dimensions. In 1873, an Italian pathologist Camillo Golgi made a landmark contribution to the field of neuroanatomy. He invented a method called silver staining of the brain, which helped to visualize the nerve cells for the first time in great details (337). However, it was Spanish anatomist Santiago Ramón y Cajal who, by using Golgi's method of staining, gave the idea that the brain is composed of individual nerve cells, which were later named neurons (338-340).

Neurogenesis

All neurons in the mammalian brain are derived from neural epithelium cells (or neural stem cells) during brain development (341). Neural stem cells have the quality of self-renewal and multipotency i.e., they can self-proliferate as well as give rise to multiple types of differentiated cells like neurons, astrocytes, and oligodendrocytes. During early brain development, neural stem

cells undergo symmetric cell divisions to self-renew and proliferate [(342), (**Figure 8**)], but after the onset of neurogenesis switch to asymmetric cell divisions (343). Through asymmetric cell divisions, neural stem cells can generate a daughter stem cell and a fate-restricted progenitor-like radial glial cell (RG), or directly a neuron (343, 344). As neurogenesis progresses, neural stem cells are essentially replaced by RG cells (345, 346). During neurogenesis, RG cells undergo asymmetric cell divisions to generate a daughter RG cell and a terminally differentiated neuron cell (344, 347, 348). RG cells display a characteristic bipolar morphology with the nucleus in the ventricular/subventricular zone and a long radial fiber extending to the pial surface (345). This morphology of RG cells helps to support neuronal migration. Neurons produced earlier during neurogenesis migrate along the radial fibers of RG cells to form the subpial preplate zone (345). Subsequent waves of neurons produced in the ventricular zone form cortical plate by migrating into the preplate and splitting it into outer superficial molecular cell layer (or layer I), which consists of Cajal-Retzius neurons, and a deep subplate. Neurons produced successively migrate through the subplate until reaching below the layer I, and therefore, form different cortical layers in an inside-out fashion (VI, V, IV, III, II, I) (349, 350). The RG cells not only generate the neurons, but are also the progenitor cells for astrocytes and oligodendrocytes during gliogenesis (345, 351). In mice, neurogenesis begins around embryonic day E9-E10, peaks at E15, and completes around E16-18.5 (352, 353). On the other hand, gliogenesis begins later during embryonic development around E15 and continues into first few postnatal weeks (354).

The idea that neurogenesis ceases to occur in postnatal brain is challenged by numerous studies. A study provided the first evidence of adult neurogenesis forming dentate granule cells in the dentate gyrus region of rat hippocampus (355, 356). Moreover, multipotent neural stem cells have been

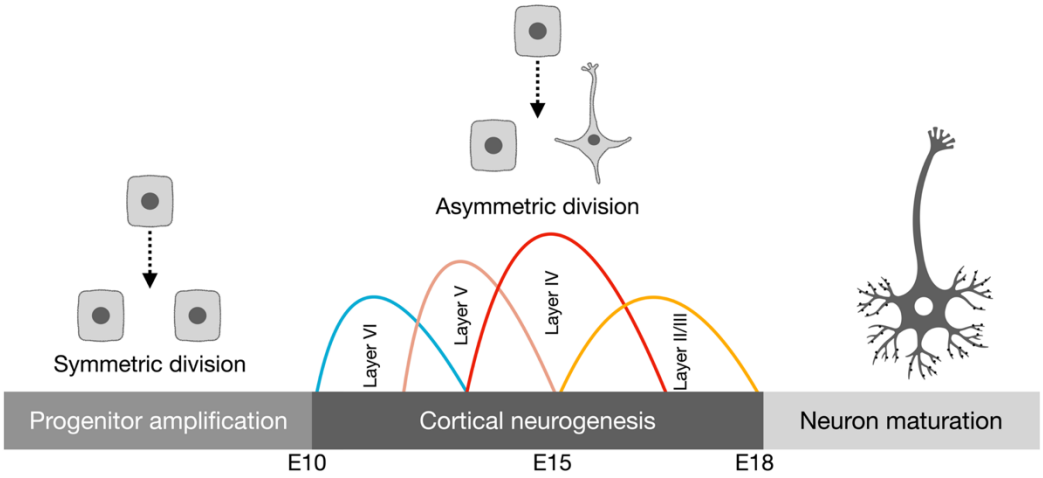

Figure 8. Cortical neurogenesis in mice. Prior to neurogenesis, the neural progenitors divide by symmetric divisions to proliferate. However, after the onset of neurogenesis (roughly embryonic day 10, E10), switch to asymmetric divisions to form one neuron cell and one progenitor cell. The brain cortex is generated in inside-out fashion where newly generated neurons migrate outward to form outer layers of the cortex (VI, V, IV, III, II). Neurogenesis peaks at E15 and completes around E18. After birth, neurons undergo extensive dendritogenesis and synaptogenesis as a part of the neuron maturation process.

derived from the striatum of adult mouse brain (357, 358). Although neurogenesis has been documented in adult mammalian brain, it is restricted to mostly two neurogenic regions namely, dentate gyrus and subventricular zone of the lateral ventricles (359, 360). With the application of BrdU as a lineage tracker, neurogenesis is also suggested to occur in adult human hippocampus (361). Therefore, adult mammalian brain retains the ability to produce new neurons, albeit in a limited capacity.

Neuron Maturation

An overview of Neuronal structure and function

A mature neuron can be divided into these sub-compartments: a cell body that contains a small volume of cytoplasm and a nucleus, an axon that contains axoplasm and displays a tree-like branching at the tip, and numerous projections emanating from the cell body with branched-patterns called dendrites (337, 339, 362). In a neuron, an impulse (or signal) travels along the length of its axon and gets relayed onto the dendrites of neighbouring neurons through a specialized structure called synapse (363-369). Therefore, neurons receive signal through the dendrites and transmit it to other cells via axon terminals. Electron microscope imaging and biochemical analyses of isolated synaptic terminals reveal that axon terminals are crowded with vesicles (363, 370, 371). These vesicles contain neurotransmitters, which are released at the synapse by exocytosis through the axonal membrane (372-375). The released neurotransmitter binds to its receptors on dendritic terminals and triggers a downstream signaling cascade, leading to the local protein synthesis from available mRNA pool (166, 376-378), thereby enabling rapid changes in synaptic connectivity.

Synaptogenesis

The cerebral cortex of mammalian brain requires a very precise neuronal circuitry for its proper function. To form this complex wiring in the brain after neurogenesis, neurons establish contacts with each other by extending their axonal and dendritic terminals. This extension is guided by a structure at the tip of the developing neurites called growth cone (379, 380). In year 1890, a pioneer work by Cajal in three days old chick embryos, led to the discovery of axonal growth cones. Cajal made an observation that the axonal tip of a commissural neuron attained a triangular shape "cone-like lump with a peripheral base" (362). Growth cone receives chemical cues from other cells in its extracellular vicinity for axonal or dendritic guidance (381), and ultimately, its precise integration with a synaptic counterpart to form a specialized structure called synapse. The growth cone migration during neurite extension is dependent on microtubule cytoskeletal rearrangements and several signaling molecules, including Ca^{2+}, small GTPases, and mitogen activated protein kinases (MAPKs) link external signaling cues to microtubule dynamic assembly and stability (382). A synapse represents the linkage between presynaptic and postsynaptic terminals of neurons. Physiologically, the presynaptic terminal releases a chemical signal messenger called a neurotransmitter (like glutamate) into the space between the two synaptic terminals called synaptic cleft (374), the neurotransmitter then binds to a receptor on the post-synaptic terminal (like NMDA receptor), and triggers a signaling cascade downstream, thus providing the basis of neuron communication. Generally, two types of synaptic transmission modalities can be described in the mammalian brain, namely, chemical synapse and electrical synapse (383-385). While chemical synapses use neurotransmitters for communication, electrical synapses transmit signal by transporting charged ions and/or messenger proteins via gap junctions (386, 387). These gap junctions are established between the pre- and post-synaptic terminals with the help of

transmembrane proteins called connexin proteins (387). In contrast to chemical synapses, an important quality of electrical synapses is that the flow of signal is bidirectional i.e., messenger molecules can flow back and forth across gap junctions. Electrical synapse was initially thought to be a precursor synapse in development to the later forming chemical synapse, which is the most abundant synapse-type in adult brain (388, 389). However, growing evidence suggests that both type of synapses are essential for synaptic transmission in adult brain and act synergistically. For example, an electron microscope connectome of rabbit retina reveals that as much as 20% of the total synapses in retina are electrical in nature (390-392).

In general, axons form the presynaptic terminal, while the postsynaptic terminal is formed by the dendritic spines. Although action potential in a neuron travels from the dendritic terminal to the axonal terminal, in 1952 Cajal made observations that several neuron types in the mammalian brain either lack dendrites or an axon, or the axon emerges from a dendrite. For example, Dorsal Root Ganglion (DRG) neurons have a unipolar morphology and contain only an axon (393, 394), while dopaminergic neurons in the substantia nigra pars compacta have an axon which is emanating from the dendrites (394). Moreover, granule cells in the olfactory bulb lack axons, release neurotransmitters from their dendrites, and form dendrodendritic synapses with mitral cells (395). These exceptional examples highlight the complexity of neural circuitry for proper communication.

Synaptic pruning and programmed cell death

During early postnatal days of brain development, neurons establish excessive number of synapses (396). In humans, synaptic density approaches its maximum during early childhood, and shows a

decline during late childhood and adolescent years before stabilizing at sexual maturity (396-400). The mitochondrial caspase-3-protease (CASP3) is localized in dendrites and its activity is linked to synaptic pruning (401). Activation of CASP3 induces long-term depression (LTD), and AMPA receptor endocytosis, thus reducing the synaptic strength and leading to the loss of synapse (401, 402). In line with this, mice lacking CASP3 display defects in spine pruning (401). CASP2 activation also displays similar phenotypes in mice (403). A defect in synaptic pruning can lead to neurodevelopmental disorders. Some studies have found that adolescent with autism spectrum disorder (ASD) have excessive number of synapses due to reduced developmental spine pruning, which is correlated to overactive mTOR and impaired autophagy (404). In contrast, brains of individuals with schizophrenia have excessive synaptic pruning (405). Embryonic brains are also reported to generate neurons in excess which are eliminated during postnatal brain development. Neurons that do not establish relevant connections are eliminated by apoptosis (406-408), a program mediated by key apoptotic protein families, including Bcl-2. The Bcl-2 family contains anti-apoptotic as well as pro-apoptotic proteins. For example, Bcl-2 and Bcl-x_L are both anti-apoptotic proteins, which dimerize and inhibit proapoptotic members like Bax (409, 410). Knocking out *Bax* in mice leads to an increase in neuron numbers in superior cervical ganglia and facial nuclei (411). Therefore, apoptotic programs are active during brain development and act by eliminating excess neurons and refining synaptic connections.

1.6. LOCAL TRANSLATION FOR SYNAPTIC PLASTICITY

In adult mammalian brain, new synaptic connections are constantly formed between neurons by cytoskeletal rearrangements. The cytoskeletal reorganization is necessary during nervous system development and in adulthood to ensure proper neuronal structure. The dynamic changes in

cytoskeleton provide neurons with the flexibility to establish and consolidate new synaptic connections quickly during the process of learning and memory formation. Neurons are highly specialized cells that can have neurites growing up to one meter in length. Therefore, to function properly, neurons rely heavily on intricate molecular networks of mRNA transport and local translation. Recent advancements in high-throughput sequencing have reliably identified thousands of mRNAs and translation machinery components enriched in neurites. Several studies over the years have now shown that mRNAs are quickly translated in neurites upon stimulation (412, 413). Many mRNAs are stored in liquid-liquid phase separated structures called 'RNA granules'. The RNA granules are transported by molecular motor proteins into the neurites and release mRNAs for translation after stimulation. Understandably, these mechanisms are necessary to give neurons the ability to produce proteins, including the ones required for structural rearrangements directly within the neurites, without having to constantly rely on the cell body. This ability of the brain to constantly rearrange neural networks has earned it the title 'plastic organ'.

RNA transport in Neurons

mRNA availability in neurites is a prerequisite for local mRNA translation and synaptic plasticity. Therefore, mRNAs are actively transported to dendrites and axons in a translationally repressed state (414-417). RNA cargo transport is facilitated by molecular motors proteins like kinesin and dynein, which ensure the precise delivery of mRNAs [(418), (**Figure 9**)]. The cytoskeleton plays a vital role in mRNA trafficking by serving as a track for molecular motor proteins (418). The role of *cis*-acting elements and *trans*-acting factors in RNA transport, the role of cytoskeletal and motor

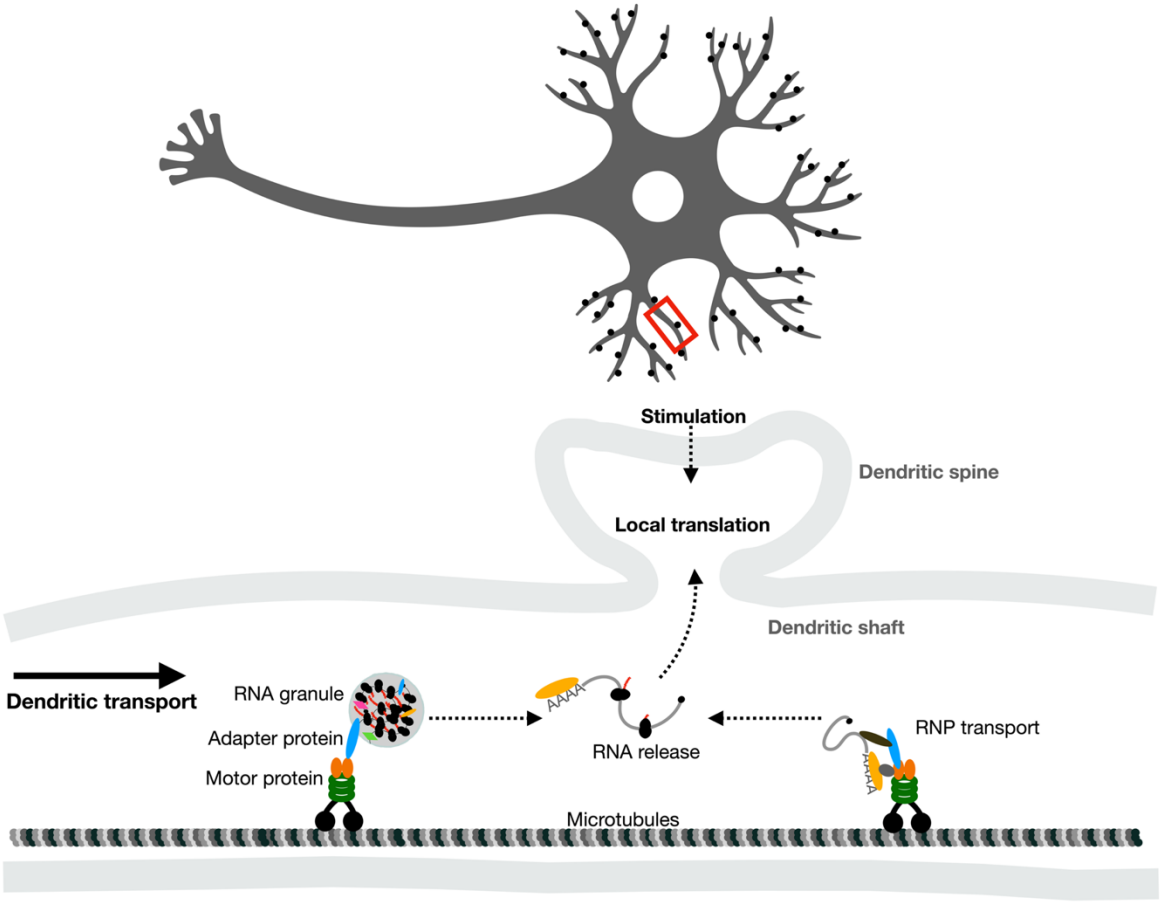

Figure 9. mRNA transport in neurons. Shows a depiction of a section of neuronal dendrite. RNAs are packaged into RNA transport granules for dendritic transport. RNA transport granules contain several RNA binding proteins and both 40S and 60S ribosomal subunits indicating "elongation-stalled" ribosomes. The RNA granules are docked onto the motor proteins (kinesin and dynein) via adapter proteins (RNA binding proteins, or other intermediate proteins), and are transported along the length of microtubules. Alternatively, several RNAs can be transported as RNPs (not containing ribosomes) to distal dendritic sites. After stimulation, mRNAs are released from the granules and RNPs for their local translation to support synaptic plasticity.

proteins in facilitating this transport, and packaging of mRNAs into RNA transport granules are discussed in detail below.

cis- and *trans*-acting elements in RNA transport

Zip codes

Recent advances in RNA deep-sequencing methods, have identified a myriad of RNA species localized in the neuronal processes (97, 378, 419-422). Various *cis*-acting elements within the RNAs and t*rans*-acting factors like RNA-binding proteins are involved in transporting RNAs in neurons. For example, several mRNAs contain localization elements (or 'zip codes') in their long 3' UTRs for dendritic transport (93, 423-429). A well-studied example is *β-actin* mRNA that contains a 54-nucleotide zipcode in its 3' UTR, which is bound by the zipcode-binding protein (ZBP1) that plays a role in its transport (423, 424, 430). Similarly, ZBP1 is also involved in the dendritic transport of *Spinophilin* mRNA, where ZBP1 knockout mice have reduced dendritic localization of *Spinophilin* mRNA (431). Interestingly, ZBP1-*β-actin* RNP colocalizes with huntingtin, and microtubule motor proteins, kinesin (KIF5A) and dynein in rodent neurons, thus highlighting the role of molecular motors in transporting ZBP1-associated RNA cargos (432).

G-quadruplex

Several mRNAs contain a secondary structure called 'G-quadruplex' in their UTRs, or although less common in coding regions (93). The consensus sequence of a G-quadruplex is (DWGG-N_{0-2})4, where D means any nucleotide except 'C' and 'W' stand for either A or U (433, 434). A significant number of well-defined dendritic mRNAs contain this structure, among these are *PSD-95, CaMKIIα, MAP1b, APP,* and *PP2Ac* (93, 433, 435-439). An important *trans*-acting

factor fragile X protein (FMRP), binds the G-quadruplex structure on these mRNAs through FMRP-RGG box (433, 440), and regulates their stability, translation, and transport (436, 437, 439, 441). Interestingly, in FMR1-kockout CAD cells, mRNAs that contain G-quadruplexes in their 3' UTRs are less enriched in neurites (441). Agreeably, subcellular fractionation and transcriptomic analyses on neurons derived from fragile X-syndrome (FXS) patients, reveals that the transcripts enriched for G-quadruplex are less neurite-enriched (441). The function of FMRP in G-quadruplex-dependent RNA transport appears independent of its function in ribosome stalling, as a mutant-FMRP that cannot bind ribosomes can still promote localization (441, 442). Mechanistically, how FMRP localizes its target mRNAs is still evolving; however, its interaction with the kinesin motor protein KIF3C suggests that FMRP can function as an adaptor between RNP complexes and motor proteins for RNA cargo transport (443).

Cytoplasmic polyadenylation element (CPE)

The CPEB protein facilitates the transport of CPE-containing mRNAs to dendrites (429, 444). While many mRNAs, including *Arc*, *CaMKIIα*, *BDNF*, and *trkB,* are actively transported to the neurites after synaptic stimulation (445, 446), not all mRNAs contain the consensus CPE. Interestingly, several dendritic mRNAs, including *CaMKIIα* and *Map2* contain CPEs in their 3'UTRs (429, 447). Specifically, the CPEB protein is demonstrated to transport the CPE-containing mRNAs, *CaMKIIα* and *Map2* to dendrites, and directly interact with the molecular motor proteins, kinesin and dynein (429). Importantly, disrupting the interaction between CPEB and motor proteins also reduces the *Map2* mRNA localization to dendrites (429). The mRNAs in CPEB-RNP particles are translationally dormant, for example, CPEB3 negatively regulates the translation of various synaptic plasticity-related mRNAs, like *PSD95* and NMDAR subunits

coding mRNAs: *NR1*, *NR2A*, and *NR2B* (448). Therefore, CPEB is a relevant *trans*-acting factor that binds CPEs and plays pivotal roles in mRNA localization and translation regulation.

Transporting brain-specific non-coding BC RNAs

The genomes of rodents and primates have independently acquired a gene that codes for a small non-coding RNA, which is specifically express in the brain called brain cytoplasmic (BC) RNA (449, 450). Rodent brains express a unique 152-nucleotide non-coding RNA named brain cytoplasmic 1 (BC1), which localizes to neuronal dendrites (449, 451-455). Similarly, the primate brain expresses a 200-nucleotide long non-coding RNA named brain cytoplasmic 200 (BC200) (450, 456), which is localized into the neurites, similar to BC1 (457, 458). BC RNAs are structurally similar (459), but were acquired independently. BC1 is coded by a gene derived from retrotransposition of $tRNA^{Ala}$ (460), while BC200 RNA coding gene is a member of Alu family of interspersed repetitive DNA elements (450, 456). BC RNAs are predicted to contain a 5' stem-loop structure, a unique 3' region, and an internal A-rich region [(459, 461), (**Figure 10**)]. Both BC RNAs are RNA polymerase III transcripts containing terminal 'UUU', and are not polyadenylated (456, 462). The 5' stem-loop structure acts as a *cis*-acting element and recruits several *trans*-acting factors for dendritic localization (452, 463). Mutations in the 5' stem-loop disrupts the dendritic localization of BC RNAs, indicating the dendrite targeting role of this 5' structure (452). Interestingly, the localization of BC1 RNA to the dendrites is microtubule-dependent, and disrupting microtubule assembly with a microtubule cytoskeleton disrupting agent, nocodazole, restricts BC RNA in the soma of neurons (464). FMRP was previously shown to bind the 5' stem-loop of BC RNAs, therefore, FMRP could act as a *trans*-acting factor for their localization (465, 466); however, later studies suggested that FMRP and BC RNAs do not interact

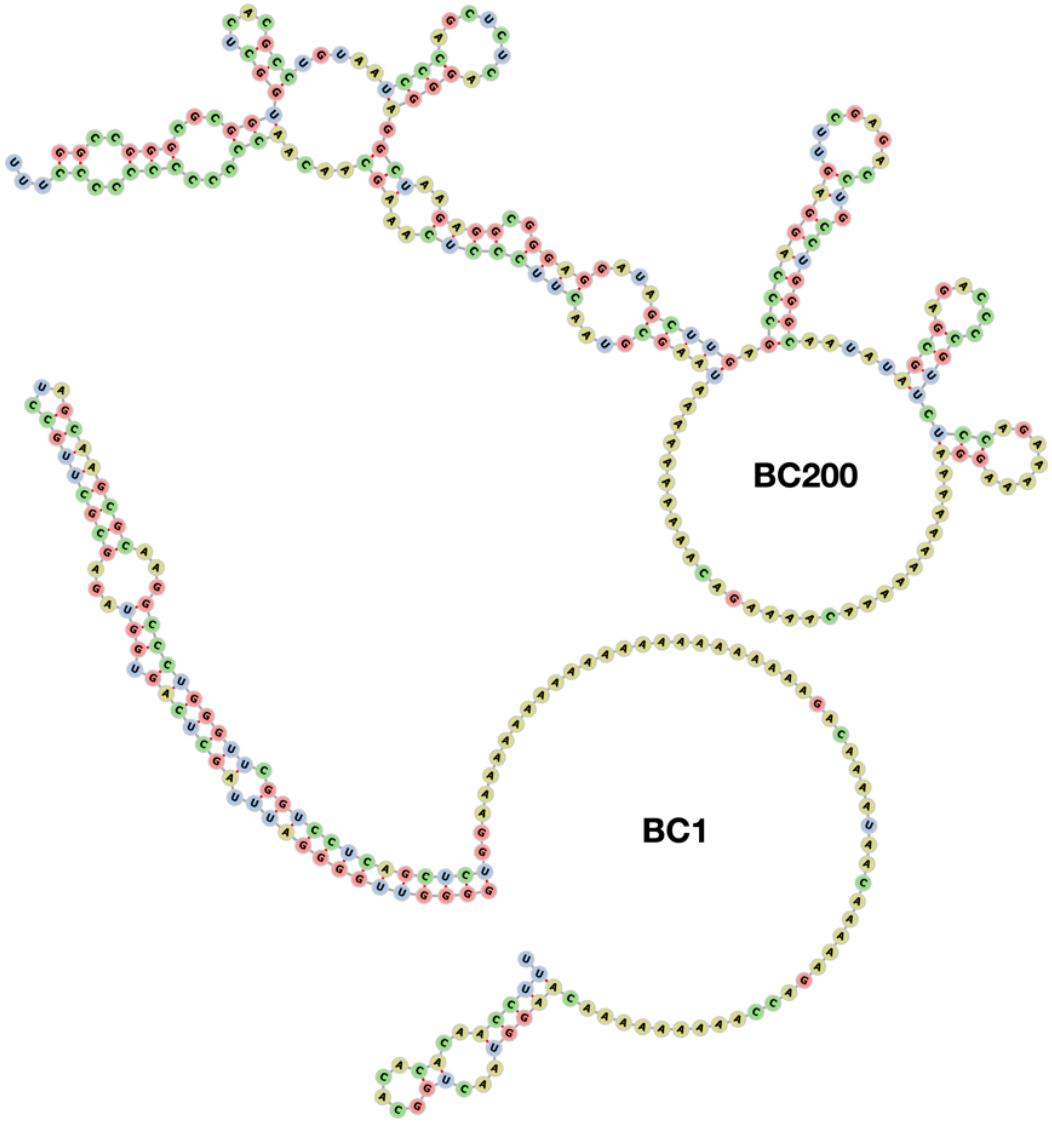

Figure 10. BC RNAs structure. Predicted structures of BC1 and BC200 RNAs by Vienna RNA Websuite (467), showing internal adenosine stretches in open conformation. BC1 RNA shows the 5' stem-loop structure and a 3' unique region.

directly, thereby casting a doubt over this interaction (468). Additionally, BC1 is highly enriched in RNP-particles containing a brain predominant RNA binding protein called Staufen (469). Staufen interacts with the motor protein kinesin, and therefore, may plays a role in BC1 RNA transport (469, 470). BC RNAs provide binding platform for several other RNA binding proteins, including PABPC1 and SYNCRIP, which can bind the internal A-rich regions (308, 471). BC1 RNA has been reported to repress translation *in vitro* and BC1-knockout mice have dysregulated levels of synaptic plasticity related genes like *PSD-95, FMRP, GluRI, GluRII* (472-474). It is currently unclear how BC RNAs regulate the translation initiation; however, *in vitro* studies suggest that BC1 RNA can bind PABPC1, and its 5' stem-loop structure can bind the RNA helicase eIF4A (472), hence BC1 may regulate their availability for the translation initiation complex assembly. These studies highlight a potential role of dendritically-localized non-coding BC RNAs in regulating local translation in dendritic compartments.

The granule theory of RNA transport

In neurons, diverse mechanisms exist for RNA transport to distal dendritic sites. While many mRNAs are transported as RNP particles, some mRNAs prefer liquid-liquid phase separated dense structures called RNA transport granules (RNA granules hereafter). These specialized structures can be found in different cell types, including oligodendrocytes, oocytes, and neurons (475-477). The neuronal RNA granule contains different types of mRNA, RNA binding proteins, 40S and 60S ribosomal subunits, elongation factors (eEF1α), microtubules-related proteins (Tubb2a, Tubb3, Map1a, Map2) and motor proteins (Kif1c, Kif5a, Dynll1, Dynll2) (477, 478). This reflects that the RNA granules are translationally competent, associate with the cytoskeleton, and are presumably motile. Indeed, in neurons RNA granules are easily visible in dendrites as distinct motile structures

with average motility of 0.1μm/sec (477). The neuronal soma also contains RNA granules; however, their high density in soma obscures their distinct morphology. This suggests that RNA granules are packaged in soma for dendritic transport. Studies over the years have demonstrated that neuronal RNA granules contain 80S ribosomes stalled at the pre-translocation step of translation elongation (478, 479). It is suggested that neuronal stimulation or depolarization leads to the release of mRNAs from the RNA granules into the actively translating mRNA pool (416).

RNA binding proteins in RNA granules

Several RNA binding proteins that are implicated in RNA transport are present in neuronal RNA granules, for example, FMRP, Staufen, PABPC1, SYNCRIP, and PURα (478-481). RNA binding proteins play pivotal roles in phase-separating target mRNAs into RNA granules, thus regulating their translation and stability during transport. Our understanding on whether these proteins play independent or coordinated roles in RNA granule assembly, is still evolving. Several important RNA granule proteins are discussed below.

FMRP

The RNA binding protein FMRP is a component of RNA granules, which is involved in RNA trafficking into dendrites (480, 482). FMRP interacts with its target RNAs through RGG box, which leads to ribosome stalling and translation repression (479, 480). FMRP also binds directly to the L5 protein in large ribosomal subunit (483, 484), and cryo-EM analysis of FMRP-ribosome complex predicts that KH1 and KH2 domains (K-homology) of FMRP may prevent tRNA from accessing the P-site on ribosome (483). However, FMRP lacking the RGG box binds ribosomes, but does not display a strong translation inhibition (483). This indicates that the RNA binding

ability of FMRP is prerequisite for its translation inhibition properties, and that the simultaneous interaction with the ribosomes is beneficial but not absolutely required. Transcriptome analysis on RNA granules has revealed that one-third of known FMRP target RNAs are packaged into RNA granules (480). Importantly, FMRP is highly enriched in the RNA granules, and less localized in polysomes (479, 480). Therefore, it is suggested that 'FMRP-stalled' polysomes are directly stored as RNA granules (479, 480).

Staufen

Staufen, a double-stranded RNA binding protein, is also involved in RNA transport in neuronal dendrites (485), and is critical for healthy spine morphology (486). It binds a stem-loop structure in target RNAs called Staufen response element (SRE) (487). The RNA targets of Staufen include members of G protein-coupled receptor family (GPCR), and majority of Staufen targets are localized to neurites (488). Staufen transports RNAs in RNP particles and RNA granules (469). Staufen containing RNP particles are enriched in dendritically localized non-coding RNA BC1, which does not associate with ribosomes (489). Staufen interacts with the motor protein kinesin and plays a role in RNA cargo transport (469, 470). Proteomic analysis of Staufen containing RNA granules has identified their components which includes, 40S and 60S ribosomal subunits, FMRP, PABPC1, motor proteins, and cytoskeletal proteins (485, 490). Therefore, Staufen transports RNAs in two distinct structures: : (i) small RNP particles that contain RNA-protein complexes, but lack ribosomes, and (ii) large dense RNA granules that contain ribosomes as well as RNA-protein complexes.

PABPC1

PABPC1 is consistently detected in RNA granules; however, its role is not clear (478, 480). PABPC1 is classified as a translation initiation factor that stimulates translation in certain contexts (142, 148), while as an mRNA stability factor in postembryonic systems (128, 160). The presence of PABPC1 in translationally dormant RNA granules is contrary to its function in translation; however, it may play a dual role in mRNA translation and stability after their release from the RNA granules. A recent study shows that PABPC1 and FMRP can physically interact, and this interaction enables FMRP to protect mRNAs from deadenylation (491). This suggests a possible role of FMRP in sequestering PABPC1 and bound mRNAs into RNA granules. Moreover, PABPC1 molecules can multimerize on mRNA tails (36), which may further support its phase separation into these dense RNP structures.

SYNCRIP

SYNCRIP (also known as hnRNPQ) is a predominantly cytoplasmic protein which belongs to a big family of heterogeneous nuclear ribonucleoproteins (hnRNPs). SYNCRIP is an RNA binding protein that was identified as a component of RNA granules in hippocampal neurons (492). SYNCRIP containing RNA granules are enriched in neuronal soma and localize to the neurites. Time-lapse microscopy experiments reveal that SYNCRIP containing granules are motile, and can travel bidirectionally in the neurites (492). The disruption of microtubules with the drug nocodazole prevents the movement of these granules, indicating that SYNCRIP-containing RNA granule motility is microtubule-dependent (492). Moreover, colocalization studies show that SYNCRIP is present in Staufen-containing RNA granules. SYNCRIP RNA interactome analysis has identified mRNAs targets for this protein. Many of these mRNAs code for proteins related to

neurogenesis, neuronal migration, and neurite outgrowth (493). Additionally, SYNCRIP targets *GAP-43* mRNA, which codes for a neuronal protein that facilitates axonal growth by regulating actin cytoskeleton dynamics (494). SYNCRIP translationally represses *GAP-43* mRNA by binding to a G-quadruplex structure in its 5' UTR (494). Therefore, SYNCRIP regulates protein synthesis of its target mRNAs and is transported in RNA granules.

PURα

PURα was first described as a transcription factor that binds a single stranded purine-rich (Adenosine repeats) element upstream of *c-myc* gene (495, 496). However, many studies have now shown that PURα is localized in the dendrites of hippocampal neurons (497). It has emerged as a major RBP involved in RNA transport in neurons, and is present in an RNA granule associated with the kinesin motor protein, KIF5 (498). It colocalizes with Staufen-containing RNA granules, and associates with several dendritically localized mRNAs, like *Map2* and non-coding RNAs BC1 and BC200 (497-499). One study showed that in mature neurons, 47% of Staufen containing RNA granules are positive for PURα. Interestingly, PURα-containing RNA granules are stationary under resting conditions; however, quickly localize into dendritic spines after activation of postsynaptic metabotropic glutamate receptor 5 (mGluR5) (499). The localization of PURα-containing RNA granules to dendrites is dependent on microtubules, as microtubules disrupters, like nocodazole and colchicine inhibit this localization (497). Moreover, PURα also colocalizes in FMRP- and Staufen-containing RNP complexes, and attaches to rough endoplasmic reticulum via kinesin motor protein KIF5 (500). These studies highlight PURα as a major component of RNA granules in neurons.

PABPC1 is not only present in FMRP-containing RNA granules, but also colocalizes with Staufen-containing RNA granules in rat brain (485). Similarly, FMRP, Staufen, PURα, SYNCRIP and other known RNA granule proteins can also colocalize in one subpopulation of granules and not in others (498, 500-502). This highlights that RNA granules are dynamic structures that contain overlapping protein components. However, as mRNAs that are localized in RNA granules may still maintain their poly(A) tails, it is not surprising that PABPC1 is sequestered into multiple neuronal RNA granule populations.

After correct delivery of mRNA cargo to distal neurites, neurons localize the RNAs in close proximity to the sites where their protein products are needed. This is usually done by docking the RNA cargo to the cytoskeleton via motor proteins (503, 504). The mRNAs are stored in repressed state and await synaptic activation (414-417). The steps involved in synaptic stimulation, and in response, local proteome modulation are discussed below.

Synaptic stimulation

Chemical synapses are the most common type of synapses in the brain. Synaptic transmission via a chemical synapse involves these steps: (i) transmission is initiated when an action potential reaches the axonal terminal causing it to depolarize and leading to, (ii) the influx of Ca^{2+} ions into the pre-synaptic terminal through voltage gated ion channels, (iii) the influx of Ca^{2+} ions activates the fusion of synaptic vesicles to the pre-synaptic membrane and release of neurotransmitter (like glutamate) by exocytosis into the synaptic cleft, (iv) glutamate binds to its receptors, mainly AMPA and NMDA, present on the excitatory post-synaptic membrane, which are ligand-gated ion channels, (v) the binding of glutamate to AMPAR leads to the influx of Na^{+} ions into the post-

synaptic terminal through AMPAR-ion channel, therefore, making it locally depolarized, and (vi) the glutamate binding to the NMDAR and simultaneous depolarization through AMPAR, causes Ca^{2+} influx through NMDAR-ion channel, thus leading to a further depolarization of post-synaptic terminal (505). The Ca^{2+} ion is an important second messenger that links membrane depolarization to downstream cell signaling cascades. These downstream biochemical machineries determine the strength and duration of a synaptic connection by regulating the local proteome abundance.

Local protein synthesis: Important players

As mentioned earlier, a myriad of studies have demonstrated that many mRNAs are transported to the neurites (97, 378, 419-422). Apart from mRNAs, the translation machinery i.e., ribosomes are also present in synaptic terminals (166, 419, 506, 507). Moreover, the mRNAs coding for translation factors, as well as the proteins themselves are transported to the synapse (97, 166, 478, 508, 509). Collectively, this gives synaptic terminals the ability to modulate their local proteome effectively. In fact, many studies have now proved that active protein synthesis takes place in pre- and postsynaptic terminals (166, 419, 510, 511). The ability of neurons to actively synthesize proteins at synaptic sites, supports the synaptic changes required during long-term memory formation (512). Several signaling molecules and effector proteins exert a tight control over protein synthesis in synaptic terminals, as discussed below.

CaMKIIα as a central molecule

The influx of Ca^{2+} ions activate downstream effector proteins that can sense elevated calcium levels. A calcium effector protein calmodulin binds up to four Ca^{2+} ions, which leads to its activation (513). Ca^{2+}/calmodulin complex binds to a serine/threonine protein kinase enzyme

called Ca^{2+}/calmodulin dependent protein kinase II (CaMKIIα) and activates its kinase activity (514). After its initial activation, CaMKIIα autophosphorylates (Thr286) itself for a long lasting Ca^{2+} independent activity (515-518). CaMKIIα is highly expressed in the hippocampus and cortex, reaching 2% and 1.3% of the total protein content, respectively (519). It is highly enriched in post-synaptic compartments and associates with NMDAR after autophosphorylation (520-523). Among many of CaMKIIα downstream substrates are included, mitogen activated serine/threonine protein kinase (MAPK) family members and protein kinase B (PKB/Akt) (524, 525). Three major types of MAPKs include extracellular signal-regulated protein kinase 1/2 (Erk1/2), c-Jun N-terminal kinase (JNK), and p38 MAPK. The phosphorylated PKB/Akt stimulates the activity of its downstream target, mTORC1 (mammalian target of rapamycin complex 1), an important serine/threonine kinase which is sensitive to nutrient conditions and regulates the translation initiation (526, 527).

The ability of CaMKIIα to sense the elevated Ca^{2+} levels, and potentiate downstream signaling cascades, suggests its role as a central molecule in neuronal synaptic signaling. It is responsible for orchestrating the activation of key downstream kinases, which are important for regulating the mRNA translation. The important pathways linking synaptic stimulation to protein synthesis are as follows.

Translation initiation control

Translation initiation is tightly regulated by mTORC1, which can sense extracellular cues like nutrient abundance (527, 528). Akt directly phosphorylates tuberin (TSC2), an inhibitor of mammalian target of rapamycin (mTOR) activity. Phospho-inhibition of TSC2 by Akt, leads to

mTOR activation via its binding to the GTP-binding protein, RHEB. mTORC1 acts as a kinase to phosphorylate its targets: eukaryotic translation initiation factor binding protein (4E-BP1), and protein S6 kinase (S6K). Phosphorylation of 4E-BP1 leads to its dissociation from eIF4E. The free eIF4E can bind the mRNA 5'cap and together with eIF4G and eIF4A, assembles the eIF4F complex for translation initiation by ribosome recruitment (134). Remarkably, a study demonstrated that inhibiting cap-dependent translation initiation leads to the depletion of polyribosomes from dendritic spine heads (511). Thus, indicating that cap-dependent translation initiation plays an important role in maintaining the local proteome in dendritic spines (511, 529). In line with this study, inhibiting the interaction between translation initiation factors eIF4E and eIF4G, which is required for ribosome recruitment, has profound effects on initial fear memory consolidation, but not on pre-existing memory reconsolidation (530). Phosphorylation of S6K activates its kinase activity, which then phosphorylates the small ribosomal protein subunit, RPS6. The significance of this phosphorylation still remains elusive; however, one study found that phosphorylation of RPS6 promotes the translation of mRNAs with short open reading frame (ORF) (531). Interestingly, in neurons, RPS6 protein is shown to get phosphorylated during neuronal activity (532).

Translation elongation control

While above studies highlight how protein synthesis is regulated at the translation initiation step, many mRNAs that are transported in neurites are repressed in the translation elongation step, as they contain stalled ribosomes awaiting reactivation (533). The phosphorylation state of the elongation factor-2 (eEF2) acts as a toggle switch for synaptic plasticity. eEF2 catalyzes the GTP-hydrolysis-dependent translocation of a ribosome on mRNA during polypeptide synthesis (534).

Phosphorylation of eEF2 by a kinase, eEF2K (or CaMKIII), renders it inactive, which stalls translation in the elongation step (535). Importantly, during stimulation-mediated neurotransmission i.e., neurotransmitter release, Ca^{2+} influx and depolarization of post-synaptic terminal, eEF2 remains dephosphorylated (active), which favours protein synthesis (536). However, during the events of "spontaneous" neurotransmitter release (at rest), when the action potentials are absent (537, 538), eEF2 is immediately phosphorylated (inactive) by eEF2K (536, 539). Intriguingly, stimulation of synaptosome preparations with the neurotransmitter glutamate mimic N-methyl-D-aspartate (NMDA), leads to the phosphorylation of eEF2 and overall decrease in protein synthesis (540). In contrast, the translation of *CaMKIIα* is rapidly upregulated following NMDAR activation (540). Therefore, while the overall mRNA translation is reduced after eEF2 phosphorylation, for unknown reasons, the translation of some synaptically important mRNAs, like *CaMKIIα, Arc*, and *MAP1B* is elevated (540-544). This suggests that eEF2 acts as a regulatory effector that couples synaptic activation to local mRNA translation.

Yet another elongation factor, eEF1A provides a regulatory link between synaptic activity and translation. eEF1A is a G-protein that utilizes a GTP molecule and bring in an aminoacylated tRNA to the A-site of a traversing ribosome during translation elongation. The eEF1A-GDP is then recycled back to GTP-bound state by eEF1B, a guanine nucleotide exchange factor (545). Other than a role in protein synthesis, eEF1A also associates with F-actin filaments and plays a non-canonical role in actin cytoskeleton rearrangements (546-548). eEF1A has two isoforms, eEF1A1 and eEF1A2. The expression of eEF1A2 progressively increases during neuron maturation, where eEF1A2 becomes the predominant isoform (549). During glutamate mediated synaptic activity through metabotropic glutamate receptors (mGluR1 and mGluR5), eEF1A2 gets phosphorylated

in c-Jun N-terminal kinase (JNK)-dependent manner (550), which leads to its dissociation from eEF1B, thereby reducing protein synthesis (545, 549). Astonishingly, eEF1A2 phosphorylation also affects its association with actin fibers, where non-phosphorylated form can associate with F-actin filaments which reduces actin dynamics and spine density (549). In contrast, the phosphorylated eEF1A2 dissociates from the F-actin filaments, which allows for actin cytoskeletal remodeling and normal spine density (549). Therefore, eEF1A2 is suggested to link local protein synthesis and cytoskeletal modifications to synaptic plasticity.

Stimulus-dependent cytoplasmic polyadenylation

Synaptic stimulation has been shown to activate the cytoplasmic polyadenylation of several mRNAs, which favours their translation (447). Several mRNAs have CPE elements in their 3' UTRs as a signal for polyadenylation. For example, *CaMKIIα* mRNA has two CPEs and undergoes polyadenylation at synapses, which upregulates its protein synthesis (447). Other examples include mRNAs: *Map2, Rcm3* (calmodulin), and *Abp* (AMPA receptor binding protein) (429, 551). Interestingly, in post-synaptic density fractions and pyramidal neurons, CPEB is shown to get phosphorylated after CaMKIIα activation (552). Moreover, inhibiting CaMKIIα activity abolishes CPEB phosphorylation (552). The phosphorylated CPEB binds CPEs and recruits the polyadenylation machinery (119, 120, 552). While several RNAs undergo stimulus-dependent cytoplasmic polyadenylation, majority of mRNAs do not, as they lack canonical CPEs. Interestingly, a recent study demonstrated that only a subset of mRNAs underwent cytoplasmic polyadenylation after neuronal stimulation (165). In this study only a modest correlation was established between poly(A) tail length and translation efficiency. However, as this correlation was

calculated from the totality of a neuron cell, investigating a correlation between poly(A) tail length and translation efficiency in the synaptic compartments would be more appropriate (165).

Collectively, these studies inform us how synaptic activity is propagated by sensors (receptors like NMDAR, mGluR) on to downstream effectors (like translation initiation and elongation factors), which play important roles in modifying the local proteome, and as a result, in modulating the synaptic architecture. Therefore, neurons can effectively modify their proteome in the axons and dendrites, which gives them the ability to form new synaptic connections and store memory. This quality of neurons to alter the synaptic structure in an activity-dependent manner forms the basis of synaptic plasticity, which is described below.

Synaptic plasticity

The ability of neurons to form and strengthen new synaptic connections and retract or erase the connections that are not meaningful, is important to achieve a well-refined neural network in the brain. To achieve this functionally 'optimized' and energetically 'favoured' network, neurons modify the efficacy of synaptic connections via many intricate systematic mechanisms. The synaptic plasticity can be achieved by two main principles, as follows.

Long-term potentiation (LTP)

LTP is a form of synaptic plasticity involving persistent strengthening of synapses between neurons which generally leads to a long-lasting excitatory postsynaptic potentials (EPSPs). Early studies on LTP were carried out using live rabbits and guinea pig hippocampal slices (553-555). In these studies, LTP was achieved when a microelectrode was used to apply a brief high frequency

stimulus to the Schaffer collaterals (axon) of a pyramidal neuron in the CA3 region, and EPSPs were recorded from a postsynaptic CA1 pyramidal neuron (554). Remarkably they observed that a persistent increase in the EPSPs was observed only when the post-synaptic membrane was briefly depolarized by applying a current through the recording electrode in conjunction with the axonal stimulus (554). Even though these early studies demonstrated methods in achieving long-lasting potentiation after synaptic stimulation, the underlying biochemical pathways remained elusive. However, decades of extensive studies have now uncovered the biochemical mechanisms important for eliciting LTP. These include the neurotransmitter release at the synapse, calcium signaling, post-synaptic membrane depolarization, local protein synthesis, and cytoskeletal rearrangements (377, 556-561). Therefore, the two main steps involved in eliciting a strong LTP are: induction and maintenance. For a strong induction, the synapse after receiving an action potential should have enhanced pre-synaptic neurotransmitter release by exocytosis, and high membrane density of the AMPA receptors on the post-synaptic terminal (562-565). Several factors can contribute to an enhanced neurotransmitter release. For example, in cultured hippocampal neurons brain derived neurotrophic factor (BDNF) is reported to enhance the release of neurotransmitter from synaptic vesicles by exocytosis and this is dependent on post-synaptic tyrosine kinase B receptor activation (563, 566-570). The synapses formed between mossy fibers of dentate gyrus granule cells and pyramidal neurons of CA3 region of hippocampus represent a unique form of LTP induction. Unlike the classical form of LTP that requires NMDA receptor activation and a rise in post-synaptic Ca^{2+} concentration, LTP of mossy fibers-CA3 pyramidal neuron synapse is NMDAR-independent, as it cannot be blocked by NMDAR antagonists (571-574). Therefore, it is generally accepted that this form of LTP is expressed pre-synaptically by

Ca^{2+} uptake through voltage gated calcium channels, thereby increasing the release of neurotransmitter (575).

Most LTP studies are conducted on excitatory synapses between Schaffer collateral axons of CA3 pyramidal neurons and dendrites of CA1 pyramidal neurons of hippocampus (554, 576, 577). At these synapses, LTP can be triggered by a short high frequency pulse stimulation, which can last for days in animal brain (578, 579). The early phase of LTP requires post-synaptic changes such as: activation of NMDAR, Ca^{2+} influx, and CaMKIIα autophosphorylation for enhanced activity (505). Early phase of LTP also requires AMPAR insertion into the PSD membrane by fusion of AMPAR-containing endosome vesicles (562, 565, 580-588). Interestingly, Ras-ERK pathway is implicated in the exocytosis of AMPAR-containing vesicles (588, 589). However, a long-lasting increase and maintenance of LTP, i.e., a phase that would last weeks or even months, requires local protein synthesis, a phase called "late-phase" of LTP (590-592). The ability to maintain the strength of LTP for a long duration is regarded as the mechanism for memory formation (593). Intriguingly, inhibiting the key mTOR pathway via using protein synthesis inhibitors like rapamycin, or disrupting eIF4E-eIF4G interactions, impairs long-term memory storage and learning (530, 590, 593-595).

Long-term depression (LTD)

In simple terms, LTD, in contrast to LTP, is described as weakening of strength between synapses. Just like LTP, early experiments that described LTD were also done on excitatory synapses between Schaffer collateral axons of CA3 pyramidal neurons and dendrites of CA1 pyramidal neurons of hippocampus (596). Earlier studies found that a series of low frequency 1-3Hz stimulation of

Schaffer collateral axons consistently induced a depression in the post-synaptic action potential of CA1 pyramidal neurons, which lasted for hours and could be reversed by short high frequency 50Hz stimulation (596, 597). Mechanistically, LTD induction was shown to be dependent on continued activation of NMDAR by a low frequency stimulation that is below the threshold of synaptic potentiation induction (596, 598). Even though both LTP and LTD induction is dependent on post-synaptic intracellular Ca^{2+} concentration and the activation of CaMKIIα (599-601), the molecular mechanisms that contribute to LTD induction are not fully understood. The consequence of LTD is a marked decrease in the density of AMPAR by endocytosis and ultimate elimination of depressed synapses (602-605).

These studies suggest that both LTP and LTD appear to work in coordination to maintain a balance between establishment and elimination of synapses in an activity-dependent manner. This in part is contributed by the number of AMPARs at the post-synapse, which determine the amplitude of depolarization currents (EPSPs), and therefore, the synaptic strength. As many studies have now concluded, for a long-term maintenance of synaptic connections, continued protein synthesis is a required phenomenon in synaptic terminals.

mRNA decay overview in neurons

In neurons, post-transcriptional mechanisms to regulate gene expression are of utmost importance. Similar to how neurons have developed intricate mechanisms to stabilize mRNAs, prior to their translation in space and time, they have also invested extensively in mechanisms to decay mRNAs. One such mechanism that has gained quite a bit of limelight in recent years is NMD pathway. It has become clear that NMD isn't merely an RNA surveillance pathway, but also plays significant

roles in degrading normal mRNA that do not harbour PTCs (276, 606, 607). Genome-wide studies in yeast and other eukaryotes have confirmed that NMD not only regulates aberrant RNAs, but also normal mRNA steady states. NMD-dependent degradation of normal RNAs is established by utilizing an EJC in the 3'UTR downstream of the stop codon (608, 609). NMD plays an important role in axon guidance by regulating the spatial and temporal expression of ROBO proteins. These proteins are located at the tip of extending axons, and are produced from alternatively spliced mRNA isoforms *Robo3.1* and *Robo3.2*. Both ROBO3.1 and ROBO3.2 proteins are extensively studied for their role in axon guidance in "commissural" axons (610). Importantly, the *Robo3.2* isoform codes for a smaller protein due to the insertion of a stop codon upstream of an exon-exon junction by frameshift mutation. This mRNA is a classical NMD target, however, it escapes NMD and is accumulated in axons in a translationally repressed state. Intriguingly, *Robo3.2* mRNA gets the opportunity to generate ROBO3.2 protein after the axons have reached spinal midline, and is eventually decayed by NMD (611). *Arc* mRNA is an unusual case, where after neuronal stimulation, it is not only transcriptionally upregulated, by its decay is also accelerated (612). *Arc* mRNA 3' UTR contains two exon-exon junctions after splicing, and therefore, contains two EJCs downstream of the stop codon (286), which can trigger NMD response (613). Interestingly, knocking down UPF1 (core NMD factor) leads to upregulation of *Arc* mRNA, thus suggesting that the expression of *Arc* is regulated by NMD (286, 611). These examples highlight that NMD not only surveys the transcriptome for quality control, but also plays an important role in spatiotemporal expression of synaptically important genes. While NMD is exemplified to regulate normal mRNA turnover, it generally requires the presence of an EJC downstream of the stop codon for its assembly (276, 285). Similar to *Arc* mRNA, many dendritically localized mRNAs contain alternatively spliced 3'UTRs, which may harbour EJCs downstream of the stop codon (97, 614-

618). However, how and if NMD is relevant for the turnover of these synaptically localized mRNAs, is unclear. Nevertheless, NMD appears to be an important pathway for normal brain function as knocking out relevant NMD factors like UFP2 results in reduced spine density and impaired LTP induction in mouse hippocampus (614).

miRNA-mediated gene silencing programs are also active in synaptic terminals. Currently, 20 or more miRNA species are known to be present in the dendrites of vertebrate neurons (619). Moreover, miRNAs are actively transcribed and transported into synaptodendritic compartments upon stimulation, where they are suggested to regulate local translation (619-624). While miRNA are generally linked to gene silencing by mRNA degradation, in certain systems including neurons, miRNAs are also suggested to repress mRNA translation in a reversible manner (625-627). Unexpectedly, miRNAs can even upregulate translation in certain context (627). A study showed that miRNA *let-7* can induce translation of its target mRNAs in cell cycle arrested cells; however, as expected, still represses translation in actively dividing cells (627). Interestingly, the levels of miRNA in neurons corelate with the activity. For example, in mouse retinal neurons, a miRNA cluster *miR-183/96/182* and miRNAs *miR-204* and *miR-211* are transcriptionally upregulated during visual stimuli and rapidly degraded during dark adaptations (620). Similar correlation can also be observed in hippocampal neurons (620). These studies highlight a remarkable adaptation of mRNA decay machineries to preserve local transcriptome and support a healthy neuronal function.

2. RATIONALE AND HYPOTHESES

Investigating *Pabpc1l2a/b:* a newly acquired mammalian-specific PABPC1-like gene

The function of prototypical PABPC i.e., PABPC1, is extensively studied in many contexts. PABPC1 stimulates mRNA translation *in vitro* and during early development by simultaneously binding the mRNA poly(A) tails and the 5'cap-bound eIF4F complex via direct interactions with the eIF4G scaffold subunit (142, 148). The crystal structure of PABPC1-eIF4G interaction has revealed the contact sites between PABPC1 RRM2 and eIF4G N-terminus (143). Higher order metazoans have acquired several PABPCs, many of which display tissue-biased expression patterns. During evolution, mammals further expanded their genetic repertoire of PABPC-like genes by acquiring an X-linked ampliconic gene, *Pabpc1l2a/b*. While a previous study detected *Pabpc1l2* mRNA expression in mouse testis and brain tissues (628), several databases have computationally predicted that *Pabpc1l2a/b* is a pseudogene. However, a comparative sequence analysis of PABPC1L2 compared to PABPC1 suggested that there is evolutionary pressure on PABPC1L2 to be able to bind RNA. With this in mind, I set out to test the hypothesis that ***Pabpc1l2a/b* indeed codes for a novel poly(A) binding protein in mammals that post-transcriptionally regulates gene expression**. The overarching goal of my Ph.D. work has been to broadly investigate *Pabpc1l2a/b*, determine if it expresses a functional protein, and to determine the role of this protein in post-transcriptionally regulating gene expression.

3. RESULTS

PREFACE: Uncovering a mammalian neural-specific poly(A) binding protein with unique properties

In sections 3.1 to 3.5., from *Sharma et al., 2023,* which is **published in *Genes & Development***, we set out to characterize the expression and shed light on the function of previously uncharacterized mammalian X-ampliconic 'PABPC-like' gene, *Pabpc1l2a/b (*collectively *Pabpc1l2)*. To this end, we have identified neural specific expression of *Pabpc1l2* mRNA and PABPC1L2 protein, which we have subsequently named neural PABP (neuPABP) as it is predominantly expressed in the brain. neuPABP maintains a unique architecture as compared to other PABPCs, containing only two RNA recognition motifs (RRMs) and maintaining a unique N-terminal domain of unknown function. neuPABP expression is activated in neurons as they mature during synaptogenesis, where neuPABP localizes to the soma and postsynaptic densities. neuPABP interacts with the non-coding RNA BC1, as well as mRNAs coding for ribosomal and mitochondrial proteins. However, in contrast to PABPC1, neuPABP does not associate with actively translating mRNAs in the brain. In keeping with this, we show that neuPABP has evolved such that it does not bind eIF4G and as a result fails to support protein synthesis *in vitro*. Taken together, these results indicate that mammals have expanded their PABPC repertoire in the brain and propose that neuPABP may support the translational repression of select mRNAs.

3.1. *Pabpc1l2* is predominantly expressed in neural tissues

The human X-chromosome contains a two-copy ampliconic *Pabp-like* gene, *Pabpc1-like 2 (Pabc1l2a/b),* with both copies lacking introns and being over 99% identical to each other at the nucleotide level (**Figure 11B**). *Pabc1l2a/b* is conserved among mammals (629), and is predicted to code for a truncated open reading frame as compared to PABPC1, containing only the first two RRMs (**Figures 11A and 12**). To assess *Pabpc1l2* expression in adult mice, we isolated total RNA from adult mouse tissues and carried out semi-quantitative RT-PCR and RT-qPCR reactions using *Pabpc1l2*-specific primers. We observed *Pabpc1l2* mRNA expression in the mouse brain tissues (e.g., cortex and hippocampus) but could not detect its expression in any other somatic tissues (**Figures 11C and 13**). In keeping with this, *Pabpc1l2* gene expression was consistently detected in the postnatal brain of P7 and 10W mice in neural cells as assessed by single-cell RNA-sequencing analyses. Detection rate was higher in neurons, lower in glial cells (oligodendroglial cells and astrocytes), and negligible in microglia and other non-neural cell types (**Figures 14 and 15**). We also analyzed *Pabpc1l2* gene expression across human tissues using publicly available data from the NIH Genotype-Tissue Expression project (630). In keeping with data acquired from mouse tissues, *Pabpc1l2* mRNA was also primarily detected in human brain tissues (**Figure 16**).

While mouse *Pabpc1l2* is predicted to code for a protein that contains only two RRMs and is classified by the NCBI as a putative pseudogene (NM_001384267.1), the predicted amino acid sequence across these motifs is highly conserved in PABPC1L2 homologs, sharing a high degree of identity and homology with the first two RRMs of PABPC1 (**Figure 12**). This suggests that as opposed to *Pabpc1l2* being a pseudogene, there has been evolutionary pressure on it to maintain

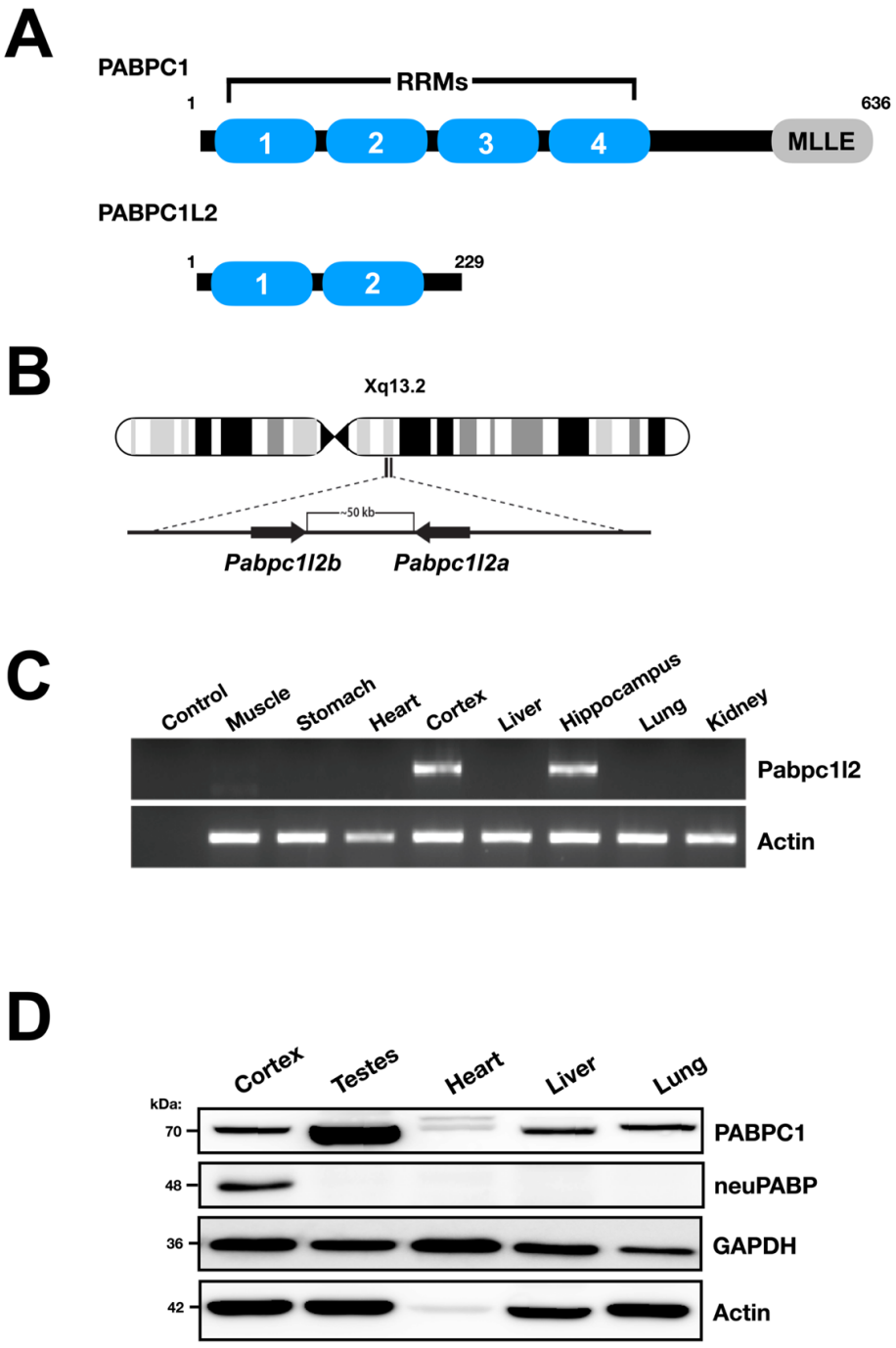

Figure 11. PABPC1L2 (neuPABP) displays a neural-specific expression pattern. (A) Schematic representation of PABPC1 and PABPC1L2 domain organization. (B) Schematic diagram of human X-chromosome showing position of *Pabpc1l2* ampliconic gene. (C) Semi-quantitative RT-PCR analysis of *Pabpc1l2* and Actin mRNAs from multiple adult mouse tissues (C57BL/6J; Age: 5 months). (D) Western blotting of PABPC1, neuPABP, GAPDH and Actin on lysates prepared from select adult mouse tissues(C57BL/6J;Age:5months).

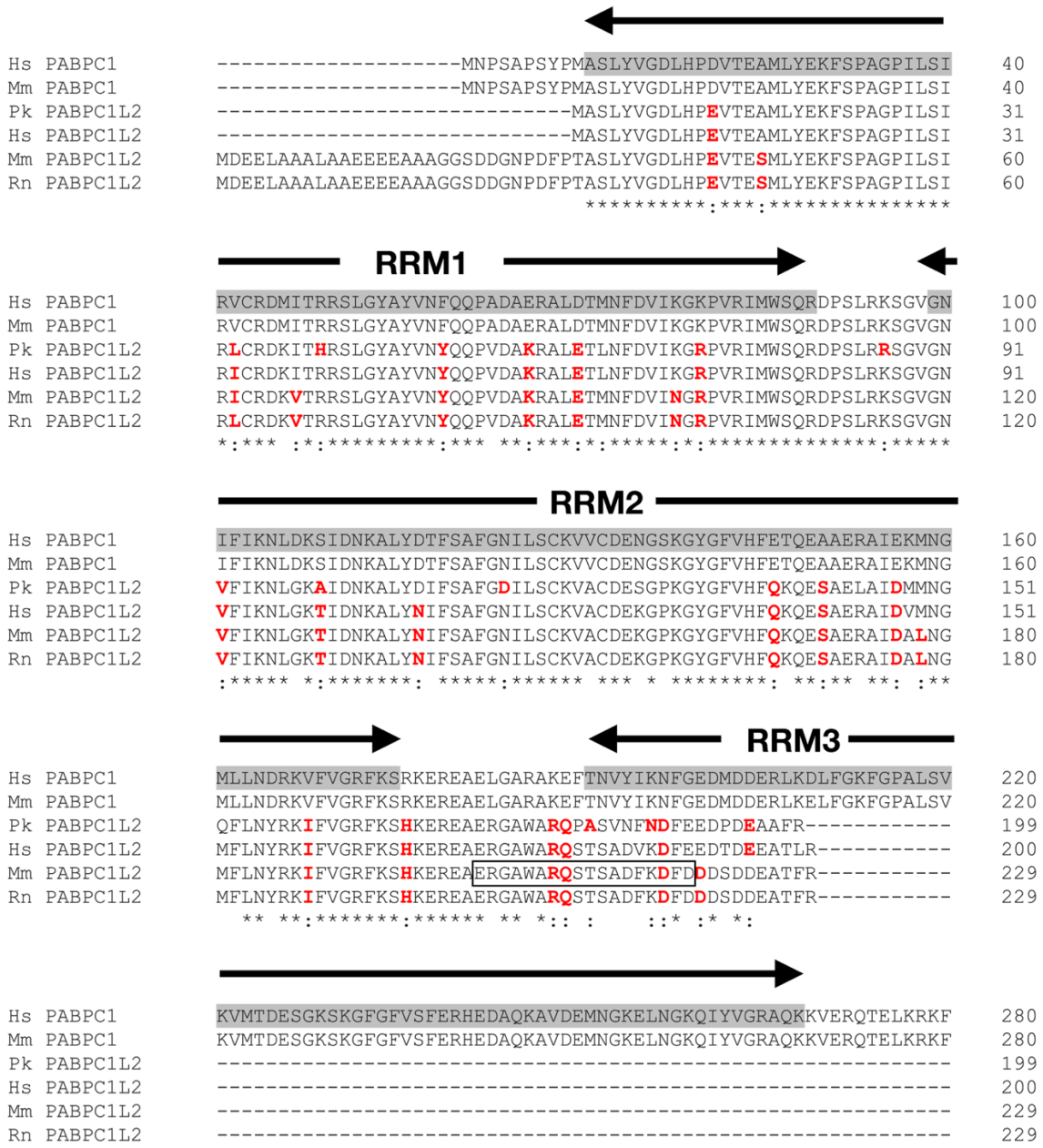

Figure 12. Comparative sequence analysis. Comparative sequence analysis of Human (Hs) and mouse (Mm) PABPC1 with human, mouse, rat (Rn) and bat (Pk) PABPC1L2 predicted open reading frames. Regions containing RNA recognition motifs (RRMs) are marked by arrows. The peptide sequence used for antiserum production to generate a mouse PABPC1L2-specific antibody is boxed.

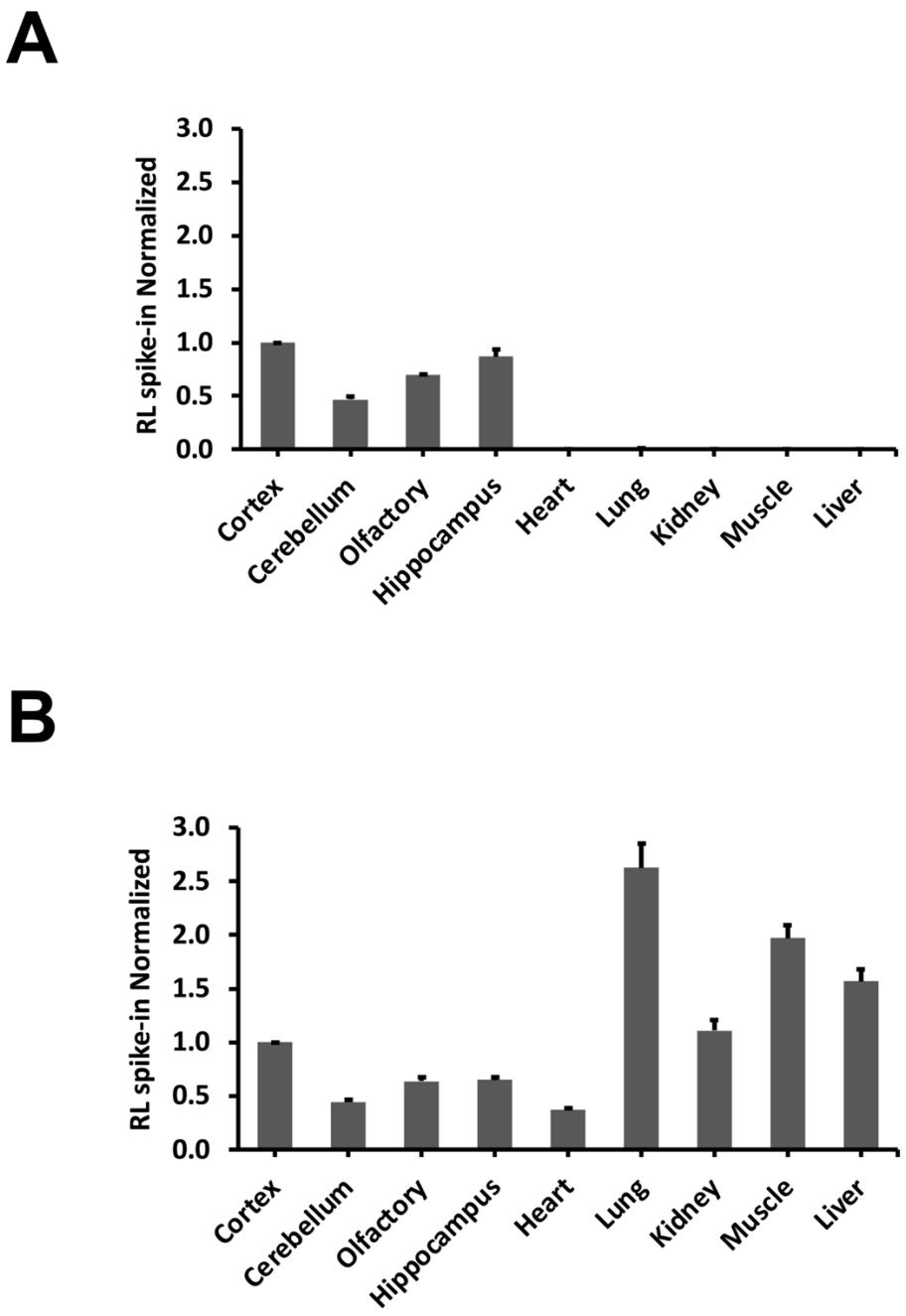

Figure 13. RT-qPCR analysis of (A) *Pabpc1l2* and (B) Pabpc1 mRNAs from multiple adult mouse tissues (C57BL/6J; Age: 5 months). An *in vitro* transcribed RLuc spike-in RNA was used for normalization across tissues. Expression of *Pabpc1l2* and *Pabpc1* in the brain cortex was set to '1' to assess the differential expression of both genes in select neural and non-neural tissues. Error bars represent SEM from three biological replicates (n=3).

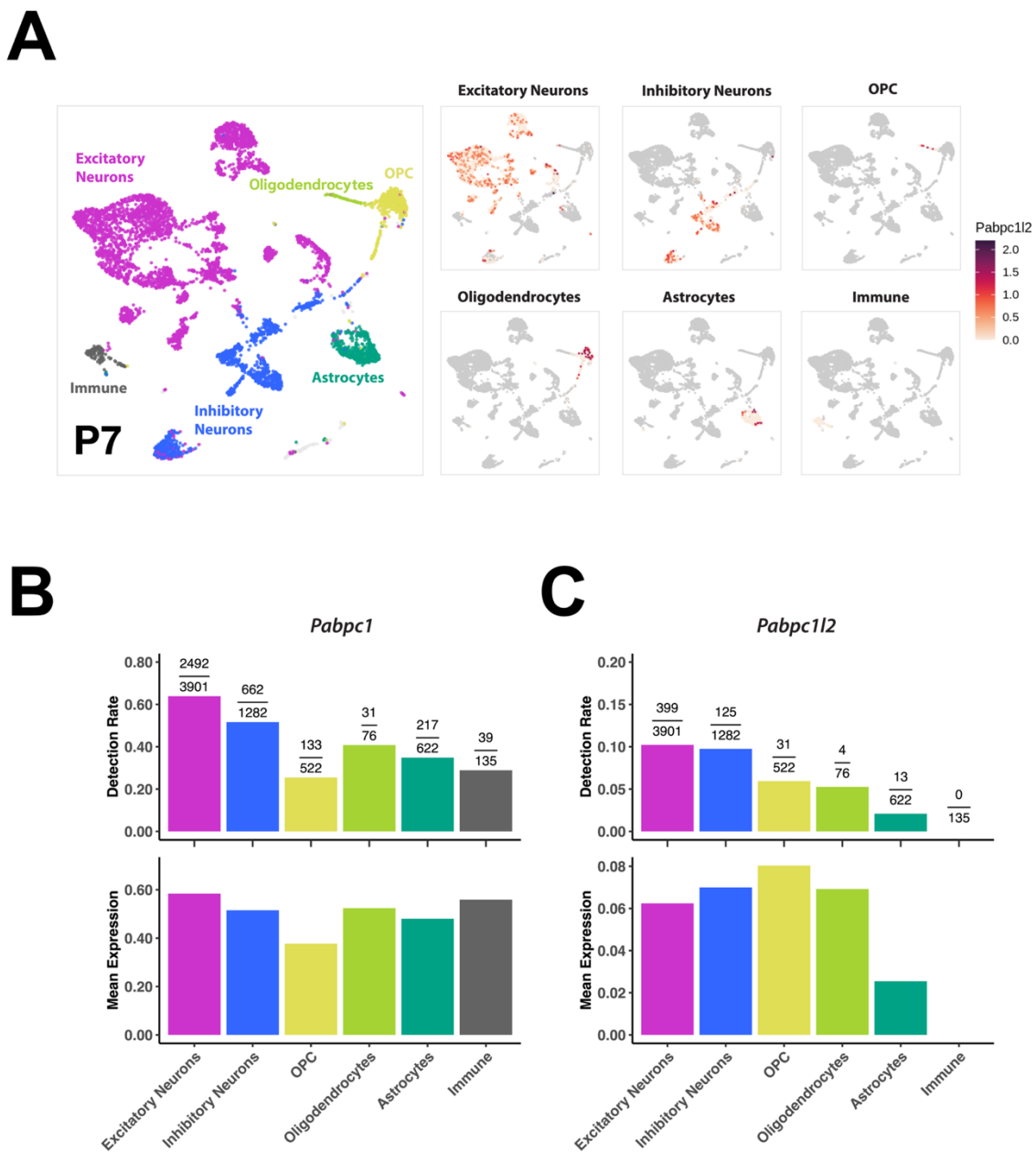

Figure 14. *Pabpc1l2* is expressed in neural cells at age of P7 (C57BL/6J; Age: Postnatal day 7) (A) Left: UMAP plot of single nuclei RNA-seq of adult mouse cortex (N =6,890). Cells are colored by cell class. Right: UMAP plots displaying the expression of *Pabpc1l2* in each cell class. Cells that do not belong to the corresponding cell class are colored in gray. Detection rate and mean expression for (B) *Pabpc1* and (C) *Pabpc1l2* in each cell class. The number of cells detected in each cell class is shown as a fraction.

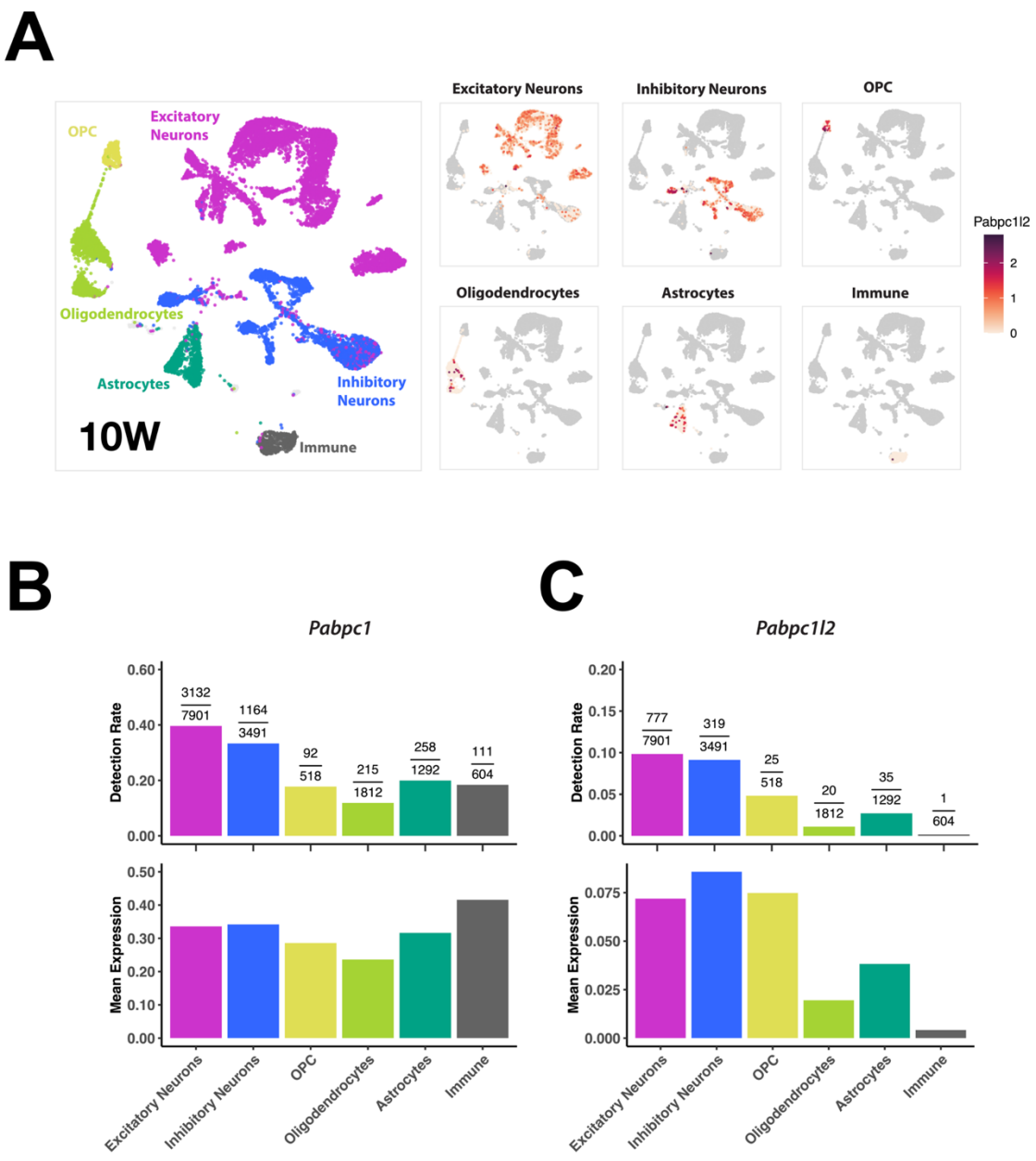

Figure 15. *Pabpc1l2* is expressed in neural cells at age of 10 weeks (C57BL/6J; Age: 2.5 months (or 10 weeks)). (A) Left: UMAP plot of single nuclei RNA-seq of adult mouse cortex (N = 16,153). Cells are colored by cell class. Right: UMAP plots displaying the expression of *Pabpc1l2* in each cell class. Cells that do not belong to the corresponding cell class are colored in gray. Detection rate and mean expression for (B) *Pabpc1* and (C) *Pabpc1l2* in each cell class. The number of cells detected in each cell class is shown as a fraction.

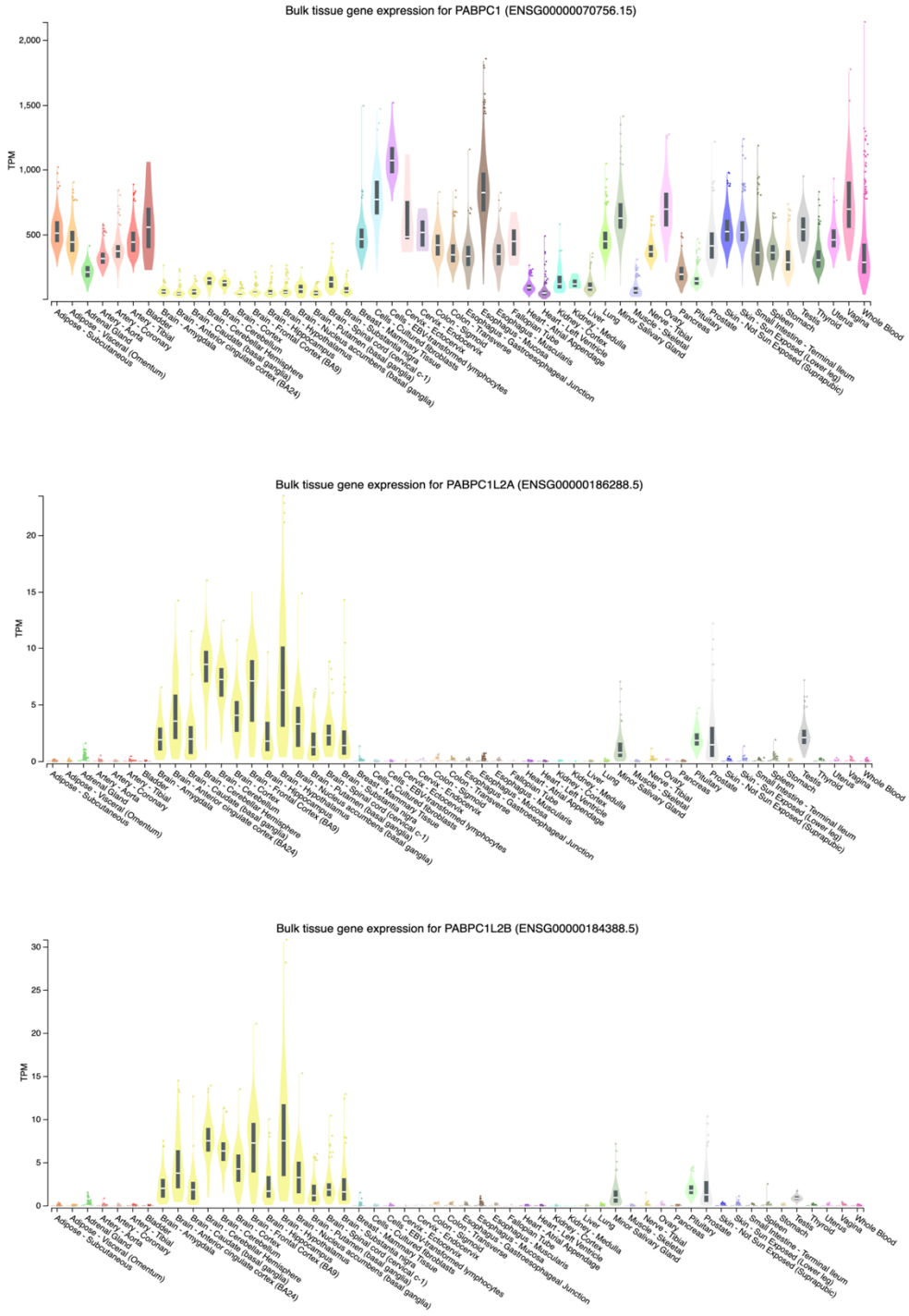

Figure 16. RNA expression of *Pabpc1* and *Pabc1l2a/b* across human tissues. Data was acquired from the Genotype-Tissue Expression (GTEx) database. Data is expressed as Transcripts Per Kilobase Million (TPM).

an open reading frame. To determine if *Pabpc1l2* is expressed at the protein level, we generated a polyclonal antibody that recognizes a peptide corresponding to the predicted mouse PABPC1L2 C-terminus (ERGAWARQSTSADFKDFD), a unique sequence that is not present in other proteins, including other PABPCs, including PABPC1 (**Figure 12**). To evaluate the specificity of our antibody, we transiently transfected HeLa cells with a plasmid coding for PABPC1L2 and carried out western blotting on lysates (**Figure 17A**). Importantly, our antibody identified ectopic PABPC1L2 in transfected cell lysates, but no corresponding band was observed in lysates derived from non-transfected cells. In keeping with *Pabpc1l2* mRNA expression patterns, western blotting analysis of mouse tissues using our antibody only detected a protein in neural tissues (**Figures 11D, 17B and 18**). In contrast, PABPC1 was detected in all somatic tissues, albeit at different levels of expression (**Figure 11D**). Thus, these data suggest that PABPC1L2 displays a neural-specific expression pattern, hence we termed it, neural PABP (neuPABP).

3.2. neuPABP contains a unique N-terminal domain of unknown function

Mouse *Pabpc1l2* mRNA is predicted to contain a 301 nt 5'UTR and an open reading frame (ORF) encoding a short protein (229 amino acids): neuPABP. However, endogenous neuPABP migrates at a higher position on SDS-PAGE (~48 kDa) than what would be predicted by its ORF. Using 5'RACE, we verified that the predicted *Pabpc1l2* mRNA 5' terminus is accurate (**Figure 19**). While it is possible that neuPABP maintains post-translational modifications that may alter its molecular weight, another explanation for this discrepancy is that the predicted ORF encoding neuPABP is incomplete. Thus, we set out to verify the sequence of full-length neuPABP. To this end, endogenous neuPABP was immunoprecipitated from adult mouse cortex lysate and subjected to mass spectrometry analysis to determine if neuPABP peptide coverage extends beyond its

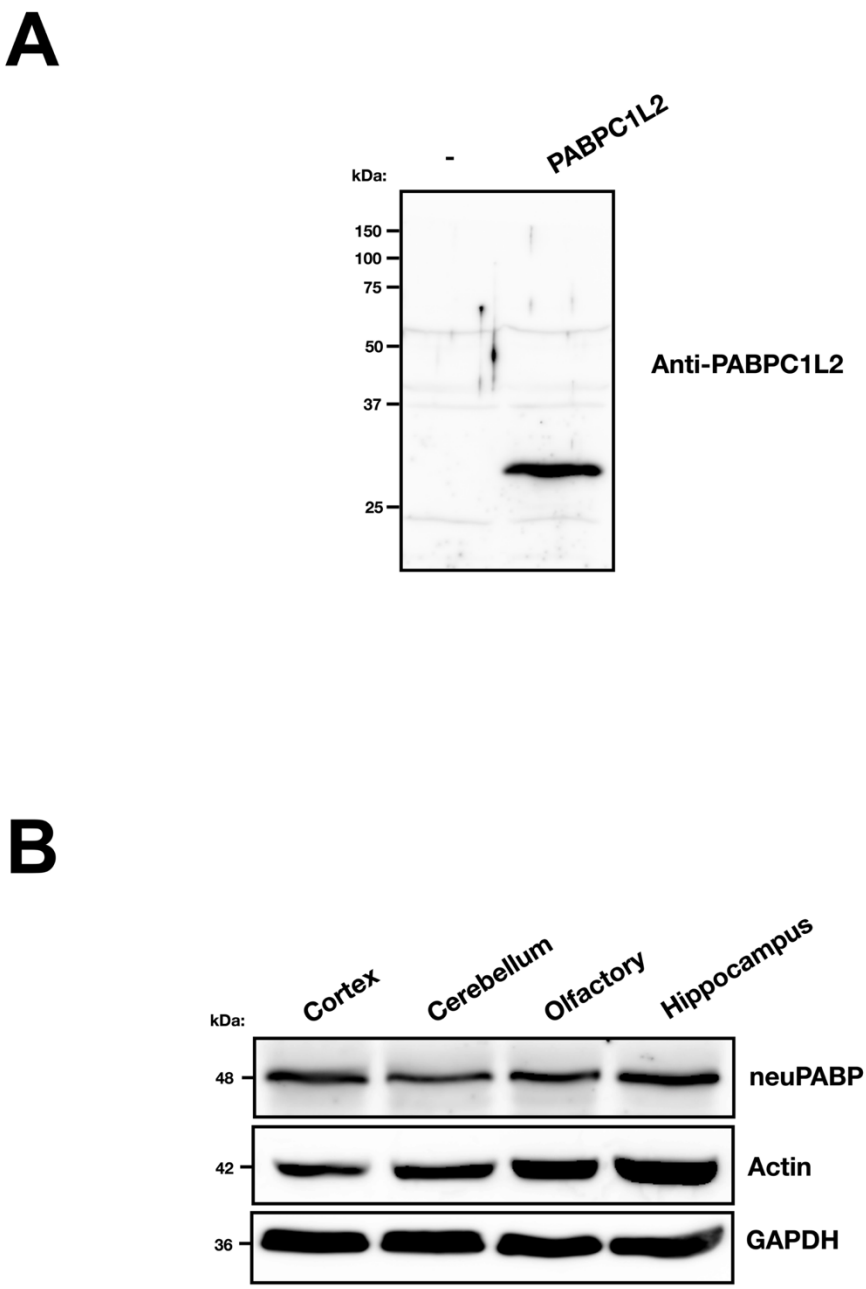

Figure 17. neuPABP antibody validation and probing of neural tissues (A) Western blot analysis using a PABPC1L2(neuPABP)-specific antibody of lysates generated from HeLa cells or HeLa cells transfected with a PABPC1L2-expressing plasmid. (B) Western blot analysis of neuPABP, Actin and GAPDH from lysates derived from adult mouse cortex, cerebellum, olfactory and hippocampus (C57BL/6J; Age: 5 months).

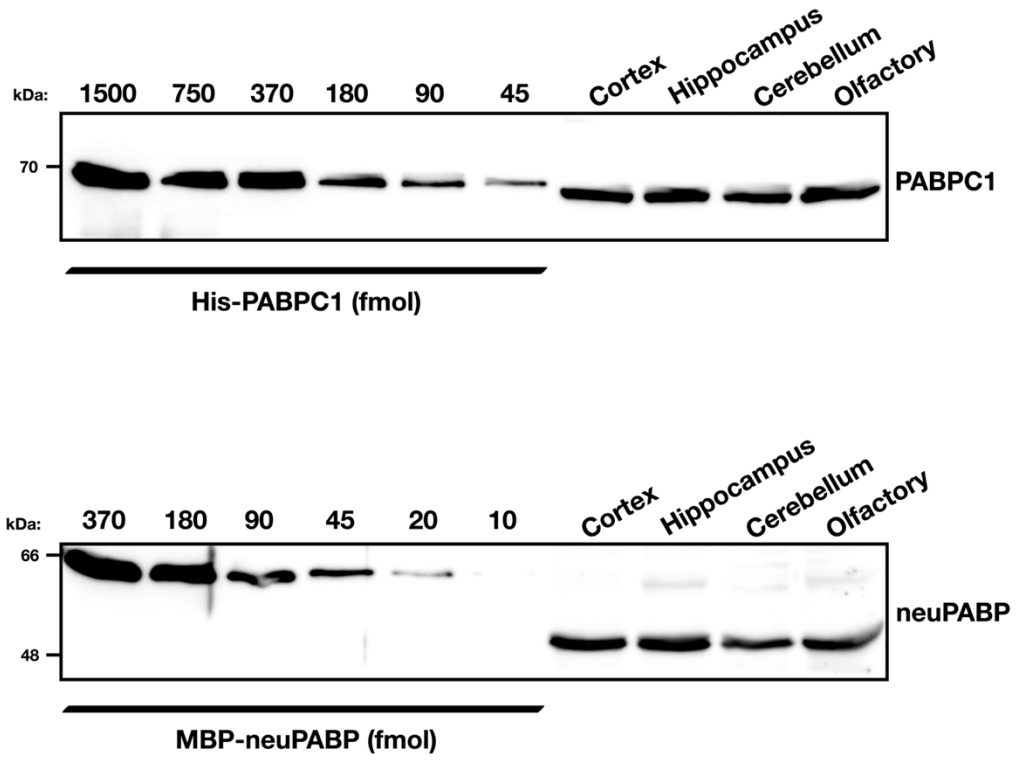

Figure 18. Quantification of PABPC1 and neuPABP expression in neural tissues. Western blot analysis on total lysates generated from adult mouse cortex, hippocampus, cerebellum and olfactory (C57BL/6J; Age: 5 months). Lysates were resolved by SDS-PAGE and western blot analysis was performed using antibodies against PABPC1 and neuPABP. Lysates were run alongside standard curves of recombinant His-tagged PABPC1 and Maltose binding protein (MBP)-tagged neuPABP to determine PABPC1 and neuPABP protein levels. PABPC1 and neuPABP levels vary between 370-180 fmol and 180-90 fmol, respectively among neural tissues.

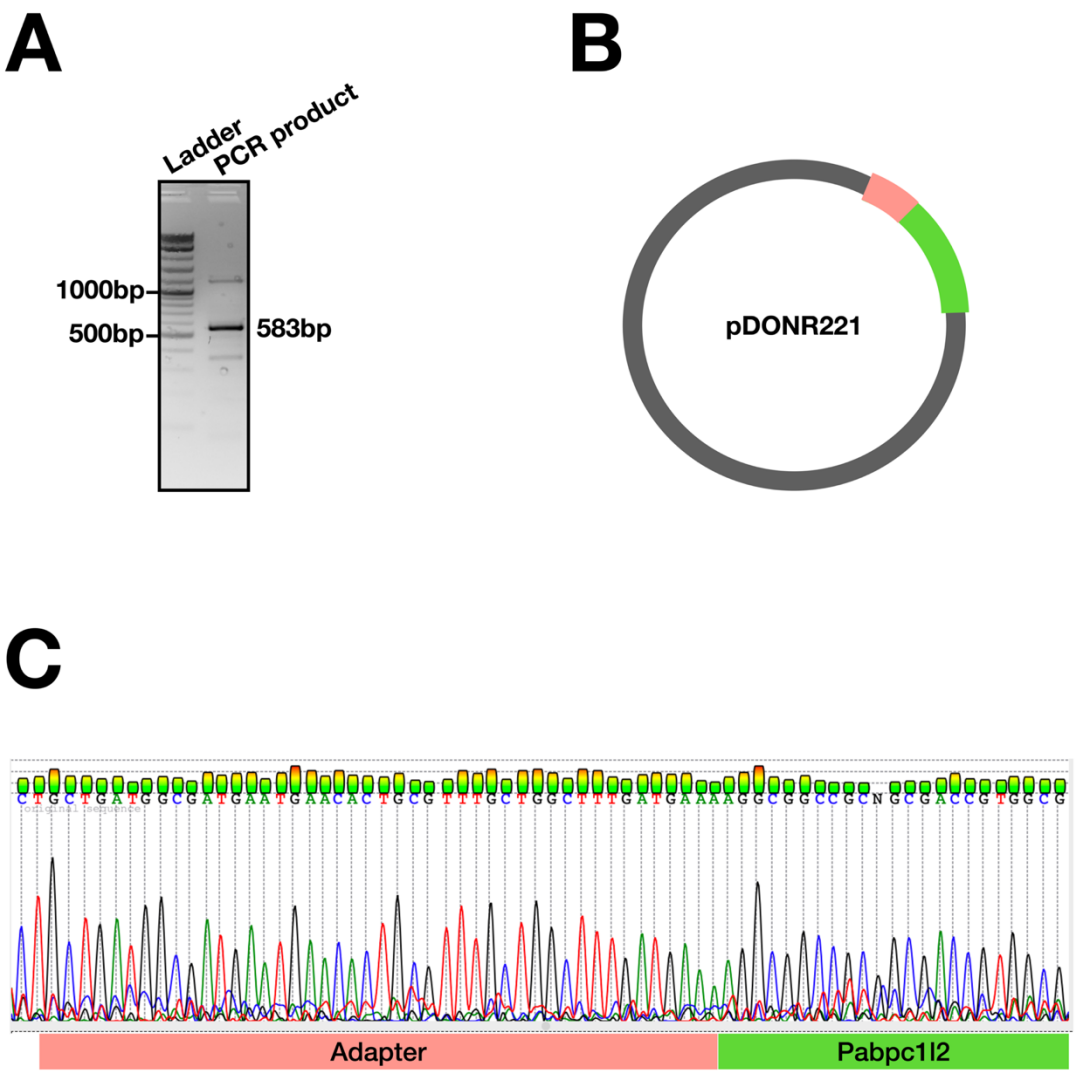

Figure 19. 5'RACE analysis of *Pabpc1l2* mRNA. RNAs were isolated from mouse primary neuronal cultures at DIV7, using Trizol reagent. RNAs were decapped, dephosphorylated, an adapter was ligated to the 5'end, and reverse transcribed (A) An adapter-specific forward and *Pabpc1l2*-specific reverse primer was used for PCR reaction. PCR products were cloned into pDONR221 (B) and sequenced. (C) Sequencing chromatogram showing the adapter sequence ligated to the *Pabpc1l2* mRNA 5'end.

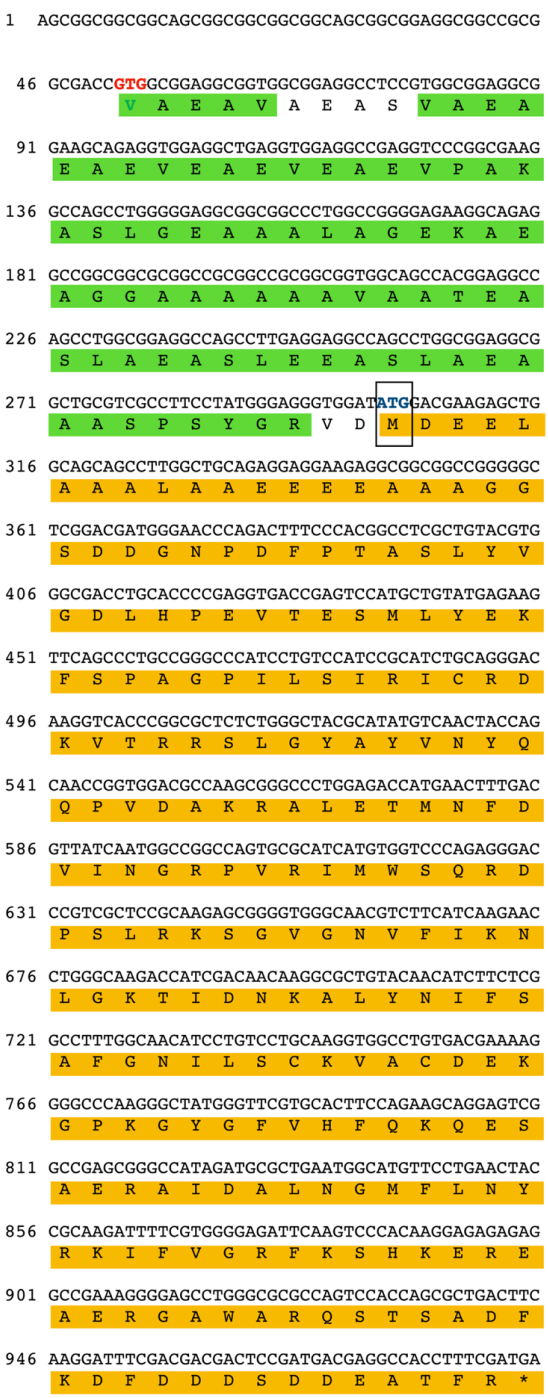

Figure 20. Nucleotide and amino acid sequence of mouse PABPC1L2 (neuPABP). Predicted ATG is boxed whereas the translation initiator GTG is red. Amino acids corresponding to the predicted neuPABP are highlighted yellow, whereas additional N-terminal peptides identified by mass spectrometry are highlighted green.

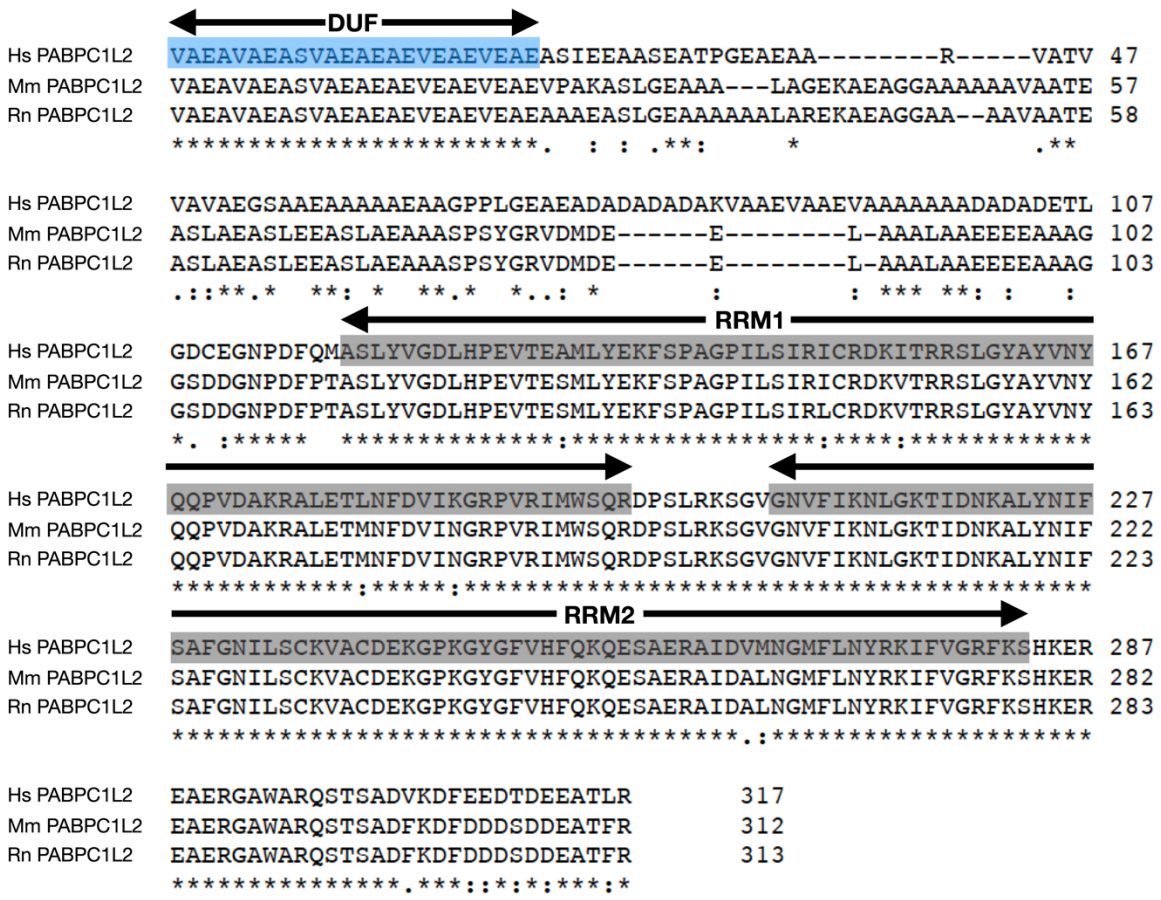

Figure 21. Comparative sequence analysis. Comparative sequence analysis of Human (Hs), Mouse (Mm) and Rat (Rn) PABPC1L2 open reading frames. Regions containing RNA recognition motifs (RRMs) and domain of unknown function (DUF) are marked by arrows.

predicted N- and C-termini. While we were unable to detect additional peptides C-terminal to the neuPABP stop codon, our analysis identified significant peptide coverage corresponding to the *Pabpc1l2* mRNA 5' UTR that is in frame with the predicted neuPABP open reading frame (**Figure 20**). This additional N-terminal sequence (83 amino acid) suggests that mouse neuPABP is 312 amino acids in length with a short (24 amino acid) conserved N-terminal domain of unknown function (DUF) comprised almost exclusively of valine, glutamate, and alanine amino acids. Interestingly, similar to the sequence conservation in RRMs, the DUF region is also predicted to be highly conserved across mammalian species **(Figures 21 and 22A).** This region has no initiator ATG codon; however, GTG at positions 53-55 (**Figure 20**) would code for the N-terminal valine identified by mass spectrometry analysis. Moreover, the sequence flanking this codon (gcggcgaccGUGgcg) is very similar to the Kozak consensus sequence for non-AUG initiators (gccgcca/gcc(nonAUG)ga/cu) (631, 632). To test this, a modified neuPABP ORF, along with all 5' terminal nucleotides, was fused to a C-terminal V5 tag and subsequently transfected into HeLa cells (**Figure 22B**). Western blotting with a V5 antibody demonstrated that this construct produced a ~48 kDa protein, similar to the size of endogenous neuPABP (**Figure 22C**). Moreover, mutating the initiator GUG in our construct to AUG generated a protein of similar size. This is in contrast to a construct with the predicted neuPABP ORF, which generated a significantly smaller protein (~28 kDa). Collectively, these data indicate that *Pabpc1l2* encodes a GUG-initiated ORF and that neuPABP contains a unique N-terminal domain that is not found in other PABPCs.

3.3. neuPABP is a bona fide PABP that is expressed during neuronal maturation

neuPABP is predicted to contain two RRMs that maintain a high degree of identity to RRMs 1 and 2 of PABPC1 (**Figure 12**). To determine if neuPABP can bind to RNA, we purified

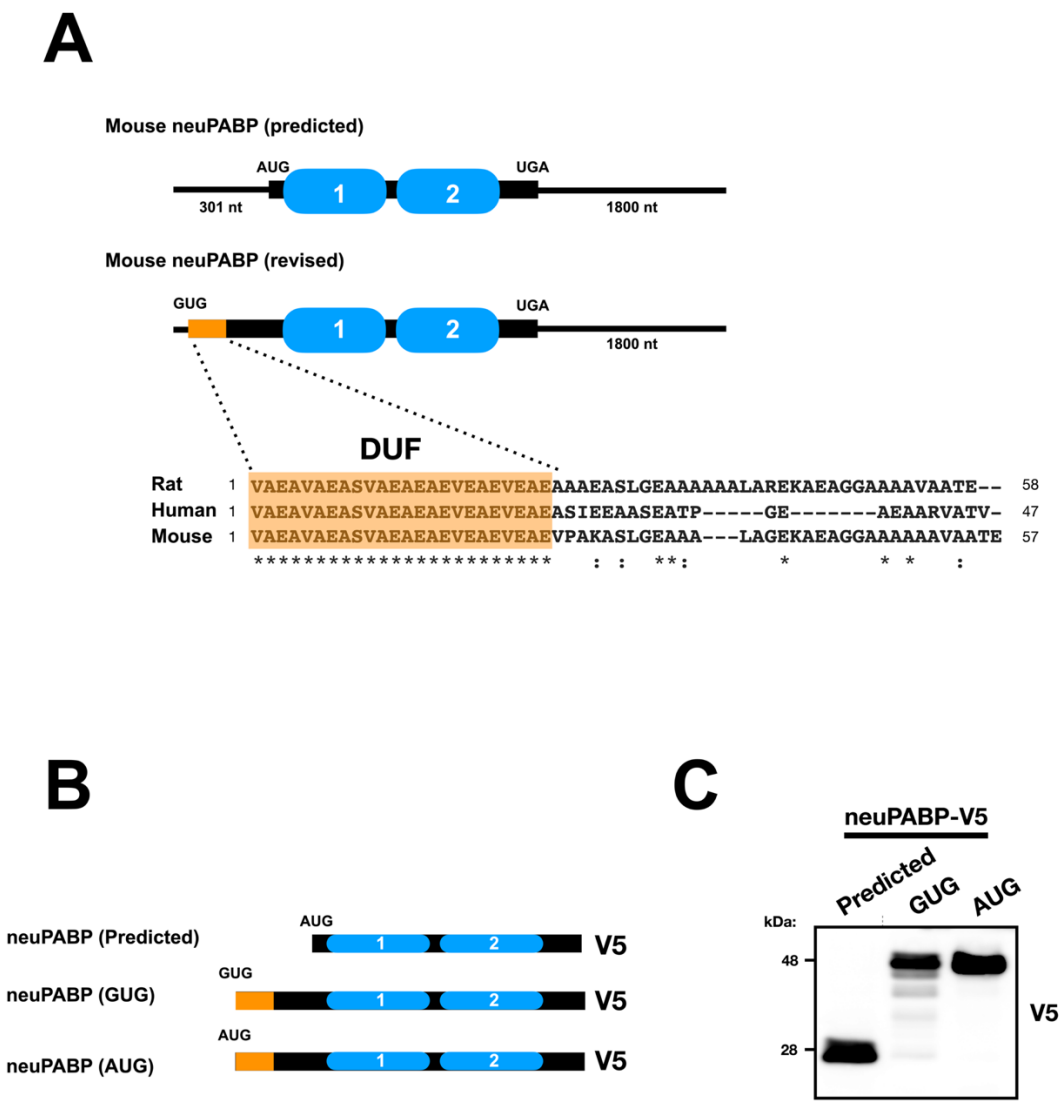

Figure 22. neuPABP is a GUG-initiated protein with a misannotated N-terminal extension. (A) Schematic diagram of predicted and revised neuPABP open reading frame, along with predicted AUG and validated GUG initiator codons, respectively. N-terminal region (highlighted in orange) corresponds to domain of unknown function (DUF) that is predicted to be conserved between human, mouse, and rat neuPABP. (B) Schematic diagram of mouse neuPABP expression constructs containing C-terminal V5 tags. (C) Western blot analysis of HeLa cells transfected with plasmids encoding V5-tagged predicted neuPABP or containing the *Pabpc1l2* 5'UTR containing the GTG codon or ATG codon.

recombinant (GST)-tagged neuPABP and carried out an *in vitro* selection— called RNAcompete (633) — by incubating GST-neuPABP with a complex collection of short RNAs. RNAcompete analysis identified 'AAAAAA' as the consensus binding motif for neuPABP, indicating the neuPABP is a true poly(A) binding protein (**Figure 23A**). To determine the affinity of neuPABP for poly(A) RNA, we purified recombinant PABPC1 and neuPABP (**Figure 23B**) and carried out electrophoretic mobility shift assays using a ^{32}P-end labelled $(A)_{25}$ oligoribonucleotide (**Figure 23C**). In keeping with the RNA compete data, we observed that neuPABP bound $(A)_{25}$ RNA with an affinity similar to that of PABPC1. Moreover, a secondary shift in neuPABP binding suggests that two neuPABP proteins can bind 25 As, as compared to PABPC1 where only a single protein can bind (242, 243).

Nuclear/cytoplasmic fractionation experiments on lysates derived from adult cortex tissue indicate that like PABPC1, neuPABP is a cytoplasmic PABP (**Figure 24A**). We next set out to determine the temporal expression of neuPABP during mouse brain development. To this end, we isolated the brains of mice at ages E13, E16, E18 as well as several postnatal ages. Lysates generated from isolated tissues were then resolved by SDS-PAGE and analyzed using antibodies against PABPC1, neuPABP, actin and beta-tubulin III (controls) **(Figure 24B)**. Strikingly, we observed that PABPC1 and neuPABP displayed opposing temporal expression patterns during brain development. PABPC1 was high expressed in embryonic tissues, but its levels were significantly lower in postnatal brain tissues. In contrast, neuPABP was barely detectable in embryonic brain tissue. However, its expression steadily increased during postnatal brain development, reaching a maximum at around P17 and remaining at this level into adulthood (**Figure 24B**). Interestingly, this period of expression coincided with synaptogenesis, where synapses are formed between

neurons and is one of the key events that takes place in rodents during the first few postnatal weeks of life (634). To determine if neuPABP displays a similar expression pattern during neuronal maturation in mice, we isolated mouse primary cortical neurons from P0 pups and cultured them to promote their maturation *in vitro*. Lysates were then generated from cultured neurons and resolved by SDS-PAGE. Similar to what we observed over the course of mouse brain development, neuPABP levels were barely detectable in newly cultured neurons. However, neuPABP expression rapidly increased over time, with its expression pattern overlapping with that of the synaptic marker PSD-95 (**Figure 24C**). Moreover, neuPABP levels in mature neurons approached those of PABPC1 as assessed by western blots using recombinant proteins ladders for direct comparisons (**Figure 25**).

In keeping with its expression during synaptogenesis, we also detected the subcellular localization of neuPABP in the synaptosomes, following synaptosome fractionation of mouse cortex. neuPABP was detected by western blotting in the PSD-95-enriched post-synaptic density (PSD) fraction (**Figure 24D**), whereas neuPABP was barely detectable in the non-PSD fraction, which was enriched in synaptophysin. This contrasts with PABPC1, which was equally detectable in both PSD and non-PSD fractions. In keeping with these data, proteomic analyses of isolated human neural tissues identified neuPABP peptides in synaptosomes and post-synaptic densities (635, 636). Taken together, these data indicate that neuPABP is a bona fide poly(A) binding protein whose expression coincides with synaptogenesis.

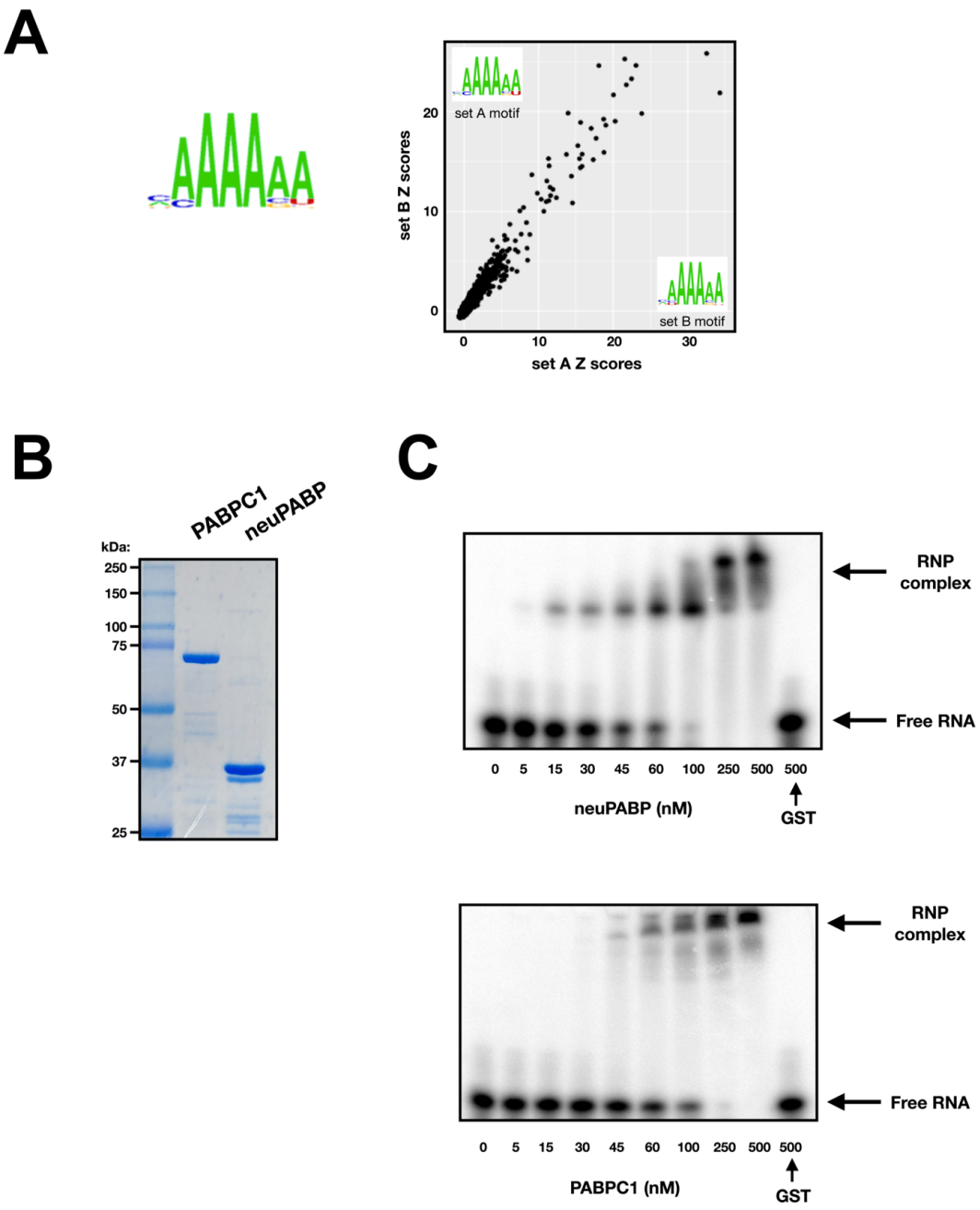

Figure 23. neuPABP specificity for poly(A) RNA. (A) Summary of RNAcompete experiments for GST-neuPABP. The sequence logo of the neuPABP RNA binding motif, along with the scatter plot displaying the *Z* scores and motifs for the two halves of the RNA pool (setA and setB) are shown. (B) Recombinant PABPC1 and neuPABP were analyzed by SDS-PAGE and Coomassie blue staining. (C) High-affinity binding of neuPABP to oligo(A) RNA. EMSA was carried out as described in methods. A constant amount of ^{32}P-oligo(A)$_{25}$ RNA was incubated with specific concentrations of neuPABP or PABPC1. The Kd value of ~50 nM was calculated from three biological experiments for both PABPC1 and neuPABP. Recombinant GST (control) did not lead to a gel shift of radiolabelled oligo.

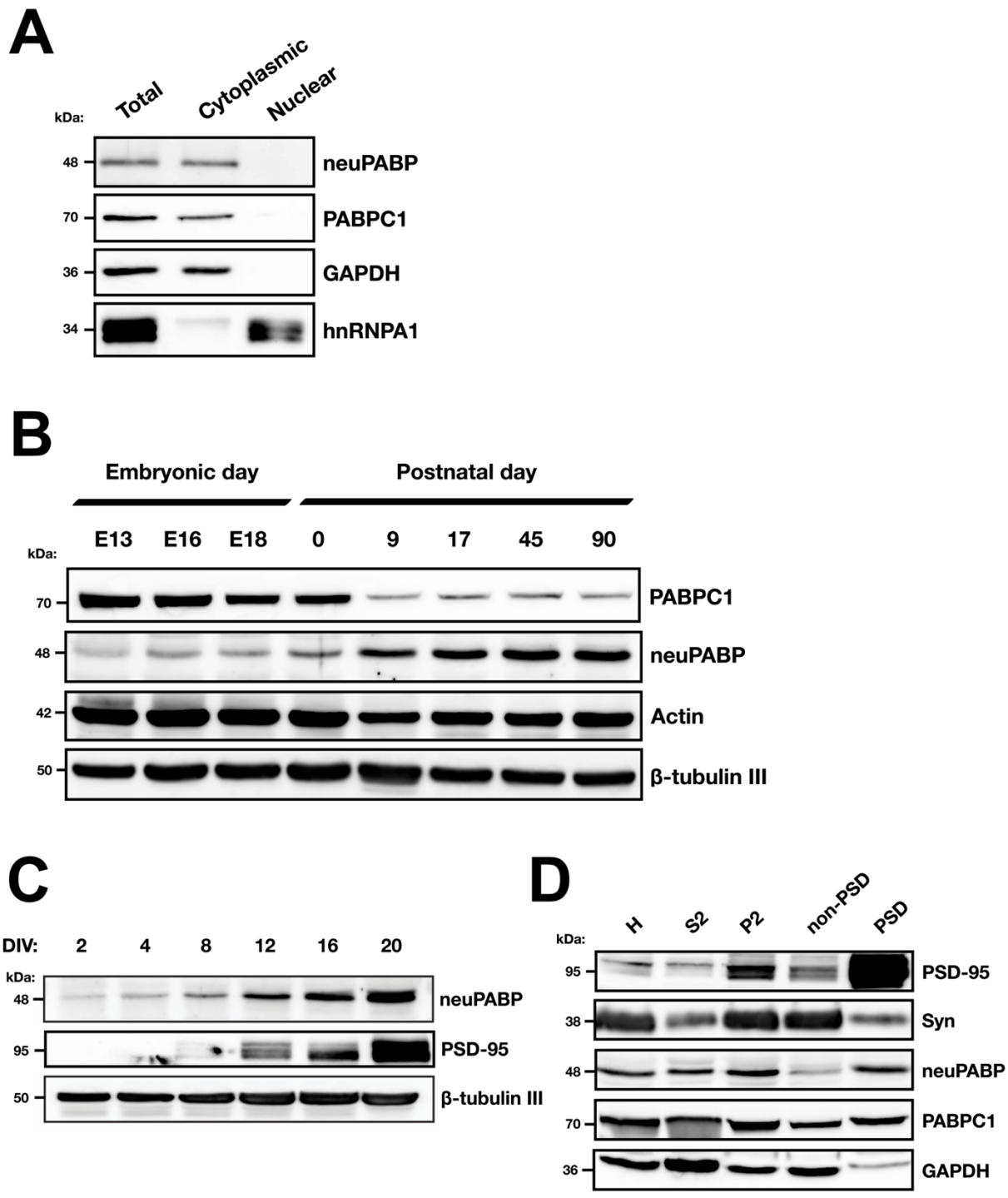

Figure 24. neuPABP is expressed during neuronal maturation. (A) Subcellular fractionation of adult mouse brain cortex (C57BL/6J; Age: 2 months) shows cytoplasmic localization of both neuPABP and PABPC1. GAPDH and hnRNPA1 were used as markers for cytoplasmic and nuclear fractions, respectively. (B) Western blot analysis of PABPC1, neuPABP, Actin and beta-tubulin III

on lysates prepared from mouse brain cortices isolated at different stages of embryonic and postnatal development. (C) Western blot analysis of neuPABP, PSD-95 and beta-tubulin III on lysates prepared from mouse primary cortical neurons. Neurons were isolated from p0 pups and cultured for defined days *in vitro* (DIV). (D) Western blot analysis of subcellular fractions of adult mouse cortex (C57BL/6J; Age: 6 months) prepared by synaptosome fractionation. Lysates were probed with the postsynaptic (PSD) marker PSD-95, the presynaptic marker synaptophysin (Syn), as well as neuPABP, PABPC1 and GAPDH. Cortex homogenates (H) were generated and supernatant (S2) and the crude synaptosomal pellet (P2) were acquired after high-speed centrifugation of S1 supernatant . The crude synaptosomal fraction was further fractionated into Triton X-100 soluble non-PSD fraction (extra-synaptic) and Triton X-100 insoluble PSD-containing fraction (synaptic).

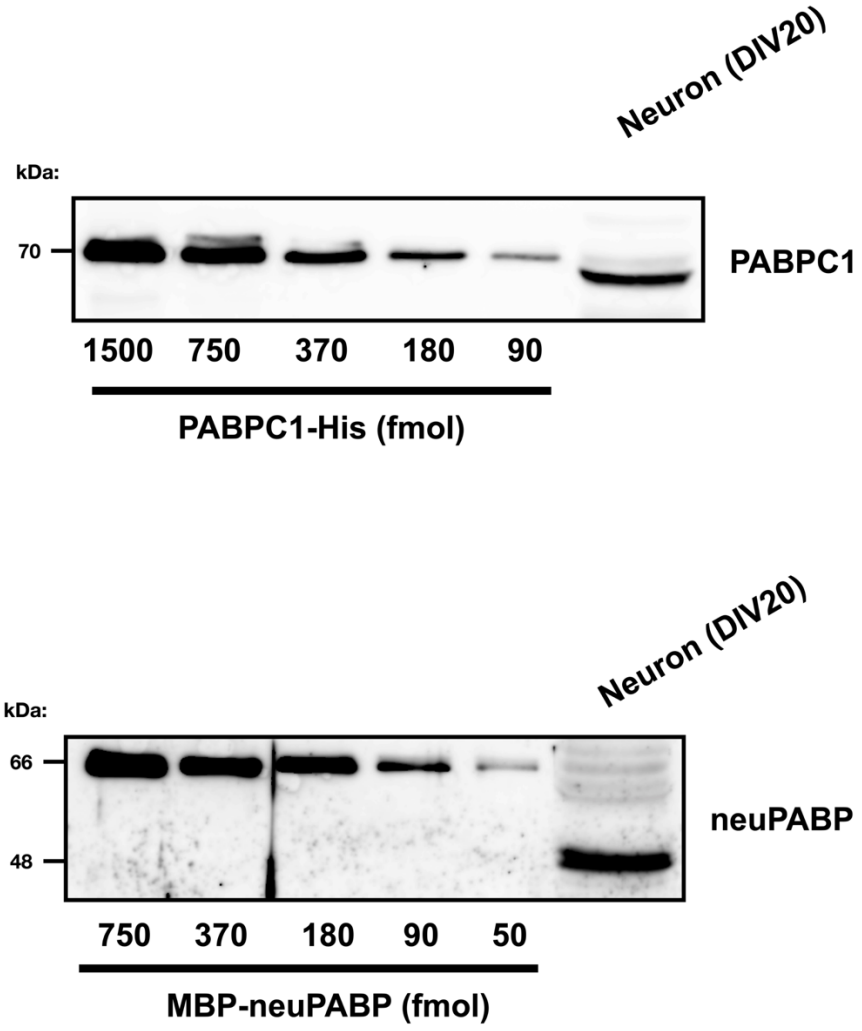

Figure 25. PABPC1 and neuPABP display equivalent expression in mature neurons. Western blot analysis of lysate generated from cultured mouse primary neurons (DIV20) and probed with antibodies against PABPC1 and neuPABP. Lysates were run alongside standard curves of recombinant His-tagged PABPC1 and Maltose binding protein (MBP)-tagged neuPABP to determine PABPC1 and neuPABP protein levels. PABPC1 and neuPABP levels displayed 1:1 ratio in mature neurons.

3.4. neuPABP interacts with BC1 RNA and select non-translating mRNAs.

As our data indicate that neuPABP can bind poly(A) RNA with similar affinity to PABPC1, we next wished to determine if neuPABP is associated with actively translating mRNAs. To this end, we isolated polysome profile fractions derived from P9 mouse cortex lysate (**Figure 26A**) and assessed the distributions of PABPC1 and neuPABP by western blotting (**Figure 26B**). Consistent with many studies, we observed PABPC1 throughout the polysome gradient, including in heavy polysome fractions that contain highly translated mRNAs (637, 638). In stark contrast, the vast majority of neuPABP did not sediment in heavy polysome fractions. Instead, neuPABP sedimented in early fractions, including those that contain free ribonucleoprotein (RNP) complexes, with a small amount of neuPABP in fractions that contain 40S subunits (**Figure 26B**). These data suggest that unlike PABPC1, neuPABP is not associated with actively translating mRNAs.

We next set out to identify RNAs associated with neuPABP by carrying out RNA-immunoprecipitation sequencing (RIP-Seq). Briefly, neuPABP-interacting RNAs were immunopurified with anti-neuPABP antibody from adult mouse hippocampal lysates in three biological replicates and sent for deep sequencing to identify neuPABP-enriched RNAs **(Figures 26C- E)**. The most highly enriched RNA associated with neuPABP was BC1 (brain cytoplasmic 1) **(Figure 26D)**, a neuron-specific non-coding RNA that contains an internal stretch of adenosines **(Figure 27A**) (461, 462). BC1 has been reported to play a role in translational repression and like neuPABP, also sediments in early polysome gradient fractions containing free RNP complexes (**Figures 27B-D)** (466, 472). Interestingly, BC1 RNA is developmentally upregulated in neurons (453), which mirrors the developmental expression of neuPABP **(Figure 28).** To verify that neuPABP can interact with BC1 RNA, HeLa cells were transfected with plasmids encoding

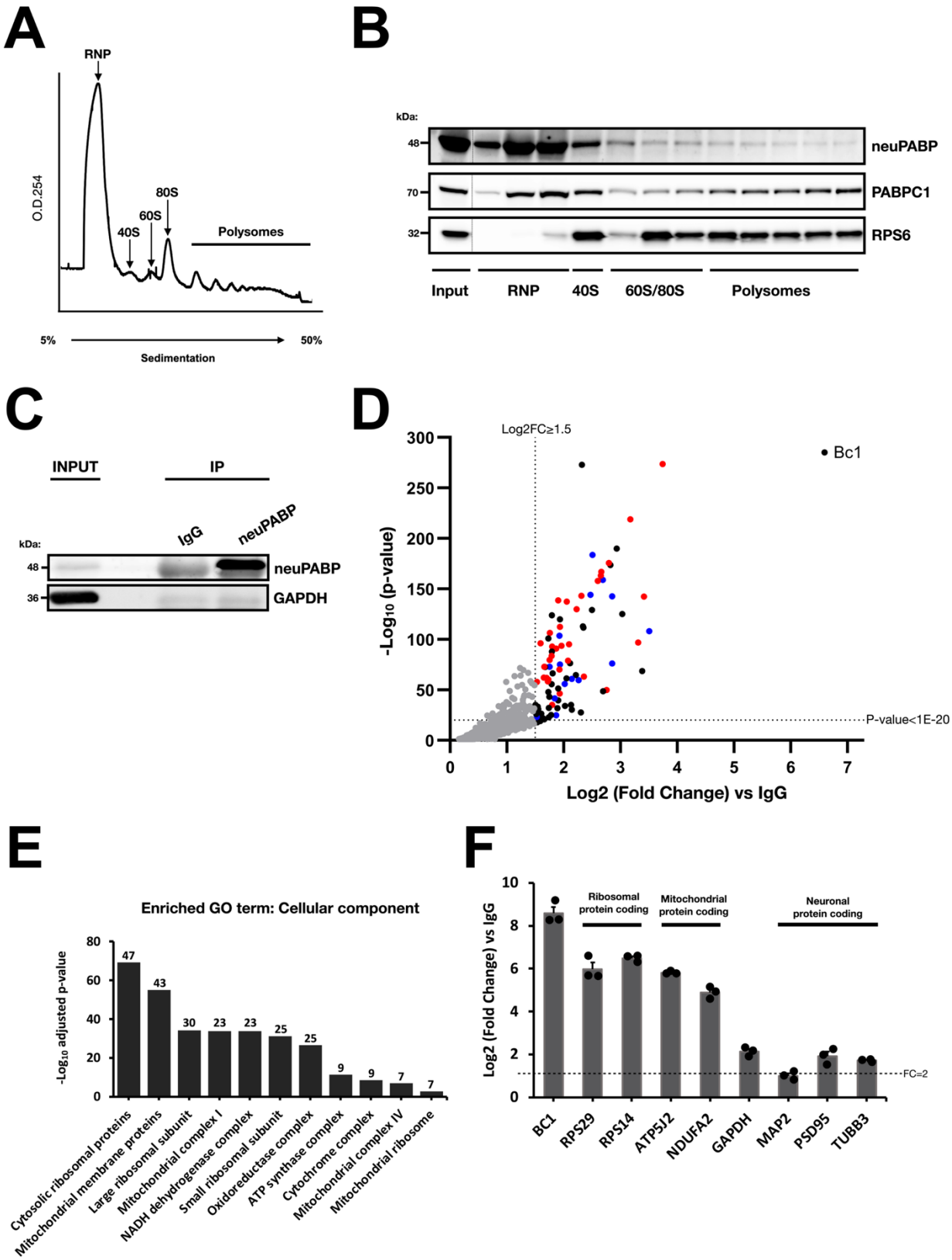
A
RNP
80S
60S
40S
Polysomes
O.D.254
5%
50%
Sedimentation
B
kDa:
48
70
32
neuPABP
PABPC1
RPS6
Input
RNP
40S
60S/80S
Polysomes
C
INPUT
IP
IgG
neuPABP
kDa:
48
36
neuPABP
GAPDH
D
Log2FC≥1.5
Bc1
-Log10 (p-value)
P-value<1E-20
Log2 (Fold Change) vs IgG
E
Enriched GO term: Cellular component
-Log10 adjusted p-value
47
43
30
23
23
25
25
9
9
7
7
Cytosolic ribosomal proteins
Mitochondrial membrane proteins
Large ribosomal subunit
Mitochondrial complex I
NADH dehydrogenase complex
Small ribosomal subunit
Oxidoreductase complex
ATP synthase complex
Cytochrome complex
Mitochondrial complex IV
Mitochondrial ribosome
F
Log2 (Fold Change) vs IgG
Ribosomal protein coding
Mitochondrial protein coding
Neuronal protein coding
FC=2
BC1
RPS29
RPS14
ATP5J2
NDUFA2
GAPDH
MAP2
PSD95
TUBB3

Figure 26. neuPABP localizes with early RNP fractions on polysome gradients and interacts with specific RNAs. (A) Polysome profile traces of lysates prepared from mouse cortices (C57BL/6J; Age: p9). (B) Lysates were fractionated by sucrose gradient centrifugation. Fractions were subsequently collected, TCA precipitated and resolved by SDS-PAGE and western blotting was subsequently performed using antibodies against neuPABP, PABPC1 and a ribosomal protein marker (RPS6). (C) Immunoprecipitation of neuPABP from adult mouse hippocampus (C57BL/6J; Age: 6 months). Immunoprecipitated complexes were subjected to SDS-PAGE and western blotting was performed using anti-neuPABP and anti-GAPDH antibodies. neuPABP-enriched RNAs were isolated using RNA purification kit (Qiagen) and identified by RNA-seq (D) Volcano scatter plot for the most significantly enriched RNAs with neuPABP vs IgG control (threshold set at Log2 FC≥1.5 and p-value at p<1E-20). BC1 RNA and mRNAs encoding ribosomal proteins (red) and nuclear-encoded mitochondrial proteins (blue) were enriched. (E) Top Wikipathway (WP) and associated gene ontology (GO) terms (cellular component) significantly enriched among proteins coded for by neuPABP-enriched mRNAs (FC≥2). The number above each column represents the number of genes associated with its corresponding term. (F) RT-qPCR analyses of neuPABP-enriched transcripts identified by RNA-seq. neuPABP was immunoprecipitated from adult mouse hippocampi (C57BL/6J; Age: 6 months) and associated RNAs were Trizol extracted. Error bars represent SEM from biological replicates (n=3), data points for biological replicates are shown as solid circles. Data were normalized to an *in vitro* transcribed RLuc spiked-in RNA.

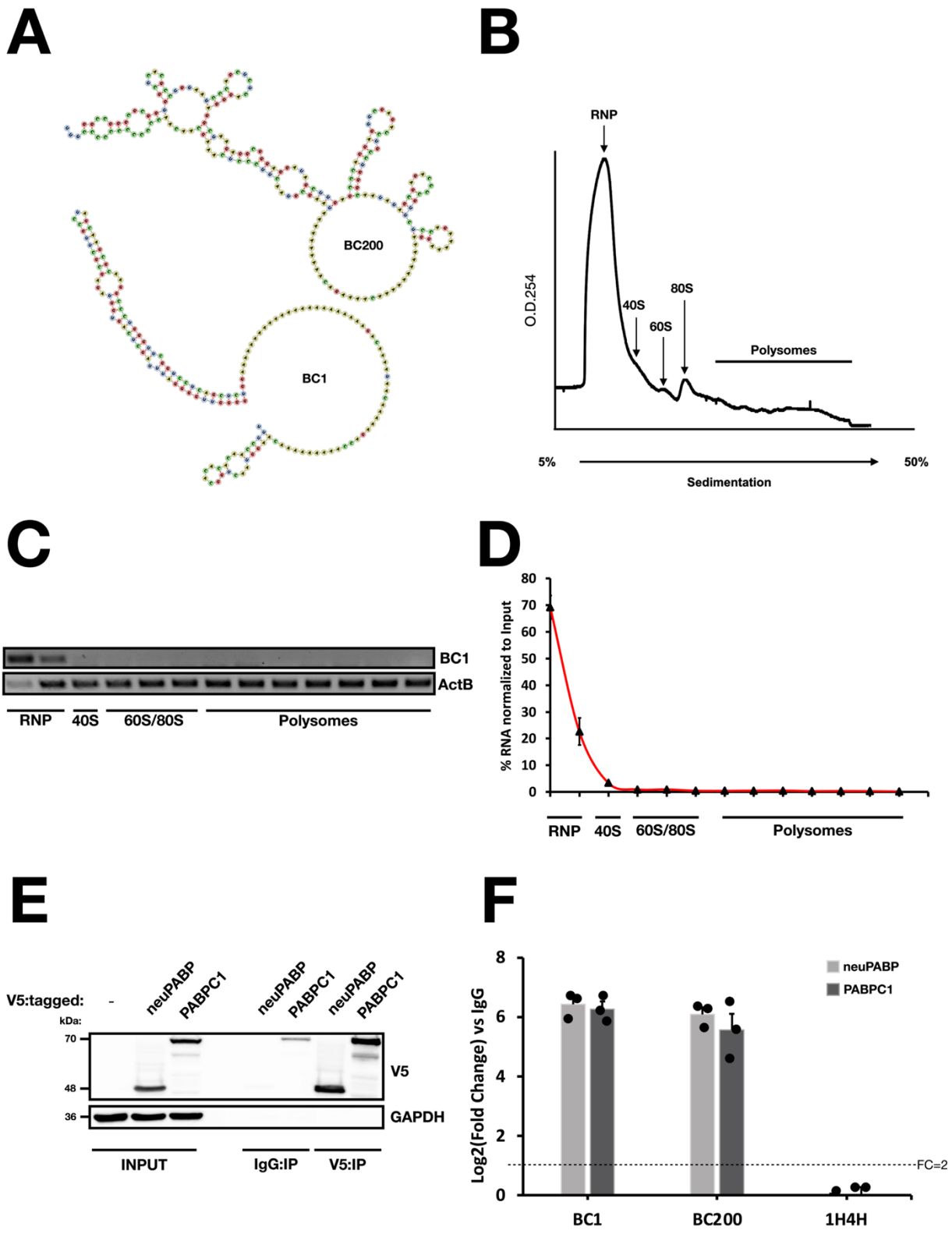
A
BC200
BC1
B
RNP
40S
60S
80S
Polysomes
O.D.254
5%
50%
Sedimentation
C
BC1
ActB
RNP
40S
60S/80S
Polysomes
D
% RNA normalized to Input
80
70
60
50
40
30
20
10
0
RNP
40S
60S/80S
Polysomes
E
V5:tagged:
-
neuPABP
PABPC1
neuPABP
PABPC1
neuPABP
PABPC1
kDa:
70
48
36
V5
GAPDH
INPUT
IgG:IP
V5:IP
F
Log2(Fold Change) vs IgG
8
6
4
2
0
neuPABP
PABPC1
FC=2
BC1
BC200
1H4H

Figure 27. neuPABP and PABPC1 display similar binding strength to BC RNAs. (A) Predicted structures of BC1 and BC200 RNAs by Vienna RNA Websuite (467), showing internal adenosine stretches in open conformation. (B-D) Lysates from adult mouse cortices (C57BL/6J; Age: 3 months) were fractionated by sucrose gradient centrifugation. (B) Shows polysome profile traces of the lysates. (C) Fractions from the polysome gradient were subsequently collected, RNA was Trizol extracted, reverse transcribed and semi-quantitative-PCR analysis was carried out on lncRNA Bc1 and Actin. (D) In parallel, qPCR analysis was carried out on BC1, and data was normalized to an Input sample (total cortex RNA) to calculate the percent distribution across fractions, error bars represent SEM from biological replicates (n=4). (E) Immunoprecipitation of V5-tagged neuPABP and V5-tagged PABPC1 from HeLa cells. (F) RNA immunoprecipitation (represented as Log2FC vs IgG) of BC1 and BC200 RNAs by V5-tagged neuPABP and V5-tagged PABPC1. A Histone RNA (1H4H), which lacks a poly(A) tail, was used as a negative control. Data were normalized to an *in vitro* transcribed RLuc spiked-in RNA. Error bars represent SEM from biological replicates (n=3), with data points for biological replicates shown as solid circles.

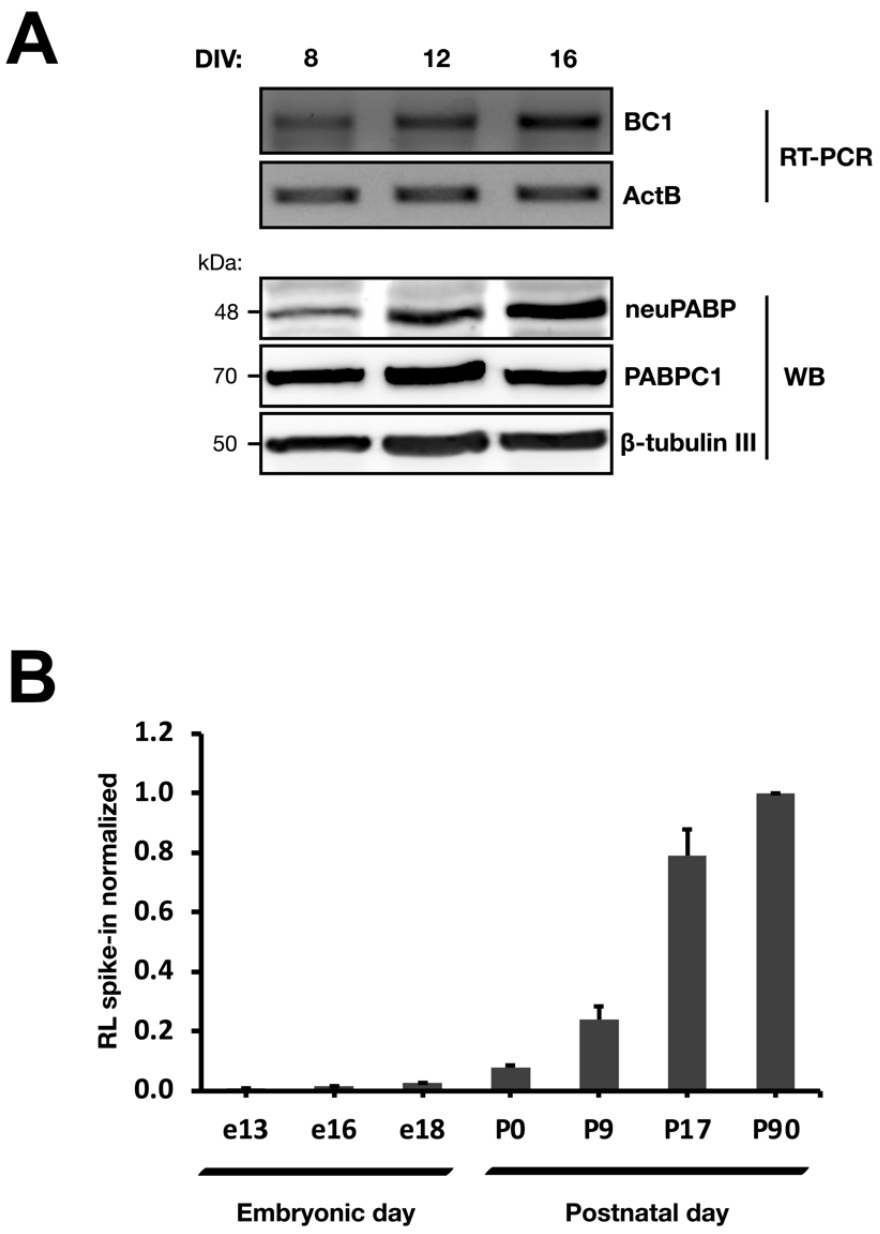

Figure 28. BC1 and neuPABP mirror expression during brain development (A) RT-PCR analysis of Bc1 and Actin (control) RNAs, and western blot (WB) analysis of neuPABP, PABPC1 and beta-tubulin III on lysates prepared from mouse primary cortical neurons. Neurons were isolated from p0 pups and cultured for defined days *in vitro* (DIV). (B) RT-qPCR analysis of Bc1 RNA from mouse brain cortices isolated at different stages of embryonic and postnatal development. An *in vitro* transcribed RLuc spike-in RNA was used for normalization. Expression of Bc1 in adult (P90) brain cortex was set to '1' to access the differential expression at different stages of brain development. Error bars represent SEM from three biological replicates (n=3).

V5-tagged neuPABP or V5-tagged PABPC1 and a plasmid that expresses the BC1 RNA. Ectopic PABPC1 and neuPABP, which were expressed at similar levels, were immunoprecipitated with V5 antibody and BC1 RNA association was assessed by RT-qPCR **(Figures 27E and F)**. We also tested if V5-tagged neuPABP could interact with BC200 RNA, a primate- and neuron-specific non-coding RNA that also contains a stretch of internal adenosines and that is expressed in Hela cells **(Figure 27A)** (456, 457, 639). While neither V5-neuPABP or V5-PABPC1 co-precipitated a histone mRNA (*1H4H*) lacking a poly(A) tail (control), BC1 and BC200 RNAs were equally enriched with both poly(A) binding proteins **(Figures 27E and F)**. In addition to interacting with BC1, our gene set enrichment analyses of neuPABP-interacting RNAs displayed an enrichment of mRNAs coding for ribosomal proteins and proteins with mitochondrial functions **(Figures 26D and E)**, which were subsequently validated by RT-qPCR analysis from hippocampal lysates (**Figure 26F**). These included ribosomal protein-encoding mRNAs (*RPS29 and RPS14*), mitochondrial protein-encoding mRNAs (*ATP5J2 and NDUFA2*). In contrast, other mRNAs coding for neuron-specific proteins (MAP2, PSD-95 and beta Tubulin III) displayed significantly lower enrichment with neuPABP.

As our data show that neuPABP sediments in early RNP fractions that contain untranslated RNAs, we next set out to determine if neuPABP directly binds the identified target RNAs in RNP fraction. As native RNA-protein interactions can be preserved by crosslinking, we formaldehyde-crosslinked adult mouse cortex tissue prior to generating lysates and carrying out polysome profiling. Early RNP fractions were isolated from polysome gradients (**Figures 29A and B)** and immunoprecipitated with IgG (control) or neuPABP antibody to isolate neuPABP-associated

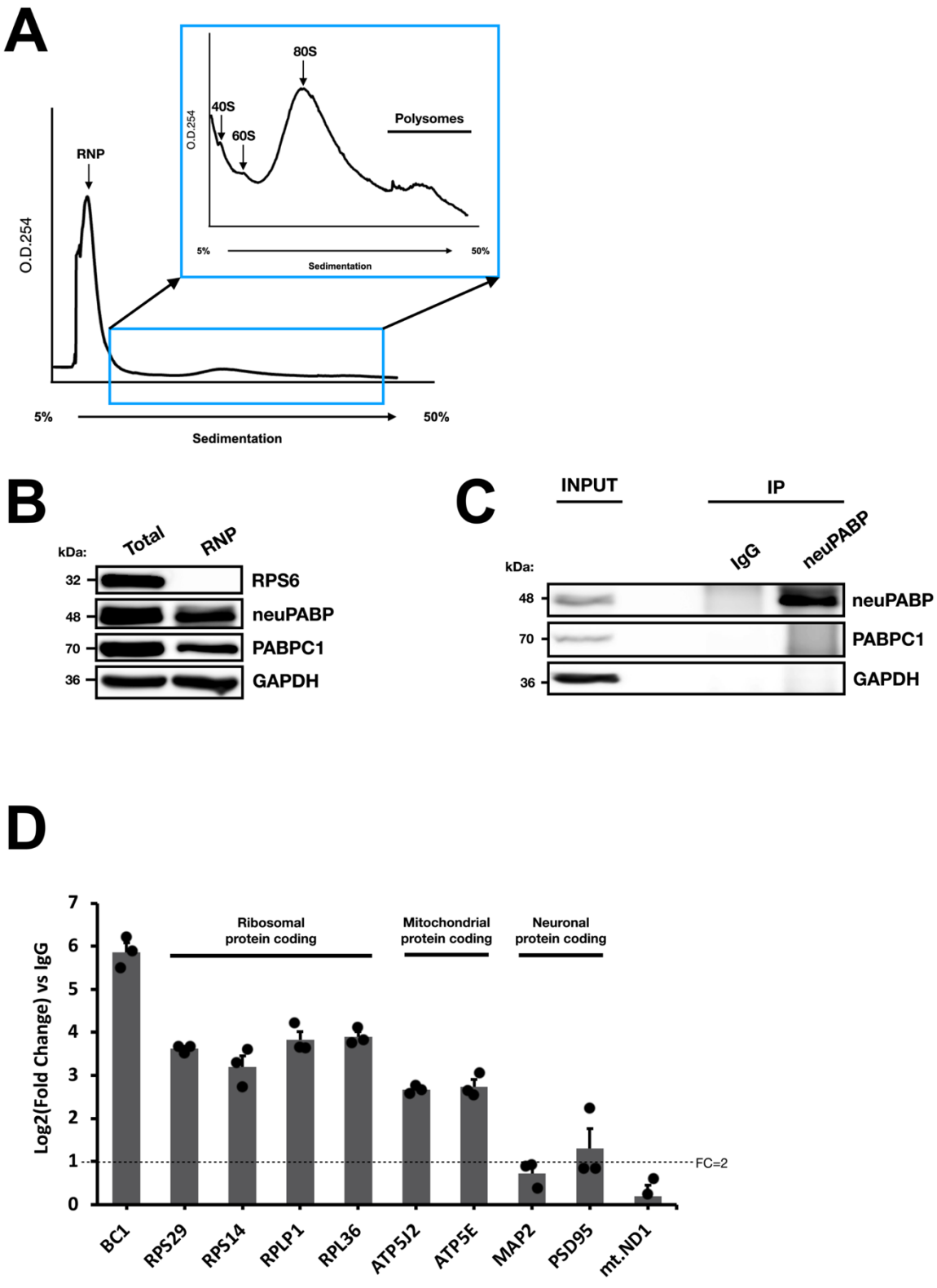
A
80S
40S
60S
Polysomes
O.D.254
RNP
5%
50%
Sedimentation
B
kDa:
Total
RNP
32
48
70
36
RPS6
neuPABP
PABPC1
GAPDH
C
INPUT
IP
IgG
neuPABP
kDa:
48
70
36
neuPABP
PABPC1
GAPDH
D
Log2(Fold Change) vs IgG
Ribosomal protein coding
Mitochondrial protein coding
Neuronal protein coding
FC=2
BC1
RPS29
RPS14
RPLP1
RPL36
ATP5J2
ATP5E
MAP2
PSD95
mt.ND1

Figure 29. neuPABP associates with untranslated mRNAs present in early RNP fraction. Cortices of adult mice (C57BL/6J; Age: 6 months) were triturated, and formaldehyde crosslinked. Lysates were prepared and fractionated by sucrose gradient centrifugation. (A) Ribosome traces of lysates prepared from formaldehyde crosslinked adult mouse cortices (C57BL/6J; Age: 6 months). (B) Free RNP fractions (depleted of ribosomal subunits) were collected from the polysome gradient, resolved by SDS-PAGE and western blotting was performed using antibodies against RPS6, neuPABP, PABPC1 and GAPDH. (C) Immunoprecipitation of neuPABP from free RNP fractions from (B). Immunoprecipitated complexes were resolved by SDS-PAGE and western blotting was performed using antibodies against neuPABP, PABPC1, and GAPDH. (D) RT-qPCR analysis of neuPABP-associated RNAs isolated from (C). Error bars represent SEM from biological replicates (n=3) and data points for biological replicates are shown as solid circles. A mitochondrial mRNA (mt.ND1) was used as a negative control. Data was normalized to an *in vitro* transcribed RLuc spiked-in RNA.

RNAs **(Figure 29C)**. Importantly, while early RNP fractions contained both neuPABP and PABPC1, PABPC1 did not co-precipitate with neuPABP **(Figure 29C)**. Nevertheless, BC1, and mRNAs coding for ribosomal and mitochondrial proteins were enriched with neuPABP as assessed by RT-qPCR analyses **(Figure 29D)**. In contrast, neuPABP pulled down significantly lower levels of two mRNAs coding for neuronal-specific proteins (PSD-95 and MAP2) and failed to interact with a mitochondrially-encoded *ND1* mRNA (control). Taken together, these data indicate that neuPABP interacts with BC1 non-coding RNA and select translationally inactive mRNAs populations.

3.5. neuPABP has lost its ability to interact with eIF4G and represses mRNA translation *in vitro*

Our data suggest that neuPABP associates with an abundant non-coding RNA, BC1. However, it also interacts with specific mRNAs that polysome profiling indicates are not being translated. As neuPABP is not associated with actively translating mRNAs, we next assessed the impact of neuPABP on protein synthesis using a Krebs cell-free *in vitro* translation (IVT) system. This system was previously used to biochemically determine that PABPC1 can function as a translation factor (142). To this end, we generated recombinant glutathione S-transferase (GST)-tagged neuPABP (**Figure 30A**) and added it to our IVT system. In contrast to recombinant glutathione S-transferase (GST), which did not affect protein synthesis, GST-tagged neuPABP inhibited the expression of a firefly luciferase (FL)-encoding polyadenylated mRNA in a dose-dependent manner (**Figure 30B**). In contrast, addition of neuPABP had no observable impact on the expression of an unadenylated FL reporter mRNA (**Figure 31**). Collectively, these data suggest that neuPABP can repress the translation of polyadenylated mRNAs *in vitro*.

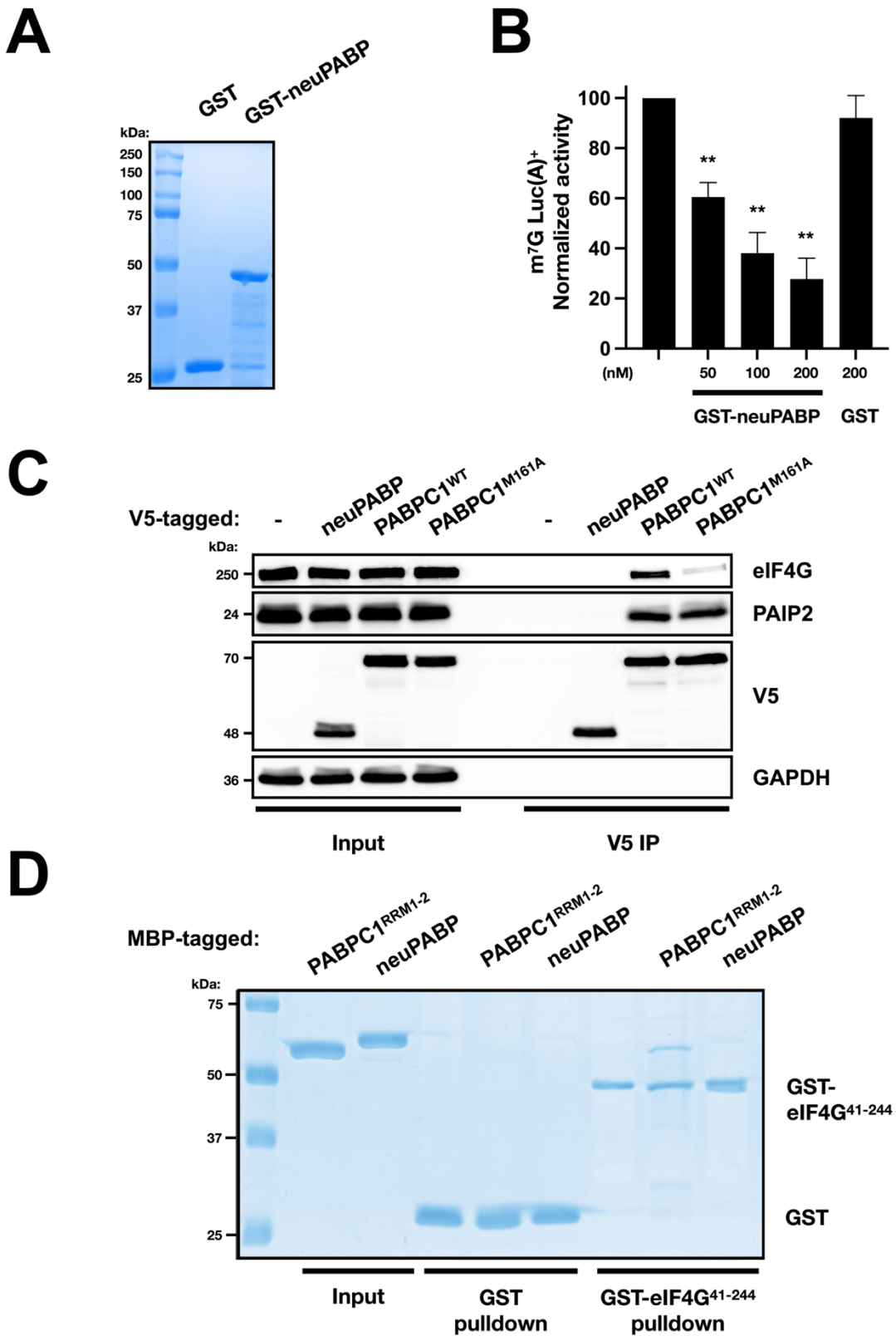
A
GST
GST-neuPABP
kDa:
250
150
100
75
50
37
25
B
m7G Luc(A)+ Normalized activity
100
80
60
40
20
0
**
**
**
(nM)
50
100
200
200
GST-neuPABP
GST
C
V5-tagged:
-
neuPABP
PABPC1WT
PABPC1M161A
-
neuPABP
PABPC1WT
PABPC1M161A
kDa:
250
24
70
48
36
eIF4G
PAIP2
V5
GAPDH
Input
V5 IP
D
MBP-tagged:
PABPC1RRM1-2
neuPABP
PABPC1RRM1-2
neuPABP
PABPC1RRM1-2
neuPABP
kDa:
75
50
37
25
GST-eIF4G41-244
GST
Input
GST pulldown
GST-eIF4G41-244 pulldown

Figure 30. neuPABP represses translation *in vitro* and does not interact with eIF4G. (A) Recombinant GST and GST-tagged neuPABP were prepared and were analyzed by SDS-PAGE and Coomassie blue staining. (B) Capped poly(A)+ luciferase reporter RNA was incubated in Krebs-2 extract. Reactions were supplemented with either buffer alone (Control), recombinant GST-neuPABP or GST alone, as indicated. Normalized luciferase activity was measured relative to control. Error bars represent SEM from biological replicates (n=3). A two-tailed Student t-test (equal variance) was conducted (versus control) to access significance, p-values<0.003, represented as '**', were calculated in GST-neuPABP treatment groups. (C) Immunoprecipitation of V5-tagged neuPABP, $PABPC1^{WT}$ or $PABPC1^{M161A}$ from HeLa cells. Immunoprecipitated complexes were subjected to SDS-PAGE and western blot analysis was performed using anti-V5, anti-eIF4G, anti-PAIP2 and anti-GAPDH antibodies. (D) Recombinant glutathione-S-transferase (GST) or GST-tagged $eIF4G^{41-244}$ were incubated with maltose-binding protein (MBP)-tagged PABPC1RRM1+2, or neuPABP. Precipitated proteins were separated by SDS-PAGE and visualized by Coomassie blue staining.

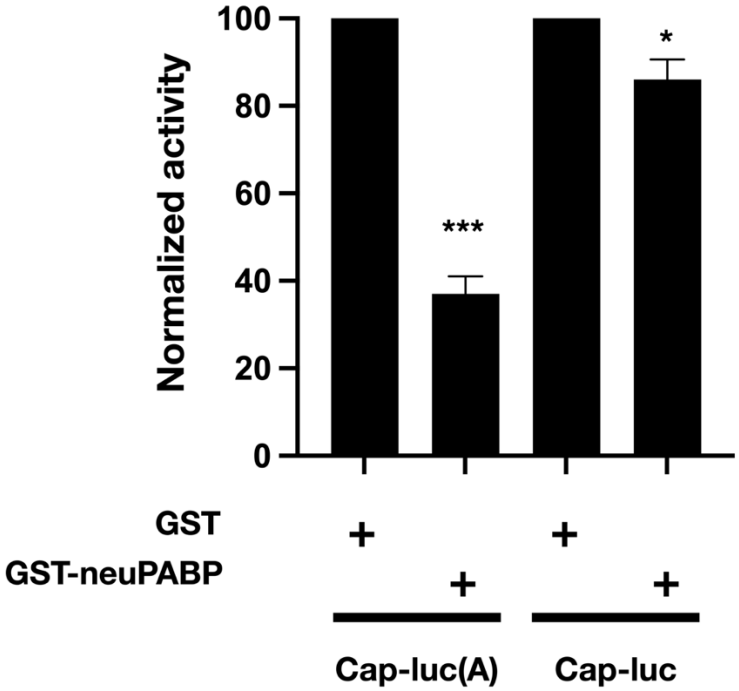

Figure 31. neuPABP represses translation in cap- and poly(A) dependent manner. Capped poly(A)+ or poly(A)- luciferase reporter RNA was incubated in Krebs-2 extract. Reactions were supplemented with either recombinant GST-neuPABP or GST alone (control), as indicated. Normalized luciferase activity was measured relative to GST. Error bars represent SEM from biological replicates (n=3). A two-tailed Student t-test (equal variance) was conducted (versus GST) to access significance, p-value<0.001, represented as '***', was calculated in GST-neuPABP treatment of Capped poly(A)+ luciferase reporter RNA.

PABPC1 stimulates mRNA translation by directly binding to eIF4G via RRM2 (142, 143). neuPABP also contains RRM2, yet paradoxically represses protein synthesis *in vitro*. To test if neuPABP can bind eIF4G, HeLa cells were transfected with plasmids encoding V5-tagged neuPABP, wild-type PABPC1 or a PABPC1 mutant (M161A) that disrupts its interaction with eIF4G (control) (142). V5-PABPC1^{WT}, V5-PABPC1^{M161A} and V5-neuPABP were affinity-purified with V5 antibody and co-immunoprecipitating proteins were resolved by SDS-PAGE followed by western blotting (**Figure 30C**). As expected, V5-PABPC1^{WT} co-precipitated both eIF4G and Paip2, whereas V5-PABPC1^{M161A} failed to efficiently interact with eIF4G. As neuPABP lacks a C-terminal MLLE domain, it was not surprising that it did not interact with Paip2, which uses this domain to interact with PABPC1 (315). However, even though neuPABP contains RRM2, it failed to associate with eIF4G. To determine if neuPABP can directly contact eIF4G, we performed *in vitro* pull-down assays using a recombinant GST-tagged fragment of eIF4G (amino acids 41-244) that directly binds PABPC1 (142), and maltose-binding protein (MBP)-fused neuPABP or a PABPC1 fragment containing RRMs 1 and 2 (**Figure 30D**). In keeping with previous reports, GST-eIF4G$^{41-244}$ efficiently bound MBP-PABPC1^{RRM1+2}. However, MBP-neuPABP failed to bind to this eIF4G fragment.

PABPC1 utilizes several amino acids in RRM2 to directly contact eIF4G (143) (**Figure 32A**). While neuPABP also contains RRM2 and binds poly(A) RNA, a comparative sequence analysis of the neuPABP RRM2 reveals non-conservative substitutions in two of the amino acids that PABPC1 utilizes to interact with eIF4G. In addition, while neuPABP maintains a methionine corresponding to M161 in PABPC1, it also contains an adjacent phenylalanine substitution.

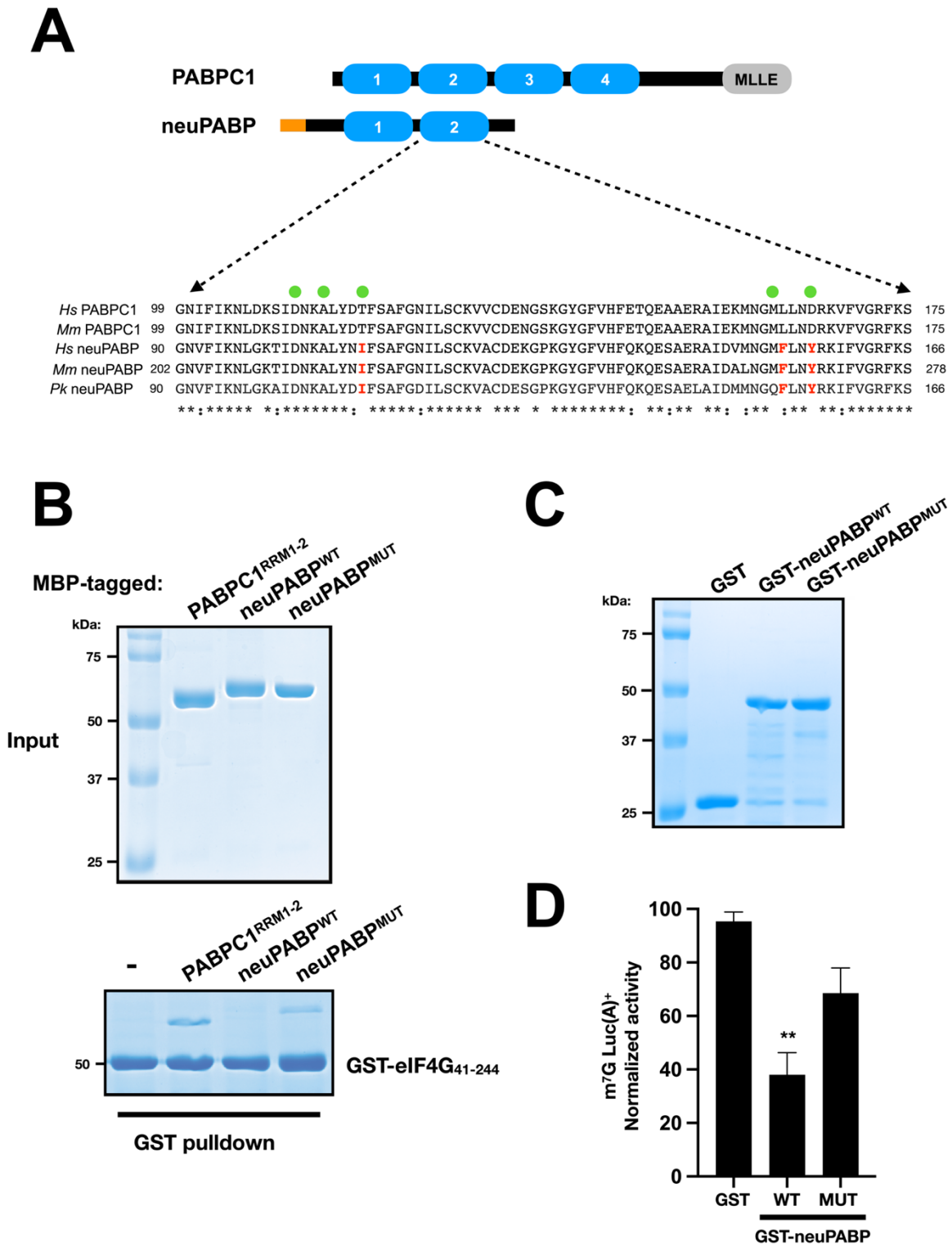
A
PABPC1
1
2
3
4
MLLE
neuPABP
1
2
Hs PABPC1 99 GNIFIKNLDKSIDNKALYDTFSAFGNILSCKVVCDENGSKGYGFVHFETQEAAERAIEKMNGMLLNDRKVFVGRFKS 175
Mm PABPC1 99 GNIFIKNLDKSIDNKALYDTFSAFGNILSCKVVCDENGSKGYGFVHFETQEAAERAIEKMNGMLLNDRKVFVGRFKS 175
Hs neuPABP 90 GNVFIKNLGKTIDNKALYNIFSAFGNILSCKVACDEKGPKGYGFVHFQKQESAERAIDVMNGMFLNYRKIFVGRFKS 166
Mm neuPABP 202 GNVFIKNLGKTIDNKALYNIFSAFGNILSCKVACDEKGPKGYGFVHFQKQESAERAIDALNGMFLNYRKIFVGRFKS 278
Pk neuPABP 90 GNVFIKNLGKAIDNKALYDIFSAFGDILSCKVACDESGPKGYGFVHFQKQESAELAIDMMNGQFLNYRKIFVGRFKS 166
B
MBP-tagged:
PABPC1RRM1-2
neuPABPWT
neuPABPMUT
kDa:
75
50
37
25
Input
-
PABPC1RRM1-2
neuPABPWT
neuPABPMUT
50
GST-eIF4G41-244
GST pulldown
C
GST
GST-neuPABPWT
GST-neuPABPMUT
kDa:
75
50
37
25
D
m7G Luc(A)+ Normalized activity
100
80
60
40
20
0
**
GST
WT
MUT
GST-neuPABP

Figure 32. neuPABP has been selected to not bind eIF4G. (A) Schematic diagrams of PABPC1 and neuPABP domain organization, along with a comparative sequence analysis of human (Hs) and mouse (Mm) PABPC1 with human, mouse, and bat (Pk) neuPABP RRM2. Amino acids that play a role in PABPC1 binding to eIF4G are denoted with a green dot. Corresponding amino acids, or those in proximity to eIF4G-intearcting residues, are red. (B) Recombinant glutathione-S-transferase (GST)-tagged $eIF4G^{41-244}$ was incubated with maltose-binding protein (MBP)-tagged $PABPC1^{RRM1+2}$, $neuPABP^{WT}$ or $neuPABP^{MUT}$ (Ile221Thr, Phe265Leu, Tyr268Asp). Precipitated proteins were separated by SDS-PAGE and visualized by Coomassie staining. (C) Recombinant GST, GST-tagged $neuPABP^{WT}$ and $neuPABP^{MUT}$ proteins were analyzed by SDS-PAGE and Coomassie blue staining. (D) Capped poly(A)+ luciferase reporter RNA was incubated in Krebs-2 extract. Reactions were supplemented with either recombinant GST, GST-$neuPABP^{WT}$ or GST-$neuPABP^{MUT}$, as indicated. Normalized luciferase activity was measured relative to GST. Error bars represent SEM from biological replicates (n=3). A two-tailed Student t-test (equal variance) was conducted (versus GST) to access significance, p-value<0.004, represented as '**', was calculated in GST-$neuPABP^{WT}$ treatment.

To determine if the ability of neuPABP fails to bind eIF4G due to substitutions in these key amino acids, we mutated these corresponding amino acids in tandem in MBP-neuPABP to those in PABPC1 [MBP-neuPABP^{MUT}(Ile221Thr, Phe265Leu, Tyr268Asp)]. While GST-eIF4G$^{41-244}$ did not interact with MBP-neuPABP^{WT}, it efficiently bound MBP-neuPABP^{MUT} (**Figure 32B**). Moreover, while GST-neuPABP^{WT} repressed protein synthesis *in vitro*, incubating GST-neuPABP^{MUT} in Krebs extract did not (**Figures 32C and D**). Taken together, these data suggest that neuPABP does not support mRNA translation due to its inability to interact with eIF4G.

The RESULTS sections 3.1 to 3.5 are from the published manuscript:

Title: *Uncovering a mammalian neural-specific poly(A) binding protein with unique properties.*
Authors: Sahil Sharma*, Sam Kajjo, Zineb Harra, Benedeta Hasaj, Victoria Delisle, Debashish Ray, Rodrigo L Gutierrez, Isabelle Carrier, Claudia Kleinman, Quaid Morris, Timothy R. Hughes, Roderick McInnes, and Marc R. Fabian*
Journal: *Genes and Development (Impact factor: 12.89)*
**First author*

PREFACE: neuPABP binds to non-translating RNAs in synapses

In sections 3.6 to 3.8, we set out to study the cellular localization and investigate the function of neuPABP in neuronal RNA metabolism. To this end, we have identified neuPABP as a synaptically localized RNA binding protein that binds to select neurite-enriched RNAs. Importantly, while PABPC1 also associates with neuPABP targeted mRNAs, we show that neuPABP and PABPC1 interact with the RNAs in a mutually exclusive manner. We also show that in contrast to PABPC1, which associates with actively translated mRNAs, neuPABP associates with translationally dormant synaptic RNAs. Additionally, similar to other well-known neuronal RNA granule proteins, like PURα and SYNCRIP, neuPABP is enriched in RNA granules and colocalizes with the RNA granule marker protein, PURα in neuronal soma and dendrites. Finally, we show that BC1 RNA levels are elevated in the brain tissues of a neuPABP^{KO} mouse model that we have acquired recently. Finally, we demonstrate that neuPABP specifically represses cap- and poly(A)-dependent translation with no impact on IRES-mediated translation of a bicistronic reporter *in cellulo.*

3.6. neuPABP binds neurite-enriched RNAs and is enriched in synaptic non-translating RNP fractions

Our RIP-seq data from mouse hippocampus showed that neuPABP binds select classes of nuclear-encoded mRNAs (ribosomal and mitochondrial proteins) and the neuron-specific non-coding BC1 RNA (**Figures 26C-F**). Interestingly, numerous transcriptomics studies have now identified RNAs localized in neuronal neurites, including mRNAs coding for ribosomal and mitochondrial proteins (97, 166, 378, 419-422). To specifically study the localization of neuPABP associated RNAs in neurites, we compared our list of 196 neuPABP bound RNAs (FC≥2) with two studies that focused on the local transcriptomes in neuronal dendrites [(97, 422), **Figure 33A**]. Our comparison yielded a list of 128 neuPABP-bound RNAs that were reported to localize in neurites by both studies **(Figure 33B).** The list included many large and small ribosomal subunit proteins coding mRNAs (37 mRNAs), as well as mitochondrial proteins coding mRNAs (23 mRNAs). These analyses suggested that majority of neuPABP bound RNAs are present in dendritic compartments. This led us to ask if neuPABP associates with target RNA in synaptic fractions. To this end, we fractionated adult mouse brain cortex tissue and collected synaptosome fractions. The quality of synaptosome fraction was confirmed by western blot analyses for pre- and postsynaptic marker proteins, synaptophysin (Syn) and PSD-95, respectively, in comparison to total brain homogenate. Importantly, only a minimal contamination was observed for a glial marker protein, GFAP **(Figures 34A and B)**. Synaptic localization was confirmed for neuPABP, PABPC1, and PABPC-interacting protein (PAIP2) which was shown previously to regulate PABPC1 function in synaptic terminals (640). Importantly, both neuPABP and PABPC1 were present in equal amount in synaptosomes as assessed by western blotting using recombinant proteins ladders for direct comparisons **(Figure 34C)**.

A

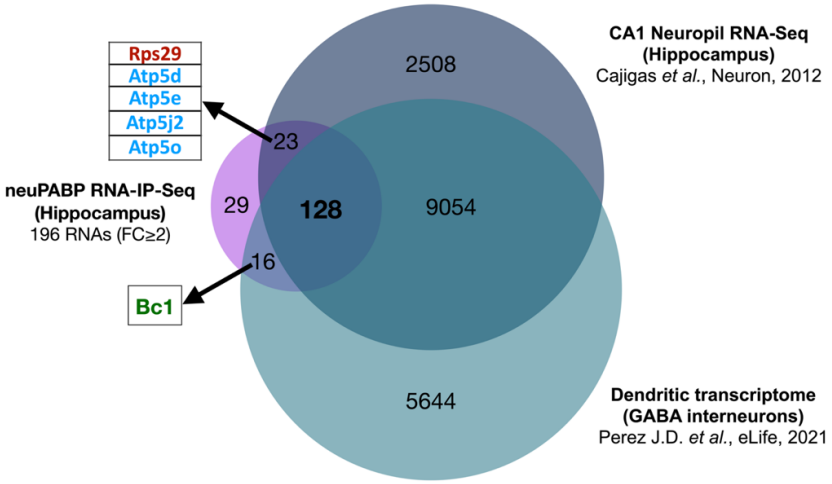

B

Ribosomal protein coding		Mitochondrial protein coding			
Small subunit	Large subunit	ATP Synthase/ ATPase	Complex I	Ribosome	Complex IV
Rps11	Rpl10	Atp6v0b	Ndufa11	Mrpl34	Cox4i1
Rps14	Rpl13		Ndufa13	Mrps18a	Cox5a
Rps15	Rpl14		Ndufa2	Mrps26	Cox5b
Rps15a	Rpl17		Ndufa3		Cox6a1
Rps16	Rpl18		Ndufa5		
Rps17	Rpl18a		Ndufa6		
Rps2	Rpl19		Ndufab1		
Rps20	Rpl21		Ndufb11		
Rps21	Rpl22l1		Ndufb5		
Rps25	Rpl23a		Ndufb7		
Rps26	Rpl26		Ndufb8		
Rps27	Rpl28		Ndufs4		
Rps5	Rpl29		Ndufs6		
Rps8	Rpl3		Ndufs7		
Rpsa	Rpl31		Ndufs8		
	Rpl36				
	Rpl39				
	Rpl41				
	Rpl6				
	Rpl8				
	Rplp0				
	Rplp1				

Figure 33. neuPABP bound RNA targets are neurite-enriched. (A) Shows an intersection between neuPABP bound RNA target list (FC≥2) and two studies that identified dendritic transcriptome, as represented by a Venn diagram. The sizes of the circles are arbitrarily relative to each gene list's log2 (number of genes in the list). 128 genes were common in all three lists. Some of the top neuPABP targets, including (*Bc1, Rps29, Atp5j2, Atp5e*) were present in either one of the lists. (B) Shows a list of ribosomal and mitochondrial proteins coding mRNAs identified among the 128 common genes.

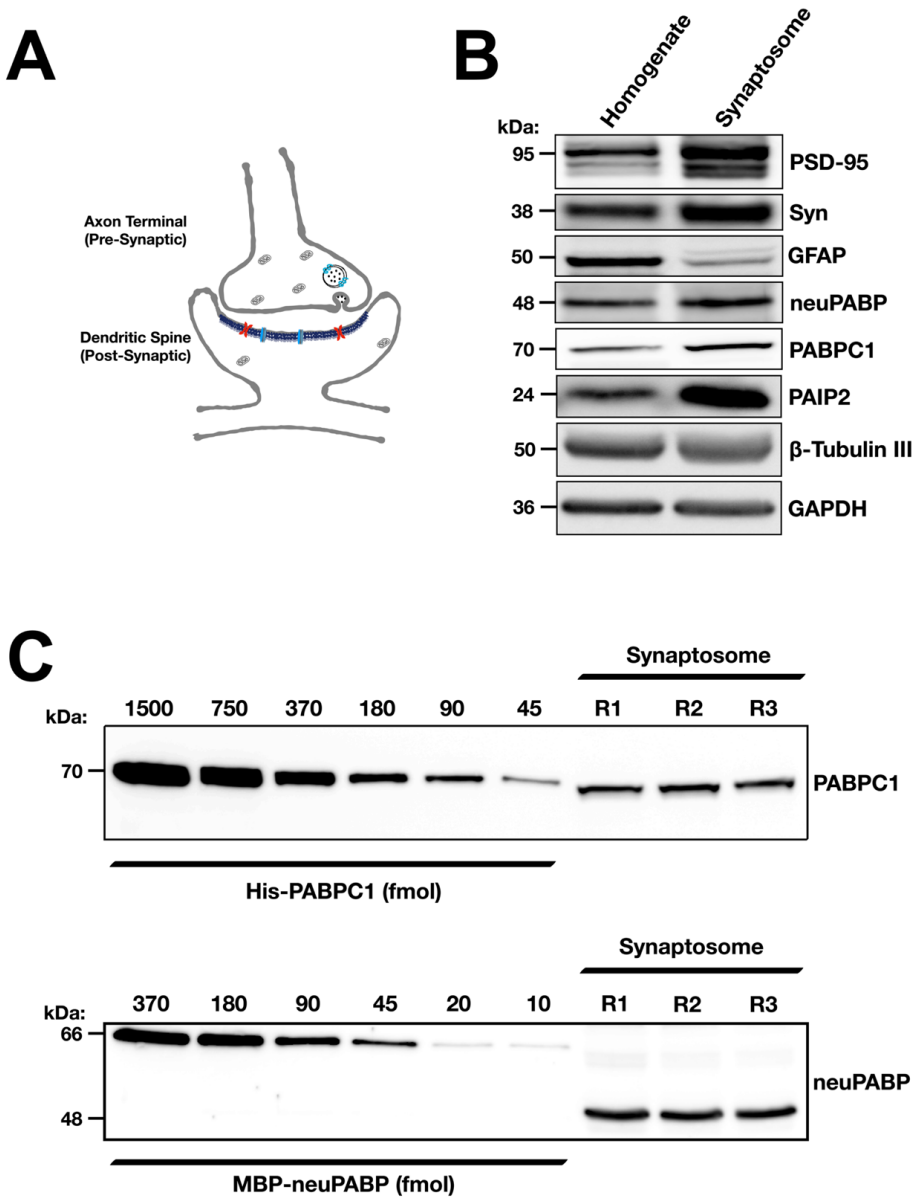

Figure 34. neuPABP and PABPC1 have comparative levels in synaptic terminals. (A) Shows a schematic representation of a synapse showing pre- and postsynaptic terminals. (B) Western blot analysis of subcellular fractions of adult mouse cortex (C57BL/6J; Age: 7 months) prepared by synaptosome fractionation. Equal amounts of lysate fractions were probed with the postsynaptic (PSD) marker PSD-95, the presynaptic marker synaptophysin (Syn), glial marker GFAP, as well as neuPABP, PABPC1, PAIP2, β-tubulin III and GAPDH. Cortex homogenates (H) were generated and the crude synaptosomal pellet (P2) was acquired after high-speed centrifugation of S1 supernatant. (C) Western blot analysis on lysates generated from adult mouse synaptosomes (C57BL/6J; Age: 7 months; shown as n=3). Lysates were resolved by SDS-PAGE and western blot analysis was performed using antibodies against PABPC1 and neuPABP. Lysates were run alongside standard curves of recombinant His-tagged PABPC1 and Maltose binding protein (MBP)-tagged neuPABP to determine PABPC1 and neuPABP protein levels, respectively. Both PABPC1 and neuPABP protein levels vary between 180-90 fmol in synaptosomes.

Next, we set out to study the interaction between neuPABP and target RNAs in synaptosomes. To preserve native RNA-protein interactions, we formaldehyde crosslinked the synaptosomes prior to generating lysates. Lysates were immunoprecipitated with IgG (control) or neuPABP antibody to isolate neuPABP-associated RNAs **(Figure 35A)**. As expected, dendritically localized BC1 RNA, and mRNAs coding for ribosomal and mitochondrial proteins were enriched with neuPABP as assessed by RT-qPCR analyses **(Figure 35B)**. In contrast, neuPABP pulled down significantly lower levels of mRNAs coding for neuronal-specific proteins, including (MAP2, PSD-95, Arc, and β-tubulin III), and failed to interact with a mitochondrially-encoded *ND1* mRNA (control). In parallel, we immunoprecipitated PABPC1 from formaldehyde crosslinked synaptosome lysates to isolate PABPC1 associate RNAs **(Figure 35A).** As anticipated, PABPC1 strongly associated with BC1 RNA (641), and mRNAs coding for ribosomal and mitochondrial proteins as assessed by RT-qPCR analyses **(Figure 35C)**. In contrast to neuPABP, PABPC1 associated with mRNAs coding for neuronal-specific proteins (MAP2, PSD-95, Arc, and β-tubulin III), albeit at lower levels as compared to ribosomal and mitochondrial protein-encoding mRNAs **(Figure 35C).** Importantly, while neuPABP and PABPC1 have overlapping RNA targets, neither neuPABP nor PABPC1 co-precipitated each other **(Figure 35A).** In addition, we carried out polysome profiling on isolated adult mouse synaptosomes **(Figure 35D)** to determine if PABPC1 and neuPABP associate with actively translating mRNA fractions. While PABPC1 associated with polysomes, the majority of neuPABP sedimented in early fractions that contain free ribonucleoproteins (RNPs), and 40S ribosomal subunits **(Figure 35E).** Collectively, these data indicate that neuPABP interacts with dendritically localized non-coding RNA BC1 and select translationally dormant mRNA populations in synaptic terminals.

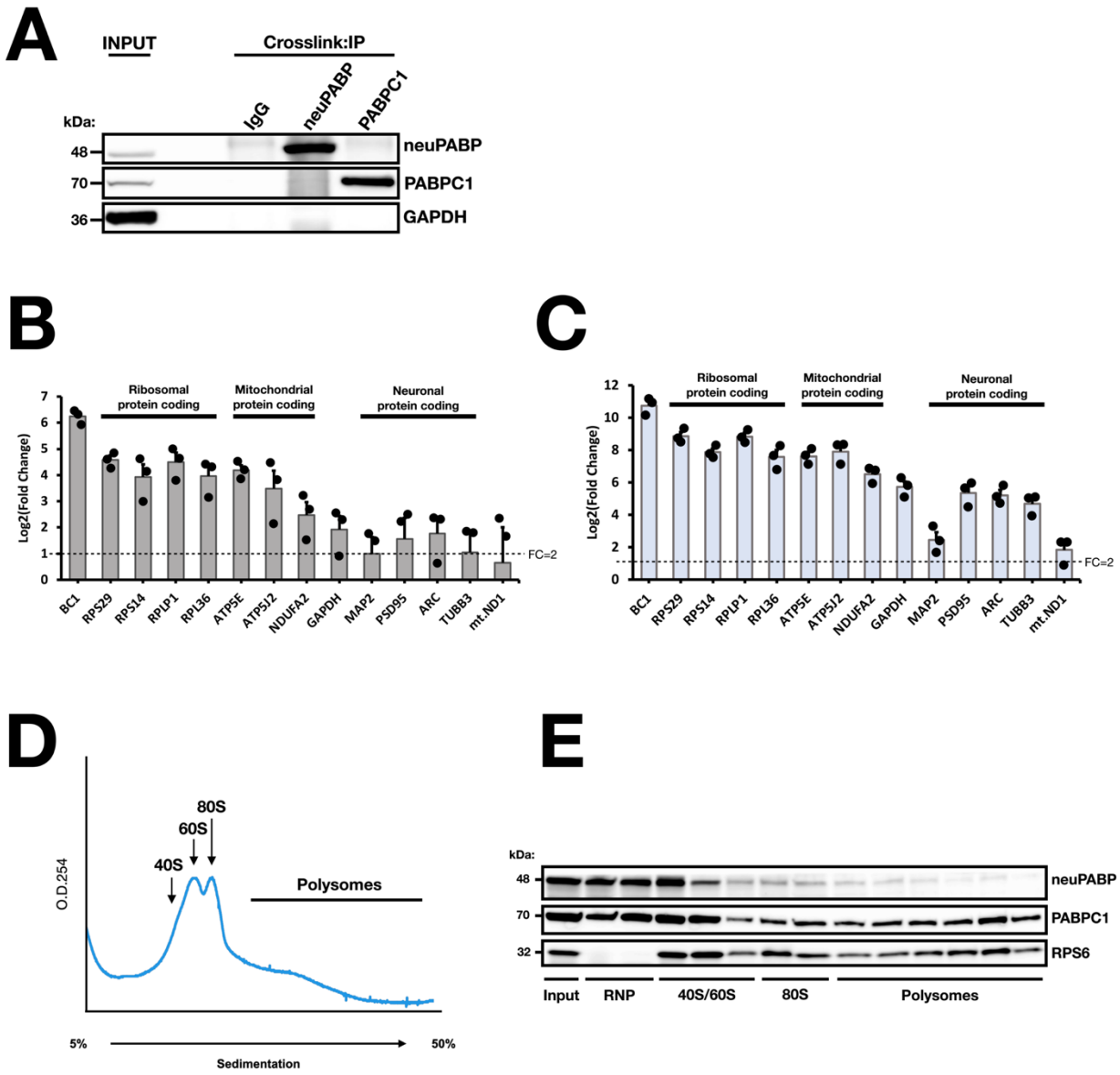

Figure 35. neuPABP and PABPC1 bind overlapping neurite-enriched RNA targets with different translation status. (A) Immunoprecipitation of neuPABP and PABPC1 from formaldehyde crosslinked adult mouse synaptosome fraction (C57BL/6J; Age: 7 months). Immunoprecipitated complexes were resolved by SDS-PAGE and western blotting was performed using antibodies against neuPABP, PABPC1, and GAPDH. (B) RT-qPCR analyses of neuPABP-associated RNAs and (C) PABPC1-associated RNAs. Error bars represent SEM from biological replicates (n=3) and data points for biological replicates are shown as solid circles. A mitochondrial mRNA (mt.ND1) was used as a negative control. Data were normalized to an *in vitro* transcribed RLuc spiked-in RNA. (D) Polysome profile traces of lysates prepared from adult mouse synaptosome (C57BL/6J; Age: 6 months). (E) Lysates were fractionated by sucrose gradient centrifugation. Fractions were subsequently collected, TCA precipitated and resolved by SDS-PAGE and western blotting was subsequently performed using antibodies against neuPABP, PABPC1 and a ribosomal protein marker (RPS6).

3.7. neuPABP is enriched in neuronal RNA granule-containing fraction

In neurons, mRNA are stored in translationally dormant state during dendritic transport (415, 478, 479, 621, 642, 643). Neurons achieve this by packaging mRNAs into liquid-liquid phase separated large RNA-protein complexes called RNA transport granules (416). These RNA granules are transported along the length of microtubular cytoskeleton by motor proteins, and release mRNAs for translation at a particular destination (498). Several RNA binding proteins prevent mRNA translation during transport, including FMRP, SYNCRIP, Staufen, and PURα (479, 492, 494, 499, 644). We identified neuPABP localization into synaptosomes **(Figures 24D and 34B**). Moreover, our *in vitro* translation assays classified neuPABP as a putative translation repressor **(Figures 30B, 31 and 32D),** and polysome fractionation from synaptic terminals and neuPABP RNA co-immunoprecipitation analyses from cortical RNP fractions showed that neuPABP associated RNAs are translationally inactive **(Figures 35E and 29).** This raised the possibility that neuPABP may be a component of neuronal RNA granules. To test this possibility, we carried out RNA granule fractionation from adult mouse cortex (416, 478), and assessed the distribution of neuPABP by western blotting **(Figures 36A-C).** Similar to other known neuronal RNA transport granule marker proteins (PURα and SYNCRIP), neuPABP and PABPC1 were enriched in RNA granule fraction, when compared to total cortex lysates **(Figure 36C)**. Importantly, the presence of both 40S and 60S ribosomal subunit proteins (RPS6 and RPLP0) suggest the presence of intact ribosomes in neuronal RNA granules (478, 479), therefore negating stress granule enrichment which contain only the 40S ribosomal subunit (645). Interestingly, β-tubulin III enrichment suggested RNA granule association with microtubules, as has been reported previously (478, 490). In contrast, translation initiation factors (eIF4E), GAPDH, and synaptic vesicle protein synaptophysin were not enriched **(Figure 36C).**

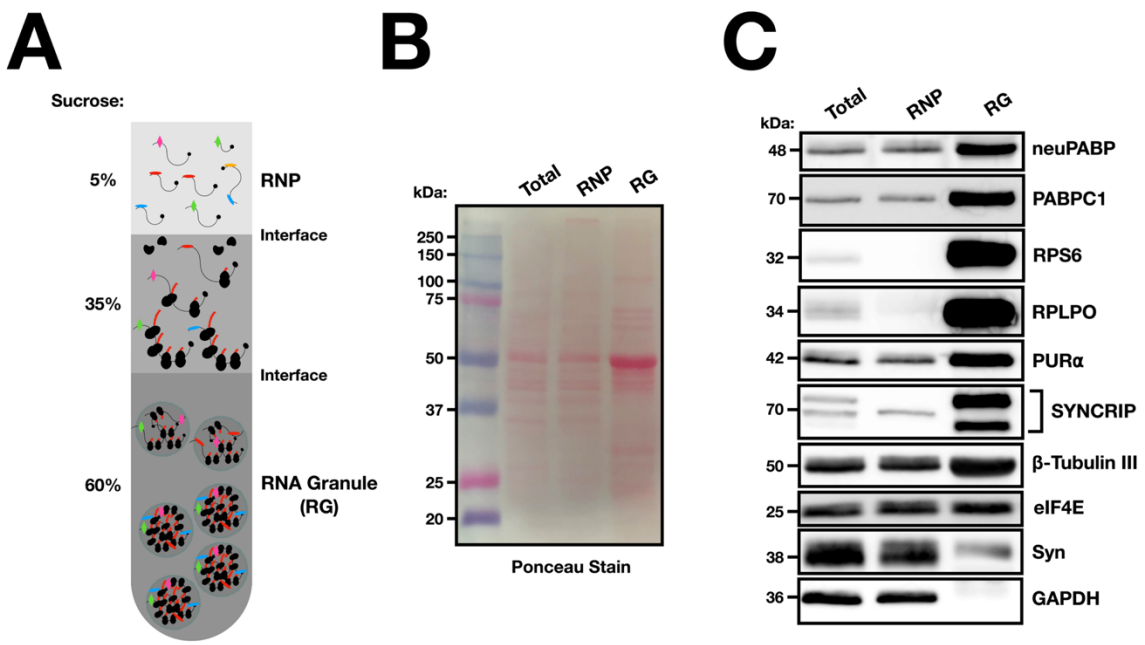

Figure 36. neuPABP is a component of neuronal RNA granule. (A) A schematic representation of a sucrose gradient used for neuronal RNA granule isolation from adult mouse brain cortex (C57BL/6J; Age: 6 months). Lysates were fractionated by sucrose gradient centrifugation. Fractions were subsequently collected, TCA precipitated and resolved by SDS-PAGE, (B) shows the Ponceau stained membrane of resolved proteins and (C) shows western blot analyses using antibodies against neuPABP, PABPC1, ribosomal subunit proteins (RPS6 and RPLP0), RNA transport granule marker proteins (PURα and SYNCRIP), β tubulin III, eIF4E, synaptophysin (Syn), and GAPDH.

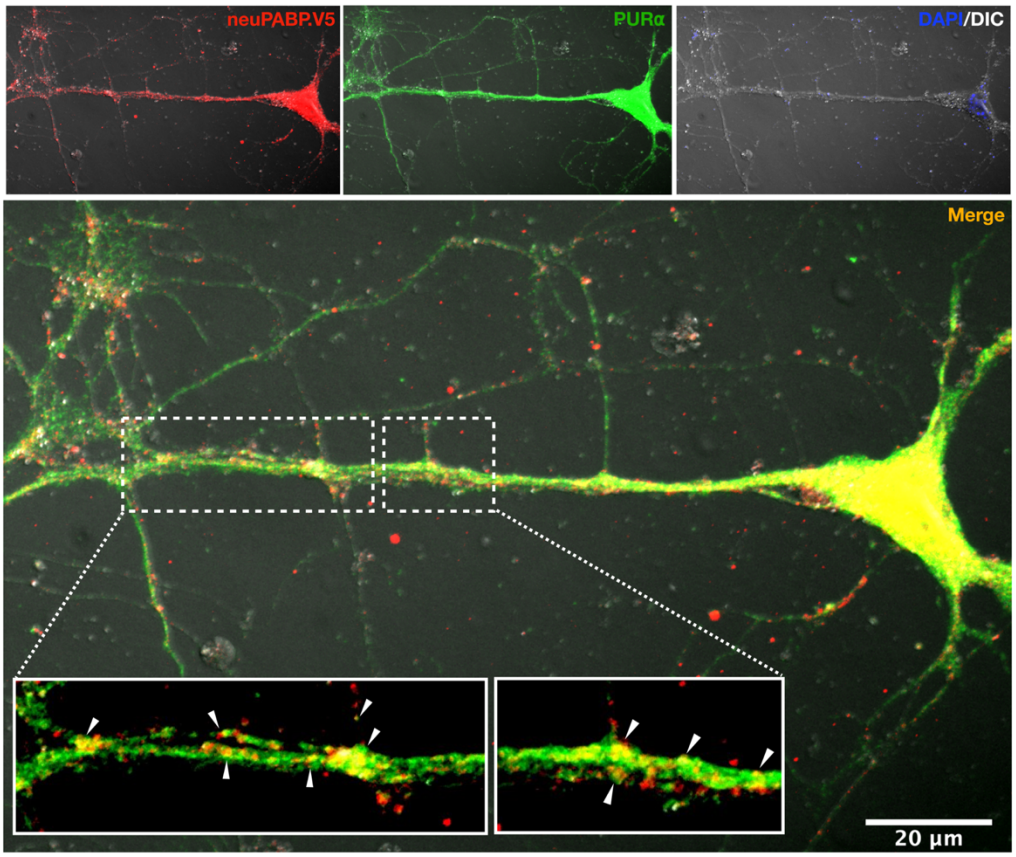

Figure 37. neuPABP colocalizes with PURα in neuronal soma and neurites
Immunofluorescence analysis (IF) on mouse primary cortical neurons. Neurons were isolated from p0 pups and cultured for 12 days *in vitro* (DIV). At DIV5 neurons were infected with a lentivirus coding for a V5-tagged neuPABP protein. IF analysis was performed on DIV12 using antibodies against V5-tag and PURα (granule marker), DAPI was used to stain the nuclei. Images were acquired using a laser scanning microscope (Zeiss), and processed using ImageJ software. A colocalization analysis was performed for red (594nm), and green (488nm) channels using Coloc2 plugin in Fiji (ImageJ). Using the Coloc2 plugin, an average Pearson correlation coefficient (r=0.84) was calculated for colocalized pixels from three neurons (n=3). White arrows indicate colocalization of V5-tagged neuPABP (red) with PURα (green).

We also tested neuPABP colocalization with an RNA granule marker protein, PURα in cultured neurons (498). To overcome the limitations of our neuPABP antibody for immunofluorescence, we expressed a V5-tagged neuPABP protein in mouse primary neurons, and carried out immunofluorescence analyses **(Figure 37).** Our analyses revealed a strong correlation between neuPABP and PURα colocalization signal (Average Pearson correlation coefficient, r=0.84). Taken together, these data suggest that neuPABP, apart from its localization in free RNP fractions, is indeed localized in neuronal RNA granules, and likely binds to mRNAs that are being transported in dendrites.

3.8. neuPABP knockout mice have elevated BC1 levels and neuPABP overexpression inhibits protein synthesis *in cellulo*

Dysregulation of local mRNA translation in dendrites leads to diverse nervous system disorders, including spinal muscular atrophy (SMN) (646) and Fragile X syndrome (647). Given the presence of neuPABP in synaptic terminals and its association with translationally dormant mRNAs and abundant non-coding BC1 RNA, the loss of neuPABP could impact local translation of its mRNA targets and BC1 RNA function. To test this, we were successful in generating *Pabpc1l2a/b* knockout (neuPABP^{KO}) mouse **(Figures 38A and B).** Recently, PABPC depletion in human cell lines was reported to severely impact the stability of selective classes of mRNAs (128, 160), which included neuPABP associated ribosomal and mitochondrial proteins coding mRNAs. Therefore, to study the impact of neuPABP on the target RNA abundance, we isolated total RNA from wild-type (WT) and neuPABP^{KO} mouse brain and carried out RT-qPCR analyses. While neuPABP target mRNA abundance was not altered in neuPABP^{KO} mice neural tissues, possibly due to other PABPCs (like PABPC1) compensating for the loss of neuPABP, we observed significantly elevated

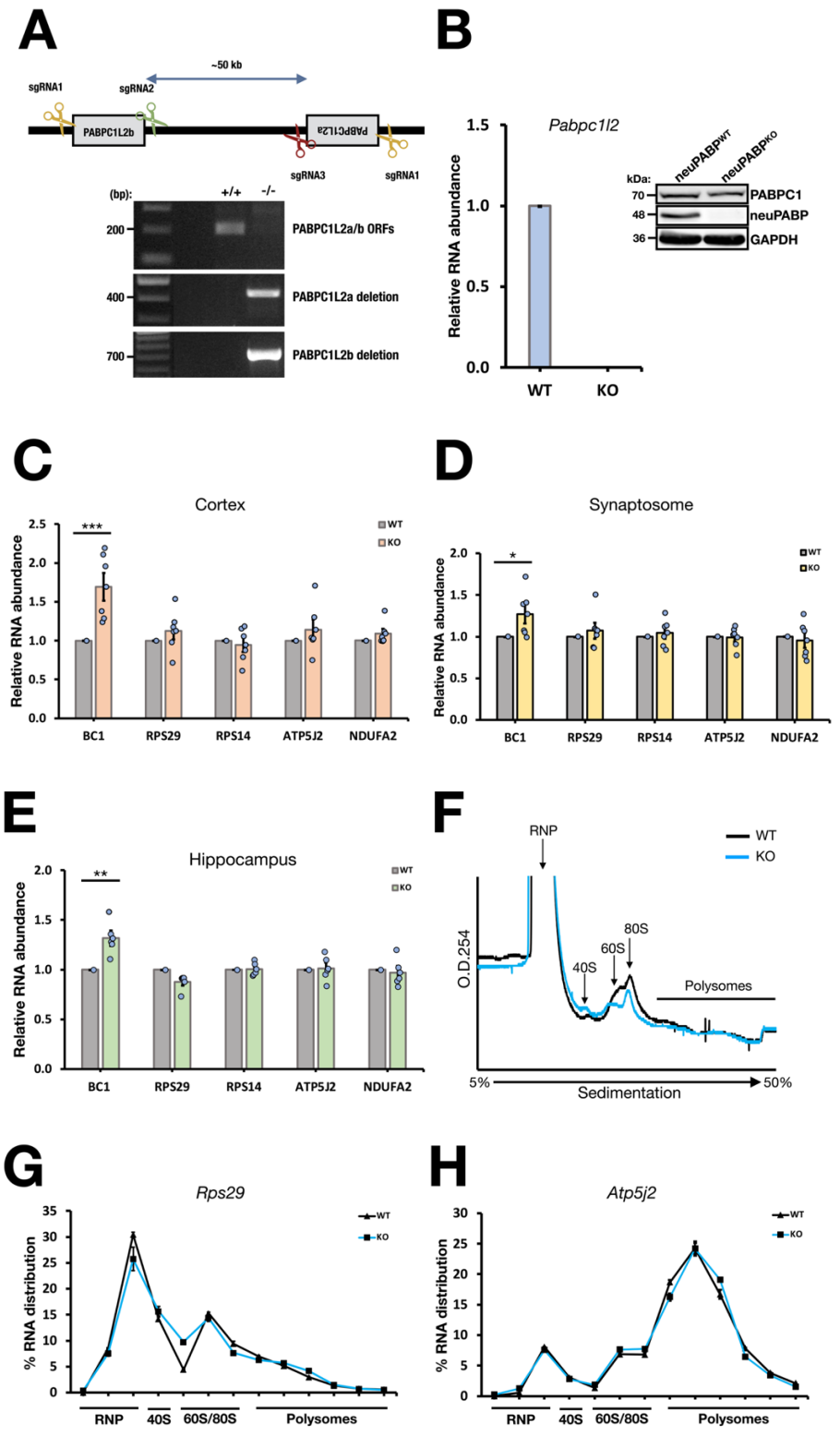

Figure 38. neuPABP^{KO} mouse brain has elevated BC1 levels. (A) Schematic representation of *Pabpc1l2a/b* CRISPR knockout (neuPABP^{KO}) mouse generation. Single guide RNAs (sgRNA) were designed to guide Cas9 nuclease to cleave at sequences flanking *Pabpc1l2a* and *Pabpc1l2b* genes. Mouse genotyping shows that both genes were deleted, as shown by the 400bp and 700bp

PCR products amplified from the gene flanking sequences left after deletion. (B) *Pabpc1l2a/b* knockout was further confirmed by RT-qPCR and western blot analyses on wild type (WT) and neuPABP^{KO} brains. Data were normalized to an *in vitro* transcribed RLuc spiked-in RNA. Error bars represent SEM from biological replicates (n=3). (C-E) Steady state comparisons of neuPABP target RNAs in the (C) brain cortices (C57BL/6J; Age: 7 to 12 months; n=7), (D) synaptosome fractions (C57BL/6J; Age: 7 to 12 months; n=7), and (E) hippocampi (C57BL/6J; Age: 7 months; n=6) of WT and age-matched neuPABP^{KO} mice. Data were normalized to an *in vitro* transcribed RLuc spiked-in RNA. Error bars represent SEM from biological replicates and data points for biological replicates are shown as solid circles. (F) Polysome profile traces of lysates prepared from hippocampi (C57BL/6J; Age: 6 months) of WT and neuPABP^{KO} mice. Lysates were fractionated by sucrose gradient centrifugation. Fractions were subsequently collected, RNAs were Trizol extracted, and RT-qPCR analyses were performed on two of the neuPABP target RNAs (G) (*Rps29)*, and (H) *(Atp5j2*) to calculate percent RNA distribution in polysome fractions, as a comparison between WT and neuPABP^{KO} hippocampi. Data were normalized to an input sample (total hippocampus RNA) to calculate the percent distribution across fractions, error bars represent SEM from biological replicates (n=3).

levels of BC1 RNA in the brain cortices of neuPABP^{KO} mice [(n=7), **(Figure 38C)**]. Similarly, elevated levels of BC1 were found in synaptosomes (n=7), and hippocampi of neuPABP^{KO} mice [(n=6), (**Figures 38D and E**)]. We also carried out polysome profiling from WT and neuPABP^{KO} mouse hippocampi (**Figure 38F**) and assessed the distribution of select mRNAs across polysome gradients by RT-qPCR. Our analyses did not suggest any impact on basal translation efficiency of these target mRNAs in neuPABP^{KO} hippocampi, as assessed by the mRNA distribution in polysome fractions **(Figures 38G and H).**

In neurons, several RNA binding proteins that regulate mRNA translation are rapidly transported into dendrites and/or accumulated in synaptic terminals after stimulation, including FMRP, FUS, and several heterogeneous nuclear ribonucleoproteins hnRNPs (483, 648-651). While it is currently unknown how and if stimulation leads to neuPABP accumulation in synaptic terminals, and whether it can actively impact local translation in neurons, we investigated the role of neuPABP in translation by utilizing a human neuroblastoma cell line —SH-SY5Y. We used a bicistronic reporter system that contains a *Renilla* luciferase ORF (RL) that is translated in 5' cap and 3' poly(A) tail-dependent manner, while a Firefly luciferase ORF (FL) that is translated by Hepatitis C virus (HCV)-IRES in 5' cap and 3' poly(A) tail-independent manner (**Figure 39A**). We cotransfected this reporter along with a FLAG-tagged neuPABP construct into SH-SY5Y cells. A GFP-expressing construct was used for normalization **(Figures 39B and C).** Our data show that adding increasing amounts of neuPABP repressed the translation of RL reporter in a dose-dependent manner (**Figure 39B**). As expected, neuPABP had no impact on the translation of IRES-controlled FL reporter (**Figure 39C**). Therefore, neuPABP has the capacity to inhibit cap- and poly(A) tail-dependent translation in human cells.

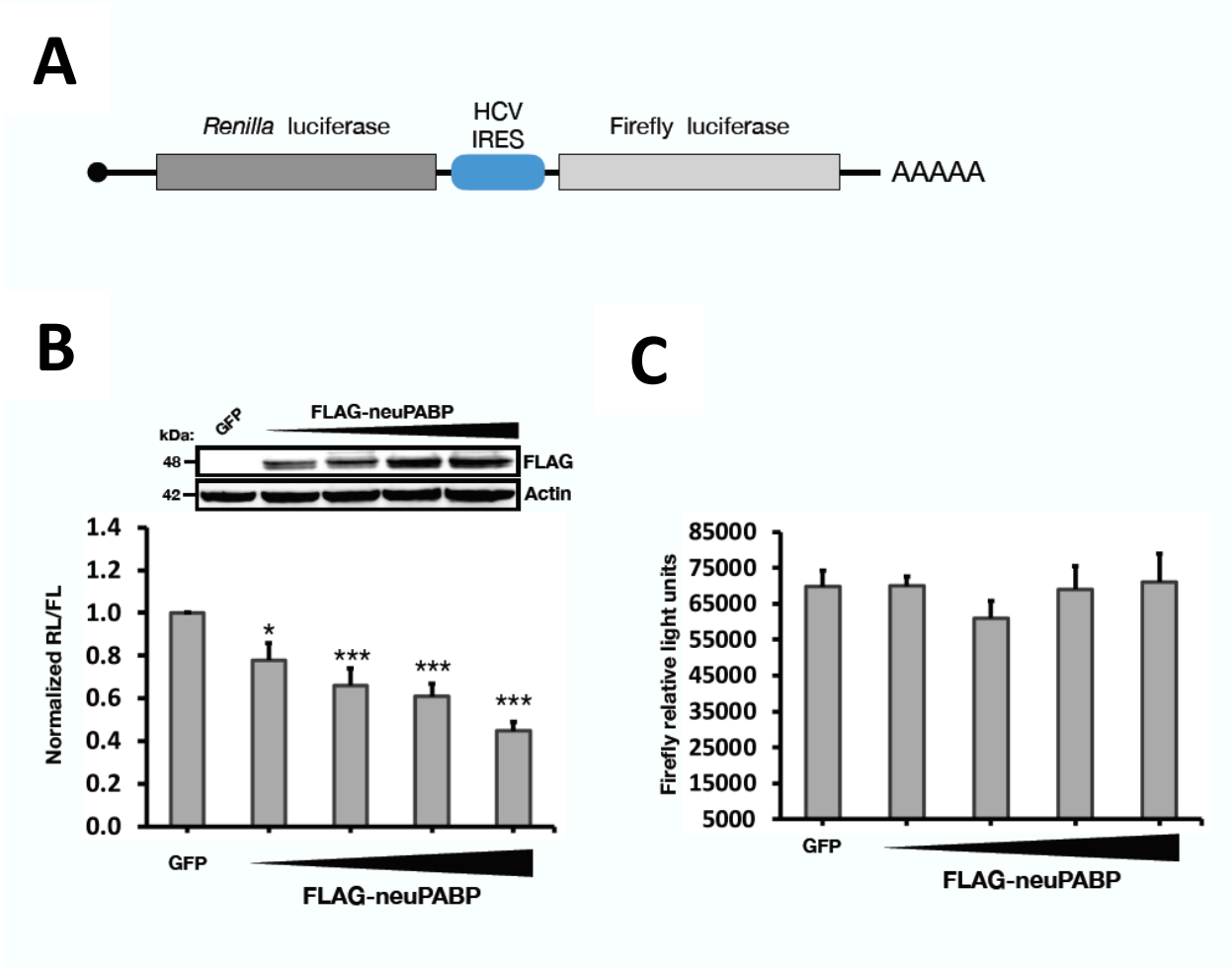

Figure 39. neuPABP expression inhibits protein synthesis *in cellulo.* Schematic diagram of a RL-HCV-FL reporter mRNA. (B and C) SH-SY5Y cells were transfected with the bicistronic reporter plasmid, along with increasing amounts of a plasmid encoding Flag-tagged neuPABP protein or GFP (control). Lysates were prepared for Western blotting and luciferase assays. Normalized RL luciferase activity (RL/FL ratio) was calculated and plotted relative to a GFP control. Raw Firefly relative light units were also plotted. Error bars represent SEM from biological replicates (n=4). A two-tailed Student t-test (equal variance) was conducted (versus control) to access significance, p-values<0.001, represented as '***'.

4. COMPREHENSIVE DISCUSSION

4.1. Overview

Here, we have identified a novel tissue-specific mammalian poly(A) binding protein, neuPABP. neuPABP is coded for by the X-linked *pabpc1l2* ampliconic gene, and is a 312 amino acid protein in mouse. neuPABP displays a brain-specific expression pattern, and is predominantly expressed in postnatal neurons as they mature during synaptogenesis and is maintained thereafter. While other PABPCs contain four RRMs, neuPABP contains only two RRMs that correspond to RRM1 and RRM2 of PABPC1. Moreover, while neuPABP lacks the linker region and MLLE domain, it contains a unique N-terminus region not found in other PABPCs, the function of which is not known. A comparison between neuPABP and PABPC1 protein sequences suggests that neuPABP RRMs are evolutionarily well conserved (~85% identity) with several conservative amino acid substitutions. As expected from sequence homology, neuPABP binds poly(A) RNA with a comparative affinity to PABPC1, but cannot bind PAIP2. Intriguingly, although neuPABP maintains RRM2, it has evolutionarily drifted from PABPC1 such that it is unable to bind eIF4G, and as a consequence, fails to support translation *in vitro*. Moreover, we show that neuPABP has the ability to repress cap-and poly(A) dependent translation *in cellulo*. In keeping with these findings, our polysome profiling and RNA-sequencing data from mouse brain indicate that neuPABP associates with select mRNAs populations that are translationally suppressed, as well as the neuronal-specific non-coding RNA BC1.

4.2. neuPABP represents a novel neural poly(A) binding protein.

PABPCs are evolutionarily conserved in eukaryotes. While yeast code for one PABPC, Pab1, mammals have evolved to code for several PABPCs. Although the prototypical PABPC i.e., PABPC1 is ubiquitously expressed among different mammalian tissues (149, 304), other PABPCs display a tissue-biased expression pattern. For example, PABPC3 (or tPABP) is expressed in round spermatids in testis (305), PABPC1L1 (or ePABP) is expressed during oocyte maturation and early embryonic development (149), and PABPC4 (or iPABP) is expressed in activated T-cells (306). neuPABP therefore represents a new PABPC that mammals have added to their repertoire that is expressed in the brain.

neuPABP displays a temporal expression pattern during neuronal maturation

Similar to other PABPCs acquired by metazoans, such as ePABP (149, 150), neuPABP also displays a unique tissue-specific and temporal expression pattern. neuPABP protein is barely detectable in embryonic brain tissues. However, its expression rapidly increases in the postnatal brain. In contrast, PABPC1 is highly abundant in the embryonic brain, while its expression steadily decreases during postnatal brain development. This is reminiscent of ePABP expression pattern during early development (150, 332). ePABP is expressed during oocyte maturation and early embryo development stages; however, its expression is turned off after the onset of zygotic transcription (150, 331, 332). PABPC1 on the other hand, is barely detectable in oocytes and early embryos (150, 331). We show that neuPABP expression steadily increases in neurons as they mature, reaching levels similar to those of PABPC1 in mature neurons. Interestingly, the temporal expression pattern of neuPABP coincides with synaptogenesis, which takes place during the first few postnatal weeks of rodent brain development (634). During this period, neurons establish

excessive number of synapses (396), which are eventually pruned during the later stages of brain development to fine tune the brain neurocircuitry (406). Whether neuPABP plays a role in maintenance of relevant synapses remains to be established. However, it is tempting to speculate that neuPABP plays a role in neuronal circuits given that neuPABP is upregulated during postnatal brain development and localizes to synaptic terminals.

Several important RNA binding proteins are temporally expressed during brain development. For example, the fragile X protein, FMRP, whose loss leads to a neurodevelopmental disorder (652), is highly expressed during early postnatal weeks of brain development, while the expression decreases around postnatal day 14 (p14) to p30 (653, 654). The DNA/RNA binding protein transactive response DNA-binding protein (TDP-43), which is implicated in familial and sporadic ALS, is also developmentally regulated (655). TDP-43 is highly expressed during embryonic brain development; however, displays a progressive decrease in protein levels during postnatal brain development. Interestingly, the single stranded DNA/RNA binding protein, PURα, whose loss leads to severe neurological problems manifested by seizures and early death, is developmentally upregulated in postnatal brain and peaks around p15 (656). While these RNA binding proteins are highly conserved from fly to humans (657-659), neuPABP represents a mammalian-specific neural RNA binding protein.

neuPABP is coded from a highly conserved X-ampliconic gene in placental mammals

The X-chromosome in placental mammals differ from marsupials in terms of newly acquired genes on XAR region (X added region), while genes in XCR (X conserved region) region share orthologues on marsupial X-chromosome (660, 661). Even though *Pabpc1l2* ampliconic gene

containing palindrome is located on Xq13.2 (628, 662), a chromosomal location within the XCR region of placental X-chromosome, similar orthologues are not present on marsupial X-chromosome. This suggests that *Pabpc1l2* gene was independently acquired after eutherian-metatherian divergence. While majority of single- and multi-copy genes on X-chromosome are shared between mouse and human, most ampliconic genes were independently acquired (629). In 1967, Susumu Ohno made a prediction that the gene content of X-chromosome in placental mammals would be highly conserved. While this holds true for the vast majority of single copy genes, most X-ampliconic genes are the exceptions to this rule (629). Remarkably, only a small number of (33 out of 107) ampliconic genes on human X-chromosome share orthologues on mouse X-chromosome, and these include *Pabpc1l2* ampliconic gene (629). This indicates that *Pabpc1l2* ampliconic gene, after its acquisition, is evolutionarily maintained in placental mammals. Intriguingly, a study that focused on identifying postmeiotic expression of X-linked multicopy genes in mouse tissues, identified *Pabpc1l2* mRNA expression in testis and brain (628). In agreement with this study, we detected *Pabpc1l2* mRNA in neural tissues, however, we did not detect *Pabpc1l2* mRNA or protein in testis.

The mammalian X-chromosome has been shown previously to have acquired genes with cognitive functions (663-666). Based on OMIM database, X-chromosome is densely packed with genes involved in healthy cognition, with ~10% of the total genes on X-chromosome associated with mental disability (664). Various protein components of neuronal complexes (NMDA/MAGUK) that are localized to the postsynaptic terminal, are encoded on the X-chromosome (667). Many of the genes on the X-chromosome encode for proteins with function such as ion channels, receptors, transcription factors, and DNA/RNA binding proteins (667). For example, the X-linked *fmr1* gene,

which codes for the RNA-binding protein, FMRP, plays a role in cognition, with its loss leading to intellectual disability and autism (668, 669). Neuroligin 3 (*NLGN3*) is also a great example of an X-linked gene with neuronal function, which is located on Xq13.1 in proximity to *Pabpc1l2* gene. Neuroligin 3 is a cell surface protein involved in remodeling synapses, and is implicated in autism spectrum disorder [(ASD), (670)]. Based on these examples, it is plausible that neuPABP may play a role in cognition.

neuPABP ORF is initiated from a non-canonical GUG codon

Translation in eukaryotes is mostly initiated at an AUG codon present in an optimal Kozak context [(A/G)CCAUGG), (135-137)]. Recent scientific leaps in ribosome footprinting techniques have revealed that translation can be initiated from near cognate non-AUG codons that resemble AUG codon but differ by only one nucleotide, for example, CUG, GUG, and UUG (185-187, 190). The usage of non-canonical start codons is a rare phenomenon in eukaryotes as these codons are less efficient than AUG (188), even when embedded in a favourable consensus Kozak motif (136). Why is initiation from a non-AUG codon favoured? The answer may lie in the sequence context surrounding the non-AUG start codon. For example, the translation initiation of NAT1/eIF4G2 is initiated at a GUG codon (190), which is present in an optimal Kozak motif and is predicted to contain a secondary hairpin structure downstream of the GUG codon. The presence of a downstream secondary structure favours the usage of a non-canonical start codon like GUG (189), presumably by slowing down the scanning 48S preinitiation complex (189). Importantly, the GUG codon mediated translation initiation of NAT1 is conserved across species (190). Similar to NAT1, the translation of *Pabpc1l2* ORF is also GUG-initiated. The nucleotide sequences around *Pabpc1l2* GUG codon i.e., "ACCGUGG", are evolutionarily conserved and present in optimal Kozak

context [(ACCAUGG), (136)]. These nucleotide sequences with purines 'A' at -3 position and 'G' at +4 position, may favour the efficient usage of the GUG as a start codon (136, 188). Interestingly, the 64-nucleotide region downstream of *Papbc1l2* GUG codon is evolutionarily well-conserved, highly GC rich, and based on RNA structure prediction tools, like Vienna RNA websuite, may form a GC base paired secondary structure (467). Therefore, these qualities of *Pabpc1l2* mRNA 5' end may have allowed for the usage of GUG as a start codon. In support of this, we show that GUG codon is able to initiate *Pabpc1l2* mRNA translation in cell lines and generate a protein of similar size to endogenous neuPABP. These observations collectively suggest that well-conserved sequence determinants proximal to the *Pabpc1l2* GUG codon, as well as downstream RNA secondary structure favors the non-AUG translation of *Pabpc1l2* mRNA.

4.3. neuPABP localizes to synapses and associates with neurite-enriched RNAs

The significance of RNA binding proteins (RBPs) at the synapse can be deciphered from patients where their complete loss or mutation can lead to impaired synaptic plasticity and neurological disorders (671). For example, mutations in the RNA binding proteins fused in sarcoma (FUS) and transactive response DNA-binding protein (TDP-43) lead to neurodegenerative diseases, including amyotrophic lateral sclerosis (ALS) and frontotemporal dementia (FD), respectively (672, 673). Similarly, mutations in *Fmr1* gene, which codes for FMRP, can also cause fragile X syndrome even in the absence of classical CGG-repeat expansions (674). Importantly, impaired RNA metabolism is at the heart of these diseases, where the loss of RBP function can affect the transport and local translation of their mRNA targets (675). These examples highlight the importance of RBPs in healthy neuronal function. Here, we have identified a new RBP, neuPABP, that is localized into the postsynaptic terminals and associates with several synaptically important RNAs that we

have identified. To effectively respond to external stimuli and propagate synaptic transmission, neurons rely on local protein synthesis in synapses (166). To do so, neurons have developed ingenious methods to transport RNAs as well as translation machinery components to the distal dendritic/axonal structures (419). This feature gives neurites the autonomy to modulate their local proteome to accommodate rapid synaptic changes, without having to rely on the cell body. Numerous transcriptomics studies over the years have now identified thousands of RNA species in the neurites (97, 166, 378, 419-422). Several RBPs are required for transporting RNAs in neurons, which include FMRP, Staufen, TDP43 and PURα (479, 492, 494, 499, 644, 676). RNA transport is achieved by the concerted action of RNA-bound RBPs and cytoskeleton (microtubules or actin filaments), which acts as a highway for RNA cargo transport (677). Importantly, RNA transport requires motor proteins (kinesin and dynein), which link up RNA cargos to the cytoskeleton and move them to distant dendritic location in ATP hydrolysis-dependent manner (677, 678). Our neuPABP-enriched transcriptome study from mouse hippocampus has identified its RNA targets. Two main classes of mRNAs are enriched with neuPABP: mRNAs coding for ribosomal and nuclear-encoded mitochondrial proteins. Intriguingly, ribosomal protein coding mRNAs have been shown to localize to dendritic processes by many studies (97, 378, 419-422, 679). Remarkably, one study showed that ribosomal proteins are locally synthesized and incorporated into functional ribosomes in dendrites (419). By utilizing metabolic labeling and mass spectrometry, this study uncovered a unique method of ribosome recycling and repair that is independent of the canonical ribosome biogenesis in the nucleolus and soma (680, 681). Similarly, mitochondrial protein coding mRNAs are also transported into axons and presynaptic terminals, where their local translation provides proteins for healthy mitochondrial function (682). These studies highlight the importance of mRNA transport in maintaining a local mRNA pool, which is

ultimately translated into healthy ribosomal and mitochondrial functions. Therefore, the identification of neuPABP target mRNAs is of high significance, as they code for protein components of core translation and metabolism machineries.

While neuPABP and its target mRNAs localize to neurites and synaptic terminals, a question became apparent: does neuPABP associate with its target RNAs in synaptic terminals? Our neuPABP formaldehyde-crosslinked immunoprecipitation (CLIP) data from synaptosome preparations show that the 'biased' binding preference of neuPABP toward ribosomal and mitochondrial protein coding transcripts also holds in synaptic terminals. Previous studies have identified several synaptic proteins coding transcripts (*Map2, PSD95, Arc*) in synaptic terminals (426, 445, 683). Even though these transcripts localize in dendritic terminals, neuPABP only shows a weak association with them. Interestingly, our CLIP data for PABPC1 show that while PABPC1 associates with mRNAs coding for neuronal-specific proteins (MAP2, PSD-95, Arc, and β-tubulin III), the enrichments are not as dramatic as for the ribosomal and mitochondrial proteins coding mRNAs. Remarkably, this pattern for PABPC1 RNA binding preference has been reported by a previous study, albeit in actively dividing HEK293T cells (684). This study showed that PABPC1 associates with mRNAs that are generally stable and have longer-half lives, which included ribosomal protein coding mRNAs. Moreover, recent studies suggested that PABPC1 serves an important function in stabilizing two main classes of transcripts: ribosomal proteins coding and mitochondrial protein coding mRNAs (128, 160). Therefore, our CLIP analyses in synaptosomes extends these findings for PABPC1 to terminally differentiated neurons. Nevertheless, our data suggests that both neuPABP and PABPC1 have overlapping targets in synaptic terminals. Do neuPABP and PABPC1 bind the mRNA targets simultaneously? Fascinatingly, our CLIP data

suggest that even though neuPABP and PABPC1 share common mRNA targets, our co-IP data show that neuPABP-bound RNAs do not contain PABPC1 and *vice versa*. This highlights that neuPABP and PABPC1 bound mRNAs represent different subpopulations of the same mRNA species.

The top neuPABP target RNA that we have identified is the highly abundant brain specific non-coding RNA, BC1. Intriguingly, our work matches well with previous studies that show that BC1 RNA is developmentally upregulated in neurons (453), which mirrors the developmental expression of neuPABP**.** The BC RNAs (BC1 and BC200) localize to dendrites and regulate mRNA translation (463, 472), and contain a dendritic targeting element in their 5' stem-loop structure (452, 463). Moreover, this stem-loop structure may serve as a binding platform for several RBPs, like FMRP, to facilitate the dendritic transport of BC RNAs (465, 466). BC RNAs also contain an internal stretch of A-rich sequence which can provide binding site for poly(A) or A/U rich RBPs, like neuPABP, PABPC1, and SYNCRIP (459, 461).

It is currently unknown how neuPABP is transported to the postsynaptic terminals and if neuPABP is even involved in RNA transport. The RBP-RNA cargo transport in neurons is mediated by cytoskeleton and motor proteins. Therefore, future studies would entail the disruption of cytoskeleton with drugs, like cytochalasin D (actin filaments), nocodazole or colchicine (microtubules), and utilize imaging and biochemical techniques to study neuPABP localization. Interestingly, a study showed that the dendritic localization of BC1 is obstructed in cultured neurons after disrupting microtubules, but not actin filaments (464). Therefore, whether BC1

facilitates neuPABP localization into dendritic postsynaptic densities or *vice versa*, is of a great interest.

neuPABP is a component of RNA transport granules

In neurons, mRNA are transported and delivered to distal dendritic/axonal sites via various methods. While several RNAs are transported as RNPs that lack ribosomal subunits, for example, non-coding BC RNAs, some prefer packaging into dense liquid-liquid phase separated structures called RNA transport granules. While neuronal transport granules share components with stress granules, there is a major key difference. In contrast to stress granules that contain 40S ribosomal subunits stalled in translation initiation, transport granules contain 80S ribosomes stalled in translation elongation phase (479, 498, 642, 645, 685, 686). Other than ribosomes, several RBPs have been identified as key components of transport granules, for example, FMRP, Staufen, PURα, PURβ, and SYNCRIP (498). Interestingly, a previous study did not detect the enrichment of PABPC1 and translation initiation factors in transport granules (416). However, a recently published study carried out proteomic analyses on neuronal transport granules isolated from rat brain cortex and human neuroblastoma SH-SY5Y cells (478), and identified several key granule marker proteins, including PABPC1. In agreement with this, we also identified PABPC1 enrichment in our RNA granule fraction. Similarly, we show that neuPABP is enriched in RNA granules along with previously identified granule marker proteins, like PURα, SYNCRIP, and 80S ribosomal proteins (RPS6 and RPLP0). Moreover, our immunofluorescence imaging data show neuPABP colocalization with PURα, a key transport granule protein (498). Live cell imaging techniques have revealed the anterograde and retrograde movements of PURα-containing granules in neurons, and these movements are dependent on myosin Va motor protein that translocate on

actin filaments (498, 499). Therefore, future live cell imaging studies coupled with actin cytoskeleton disruption agent cytochalasin D, would shed some light on neuPABP-PURα granule dynamics. Additionally, similar to a previous study that coimmunoprecipitated and characterized motor protein KIF5-associated RNA granules and their components, which included PURα (498), it will be interesting to examine the association of neuPABP-containing RNA granules with cytoskeleton by direct pulldown of motor proteins.

A putative role for neuPABP in translational regulation

Translational control of gene expression is critical for regulating both general protein synthesis and synthesis of specific proteins in response to neuronal activity pertaining to long lasting synaptic plasticity (LTP) and memory formation (687-690). In neurons, several RBPs are localized into synaptodendritic compartments and regulate temporal protein synthesis to fine tune a synaptic response to external stimulus **(Figure 40)**. For example, FMRP regulates mRNA translation by stalling the ribosomes in the elongation phase and packaging the stalled polysomes into RNA granules for transport (442, 479, 691). HuD (ELAV4), an AU-rich neuronal RNA binding protein, localizes to the dendrites after stimulation and supports translation of immediate early gene transcripts (*Neuritin, GAP-43, CaMKIIα*), whose protein products are essential for synaptic plasticity (692). PABPC1, an important protein that stimulates translation *in vitro* and during early development (142, 148), is negatively regulated by PAIP2, which binds and displaces PABPC1 from poly(A) tails (315, 693, 694). Intriguingly, a study showed that PABPC1 increasingly associated with *CaMKIIα* mRNA in mouse hippocampus after training. Interestingly, PABPC1 showed even stronger binding to *CaMKIIα* mRNA in trained *Paip2a-/-* mice, where *CaMKIIα* mRNA showed increased polysome association and protein synthesis (640). Moreover, they saw

that *Paip2a*$^{-/-}$ mice displayed a lower threshold for late phase-LTP induction (L-LTP) and enhanced spatial memory formation after weak training, while memory impairment was observed following strong training, possibly due to excessive translation stimulation by PABPC1 after *Paip2a* loss (640). These studies highlight that a balanced translation output following stimulus is necessary for healthy synaptic function. Unlike PABPC1, which contains MLLE domain for PAIP2 binding, neuPABP lacks MLLE, cannot bind PAIP2, and therefore, may not be regulated by PAIP2. However, PAIP2 and neuPABP may function independently to regulate PABPC1 function in translation by displacement and replacement strategies, respectively. Importantly, our neuPABP and PABPC1 CLIP experiments from synaptic terminals suggest that even though both proteins share mRNA targets, they do not coexist on the same RNA. This indicates that these proteins may bind mRNAs with distinct translation status. Indeed, our polysome profiling data from mouse cortex and synaptic fractions shows that neuPABP and PABPC1 have distinct polysome profiles. While PABPC1 was detected throughout polysome fractions, including in heavy polysome fractions that contain actively translated mRNAs (637, 638), neuPABP sedimented in early fractions that contain untranslated free ribonucleoprotein (RNP) and 40S ribosomal subunits. Moreover, our data show that neuPABP directly associates with translationally dormant RNAs in the RNP fractions. While it seems clear that neuPABP and PABPC1 bound RNAs have distinct translation status, the status of PABPC1 associated RNAs in RNP fractions remains unclear. PABPC1 binds poly(A) tails and stimulates translation by contacting eIF4G subunit of eIF4F complex (142, 148). In addition, PABPC1 was previously reported to stabilize the eIF4F complex on 5' cap *in vitro* and in plants (142, 695-697).

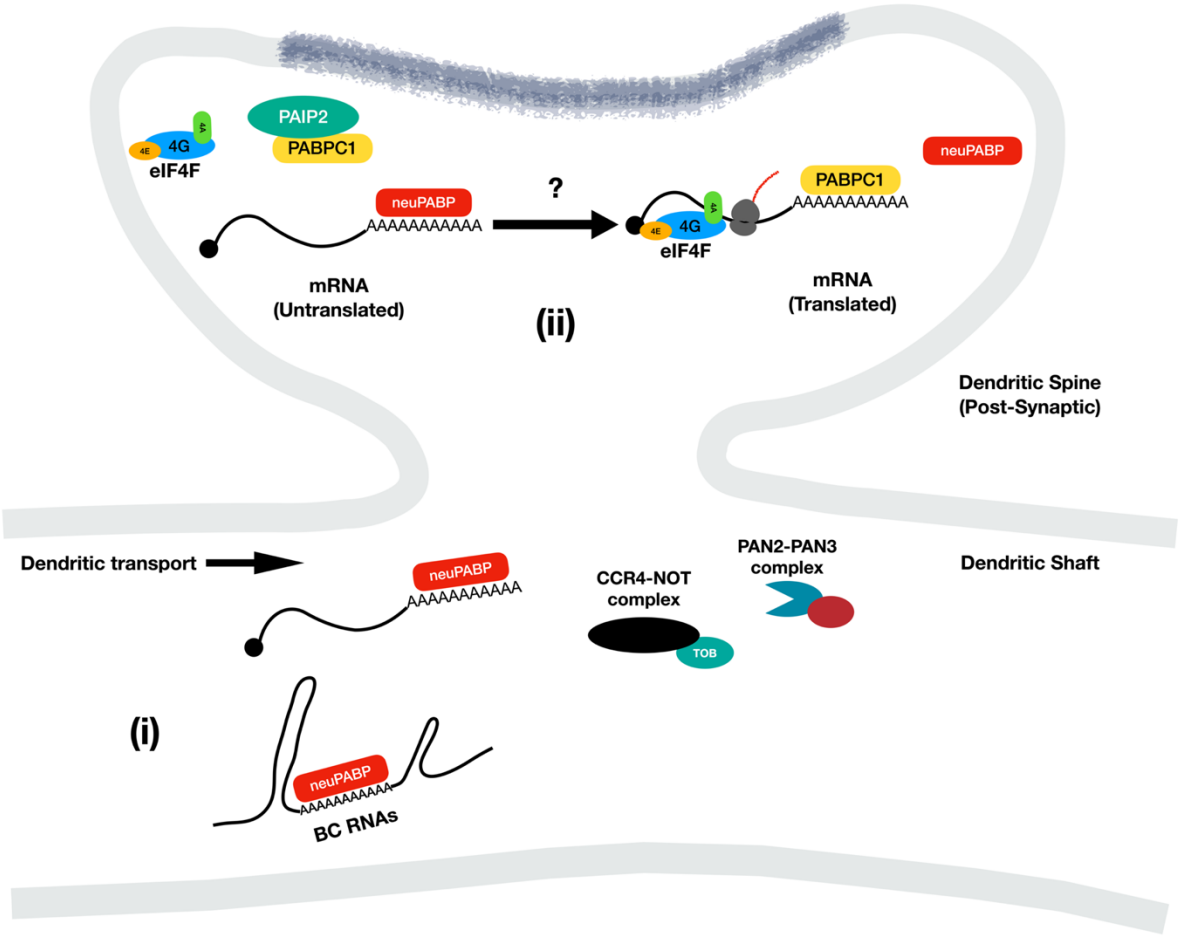

Figure 40. Model for biological role of neuPABP. (i) neuPABP binds to BC1 RNA and select translationally dormant mRNAs which may be transported to post-synaptic compartments. As neuPABP also lacks the PABPC1 MLLE domain, it may protect mRNAs from mRNA decay factors that can interact with this domain, including the PAN2-PAN3 complex and Tob, which interacts with the CCR4-NOT deadenylase complex. (ii) It is possible that in specific contexts (depicted as a question mark), PABPC1 may displace neuPABP from mRNA poly(A) tails, bind eIF4G and stimulates their mRNA translation.

In line with these studies, our data shows that PABPC1 binds eIF4G both *in vitro* and *in cellulo*, in contrast, neuPABP fails to interact with eIF4G as it contains non-conservative amino acid substitutions in eIF4G binding sites. Do PABPC1-bound mRNAs in early RNP fractions contain eIF4F complex? To answer this, it is of interest to us to pulldown neuPABP and PABPC1 from early RNP fractions and study if the bound RNAs contain eIF4F complex components. This would further enhance our current understanding of neuPABP function in translation regulation.

In vitro protein synthesis assays are important tools to study the impact of a protein on translation. These assays have been used previously to investigate proteins with a potential regulatory role in translation. For example, PABPC1 was described as a translation factor that stimulates translation using an *in vitro* translation system (142), FMRP, a well-studied protein in neurons was classified as a negative regulator of translation by using *in vitro* protein synthesis assays (691, 698). The use of *in vitro* translation assays have advantages such that the effect of a protein on translation can be studied quickly by modulating its concentration or inserting mutations. Therefore, by utilizing *in vitro* translation assay, we have characterized neuPABP as a putative translation repressor.

We have recently generated a *Pabpc1l2* knockout mouse. While the distribution profile of neuPABP-associated mRNAs in polysomes is similar between *Pabpc1l2*^{KO} and WT mice hippocampi, future studies involving neuron stimulation, for example with BDNF (376, 688, 699), would be necessary to challenge the system to study any translation defects. A new method to study the synthesis of specific proteins was devised in neurons (700). This method combines puromycylation of newly synthesized peptides with proximity ligation assay (Puro-PLA). Briefly, neuronal cultures are treated with puromycin, followed by immunofluorescence. Two primary

antibodies, one targeting puromycin tag and the other targeting the protein of interest (ideally N-terminus) are used (419, 700). Next, secondary antibodies coupled to oligonucleotide probes are used. When two probes are in close proximity, they ligate with the help of linker oligonucleotides and a ligase enzyme to form a circle, which is amplified by rolling circle amplification. The amplified circular sequences are then detected by complementary fluorescently-labeled probes. Puro-PLA method has been tested extensively in neurons and can detect translation of ribosomal protein coding mRNAs in dendrites (419). Utilizing this method, the translation of neuPABP-associated mRNAs should be studied in WT and *Pabpc1l2*^{KO} neurons pre-and post-stimulation. Moreover, these studies can be coupled with ribosome footprinting to simultaneously access mRNA association with translating ribosomes. Local mRNA translation in neurons is required for maintaining a long-lasting synaptic strength (L-LTP) (690). Similar to *Paip2a*$^{-/-}$ mice that displayed a lower threshold for L-LTP induction (640), it will be interesting to investigate if *Pabpc1l2*^{KO} mice also display similar electrophysiological phenotypes. Therefore, future studies should combine local protein synthesis and electrophysiological studies to better understand the impact of local proteome changes on LTP induction in *Pabpc1l2*^{KO} mice.

Interestingly, our translation assay in SH-SY5Y cells using a bicistronic reporter, demonstrates that neuPABP can repress cap- and poly(A) dependent translation in a dose dependent manner. These data suggest that the impact of neuPABP on translation can be modulated by a change in its levels. Do neurons modulate local concentration of neuPABP in synaptic terminals following stimulation? This is an important question that will be addressed in future studies. For example, neuron cultures should be stimulated (for example, BDNF or KCl), and synaptic terminals can be fractionated to quantify changes in neuPABP protein levels pre- and post-stimulation. Interestingly,

our data and previous studies suggest PABPC1 localization in dendritic compartments (641), where it associates strongly with *CaMKIIα* mRNA after training in WT and *Paip2a*$^{-/-}$ mice (640). Likewise, a study demonstrated a strong association of HuD with dendritic mRNAs (*Neuritin, Homer1a, GAP-43, Neuroligins, Verge* and *CaMKIIα*) after KCl stimulation of cultured neurons (692). Currently, it is not known if neuPABP is associated strongly or released from target RNAs after stimulation. Therefore, to test this, future studies should focus on CLIP experiments from cultured neurons using different stimulation methods. These experiments will deepen our understanding of the fate of neuPABP-bound RNAs.

Brain cytoplasmic (BC) RNAs have been extensively reported to localize into dendritic compartments, and act by repressing local translation of mRNAs (452, 464, 466, 473, 701, 702). Interestingly, BC RNAs are suggested to repress translation by sequestrating eIF4A and PABPC1, both of which can bind BC RNAs, and thereby inhibiting the formation of 48S preinitiation complex (472), Our polysome profiling data show that both neuPABP and BC1 RNA are localized in early RNP fractions that contain untranslated RNAs. Moreover, we show that neuPABP cannot bind eIF4G. Therefore, these data collectively suggest a possible unexplored role of neuPABP-BC1 RNP in translation initiation control in dendrites. Interestingly, a recent study reported the expression of BC1 RNA in germinal vesicle (GV) stage oocytes. They showed that BC1 RNA overexpression in GV oocytes repressed the translation of an injected luciferase reporter bearing a strong 5' terminal oligopyrimidine (TOP) motif sequence (703). Intriguingly, ribosomal protein coding mRNAs that neuPABP targets, are TOP motif-containing mRNAs (704). While neuPABP expression in GV oocytes is currently unknown, in neurons BC1-neuPABP may function together to regulate TOP mRNA translation. Our RNA abundance analysis from neuPABP^{KO} mouse brain

showed significantly elevated levels of BC1 RNA. While the consequences that elevated BC1 levels may have on neuronal function are currently unclear, a study found elevated levels of BC200 RNA in Alzheimer's brain regions that were involved in the disease progression; however, no causal link was established (458). How neuPABP regulates BC1 levels and function remains unclear.

More recently, several studies revealed the function of PABPC1 in mRNA stability. These studies found that PABPC1 supports the stability of generally stable mRNAs that code for proteins with constitutive functions (128). Depletion of PABPC1 from human cell lines led to the degradation of these mRNAs which was dependent on 3' terminal uridylation by TUT4/TUT7 (37, 128, 160, 241). Therefore, while PABPC1 does promote deadenylation, it seems to prevent mRNA decay by preventing terminal uridylation (37). Before we ask if neuPABP can block terminal uridylation, a more pressing question is: can neuPABP block deadenylation? Evidently, many factors that regulate mRNA stability interact with PABPC1 via MLLE domain. These include: PAN3 subunit of PAN2-PAN3 deadenylase complex (36), Tob proteins and GW182 protein of miRISC complex, both of which can recruit CCR4-NOT deadenylase complex to target mRNAs (228, 269, 705-707). However, in contrast to PABPC1, neuPABP lacks MLLE domain, and therefore, may not recruit deadenylation factors to neuPABP-bound mRNAs. An alternate possibility is that once PABPC1 bound mRNAs are deadenylated by the concerted action of major deadenylases i.e., PAN2-PAN3 and CCR4-NOT, short mRNA poly(A) tails (<25 adenosines) that can no longer accommodate a PABPC1 molecule (37, 242, 243, 708), may become substrate for neuPABP binding. neuPABP contains only two RRMs, which can easily bind very short poly(A) sequences (12-25 adenosines) (143, 308, 311). Moreover, neuPABP not only lacks RRMs 3 and 4, but also lacks the linker region

that PABPC1 use to oligomerize on mRNA poly(A) tails (36, 708). Specifically, RRM1 of a PABPC1 molecule contacts the linker region of an adjacent PABPC1 molecule for oligomerization (36, 309-311). Additionally, neuPABP has acquired a new N-terminus that is not present in other PABPCs. Together, these unique properties of neuPABP may prevent it from oligomerizing with itself or other PABPCs on poly(A) tails. In line with this, our data show that neuPABP and PABPC1 do not coexist on RNAs. Taken together, it is possible that short-tailed mRNAs prefer neuPABP over PABPC1. Consequently, similar to PABPC1, neuPABP may protect its mRNA targets from TUT4/TU7 mediated uridylation. To test these possibilities, nanopore sequencing of neuPABP-associated mRNA poly(A) tails is required. A parallel sequencing experiment on PABPC1-bound mRNA poly(A) tails would also be necessary for a direct comparison of poly(A) tail lengths as well as 3'end modifications.

In line with previous studies, our data show that PABPC1 can coimmunoprecipitate eIF4G from human cell lysates (143). Moreover, PABPC1 and eIF4G cooccupancy on mRNAs correlates very strongly in *Drosophila* and human cell lines (161). In contrast to this, we show that neuPABP not only fails to interact with eIF4G *in vitro*, but is unable to coimmunoprecipitate eIF4G from human cell lysates, even when native mRNAs were maintained in RNAse free conditions. This suggest that neuPABP-containing mRNAs may not be able to recruit eIF4G. Previous studies suggest that eIF4E binds weakly to the 5' cap, when outside the context of eIF4F complex, however, interaction with eIF4G is required for a stable eIF4E-5' cap binding (695). Do neuPABP bound mRNAs maintain a 5' cap structure and bind eIF4E? Future studies should involve terminator 5' phosphate-dependent nuclease assay to examine if neuPABP-bound RNAs still maintain a 5' cap, as mRNAs that lack the 5'cap will be susceptible to degradation by 5'-3' ribonucleases (709).

4.4. Conclusions

Post-transcriptional regulatory mechanisms are critical in exerting a tight control over spatiotemporal gene expression. Neurons have developed intricate mechanisms to transport mRNAs and translation regulatory machineries to the neurites, which allows for the synthesis of specific proteins in response to synaptic activity. The localized gene expression programs grant neurons with the ability to rapidly modify their local proteome to support long lasting synaptic plasticity and memory storage. Several RBPs have emerged as key modulators of local protein synthesis, and the multifaceted roles they play in RNA fate determination are of great scientific interest. Despite the identification of RBPs and RNAs in the neurites, the precise role of RBPs in RNA metabolism is only starting to unravel. Through the work presented in my thesis, I have uncovered a new mammalian brain-specific RBP, whose expression peaks in mature neurons, and therefore, we have named it neuPABP. Moreover, we were successful in identifying neuPABP-associated RNAs in the brain, and our work classifies neuPABP as a putative translation repressor. This work will facilitate future studies to further investigate the role of neuPABP in regulating local mRNA translation. Importantly, the identification of neuPABP associated mRNAs will have implications for subsequent studies investigating the impact of local protein synthesis on ribosomal and/or mitochondrial functions in neurites. In addition, the identification of neuPABP-BC1 association is significant, which may shed some light on BC1 functionality. Overall, this work has unveiled a new neuronal RBP that may function to regulate protein synthesis of select mRNAs and will broaden our understanding about the diverse roles of RBPs in supporting synaptic function.

5. METHODS

5.1. Uncovering neuPABP

Antibodies

Antibodies were purchased from Abcam (PABPC1, hnRNPA1, PSD-95, RPS6, Synaptophysin), Cell signaling (PABPC1, V5, eIF4G, β-Actin), Biolegend (β3tubulin), Invitrogen (V5-tag), Santa Cruz (GAPDH), Sigma-Aldrich (PAIP2). A peptide encompassing the C-terminal end of mouse neuPABP (ERGAWARQSTSADFKDFD) that is not conserved in other mammalian PABPC proteins was injected into rabbits for neuPABP antibody production (Thermofisher).

DNA Constructs, cell lines and primary cultures

Bacterial expression vectors

N-terminal GST-tagged neuPABP and eIF4G (41-244) expression clones were generated by cloning into pGEX-6P1 plasmid (Addgene). neuPABP and eIF4G (41-244) coding sequences were PCR-amplified, restriction digested with enzymes BamHI, SalI for neuPABP, and NotI, SalI for eIF4G (41-244), and ligated in frame with the N-terminal GST-tag in pGEX-6P1 plasmid, N-terminal His-tagged PABPC1 expressing pET-28b-PABPC1 plasmid was a gift from Dr. Sonenberg at McGill University. N-terminal malE-tagged neuPABP and PABPC1 (RRM1+2) expression clones were generated by cloning into pMAL-c5X plasmid (NEB) using restriction enzyme sites NotI and SacI. neuPABP and PABPC1(RRM1+2) coding sequences were PCR-amplified, restriction digested with enzymes NotI and SacI, and ligated in frame with the N-terminal malE-tag in pMAL-c5X plasmid.

Mammalian expression vectors

C-terminal V5-tagged neuPABP and PABPC1 expression clones were generated by Gateway cloning (ThermoFisher). Coding sequences were PCR-amplified using gene-specific gateway primers that contained flanking attB sites for recombination with attP sites in the donor pDONR221 plasmid, to generate entry clones with attL sites. Further, neuPABP and PABPC1 expression clones were generated by recombining the attL sites in the pDONR221-neuPABP and PABPC1 entry clones and the attR sites in pLEX-307 destination vector (Addgene), and lncRNA Bc1 gene sequence was cloned into PLKO.1 puro vector (Sigma). Bc1 gene sequence was PCR amplified using primers containing restriction enzyme sites for EcoRI and XmaI, restriction digested, and ligated into PLKO.1 puro plasmid that was digested with EcoRI and AgeI (BshTI).

Cell Lines

Human epithelial carcinoma HeLa cells and Human embryonic kidney HEK293T cells were purchased from ATCC. Cell lines were maintained in Dulbecco's modified Eagle's medium (DMEM) supplemented with 10% fetal bovine serum, 50 U/ml of penicillin and 50 µg/ml of streptomycin.

Primary neuronal cultures

Mouse primary cortical neuron cultures were prepared from P0 pup cortices. Mouse pups were collected soon after birth and decapitated as per animal handling protocol. Brains were immediately harvested into cold Dulbecco's modified Eagle's medium-F12 media (DMEM/F-12), and cerebellum and olfactory bulbs were removed. Cortices were gently triturated in pre-warmed DMEM/F12 medium by pipetting with Pasteur pipette to get homogenous cell suspension, and

centrifuged (700rpm, 2min). Only half of the supernatant was removed from the top, replaced with PPD saline (0.1% Papain, 0.01% deoxyribonuclease-I, 0.1% neutral protease-Dispase-II, 10mM $MgCl_2$ in HBSS(without Ca^{2+} and Mg^{2+})), mixed with Pasteur pipette, incubated (37C, 30min), and in between pipetting gently every 10min. Cells were centrifuged (800rpm, 10min), resuspended in DNase-I saline (0.1% deoxyribonuclease-I in DMEM), and incubated at (37C, 15 min). Cells were then collected by centrifugation (800rpm, 10min), resuspended in Complete Neuronal medium (Neurobasal medium containing 1X B27 supplement, 2mM L-Glutamine, 0.5X Pen/Strep), and plated on Poly-L-Lysine coated culture flasks. 72 hours post-plating, Ara-C (Arabinosylcytosine) drug (3uM) was added to control glial cell overgrowth. Sterile conditions were maintained throughout the procedure.

5'RACE (Rapid Amplification of cDNA Ends)

RNAs were isolated from mouse primary neuronal cultures at DIV7, using Trizol reagent. RNAs were dephosphorylated using FastAP (Alkaline Phosphatase) kit (ThermoFisher) and decapped using RppH (RNA 5' Pyrophosphohydrolase) kit (NEB). RNA adapter: (5'GCUGAUGGCGAUGAAUGAACACUGCGUUUGCUGGCUUUGAUGAAA3') was ligated to 5'monophosphate ends of the decapped RNAs by using T4 RNA Ligase 1 (NEB). RNAs were reverse transcribed using AffinityScript kit (Agilent). A PCR amplification using KAPA HotStart kit (MilliporeSigma) was carried out using adapter specific forward primer: (5'GCTGATGGCGATGAATGAACACTG3') and *pabpc1l2* sequence specific reverse primer: (5'CACCGGTTGCTGGTAGTTGA3'). A fraction of PCR reaction was further amplified using adapter specific forward and *pabpc1l2* sequence specific reverse Gateway primers containing attB sites:

(5'GGGGACAAGTTTGTACAAAAAAGCAGGCTACCGCTGATGGCGATGAATGAACACT G3') and (5'GGGGACCACTTTGTACAAGAAAGCTGGGTCCCAGGCTGGCCTCCTCAA3'), respectively and cloned into a Gateway donor plasmid pDONR™221 (ThermoFisher). Plasmid constructs were sequenced to identify *pabpc1l2* mRNA 5'end.

Recombinant protein purification

GST-tagged recombinant proteins were expressed in Rosetta-2(DE3) *E. coli* cells (Millipore) and purified by using Glutathione agarose resin (ThermoFisher). GST cleavage was performed using HRV-3C protease (ThermoFisher). His-tagged recombinant proteins were purified by using Ni-NTA beads (Qiagen). MBP-tagged recombinant proteins were purified by using Amylose resin (NEB). (**Note:** Recombinant protein purification protocol is detailed in Section 3.2)

GST-pulldown assays

GST or GST-eIF4G (1-244) recombinant bait proteins (200 pmol) were allowed to bind to 25ul of packed glutathione beads in binding buffer (50mM Tris, 150mM NaCl, 0.5% NP-40, 5% Glycerol, 1.5mM DTT), for 2 hours at 4C, with gentle rotation. MBP-tagged neuPABP or PABPC1 (RRM1+2) prey proteins (160 pmol) were then added, and the reactions were incubated overnight at 4C, with gentle rotation. Beads were washed to remove unbound proteins , boiled in Laemmli buffer to release the bound proteins, and resolved on an SDS-PAGE gel. Resolved proteins were visualized by Coomassie blue staining.

RNAcompete

The RNA pool generation, RNAcompete pulldown assays, and microarray hybridizations were performed as previously described (633, 710, 711). Briefly, RNAcompete experiments employed defined RNA pools that are generated from 244K Agilent custom DNA microarrays. Pool design is based on a de Bruijn sequence of order 11 that was subsequently modified to minimize secondary structure in the designed sequences and minimize intramolecular RNA cross-hybridization. After these modifications, not every 11-mer is represented but each 9-mer is represented at least 16 times. To facilitate internal data comparisons, the pool is split computationally into two sets: Set A and Set B. Each set contains at least 155 copies of all 7-mers except GCTCTTC and CGAGAAG which are removed because they correspond to the SapI/ BspQI restriction site used during DNA template pool generation. A φ2.5 bacteriophage T7 promoter initiating with an AGA or AGG sequence is added at the beginning of each probe sequence in the DNA template pool to enable RNA synthesis. The final RNA pool consists of 241,399 individual sequences up to 41 nucleotides in length (633). The microarray design is detailed in (633) and can be ordered from Agilent Technologies using AMADID# 024519. In RNAcompete assays, 20 pmoles of GST-tagged neuPABP and RNA pool (1.5 nmoles) were incubated in 1 mL of Binding Buffer (20 mM Hepes pH 7.8, 80 mM KCl, 20 mM NaCl, 10% glycerol, 2 mM DTT, 0.1 mg/mL BSA) containing 20 μL glutathione Sepharose 4B (GE Healthcare) beads (pre-washed 3 times in Binding Buffer) for 30 minutes at 4°C, and subsequently washed four times for two minutes with Binding Buffer at 4°C. One-sided Z-scores were calculated for the motifs as described previously (633).

Electrophoretic Mobility Shift Assay

150 pmol of RNA oligo$(A)_{25}$ was 5' end-radiolabeled with 10 μCi of [γ32-P]-ATP (Perkin Elmer)

by using the enzyme T4 polynucleotide kinase (ThermoFisher) for 1 hour at 37C. The end-labeled oligoribonucleotide was diluted (to 2 pmol per μL) with double distilled water, column purified (Roche), 2pmol RNA oligonucleotide was used for each EMSA reaction. RNA-protein EMSA binding reactions as well as protein dilutions were made in standard phosphate buffer saline (NaCl: 137 mM, KCl: 2.7 mM, Na2HPO4: 10 mM, KH2PO4: 1.8 mM) supplemented with 160ng/mL double stranded DNA and 40U/mL RNase inhibitor (Promega). 2 pmol of radiolabelled RNA oligonucleotide (per reaction) was mixed with different amounts of recombinant protein (neuPABP or PABPC1) in a final reaction volume of 20 uL, and incubated at 30C for 1 hour. Binding reactions were supplemented with glycerol containing bromophenol blue dye (to 5% glycerol concentration) and were electrophoresed on a 10% non-denaturing polyacrylamide/bis-acrylamide (29:1, w/w) gel in Tris-borate-EDTA running buffer (120V, 60-120 min, on ice). Gels were analyzed using a PhosphorImager (GE Healthcare). Free RNA as well as gel-shifted RNA bands were quantified for each gel lane by ImageJ. The fraction of bound RNA in each lane was calculated by using the expression: bound/(bound + unbound). The dissociation constant (K_D) values were calculated by GraphPad Prism software as the protein concentration (nM) at which only 50% of free RNA remained unbound.

***in vitro* translation experiments**

Krebs-2 cell-free lysates were prepared as described previously for in vitro translation experiments (712, 713). Capped poly(A)+ and poly(A)- luciferase RNAs were incubated in Krebs-2 extract, *in vitro* translation reactions were incubated at 30C for 1hour, and translation output from the reporter mRNAs was accessed by a luciferase assay (Promega).

Tissue expression analysis

Western blotting

Adult mice (C57BL/6J; 5 months old) were sacrificed as per animal euthanization protocol, different tissues were dissected out, including different brain regions and lysates were prepared in a lysis buffer (50mM Tris-HCl (pH-7.5), 150mM NaCl, 0.5% NP-40, 2mM EDTA, 1mM DTT). Western blotting was performed to assess the expression of neuPABP PABPC1 and other proteins.

RT-PCR and RT-qPCR analyses

Adult mice (C57BL/6J; 5 months old) were sacrificed as per animal euthanization protocol. Different tissues/brain regions were dissected out and total RNA was isolated using Trizol reagent. RNAs were reverse-transcribed (ThermoFisher) and semi-quantitative PCR and qPCR analyses were performed to access the differential expression of *pabpc1l2* among mouse tissues.

Single-nuclei RNA-seq data processing

10x multiome RNA + ATAC data for healthy mouse cortex at postnatal timepoints P7 and 10W were obtained from GSE199885. Sequencing reads were reprocessed to allow the quantification of *Pabpc1l2*, as the genomic annotations for *Pabpc1l2*a/b are absent in the mm10 reference genome build used in the original publication (714). A custom reference was built, adding the coordinates for *Pabpc1l2b* (chrX:103,013,563-103,016,208) to the gene annotation. In addition, since there is high homology in *Pabpc1l2*a/b genes resulting in multimapping reads, the sequence for *Pabpc1l2a* (chrX:103,064,742-103,067,538) was masked using bedtools maskfasta. Thus, the expression of the two *Pabpc1l2a/b* genes is profiled as a single feature (*Pabpc1l2*) in downstream analysis, and no attempt is done to distinguish expression of *Pabpc1l2a* and *Pabpc1l2b* separately.

Sequencing reads were then aligned and demultiplexed using cellranger-arc v2.0.0 (10x Genomics) using this modified mm10 reference genome build coupled with the modified Ensembl 98 gene annotation. Quality control (QC) and data processing steps were performed using Signac v1.3.0 (715) and Seurat v4.0.0 (716) as described in the original publication (714). Briefly, QC metrics for RNA and ATAC modalities were jointly used to filter cells. In the RNA modality, cells were filtered on the number of genes, unique molecular identifiers (UMIs), and mitochondrial content. In the ATAC modality, cells were filtered on the number of peaks detected, transcription start site enrichment, and nucleosome signal. Next, RNA libraries were scaled to 10,000 UMIs per-cell, log normalized, and UMI counts and mitochondrial content were regressed out. 10W samples were integrated by merging the samples without batch correction, followed with scaling and normalization. Dimensionality reduction was performed using PCA on the top 2,000 most variable features. The first 25 principal components were used as input for projection into two dimensions (uniform manifold approximation and projection (arXiv:1802.03426) and for clustering [shared nearest-neighbor algorithm (716)]. Doublets were identified using scDblFinder (717) with the recommended cluster-based approach and subsequently the doublets were filtered. Lastly, annotations of cell types was performed using four machine learning-based prediction methods (SciBet, SingleCellNet, SingleR, and Support Vector Machines) (718-720). For this, two murine brain cell type atlases were used: non-neuronal cell-types were annotated using a developmental murine atlas (721). Cells predicted as neurons were subsequently annotated using a more detailed neuronal enriched atlas (722). A consensus cell type annotation was assigned when at least two methods agreed. Finally, cell type labels were aggregated into broad cell type classes.

Subcellular fractionation

Whole cell, cytoplasmic and nuclear fractions

The protocol for cell fractionation of mouse brain cortex (C57BL/6J; Age: 2 months) was adapted and optimized from a previously published paper describing a rapid and efficient method to sub-fractionate human cell-lines (723). Briefly, an adult mouse was euthanized as per animal handling protocols, brain was dissected out and cerebellum and olfactory bulbs were removed. The brain hemispheres were separated, and cerebral cortex was dissected out from one hemisphere. The cortex tissue was triturated in phosphate buffer saline (PBS) by pipetting, centrifuged (200X g, 3min). The pellet was again triturated in PBS and incubated on ice (3min) to allow the tissue chunks to settle down. Cell suspension was obtained from the top by avoiding the tissue chunks. A part of this cell suspension was then centrifuged (2500 X g, 3 min). The cell pellet thus obtained was triturated in Lysis buffer (0.1% NP-40 in PBS) by pipetting 6-7 times using a p1000 micropipette. One third of this homogenous cell suspension was kept as “Whole cell fraction”, the remaining homogenate was pipetted 3 more times, and centrifuged (7000 X g, 30sec). One half of the supernatant was kept as “cytoplasmic fraction”, while the remaining supernatant was discarded. The pellet was again triturated in the lysis buffer by pipetting 5 times, centrifuged (7000 X g, 30sec), and supernatant was discarded. The residual pellet was kept as “Nuclear fraction”. Laemmli buffer containing Benzonase (Millipore) was added to each collected fraction, and western blot analysis was performed for nuclear and cytosolic proteins was performed.

Crude synaptosome preparation

Subcellular fractionation of adult mouse brain cortex (C57BL/6J; Age: 6 months) was carried out using a protocol adapted from (473, 724, 725). Briefly, adult mouse brain was dissected out and

cerebellum and olfactory bulbs were removed. The cortex tissue was homogenized in homogenization buffer (320 mM Sucrose, 5 mM HEPES-NaOH (pH 7.4), 2 mg/mL BSA, and 1 mM EDTA), by 15 strokes using a Dounce homogenizer to obtain brain homogenate fraction (H), which was centrifuged (1000 X g, 10 min, 4C) to obtain supernatant S1. The S1 supernatant was centrifuged (14000 X g, 20 min, 4C) to obtain cytosolic supernatant S2 fraction, and crude synaptosome containing pellet P2 fraction. We further fractionated the crude synaptosomes into Triton X-100 detergent soluble "non-PSD" fraction and detergent insoluble "PSD-enriched" fraction. P2 fraction was once resuspended in Resuspension buffer (5mM HEPES-NaOH (pH-7.4), 1mM EDTA), and centrifuged (14000 X g, 15 min, 4C). The washed pellet thus obtained was resuspended in Buffer-A (5mM HEPES-NaOH (pH-7.4), 100mM NaCl, 0.5% Triton X-100), rotated (15 min, 4C), centrifuged (14000 X g, 15 min, 4C), to obtain Triton X-100 soluble "non-PSD" fraction as the supernatant. The remaining pellet was resuspended in Buffer-B (5mM HEPES NaOH (pH-7.4), 0.15mM NaCl, 1% Triton X-100, 1% SDS, 1% Deoxycholic acid, 1mM DTT), rotated (75min, 4C), centrifuged (14000 X g, 15 min, 4C), to obtain Triton X-100 insoluble "PSD-enriched" fraction as the supernatant. The brain homogenate, cytosolic and crude synaptosomal fractions were lysed completely by supplementing with RIPA buffer (10mM Tris-HCl (pH-8.0), 140mM NaCl, 1% Triton X-100, 0.1% Deoxycholic acid, 0.1% SDS, 1mM EDTA). The buffers used in crude synaptosomal preparation were supplemented with Protease inhibitors cocktail and 1mM Phenylmethylsulfonyl fluoride (PMSF).

Mass-spectrometry analysis

Adult mouse brain (C57BL/6J; Age: 2 months) was dissected out, cerebellum and olfactory bulbs were removed, and cerebral cortex was isolated. Briefly, fresh cortex tissue was triturated in cold

phosphate buffer saline by pipetting, and centrifuged (200X g, 3min). Tissue pellet was lysed in a lysis buffer (50mM Tris-HCl (pH-7.5), 150mM NaCl, 0.5% NP-40, 2mM EDTA, 1mM DTT), and centrifuged (20,000 X g, 15min, 4C) to obtain the lysate. Tissue lysate was clarified with Protein G Agarose beads (MILLIPORE), total protein quantified, and immunoprecipitated with neuPABP antibody. Protein complexes were eluted with neuPABP-specific peptide (ERGAWARQSTSADFKDFD) and resolved by SDS-PAGE. Gels were subsequently stained with colloidal stain, neuPABP protein was excised, digested with trypsin or subtilisin and analyzed by the LDI Proteomics Centre (Montreal, Canada).

Polysome profiling

Mouse brain (C57BL/6J; p9 mouse pup) was dissected out, and cerebellum and olfactory bulbs were removed. The remaining brain tissue was triturated by pipetting in dissection buffer (10mM HEPES-NaOH (pH-7.5), cycloheximide (0.1mg/mL)), centrifuged (300 X g, 3 min). The tissue pellet was lysed in polysome lysis buffer (10mM HEPES-NaOH (pH-7.5), 150mM NaCl, 5mM $MgCl_2$, 0.5mM DTT, 1% NP-40, cycloheximide (0.1mg/mL)), and centrifuged twice (20,000 X g, 10 min, 4C). Lysates were loaded on a linear sucrose gradient (5-50%), centrifuged (130,000 X g, 2 hours, 4C). Gradient fractions (4 to 16) were collected as described previously (726), proteins were TCA precipitated from each fraction and dissolved in Laemmli buffer to perform western blot analysis.

For lncRNA Bc1, polysome fractionation was done from adult mice (C57BL/6J; Age: 3 months). RNA from each polysome gradient fraction was Trizol extracted, reverse transcribed and semi-quantitative-PCR analysis was carried out on lncRNA Bc1 and Actin. In parallel, qPCR analysis

was carried out on lncRNA Bc1 and data was normalized to the total cortex RNA (Input) to calculate percent distribution across fractions.

RIP RNA-sequencing (RIP-Seq)

Mouse hippocampi (C57BL/6J; Age: 6 months) were dissected out and flash frozen on dry ice. Tissue was lysed in a lysis buffer (50mM Tris-HCl (pH-7.5), 150mM NaCl, 0.5% NP-40, 2mM EDTA, 1mM DTT), and centrifuged (20,000 X g, 15min, 4C) to obtain the lysate. Tissue lysates were clarified with Protein G Agarose beads (MILLIPORE), total proteins quantified, and immunoprecipitation carried out by first incubating with antibodies: IgG (control) or neuPABP, followed by a pulldown of immunoprecipitants with Protein-G agarose beads. Immunoprecipitation of neuPABP was confirmed by western blotting. neuPABP bound RNAs were extracted directly from the beads by using an RNA purification kit (Qiagen). Biological triplicate libraries were prepared from immunoprecipitated RNAs. RNA was depleted of ribosomal RNA and libraries were prepared using the KAPA Stranded RNA-Seq Kit with RiboErase (Roche). Sequencing reactions were carried out by paired-end 150 bp sequencing on a Nextseq500 platform (Genomics Platform at the Institute for Research in Immunology and Cancer, Montreal). Sequences were trimmed for sequencing adapters and low quality 3' bases using Trimmomatic version 0.35 (727) and aligned to the reference mouse genome version GRCm38 (gene annotation from Gencode version M25, based on Ensembl 100) using STAR version 2.7.1a (728). Gene expressions were obtained both as readcount directly from STAR as well as computed using RSEM (729) in order to obtain normalized gene and transcript level expression, in TPM values, for stranded RNA libraries. DESeq2 version 1.22.2 was then used to normalize gene readcounts (730).

Volcano plot and Gene Ontology analysis

Volcano plot was generated using a list of transcripts with Fold Change≥1.10 (~2200 transcripts which had p-value<0.05 . A Log2FC≥1.5 cut-off was further used in Volcano plot to highlight highly enriched transcripts. Gene set enrichment analyses for Wikipathway (WP) terms enriched among neuPABP-enriched transcripts (FC≥2) were performed using the g:Profiler online platform (731).

RNA immunoprecipitation with V5 antibody

HeLa cells were co-transfected with V5-tagged neuPABP or PABPC1 expressing constructs and a lncRNA BC1 expressing plasmid. 48 hours post-transfection, lysates were prepared in a lysis buffer (50mM Tris-HCl (pH-7.5), 150mM NaCl, 0.5% NP-40, 2mM EDTA, 1mM DTT) and precleared using Protein-G agarose beads (Millipore). Lysates were incubated with rabbit antibodies: IgG (control), or V5-tag antibody (cell signaling), followed by a pulldown of immunoprecipitants with Protein-G agarose beads. Immunoprecipitation of V5-tagged proteins was confirmed by western blotting. Co-immunoprecipitated RNA was extracted by using Trizol reagent and reverse transcribed. qPCR analysis was carried out to access fold enrichments (vs IgG control) of lncRNAs BC1 and BC200 with V5-tagged proteins. A non-polyadenylated Histone (1H4H) mRNA was used as a negative control.

Formaldehyde-crosslinked RNA immunoprecipitation

Formaldehyde crosslinking of mouse cortex

Brain cortices of adult mice (C57BL/6J; Age: 6 months) were dissected out and gently triturated in dissection buffer (Hank's balanced salt solution containing 10mM HEPES (pH-7.5)), spun at

1000Xg to collect the triturated tissue as a pellet. The pellet was then gently resuspended in dissection buffer containing 0.1% Formaldehyde and incubated at room temperature for 10 minutes. Formaldehyde was quenched by adding Glycine to a final concentration of 200mM, for 5 minutes. Tissue suspension was chilled on ice and pelleted by spinning at 1000Xg. Tissue pellet was washed twice (without resuspending) with dissection buffer containing glycine at a final concentration of 200mM.

Tissue lysis and Polysome RNP fractionation

The crosslinked tissue pellet was lysed in polysome lysis buffer (10mM HEPES-NaOH (pH-7.5), 150mM NaCl, 5mM MgCl2, 0.5mM DTT, 1% NP-40, cycloheximide (0.1mg/mL)), and centrifuged twice (20,000 X g, 10 min, 4C). Lysates were loaded on a linear sucrose gradient (5-50%), centrifuged (130,000 X g, 2 hours, 4C). Gradient fractions (1,2) corresponding to the RNP fraction were collected and combined. Proteins from a part of RNP fraction were TCA precipitated and dissolved in Laemmli buffer to perform western blot analysis to access the depletion of ribosomal subunits in comparison to the total cortex lysate (Marker: RPS6).

Crosslink-(RNP) RNA immunoprecipitation

The RNP fraction was diluted (1:2 dilution) in RIPA buffer (25mM Tris-HCl (pH-7.5), 150mM NaCl, 2mM EDTA, 1% NP-40, 0.1% SDS, 0.1% Sodium deoxycholate, 1mM DTT), and immunoprecipitation was carried out by first incubating with antibodies: IgG (control) or neuPABP, followed by a pulldown of immunoprecipitants with Protein-G agarose beads (Millipore). Immunoprecipitation of neuPABP was confirmed by western blotting. Co-immunoprecipitated RNAs were eluted from the beads in elution buffer (50mM Tris-HCl (pH-

8.0), 2mM EDTA, 1% SDS, 10mM DTT) containing Proteinase-K (NEB) (100U/mL). Reverse crosslinking was performed on the thermomixer (1200rpm, 60C for 30 minutes, and 70C for 15 minutes). Eluted RNAs were further isolated by using Trizol reagent (ThermoFisher). qPCR analysis was carried out to access fold enrichments (vs IgG control) of lncRNAs BC1 and other neuPABP target and non-target mRNAs. A mitochondrial genome encoded mRNA (*mt.ND1*) was used as a control to negate post-lysis reassociation artifacts.

Statistics

All experiments were carried out at least in triplicates. Graphs for *in vitro* translation assays were generated using GraphPad Prism software and Excel. Means and standard error of the mean (SEM) from biological replicates (n=3) were calculated. For *in vitro* translation assays, a two-tailed Student t-test (equal variance) was carried out to assess the significance of the data in Excel. $p>0.05$ are denoted as n.s., $p<0.05$ as '*', $p<0.01$ as '**', and $p<0.001$ as '***'.

The METHODS section 5.1 is from the published manuscript:

Title: *Uncovering a mammalian neural-specific poly(A) binding protein with unique properties.*
Authors: Sahil Sharma*, Sam Kajjo, Zineb Harra, Benedeta Hasaj, Victoria Delisle, Debashish Ray, Rodrigo L Gutierrez, Isabelle Carrier, Claudia Kleinman, Quaid Morris, Timothy R. Hughes, Roderick McInnes, and Marc R. Fabian*
Journal: *Genes and Development (Impact factor: 12.89)*
**First author*

5.2. neuPABP, a synaptically localized RNA binding protein

Antibodies

Antibodies were purchased from Abcam (PABPC1, PSD-95, RPS6, Synaptophysin, GFAP), Proteintech (RPLP0), Cell signaling (PABPC1), Biolegend (β-tubulin III), Santa Cruz (GAPDH), MBL life science (eIF4E), and Sigma-Aldrich (PAIP2 and FLAG). A peptide encompassing the C-terminal end of mouse neuPABP (ERGAWARQSTSADFKDFD) that is not conserved in other mammalian PABPC proteins was injected into rabbits for neuPABP antibody production (Thermofisher).

DNA Constructs, cell lines and primary cultures

Bacterial expression vectors

N-terminal His-tagged PABPC1 expressing pET-28b-PABPC1 plasmid was gifted by Dr. Sonenberg at McGill University. N-terminal malE-tagged neuPABP expression clone was generated by cloning into pMAL-c5X plasmid (NEB) using restriction enzyme sites NotI and SacI. neuPABP coding sequence was PCR-amplified, restriction digested with enzymes NotI and SacI, and ligated in frame with the N-terminal malE-tag in pMAL-c5X plasmid.

Mammalian expression vectors

The bicistronic luciferase reporter system was a generous gift from Dr. Selena Sagan at McGill University. This reporter system contains: a Renilla luciferase reporter, Hepatitis C virus IRES-element, a Firefly luciferase reporter, and a bovine growth hormone polyadenylation signal sequence (bgh-poly(A)), in this order. The transcription of the reporter is under the control of a

CMV promoter in a pcDNA3 vector background. N-terminal FLAG-tagged neuPABP construct was generated by cloning the coding sequences into pBABE-3XFLAG-puro vector.

Cell Lines

Human neuroblastoma SH-SY5Y cells were purchased from ATCC. Cell lines were maintained in Dulbecco's modified Eagle's medium (DMEM/F12) supplemented with 10% fetal bovine serum, 50 U/ml of penicillin and 50 µg/ml of streptomycin.

Primary neuronal cultures

Mouse primary cortical neuron cultures were prepared from P0 pup cortices. Mouse pups were collected soon after birth and decapitated as per animal handling protocol. Brains were immediately harvested into cold Dulbecco's modified Eagle's medium-F12 media (DMEM/F-12), and cerebellum and olfactory bulbs were removed. Cortices were gently triturated in pre-warmed DMEM/F12 medium by pipetting with Pasteur pipette to get homogenous cell suspension, and centrifuged (700rpm, 2min). Only half of the supernatant was removed from the top, replaced with PPD saline (0.1% Papain, 0.01% deoxyribonuclease-I, 0.1% neutral protease-Dispase-II, 10mM $MgCl_2$ in HBSS(without Ca^{2+} and Mg^{2+})), mixed with Pasteur pipette, incubated (37C, 30min), and in between pipetting gently every 10min. Cells were centrifuged (800rpm, 10min), resuspended in DNase-I saline (0.1% deoxyribonuclease-I in DMEM), and incubated at (37C, 15 min). Cells were then collected by centrifugation (800rpm, 10min), resuspended in Complete Neuronal medium (Neurobasal medium containing 1X B27 supplement, 2mM L-Glutamine, 0.5X Pen/Strep), and plated on Poly-L-Lysine coated culture flasks. 72 hours post-plating, Ara-C

(Arabinosylcytosine) drug (3uM) was added to control glial cell overgrowth. Sterile conditions were maintained throughout the procedure.

Recombinant protein purification

To produce and purify neuPABP and PABPC1 recombinant proteins, E. coli BL2 (DE3) competent cells were transformed with pMAL-C5x-nPABP and pET28b-PABPC1constructs.

GST-fusion protein purification

GST-tagged recombinant proteins were produced by growing the bacterial cultures at 37C, followed by induction with 1mM isopropyl-β-D-thiogalactopyranoside (IPTG) for 4 hours. To purify recombinant proteins, cells were centrifuged (6000 X g, 15min, 4C), and resuspended in Tris-buffered saline solution (containing 1mM PMSF). Cells were lysed by sonication (5 rounds of 15sec pulse at 45% amplitude), followed by lysis with 1% Triton X-100 (rotation, 10min, 4C). Lysates were centrifuged (20000 X g, 20min, 4C), supernatants were incubated with glutathione agarose beads (ThermoFisher) (rotation, 1 hour, 4C), bound beads were washed several times with Tris-buffered saline (containing 0.1% Triton X-100), followed by a final wash with standard Tris-buffered saline. Recombinant proteins were eluted in a GST-elution buffer (50mM Tris-HCl (pH-8.0), 150mM NaCl, 10mM Glutathione). In some instances, recombinant proteins were eluted from the beads by cleaving the GST-tag with a highly specific HRV-3C protease (ThermoFisher). Protein concentration was measured by Bradford assay (BIO-RAD), as well as by a comparison to BSA protein curve on Coomassie-stained SDS-PAGE gel.

His-fusion protein purification

His-tagged recombinant proteins were produced by growing the bacterial cultures at 37C, followed by induction with 1mM isopropyl-β-D-thiogalactopyranoside (IPTG) for 4 hours. To purify recombinant proteins, cells were centrifuged (6000 X g, 15min, 4C), and resuspended in high salt Tris-buffered saline solution (containing 500mM NaCl, 20mM imidazole, 1mM EDTA, 1mM PMSF). Cells were lysed by sonication (5 rounds of 15sec pulse at 45% amplitude), centrifuged (20000 X g, 20min, 4C), supernatants were incubated with Ni-NTA agarose beads (Qiagen) (rotation, 1 hour, 4C), bound beads were washed several times with high salt Tris-buffered saline (500mM NaCl, 20mM imidazole), followed by a final wash with standard Tris-buffered saline (containing 20mM imidazole). Recombinant proteins were eluted in a His-elution buffer (Tris buffered saline containing 500mM imidazole). Protein concentration was measured by Bradford assay (BIO-RAD), as well as by a comparison to BSA protein curve on Coomassie-stained SDS-PAGE gel.

MBP-fusion protein purification

MBP-tagged recombinant proteins were produced by growing the bacterial cultures at 37C, followed by induction with 1mM isopropyl-β-D-thiogalactopyranoside (IPTG) for 4 hours. To purify recombinant proteins, cells were centrifuged (6000 X g, 15min, 4C), and resuspended in high salt Tris-buffered saline solution (containing 500mM NaCl, 1mM EDTA, 1mM PMSF). Cells were lysed by sonication (5 rounds of 15sec pulse at 45% amplitude), centrifuged (20000 X g, 20min, 4C), supernatants were incubated with Amylose resin (NEB) (rotation, 1 hour, 4C), bound beads were washed several times with high salt Tris-buffered saline (1000mM NaCl), followed by a final wash with standard Tris-buffered saline. Recombinant proteins were eluted in MBP-elution

buffer (Tris buffered saline containing 10mM maltose). Protein concentration was measured by Bradford assay (BIO-RAD), as well as by a comparison to BSA protein curve on Coomassie-stained SDS-PAGE gel.

Formaldehyde-crosslinked RNA immunoprecipitation from Synaptosome

Crude Synaptosome preparation

Subcellular fractionation of adult mouse brain cortex (C57BL/6J; Age: 7 months) was carried out using a protocol adapted from (473, 724, 725). Briefly, adult mouse brain was dissected out and cerebellum and olfactory bulbs were removed. The cortex tissue was homogenized in homogenization buffer (320 mM Sucrose, 5 mM HEPES-NaOH (pH 7.4), 2 mg/mL BSA, and 1 mM EDTA), by 15 strokes using a Dounce homogenizer to obtain brain homogenate fraction (H), which was centrifuged (1000 X g, 10 min, 4C) to obtain supernatant S1. The S1 supernatant was centrifuged (14000 X g, 20 min, 4C) to obtain cytosolic supernatant S2 fraction, and crude synaptosome containing pellet P2 fraction.

Formaldehyde crosslinking of crude synaptosome

The P2 pellet was gently resuspended in HBSS buffer containing 0.1% Formaldehyde and incubated at room temperature for 10 minutes. Formaldehyde was quenched by adding Glycine to a final concentration of 200mM, for 5 minutes. Tissue suspension was chilled on ice and pelleted by spinning (14000Xg, 10 min, 4C). Tissue pellet was washed twice (without resuspending) with HBSS buffer containing glycine at a final concentration of 200mM.

Crosslink-RNA immunoprecipitation

The crosslinked P2-pellet was lysed in RIPA buffer (25mM Tris-HCl (pH-7.5), 150mM NaCl, 2mM EDTA, 1% NP-40, 0.1% SDS, 0.1% Sodium deoxycholate, 1mM DTT) to obtain the lysate. Tissue lysate was clarified with Protein G Agarose beads (MILLIPORE), total proteins quantified, and immunoprecipitation carried out by first incubating with antibodies: IgG (control), neuPABP, and PABPC1 (Abcam, #21060), followed by a pulldown of immunoprecipitants with Protein-G agarose beads. Immunoprecipitation of neuPABP, and PABPC1 was confirmed by western blotting. RNAs that coimmunoprecipitated with neuPABP and PABPC1 were eluted from the beads in elution buffer (50mM Tris-HCl (pH-8.0), 2mM EDTA, 1% SDS, 10mM DTT) containing Proteinase-K (NEB) (100U/mL). Reverse crosslinking was performed on the thermomixer (1200rpm, 60C for 30 minutes, and 70C for 15 minutes). Eluted RNAs were further isolated by using Trizol reagent (ThermoFisher). qPCR analysis was carried out to access fold enrichment (vs. IgG control) of lncRNAs BC1 and select mRNAs with both neuPABP and PABPC1. A mitochondrial genome encoded mRNA (*mt.ND1*) was used as a control to negate post-lysis reassociation artifacts.

Polysome profiling of Synaptosome

Subcellular fractionation of adult mouse brain cortex (C57BL/6J; Age: 6 months) was carried out using a protocol adapted from (473, 724, 725). Briefly, adult mouse brain was dissected out and cerebellum and olfactory bulbs were removed. The cortex tissue was homogenized in dissection buffer (10mM HEPES-NaOH (pH-7.5), cycloheximide (0.1mg/mL)), by 15 strokes using a Dounce homogenizer to obtain brain homogenate fraction (H), which was centrifuged (1000 X g, 10 min, 4C) to obtain supernatant S1. The S1 supernatant was centrifuged (14000 X g, 20 min,

4C) to obtain cytosolic supernatant S2 fraction, and crude synaptosome containing pellet P2 fraction.

The crude synaptosome 'P2 pellet' was lysed in polysome lysis buffer (10mM HEPES-NaOH (pH-7.5), 150mM NaCl, 5mM $MgCl_2$, 0.5mM DTT, 1% NP-40, cycloheximide (0.1mg/mL)), and centrifuged twice (20,000 X g, 10 min, 4C) to obtain lysate. The lysate was loaded on a linear sucrose gradient (5-50%) and centrifuged (130,000 X g, 2 hours, 4C). Gradient fractions (5 to 17) were collected as described previously (726), proteins were TCA precipitated from each fraction and dissolved in Laemmli buffer to perform western blot analysis.

RNA granule fractionation

The protocol for RNA granule fractionation was adapted from published papers with a few modifications (416, 478). Briefly, mouse brain (C57BL/6J; Age: 6 months) was dissected out, and cerebellum and olfactory bulbs were removed. The remaining brain cortex tissue was triturated by pipetting in dissection buffer (10mM HEPES-NaOH (pH-7.5), cycloheximide (0.1mg/mL)), centrifuged (300 X g, 3 min). The tissue pellet was lysed in granule lysis buffer (10mM HEPES-NaOH (pH-7.5), 150mM NaCl, 5mM $MgCl_2$, 0.5mM DTT, 1% NP-40, cycloheximide (0.1mg/mL)), and centrifuged twice (20,000 X g, 10 min, 4°C) to obtain lysate. Tissue lysate was loaded on a sucrose gradient (5% top (3mL), 35% middle (3mL), and 60% bottom (6mL) cushion), centrifuged (130,000 X g, 2 hours, 4°C). The 5% top layer of the sucrose gradient was collected as 'RNP fraction', the 35% middle layer of sucrose mostly contains polysomes, which was carefully removed until 60% sucrose boundary, and discarded. Tube walls and top of the 60% sucrose cushion was washed three times with granule lysis buffer (1ml per wash), by carefully

dispensing the lysis buffer on to the tube walls. Finally, the 60% sucrose cushion was collected as 'RNA granule fraction'. Proteins were TCA precipitated from each collected fraction and western blot analysis was performed for neuPABP, PABPC1, ribosomal proteins (RPS6, RPLP0), granule markers (PURA, SYNCRIP), microtubule protein (β-tubulin III), translation initiation factor eIF4E. A synaptic vesicle protein (Synaptophysin), and GAPDH were used as a control for non-enrichment.

Bicistronic luciferase assay

SH-SY5Y cells were co-transfected with the bicistronic luciferase reporter and N-terminally FLAG-tagged neuPABP or PABPC1 expressing constructs. 24 hours post-transfection, cells were collected and lysed in Passive lysis buffer (Promega), and RL and FL activities were measured using Dual-Luciferase Assay (Promega). In parallel, the expression of FLAG-tagged proteins was validated by western blot analyses. RL to FL ratios were calculated and plotted as normalized luciferase activity. A nuclear GFP expressing construct was used as a control for normalization. Experiments were conducted in biological replicates (n=4).

***Pabpc1l2a/b* knockout (*pabpc1l2*$^{-/-}$) mouse generation**

Pabpc1l2a/b knockout (collectively *pabpc1l2*$^{-/-}$) mice were generated at the Centre for Phenogenomics (Toronto) by coinjecting Cas9 ribonucleoprotein complexes and single guide RNAs (sgRNAs) into the zygotes of C57BL/6J mice. Briefly, *pabpc1l2a* and *pabpc1l2b* alleles were targeted for deletion by generating a sgRNA (sgRNA1): 5' CGAGCCCCCGGCCCGCGTTC 3' targeting the 5' of *pabp1l2b* and 3' of *pabpc1l2a* (based on their chromosome location and not transcription start site as *pabpc1l2a* is antisense), and two

sgRNAs (sgRNA2 and sgRNA3): 5' ACTCTCCTGCACTACAGGTG 3' and 5' GAAATCATACTACATTTCGA 3' targeting the intergenic regions separating these two genes. The positioning of sgRNAs was as below:

Gm21998-**gRNA1**-*Pabpc1l2b*-**gRNA2**-Gm9143-**gRNA3**-*Pabpc1l2a*-**gRNA1**-Gm3928

Genotyping PCR primers were designed against the genomic regions (Gm21998, Gm9143, and Gm3928) that remained intact after *Pabpc1l2a/b* gene deletions. A genotyping PCR using the KAPA HotStart genotyping kit (MilliporeSigma) was carried out to confirm the deletion of both genes. An F1 progeny consisted of heterozygous females and hemizygous males. The F1 progeny was crossed (*pabpc1l2*$^{-/-}$ (male) and *pabpc1l2*$^{-/+}$ (female)) to obtain a homozygous female. Finally, the *pabpc1l2*$^{-/-}$ mice were crossed to obtain *pabpc1l2* knockout mouse line. The gene knockout was also confirmed by RT-qPCR and western blot analyses.

Statistics

All experiments were carried out at least in triplicates. Means and standard error of the mean (SEM) from biological replicates (n=3) were calculated. For *in cellulo* translation assays and RNA steady states from brain tissues, a two-tailed Student t-test (equal variance) was carried out to assess the significance of the data in Excel. $p>0.05$ are denoted as n.s., $p<0.05$ as '*', $p<0.01$ as '**', and $p<0.001$ as '***'.

6. REFERENCES

1. French KL, Hallmann C, Hope JM, Schoon PL, Zumberge JA, Hoshino Y, et al. Reappraisal of hydrocarbon biomarkers in Archean rocks. *Proc Natl Acad Sci U S A*. 2015;**112**(19):5915-20.
2. Stent GS. The Operon: On Its Third Anniversary. Modulation of Transfer Rna Species Can Provide a Workable Model of an Operator-Less Operon. *Science*. 1964;**144**(3620):816-20.
3. Byrne R, Levin JG, Bladen HA, Nirenberg MW. The in Vitro Formation of a DNA-Ribosome Complex. *Proc Natl Acad Sci U S A*. 1964;**52**(1):140-8.
4. Miller OL, Jr., Hamkalo BA, Thomas CA, Jr. Visualization of bacterial genes in action. *Science*. 1970;**169**(3943):392-5.
5. Irastortza-Olaziregi M, Amster-Choder O. Coupled Transcription-Translation in Prokaryotes: An Old Couple With New Surprises. *Front Microbiol*. 2020;**11**:624830.
6. Sentenac A. Eukaryotic RNA polymerases. *CRC Crit Rev Biochem*. 1985;**18**(1):31-90.
7. Nikolov DB, Burley SK. RNA polymerase II transcription initiation: a structural view. *Proc Natl Acad Sci U S A*. 1997;**94**(1):15-22.
8. Fischer V, Schumacher K, Tora L, Devys D. Global role for coactivator complexes in RNA polymerase II transcription. *Transcription*. 2019;**10**(1):29-36.
9. Coppola JA, Field AS, Luse DS. Promoter-proximal pausing by RNA polymerase II in vitro: transcripts shorter than 20 nucleotides are not capped. *Proc Natl Acad Sci U S A*. 1983;**80**(5):1251-5.
10. Ramanathan A, Robb GB, Chan SH. mRNA capping: biological functions and applications. *Nucleic Acids Res*. 2016;**44**(16):7511-26.
11. Mazza C, Segref A, Mattaj IW, Cusack S. Large-scale induced fit recognition of an m(7)GpppG cap analogue by the human nuclear cap-binding complex. *EMBO J*. 2002;**21**(20):5548-57.
12. Rambout X, Maquat LE. NCBP3: A Multifaceted Adaptive Regulator of Gene Expression. *Trends Biochem Sci*. 2021;**46**(2):87-96.
13. Lejeune F, Ishigaki Y, Li X, Maquat LE. The exon junction complex is detected on CBP80-bound but not eIF4E-bound mRNA in mammalian cells: dynamics of mRNP remodeling. *EMBO J*. 2002;**21**(13):3536-45.
14. Sen R, Barman P, Kaja A, Ferdoush J, Lahudkar S, Roy A, et al. Distinct Functions of the Cap-Binding Complex in Stimulation of Nuclear mRNA Export. *Mol Cell Biol*. 2019;**39**(8).
15. Will CL, Luhrmann R. Spliceosome structure and function. *Cold Spring Harb Perspect Biol*. 2011;**3**(7).
16. Wilkinson ME, Charenton C, Nagai K. RNA Splicing by the Spliceosome. *Annu Rev Biochem*. 2020;**89**:359-88.
17. Bentley DL. Rules of engagement: co-transcriptional recruitment of pre-mRNA processing factors. *Curr Opin Cell Biol*. 2005;**17**(3):251-6.
18. Raitskin O, Angenitzki M, Sperling J, Sperling R. Large nuclear RNP particles--the nuclear pre-mRNA processing machine. *J Struct Biol*. 2002;**140**(1-3):123-30.
19. Le Hir H, Izaurralde E, Maquat LE, Moore MJ. The spliceosome deposits multiple proteins 20-24 nucleotides upstream of mRNA exon-exon junctions. *EMBO J*. 2000;**19**(24):6860-9.

20. Le Hir H, Sauliere J, Wang Z. The exon junction complex as a node of post-transcriptional networks. *Nat Rev Mol Cell Biol*. 2016;**17**(1):41-54.
21. Kuhn U, Gundel M, Knoth A, Kerwitz Y, Rudel S, Wahle E. Poly(A) tail length is controlled by the nuclear poly(A)-binding protein regulating the interaction between poly(A) polymerase and the cleavage and polyadenylation specificity factor. *J Biol Chem*. 2009;**284**(34):22803-14.
22. Fischer T, Strasser K, Racz A, Rodriguez-Navarro S, Oppizzi M, Ihrig P, et al. The mRNA export machinery requires the novel Sac3p-Thp1p complex to dock at the nucleoplasmic entrance of the nuclear pores. *EMBO J*. 2002;**21**(21):5843-52.
23. Rout MP, Aitchison JD. The nuclear pore complex as a transport machine. *J Biol Chem*. 2001;**276**(20):16593-6.
24. Strambio-De-Castillia C, Niepel M, Rout MP. The nuclear pore complex: bridging nuclear transport and gene regulation. *Nat Rev Mol Cell Biol*. 2010;**11**(7):490-501.
25. Apponi LH, Leung SW, Williams KR, Valentini SR, Corbett AH, Pavlath GK. Loss of nuclear poly(A)-binding protein 1 causes defects in myogenesis and mRNA biogenesis. *Hum Mol Genet*. 2010;**19**(6):1058-65.
26. Afonina E, Stauber R, Pavlakis GN. The human poly(A)-binding protein 1 shuttles between the nucleus and the cytoplasm. *J Biol Chem*. 1998;**273**(21):13015-21.
27. Lemay JF, Lemieux C, St-Andre O, Bachand F. Crossing the borders: poly(A)-binding proteins working on both sides of the fence. *RNA Biol*. 2010;**7**(3):291-5.
28. Maquat LE, Tarn WY, Isken O. The pioneer round of translation: features and functions. *Cell*. 2010;**142**(3):368-74.
29. Kim KM, Cho H, Choi K, Kim J, Kim BW, Ko YG, et al. A new MIF4G domain-containing protein, CTIF, directs nuclear cap-binding protein CBP80/20-dependent translation. *Genes Dev*. 2009;**23**(17):2033-45.
30. Ishigaki Y, Li X, Serin G, Maquat LE. Evidence for a pioneer round of mRNA translation: mRNAs subject to nonsense-mediated decay in mammalian cells are bound by CBP80 and CBP20. *Cell*. 2001;**106**(5):607-17.
31. Hwang J, Sato H, Tang Y, Matsuda D, Maquat LE. UPF1 association with the cap-binding protein, CBP80, promotes nonsense-mediated mRNA decay at two distinct steps. *Mol Cell*. 2010;**39**(3):396-409.
32. Durand S, Lykke-Andersen J. SnapShot: Nonsense-mediated mRNA decay. *Cell*. 2011;**145**(2):324- e2.
33. Chang H, Lim J, Ha M, Kim VN. TAIL-seq: genome-wide determination of poly(A) tail length and 3' end modifications. *Mol Cell*. 2014;**53**(6):1044-52.
34. Subtelny AO, Eichhorn SW, Chen GR, Sive H, Bartel DP. Poly(A)-tail profiling reveals an embryonic switch in translational control. *Nature*. 2014;**508**(7494):66-71.
35. Lima SA, Chipman LB, Nicholson AL, Chen YH, Yee BA, Yeo GW, et al. Short poly(A) tails are a conserved feature of highly expressed genes. *Nat Struct Mol Biol*. 2017;**24**(12):1057-63.
36. Schafer IB, Yamashita M, Schuller JM, Schussler S, Reichelt P, Strauss M, et al. Molecular Basis for poly(A) RNP Architecture and Recognition by the Pan2-Pan3 Deadenylase. *Cell*. 2019;**177**(6):1619-31 e21.
37. Yi H, Park J, Ha M, Lim J, Chang H, Kim VN. PABP Cooperates with the CCR4-NOT Complex to Promote mRNA Deadenylation and Block Precocious Decay. *Mol Cell*. 2018;**70**(6):1081-8 e5.

38. Chang CT, Bercovich N, Loh B, Jonas S, Izaurralde E. The activation of the decapping enzyme DCP2 by DCP1 occurs on the EDC4 scaffold and involves a conserved loop in DCP1. *Nucleic Acids Res*. 2014;**42**(8):5217-33.
39. van Dijk E, Cougot N, Meyer S, Babajko S, Wahle E, Seraphin B. Human Dcp2: a catalytically active mRNA decapping enzyme located in specific cytoplasmic structures. *EMBO J*. 2002;**21**(24):6915-24.
40. Wang Z, Jiao X, Carr-Schmid A, Kiledjian M. The hDcp2 protein is a mammalian mRNA decapping enzyme. *Proc Natl Acad Sci U S A*. 2002;**99**(20):12663-8.
41. Hsu CL, Stevens A. Yeast cells lacking 5'-->3' exoribonuclease 1 contain mRNA species that are poly(A) deficient and partially lack the 5' cap structure. *Mol Cell Biol*. 1993;**13**(8):4826-35.
42. Pestova TV, Kolupaeva VG, Lomakin IB, Pilipenko EV, Shatsky IN, Agol VI, et al. Molecular mechanisms of translation initiation in eukaryotes. *Proc Natl Acad Sci U S A*. 2001;**98**(13):7029-36.
43. Shatkin AJ. mRNA cap binding proteins: essential factors for initiating translation. *Cell*. 1985;**40**(2):223-4.
44. Furuichi Y, LaFiandra A, Shatkin AJ. 5'-Terminal structure and mRNA stability. *Nature*. 1977;**266**(5599):235-9.
45. Shimotohno K, Kodama Y, Hashimoto J, Miura KI. Importance of 5'-terminal blocking structure to stabilize mRNA in eukaryotic protein synthesis. *Proc Natl Acad Sci U S A*. 1977;**74**(7):2734-8.
46. Konarska MM, Padgett RA, Sharp PA. Recognition of cap structure in splicing in vitro of mRNA precursors. *Cell*. 1984;**38**(3):731-6.
47. Edery I, Sonenberg N. Cap-dependent RNA splicing in a HeLa nuclear extract. *Proc Natl Acad Sci U S A*. 1985;**82**(22):7590-4.
48. Flaherty SM, Fortes P, Izaurralde E, Mattaj IW, Gilmartin GM. Participation of the nuclear cap binding complex in pre-mRNA 3' processing. *Proc Natl Acad Sci U S A*. 1997;**94**(22):11893-8.
49. Gorlich D, Kraft R, Kostka S, Vogel F, Hartmann E, Laskey RA, et al. Importin provides a link between nuclear protein import and U snRNA export. *Cell*. 1996;**87**(1):21-32.
50. Shen EC, Stage-Zimmermann T, Chui P, Silver PA. 7The yeast mRNA-binding protein Npl3p interacts with the cap-binding complex. *J Biol Chem*. 2000;**275**(31):23718-24.
51. Rasmussen EB, Lis JT. In vivo transcriptional pausing and cap formation on three Drosophila heat shock genes. *Proc Natl Acad Sci U S A*. 1993;**90**(17):7923-7.
52. Belanger F, Stepinski J, Darzynkiewicz E, Pelletier J. Characterization of hMTr1, a human Cap1 2'-O-ribose methyltransferase. *J Biol Chem*. 2010;**285**(43):33037-44.
53. Shuman S. Structure, mechanism, and evolution of the mRNA capping apparatus. *Prog Nucleic Acid Res Mol Biol*. 2001;**66**:1-40.
54. Yue Z, Maldonado E, Pillutla R, Cho H, Reinberg D, Shatkin AJ. Mammalian capping enzyme complements mutant Saccharomyces cerevisiae lacking mRNA guanylyltransferase and selectively binds the elongating form of RNA polymerase II. *Proc Natl Acad Sci U S A*. 1997;**94**(24):12898-903.
55. Chu C, Das K, Tyminski JR, Bauman JD, Guan R, Qiu W, et al. Structure of the guanylyltransferase domain of human mRNA capping enzyme. *Proc Natl Acad Sci U S A*. 2011;**108**(25):10104-8.

56. Saha N, Schwer B, Shuman S. Characterization of human, Schizosaccharomyces pombe, and Candida albicans mRNA cap methyltransferases and complete replacement of the yeast capping apparatus by mammalian enzymes. *J Biol Chem*. 1999;**274**(23):16553-62.
57. Cho EJ, Takagi T, Moore CR, Buratowski S. mRNA capping enzyme is recruited to the transcription complex by phosphorylation of the RNA polymerase II carboxy-terminal domain. *Genes Dev*. 1997;**11**(24):3319-26.
58. Proudfoot NJ, Furger A, Dye MJ. Integrating mRNA processing with transcription. *Cell*. 2002;**108**(4):501-12.
59. Gu B, Eick D, Bensaude O. CTD serine-2 plays a critical role in splicing and termination factor recruitment to RNA polymerase II in vivo. *Nucleic Acids Res*. 2013;**41**(3):1591-603.
60. McCracken S, Fong N, Yankulov K, Ballantyne S, Pan G, Greenblatt J, et al. The C-terminal domain of RNA polymerase II couples mRNA processing to transcription. *Nature*. 1997;**385**(6614):357-61.
61. Marzluff WF, Wagner EJ, Duronio RJ. Metabolism and regulation of canonical histone mRNAs: life without a poly(A) tail. *Nat Rev Genet*. 2008;**9**(11):843-54.
62. Millevoi S, Vagner S. Molecular mechanisms of eukaryotic pre-mRNA 3' end processing regulation. *Nucleic Acids Res*. 2010;**38**(9):2757-74.
63. Fuke H, Ohno M. Role of poly (A) tail as an identity element for mRNA nuclear export. *Nucleic Acids Res*. 2008;**36**(3):1037-49.
64. Long RM, Elliott DJ, Stutz F, Rosbash M, Singer RH. Spatial consequences of defective processing of specific yeast mRNAs revealed by fluorescent in situ hybridization. *RNA*. 1995;**1**(10):1071-8.
65. Huang Y, Carmichael GG. Role of polyadenylation in nucleocytoplasmic transport of mRNA. *Mol Cell Biol*. 1996;**16**(4):1534-42.
66. Hammell CM, Gross S, Zenklusen D, Heath CV, Stutz F, Moore C, et al. Coupling of termination, 3' processing, and mRNA export. *Mol Cell Biol*. 2002;**22**(18):6441-57.
67. Edmonds M, Vaughan MH, Jr., Nakazato H. Polyadenylic acid sequences in the heterogeneous nuclear RNA and rapidly-labeled polyribosomal RNA of HeLa cells: possible evidence for a precursor relationship. *Proc Natl Acad Sci U S A*. 1971;**68**(6):1336-40.
68. McLaughlin CS, Warner JR, Edmonds M, Nakazato H, Vaughan MH. Polyadenylic acid sequences in yeast messenger ribonucleic acid. *J Biol Chem*. 1973;**248**(4):1466-71.
69. Wahle E, Keller W. The biochemistry of polyadenylation. *Trends Biochem Sci*. 1996;**21**(7):247-50.
70. Colgan DF, Manley JL. Mechanism and regulation of mRNA polyadenylation. *Genes Dev*. 1997;**11**(21):2755-66.
71. Beaudoing E, Freier S, Wyatt JR, Claverie JM, Gautheret D. Patterns of variant polyadenylation signal usage in human genes. *Genome Res*. 2000;**10**(7):1001-10.
72. Chan SL, Huppertz I, Yao C, Weng L, Moresco JJ, Yates JR, 3rd, et al. CPSF30 and Wdr33 directly bind to AAUAAA in mammalian mRNA 3' processing. *Genes Dev*. 2014;**28**(21):2370-80.
73. Schonemann L, Kuhn U, Martin G, Schafer P, Gruber AR, Keller W, et al. Reconstitution of CPSF active in polyadenylation: recognition of the polyadenylation signal by WDR33. *Genes Dev*. 2014;**28**(21):2381-93.

74. Sullivan KD, Steiniger M, Marzluff WF. A core complex of CPSF73, CPSF100, and Symplekin may form two different cleavage factors for processing of poly(A) and histone mRNAs. *Mol Cell*. 2009;**34**(3):322-32.
75. Kolev NG, Yario TA, Benson E, Steitz JA. Conserved motifs in both CPSF73 and CPSF100 are required to assemble the active endonuclease for histone mRNA 3'-end maturation. *EMBO Rep*. 2008;**9**(10):1013-8.
76. Neve J, Patel R, Wang Z, Louey A, Furger AM. Cleavage and polyadenylation: Ending the message expands gene regulation. *RNA Biol*. 2017;**14**(7):865-90.
77. Schul W, Groenhout B, Koberna K, Takagaki Y, Jenny A, Manders EM, et al. The RNA 3' cleavage factors CstF 64 kDa and CPSF 100 kDa are concentrated in nuclear domains closely associated with coiled bodies and newly synthesized RNA. *EMBO J*. 1996;**15**(11):2883-92.
78. Gilmartin GM, Nevins JR. Molecular analyses of two poly(A) site-processing factors that determine the recognition and efficiency of cleavage of the pre-mRNA. *Mol Cell Biol*. 1991;**11**(5):2432-8.
79. Christofori G, Keller W. Poly(A) polymerase purified from HeLa cell nuclear extract is required for both cleavage and polyadenylation of pre-mRNA in vitro. *Mol Cell Biol*. 1989;**9**(1):193-203.
80. Takagaki Y, Ryner LC, Manley JL. Separation and characterization of a poly(A) polymerase and a cleavage/specificity factor required for pre-mRNA polyadenylation. *Cell*. 1988;**52**(5):731-42.
81. Wahle E. A novel poly(A)-binding protein acts as a specificity factor in the second phase of messenger RNA polyadenylation. *Cell*. 1991;**66**(4):759-68.
82. Bienroth S, Keller W, Wahle E. Assembly of a processive messenger RNA polyadenylation complex. *EMBO J*. 1993;**12**(2):585-94.
83. Tian B, Hu J, Zhang H, Lutz CS. A large-scale analysis of mRNA polyadenylation of human and mouse genes. *Nucleic Acids Res*. 2005;**33**(1):201-12.
84. Arora A, Goering R, Lo HYG, Lo J, Moffatt C, Taliaferro JM. The Role of Alternative Polyadenylation in the Regulation of Subcellular RNA Localization. *Front Genet*. 2021;**12**:818668.
85. Tian B, Manley JL. Alternative polyadenylation of mRNA precursors. *Nat Rev Mol Cell Biol*. 2017;**18**(1):18-30.
86. Gruber AR, Martin G, Keller W, Zavolan M. Cleavage factor Im is a key regulator of 3' UTR length. *RNA Biol*. 2012;**9**(12):1405-12.
87. Li W, You B, Hoque M, Zheng D, Luo W, Ji Z, et al. Systematic profiling of poly(A)+ transcripts modulated by core 3' end processing and splicing factors reveals regulatory rules of alternative cleavage and polyadenylation. *PLoS Genet*. 2015;**11**(4):e1005166.
88. Moore MJ. From birth to death: the complex lives of eukaryotic mRNAs. *Science*. 2005;**309**(5740):1514-8.
89. Sandberg R, Neilson JR, Sarma A, Sharp PA, Burge CB. Proliferating cells express mRNAs with shortened 3' untranslated regions and fewer microRNA target sites. *Science*. 2008;**320**(5883):1643-7.
90. Mayr C, Bartel DP. Widespread shortening of 3'UTRs by alternative cleavage and polyadenylation activates oncogenes in cancer cells. *Cell*. 2009;**138**(4):673-84.

91. Perry RB, Doron-Mandel E, Iavnilovitch E, Rishal I, Dagan SY, Tsoory M, et al. Subcellular knockout of importin beta1 perturbs axonal retrograde signaling. *Neuron*. 2012;**75**(2):294-305.
92. Beaudoin JD, Perreault JP. Exploring mRNA 3'-UTR G-quadruplexes: evidence of roles in both alternative polyadenylation and mRNA shortening. *Nucleic Acids Res*. 2013;**41**(11):5898-911.
93. Subramanian M, Rage F, Tabet R, Flatter E, Mandel JL, Moine H. G-quadruplex RNA structure as a signal for neurite mRNA targeting. *EMBO Rep*. 2011;**12**(7):697-704.
94. Lianoglou S, Garg V, Yang JL, Leslie CS, Mayr C. Ubiquitously transcribed genes use alternative polyadenylation to achieve tissue-specific expression. *Genes Dev*. 2013;**27**(21):2380-96.
95. Singh I, Lee SH, Sperling AS, Samur MK, Tai YT, Fulciniti M, et al. Widespread intronic polyadenylation diversifies immune cell transcriptomes. *Nat Commun*. 2018;**9**(1):1716.
96. Lee SH, Singh I, Tisdale S, Abdel-Wahab O, Leslie CS, Mayr C. Widespread intronic polyadenylation inactivates tumour suppressor genes in leukaemia. *Nature*. 2018;**561**(7721):127-31.
97. Cajigas IJ, Tushev G, Will TJ, tom Dieck S, Fuerst N, Schuman EM. The local transcriptome in the synaptic neuropil revealed by deep sequencing and high-resolution imaging. *Neuron*. 2012;**74**(3):453-66.
98. Andreassi C, Zimmermann C, Mitter R, Fusco S, De Vita S, Saiardi A, et al. An NGF-responsive element targets myo-inositol monophosphatase-1 mRNA to sympathetic neuron axons. *Nat Neurosci*. 2010;**13**(3):291-301.
99. An JJ, Gharami K, Liao GY, Woo NH, Lau AG, Vanevski F, et al. Distinct role of long 3' UTR BDNF mRNA in spine morphology and synaptic plasticity in hippocampal neurons. *Cell*. 2008;**134**(1):175-87.
100. Lau AG, Irier HA, Gu J, Tian D, Ku L, Liu G, et al. Distinct 3'UTRs differentially regulate activity-dependent translation of brain-derived neurotrophic factor (BDNF). *Proc Natl Acad Sci U S A*. 2010;**107**(36):15945-50.
101. Fox CA, Sheets MD, Wickens MP. Poly(A) addition during maturation of frog oocytes: distinct nuclear and cytoplasmic activities and regulation by the sequence UUUUUAU. *Genes Dev*. 1989;**3**(12B):2151-62.
102. McGrew LL, Richter JD. Translational control by cytoplasmic polyadenylation during Xenopus oocyte maturation: characterization of cis and trans elements and regulation by cyclin/MPF. *EMBO J*. 1990;**9**(11):3743-51.
103. de Moor CH, Richter JD. The Mos pathway regulates cytoplasmic polyadenylation in Xenopus oocytes. *Mol Cell Biol*. 1997;**17**(11):6419-26.
104. Stebbins-Boaz B, Hake LE, Richter JD. CPEB controls the cytoplasmic polyadenylation of cyclin, Cdk2 and c-mos mRNAs and is necessary for oocyte maturation in Xenopus. *EMBO J*. 1996;**15**(10):2582-92.
105. Ivshina M, Lasko P, Richter JD. Cytoplasmic polyadenylation element binding proteins in development, health, and disease. *Annu Rev Cell Dev Biol*. 2014;**30**:393-415.
106. Pique M, Lopez JM, Foissac S, Guigo R, Mendez R. A combinatorial code for CPE-mediated translational control. *Cell*. 2008;**132**(3):434-48.
107. Wilt FH. Polyadenylation of maternal RNA of sea urchin eggs after fertilization. *Proc Natl Acad Sci U S A*. 1973;**70**(8):2345-9.

108. Slater I, Gillespie D, Slater DW. Cytoplasmic adenylylation and processing of maternal RNA. *Proc Natl Acad Sci U S A*. 1973;**70**(2):406-11.
109. Paris J, Osborne HB, Couturier A, Le Guellec R, Philippe M. Changes in the polyadenylation of specific stable RNA during the early development of Xenopus laevis. *Gene*. 1988;**72**(1-2):169-76.
110. McGrew LL, Dworkin-Rastl E, Dworkin MB, Richter JD. Poly(A) elongation during Xenopus oocyte maturation is required for translational recruitment and is mediated by a short sequence element. *Genes Dev*. 1989;**3**(6):803-15.
111. Gebauer F, Xu W, Cooper GM, Richter JD. Translational control by cytoplasmic polyadenylation of c-mos mRNA is necessary for oocyte maturation in the mouse. *EMBO J*. 1994;**13**(23):5712-20.
112. Yang F, Wang W, Cetinbas M, Sadreyev RI, Blower MD. Genome-wide analysis identifies cis-acting elements regulating mRNA polyadenylation and translation during vertebrate oocyte maturation. *RNA*. 2020;**26**(3):324-44.
113. Lim J, Lee M, Son A, Chang H, Kim VN. mTAIL-seq reveals dynamic poly(A) tail regulation in oocyte-to-embryo development. *Genes Dev*. 2016;**30**(14):1671-82.
114. Weill L, Belloc E, Bava FA, Mendez R. Translational control by changes in poly(A) tail length: recycling mRNAs. *Nat Struct Mol Biol*. 2012;**19**(6):577-85.
115. Reyes JM, Ross PJ. Cytoplasmic polyadenylation in mammalian oocyte maturation. *Wiley Interdiscip Rev RNA*. 2016;**7**(1):71-89.
116. Hake LE, Richter JD. CPEB is a specificity factor that mediates cytoplasmic polyadenylation during Xenopus oocyte maturation. *Cell*. 1994;**79**(4):617-27.
117. Kim JH, Richter JD. Opposing polymerase-deadenylase activities regulate cytoplasmic polyadenylation. *Mol Cell*. 2006;**24**(2):173-83.
118. Stebbins-Boaz B, Cao Q, de Moor CH, Mendez R, Richter JD. Maskin is a CPEB-associated factor that transiently interacts with elF-4E. *Mol Cell*. 1999;**4**(6):1017-27.
119. Mendez R, Hake LE, Andresson T, Littlepage LE, Ruderman JV, Richter JD. Phosphorylation of CPE binding factor by Eg2 regulates translation of c-mos mRNA. *Nature*. 2000;**404**(6775):302-7.
120. Mendez R, Murthy KG, Ryan K, Manley JL, Richter JD. Phosphorylation of CPEB by Eg2 mediates the recruitment of CPSF into an active cytoplasmic polyadenylation complex. *Mol Cell*. 2000;**6**(5):1253-9.
121. Robbins E, Borun TW. The cytoplasmic synthesis of histones in hela cells and its temporal relationship to DNA replication. *Proc Natl Acad Sci U S A*. 1967;**57**(2):409-16.
122. Zhao J, Kennedy BK, Lawrence BD, Barbie DA, Matera AG, Fletcher JA, et al. NPAT links cyclin E-Cdk2 to the regulation of replication-dependent histone gene transcription. *Genes Dev*. 2000;**14**(18):2283-97.
123. Dominski Z, Marzluff WF. Formation of the 3' end of histone mRNA. *Gene*. 1999;**239**(1):1-14.
124. Dominski Z, Tong L. U7 deciphered: the mechanism that forms the unusual 3' end of metazoan replication-dependent histone mRNAs. *Biochem Soc Trans*. 2021;**49**(5):2229-40.
125. Sanchez R, Marzluff WF. The stem-loop binding protein is required for efficient translation of histone mRNA in vivo and in vitro. *Mol Cell Biol*. 2002;**22**(20):7093-104.

126. Pandey NB, Marzluff WF. The stem-loop structure at the 3' end of histone mRNA is necessary and sufficient for regulation of histone mRNA stability. *Mol Cell Biol*. 1987;**7**(12):4557-9.
127. Hoefig KP, Rath N, Heinz GA, Wolf C, Dameris J, Schepers A, et al. Eri1 degrades the stem-loop of oligouridylated histone mRNAs to induce replication-dependent decay. *Nat Struct Mol Biol*. 2013;**20**(1):73-81.
128. Kajjo S, Sharma S, Chen S, Brothers WR, Cott M, Hasaj B, et al. PABP prevents the untimely decay of select mRNA populations in human cells. *EMBO J*. 2022;**41**(6):e108650.
129. Fabian MR, Frank F, Rouya C, Siddiqui N, Lai WS, Karetnikov A, et al. Structural basis for the recruitment of the human CCR4-NOT deadenylase complex by tristetraprolin. *Nat Struct Mol Biol*. 2013;**20**(6):735-9.
130. Marcotrigiano J, Gingras AC, Sonenberg N, Burley SK. Cocrystal structure of the messenger RNA 5' cap-binding protein (eIF4E) bound to 7-methyl-GDP. *Cell*. 1997;**89**(6):951-61.
131. Sachs AB, Sarnow P, Hentze MW. Starting at the beginning, middle, and end: translation initiation in eukaryotes. *Cell*. 1997;**89**(6):831-8.
132. Gingras AC, Raught B, Sonenberg N. eIF4 initiation factors: effectors of mRNA recruitment to ribosomes and regulators of translation. *Annu Rev Biochem*. 1999;**68**:913-63.
133. Matsuo H, Li H, McGuire AM, Fletcher CM, Gingras AC, Sonenberg N, et al. Structure of translation factor eIF4E bound to m7GDP and interaction with 4E-binding protein. *Nat Struct Biol*. 1997;**4**(9):717-24.
134. Jackson RJ, Hellen CU, Pestova TV. The mechanism of eukaryotic translation initiation and principles of its regulation. *Nat Rev Mol Cell Biol*. 2010;**11**(2):113-27.
135. Kozak M. Possible role of flanking nucleotides in recognition of the AUG initiator codon by eukaryotic ribosomes. *Nucleic Acids Res*. 1981;**9**(20):5233-52.
136. Kozak M. Point mutations define a sequence flanking the AUG initiator codon that modulates translation by eukaryotic ribosomes. *Cell*. 1986;**44**(2):283-92.
137. Kozak M. Compilation and analysis of sequences upstream from the translational start site in eukaryotic mRNAs. *Nucleic Acids Res*. 1984;**12**(2):857-72.
138. Eliseev B, Yeramala L, Leitner A, Karuppasamy M, Raimondeau E, Huard K, et al. Structure of a human cap-dependent 48S translation pre-initiation complex. *Nucleic Acids Res*. 2018;**46**(5):2678-89.
139. Unbehaun A, Borukhov SI, Hellen CU, Pestova TV. Release of initiation factors from 48S complexes during ribosomal subunit joining and the link between establishment of codon-anticodon base-pairing and hydrolysis of eIF2-bound GTP. *Genes Dev*. 2004;**18**(24):3078-93.
140. Jennings MD, Pavitt GD. eIF5 is a dual function GAP and GDI for eukaryotic translational control. *Small GTPases*. 2010;**1**(2):118-23.
141. Das S, Ghosh R, Maitra U. Eukaryotic translation initiation factor 5 functions as a GTPase-activating protein. *J Biol Chem*. 2001;**276**(9):6720-6.
142. Kahvejian A, Svitkin YV, Sukarieh R, M'Boutchou MN, Sonenberg N. Mammalian poly(A)-binding protein is a eukaryotic translation initiation factor, which acts via multiple mechanisms. *Genes Dev*. 2005;**19**(1):104-13.

143. Safaee N, Kozlov G, Noronha AM, Xie J, Wilds CJ, Gehring K. Interdomain allostery promotes assembly of the poly(A) mRNA complex with PABP and eIF4G. *Mol Cell*. 2012;**48**(3):375-86.
144. Wells SE, Hillner PE, Vale RD, Sachs AB. Circularization of mRNA by eukaryotic translation initiation factors. *Mol Cell*. 1998;**2**(1):135-40.
145. Alekhina OM, Terenin IM, Dmitriev SE, Vassilenko KS. Functional Cyclization of Eukaryotic mRNAs. *Int J Mol Sci*. 2020;**21**(5).
146. Marshall E, Stansfield I, Romano MC. Ribosome recycling induces optimal translation rate at low ribosomal availability. *J R Soc Interface*. 2014;**11**(98):20140589.
147. Groft CM, Burley SK. Recognition of eIF4G by rotavirus NSP3 reveals a basis for mRNA circularization. *Mol Cell*. 2002;**9**(6):1273-83.
148. Wakiyama M, Imataka H, Sonenberg N. Interaction of eIF4G with poly(A)-binding protein stimulates translation and is critical for Xenopus oocyte maturation. *Curr Biol*. 2000;**10**(18):1147-50.
149. Seli E, Lalioti MD, Flaherty SM, Sakkas D, Terzi N, Steitz JA. An embryonic poly(A)-binding protein (ePAB) is expressed in mouse oocytes and early preimplantation embryos. *Proc Natl Acad Sci U S A*. 2005;**102**(2):367-72.
150. Voeltz GK, Ongkasuwan J, Standart N, Steitz JA. A novel embryonic poly(A) binding protein, ePAB, regulates mRNA deadenylation in Xenopus egg extracts. *Genes Dev*. 2001;**15**(6):774-88.
151. Sun F, Fang H, Li R, Gao T, Zheng J, Chen X, et al. Nuclear reprogramming: the zygotic transcription program is established through an "erase-and-rebuild" strategy. *Cell Res*. 2007;**17**(2):117-34.
152. Debey P, Szollosi MS, Szollosi D, Vautier D, Girousse A, Besombes D. Competent mouse oocytes isolated from antral follicles exhibit different chromatin organization and follow different maturation dynamics. *Mol Reprod Dev*. 1993;**36**(1):59-74.
153. Tan JH, Wang HL, Sun XS, Liu Y, Sui HS, Zhang J. Chromatin configurations in the germinal vesicle of mammalian oocytes. *Mol Hum Reprod*. 2009;**15**(1):1-9.
154. Bonnet-Garnier A, Feuerstein P, Chebrout M, Fleurot R, Jan HU, Debey P, et al. Genome organization and epigenetic marks in mouse germinal vesicle oocytes. *Int J Dev Biol*. 2012;**56**(10-12):877-87.
155. Schultz RM, Stein P, Svoboda P. The oocyte-to-embryo transition in mouse: past, present, and future. *Biol Reprod*. 2018;**99**(1):160-74.
156. Anger M, Radonova L, Horakova A, Sekach D, Charousova M. Impact of Global Transcriptional Silencing on Cell Cycle Regulation and Chromosome Segregation in Early Mammalian Embryos. *Int J Mol Sci*. 2021;**22**(16).
157. Huarte J, Stutz A, O'Connell ML, Gubler P, Belin D, Darrow AL, et al. Transient translational silencing by reversible mRNA deadenylation. *Cell*. 1992;**69**(6):1021-30.
158. Winata CL, Korzh V. The translational regulation of maternal mRNAs in time and space. *FEBS Lett*. 2018;**592**(17):3007-23.
159. Vassalli JD, Huarte J, Belin D, Gubler P, Vassalli A, O'Connell ML, et al. Regulated polyadenylation controls mRNA translation during meiotic maturation of mouse oocytes. *Genes Dev*. 1989;**3**(12B):2163-71.
160. Xiang K, Bartel DP. The molecular basis of coupling between poly(A)-tail length and translational efficiency. *Elife*. 2021;**10**.

161. Rissland OS, Subtelny AO, Wang M, Lugowski A, Nicholson B, Laver JD, et al. The influence of microRNAs and poly(A) tail length on endogenous mRNA-protein complexes. *Genome Biol*. 2017;**18**(1):211.
162. Gorlach M, Burd CG, Dreyfuss G. The mRNA poly(A)-binding protein: localization, abundance, and RNA-binding specificity. *Exp Cell Res*. 1994;**211**(2):400-7.
163. Nagaraj N, Wisniewski JR, Geiger T, Cox J, Kircher M, Kelso J, et al. Deep proteome and transcriptome mapping of a human cancer cell line. *Mol Syst Biol*. 2011;**7**:548.
164. Park JE, Yi H, Kim Y, Chang H, Kim VN. Regulation of Poly(A) Tail and Translation during the Somatic Cell Cycle. *Mol Cell*. 2016;**62**(3):462-71.
165. Eisen TJ, Li JJ, Bartel DP. The interplay between translational efficiency, poly(A) tails, microRNAs, and neuronal activation. *RNA*. 2022;**28**(6):808-31.
166. Hafner AS, Donlin-Asp PG, Leitch B, Herzog E, Schuman EM. Local protein synthesis is a ubiquitous feature of neuronal pre- and postsynaptic compartments. *Science*. 2019;**364**(6441).
167. Marzluff WF. Metazoan replication-dependent histone mRNAs: a distinct set of RNA polymerase II transcripts. *Curr Opin Cell Biol*. 2005;**17**(3):274-80.
168. Dominski Z, Zheng LX, Sanchez R, Marzluff WF. Stem-loop binding protein facilitates 3'-end formation by stabilizing U7 snRNP binding to histone pre-mRNA. *Mol Cell Biol*. 1999;**19**(5):3561-70.
169. Gorgoni B, Andrews S, Schaller A, Schumperli D, Gray NK, Muller B. The stem-loop binding protein stimulates histone translation at an early step in the initiation pathway. *RNA*. 2005;**11**(7):1030-42.
170. Gallie DR, Lewis NJ, Marzluff WF. The histone 3'-terminal stem-loop is necessary for translation in Chinese hamster ovary cells. *Nucleic Acids Res*. 1996;**24**(10):1954-62.
171. Ling J, Morley SJ, Pain VM, Marzluff WF, Gallie DR. The histone 3'-terminal stem-loop-binding protein enhances translation through a functional and physical interaction with eukaryotic initiation factor 4G (eIF4G) and eIF3. *Mol Cell Biol*. 2002;**22**(22):7853-67.
172. Cakmakci NG, Lerner RS, Wagner EJ, Zheng L, Marzluff WF. SLIP1, a factor required for activation of histone mRNA translation by the stem-loop binding protein. *Mol Cell Biol*. 2008;**28**(3):1182-94.
173. Gupta N, Lorsch JR, Hinnebusch AG. Yeast Ded1 promotes 48S translation pre-initiation complex assembly in an mRNA-specific and eIF4F-dependent manner. *Elife*. 2018;**7**.
174. Brito Querido J, Sokabe M, Kraatz S, Gordiyenko Y, Skehel JM, Fraser CS, et al. Structure of a human 48S translational initiation complex. *Science*. 2020;**369**(6508):1220-7.
175. Duncan R, Milburn SC, Hershey JW. Regulated phosphorylation and low abundance of HeLa cell initiation factor eIF-4F suggest a role in translational control. Heat shock effects on eIF-4F. *J Biol Chem*. 1987;**262**(1):380-8.
176. Rau M, Ohlmann T, Morley SJ, Pain VM. A reevaluation of the cap-binding protein, eIF4E, as a rate-limiting factor for initiation of translation in reticulocyte lysate. *J Biol Chem*. 1996;**271**(15):8983-90.
177. Park EH, Lee JM, Blais JD, Bell JC, Pelletier J. Internal translation initiation mediated by the angiogenic factor Tie2. *J Biol Chem*. 2005;**280**(22):20945-53.
178. Park EH, Lee JM, Pelletier J. The Tie2 5' untranslated region is inhibitory to 5' end-mediated translation initiation. *FEBS Lett*. 2006;**580**(5):1309-19.
179. Graber TE, Holcik M. Cap-independent regulation of gene expression in apoptosis. *Mol Biosyst*. 2007;**3**(12):825-34.

180. Pinkstaff JK, Chappell SA, Mauro VP, Edelman GM, Krushel LA. Internal initiation of translation of five dendritically localized neuronal mRNAs. *Proc Natl Acad Sci U S A*. 2001;**98**(5):2770-5.
181. Sun C, Querol-Audi J, Mortimer SA, Arias-Palomo E, Doudna JA, Nogales E, et al. Two RNA-binding motifs in eIF3 direct HCV IRES-dependent translation. *Nucleic Acids Res*. 2013;**41**(15):7512-21.
182. Balvay L, Soto Rifo R, Ricci EP, Decimo D, Ohlmann T. Structural and functional diversity of viral IRESes. *Biochim Biophys Acta*. 2009;**1789**(9-10):542-57.
183. Marques R, Lacerda R, Romao L. Internal Ribosome Entry Site (IRES)-Mediated Translation and Its Potential for Novel mRNA-Based Therapy Development. *Biomedicines*. 2022;**10**(8).
184. Pisarev AV, Shirokikh NE, Hellen CU. Translation initiation by factor-independent binding of eukaryotic ribosomes to internal ribosomal entry sites. *C R Biol*. 2005;**328**(7):589-605.
185. Kearse MG, Wilusz JE. Non-AUG translation: a new start for protein synthesis in eukaryotes. *Genes Dev*. 2017;**31**(17):1717-31.
186. Clements JM, Laz TM, Sherman F. Efficiency of translation initiation by non-AUG codons in Saccharomyces cerevisiae. *Mol Cell Biol*. 1988;**8**(10):4533-6.
187. Zitomer RS, Walthall DA, Rymond BC, Hollenberg CP. Saccharomyces cerevisiae ribosomes recognize non-AUG initiation codons. *Mol Cell Biol*. 1984;**4**(7):1191-7.
188. Kozak M. Context effects and inefficient initiation at non-AUG codons in eucaryotic cell-free translation systems. *Mol Cell Biol*. 1989;**9**(11):5073-80.
189. Kozak M. Downstream secondary structure facilitates recognition of initiator codons by eukaryotic ribosomes. *Proc Natl Acad Sci U S A*. 1990;**87**(21):8301-5.
190. Takahashi K, Maruyama M, Tokuzawa Y, Murakami M, Oda Y, Yoshikane N, et al. Evolutionarily conserved non-AUG translation initiation in NAT1/p97/DAP5 (EIF4G2). *Genomics*. 2005;**85**(3):360-71.
191. Hann SR, King MW, Bentley DL, Anderson CW, Eisenman RN. A non-AUG translational initiation in c-myc exon 1 generates an N-terminally distinct protein whose synthesis is disrupted in Burkitt's lymphomas. *Cell*. 1988;**52**(2):185-95.
192. Blackwood EM, Lugo TG, Kretzner L, King MW, Street AJ, Witte ON, et al. Functional analysis of the AUG- and CUG-initiated forms of the c-Myc protein. *Mol Biol Cell*. 1994;**5**(5):597-609.
193. Castelli LM, Huang WP, Lin YH, Chang KY, Hautbergue GM. Mechanisms of repeat-associated non-AUG translation in neurological microsatellite expansion disorders. *Biochem Soc Trans*. 2021;**49**(2):775-92.
194. Banez-Coronel M, Ayhan F, Tarabochia AD, Zu T, Perez BA, Tusi SK, et al. RAN Translation in Huntington Disease. *Neuron*. 2015;**88**(4):667-77.
195. Jazurek-Ciesiolka M, Ciesiolka A, Komur AA, Urbanek-Trzeciak MO, Krzyzosiak WJ, Fiszer A. RAN Translation of the Expanded CAG Repeats in the SCA3 Disease Context. *J Mol Biol*. 2020;**432**(24):166699.
196. Zu T, Gibbens B, Doty NS, Gomes-Pereira M, Huguet A, Stone MD, et al. Non-ATG-initiated translation directed by microsatellite expansions. *Proc Natl Acad Sci U S A*. 2011;**108**(1):260-5.
197. A novel gene containing a trinucleotide repeat that is expanded and unstable on Huntington's disease chromosomes. The Huntington's Disease Collaborative Research Group. *Cell*. 1993;**72**(6):971-83.

198. Pieretti M, Zhang FP, Fu YH, Warren ST, Oostra BA, Caskey CT, et al. Absence of expression of the FMR-1 gene in fragile X syndrome. *Cell*. 1991;**66**(4):817-22.
199. Nelson DL, Orr HT, Warren ST. The unstable repeats--three evolving faces of neurological disease. *Neuron*. 2013;**77**(5):825-43.
200. Greco CM, Berman RF, Martin RM, Tassone F, Schwartz PH, Chang A, et al. Neuropathology of fragile X-associated tremor/ataxia syndrome (FXTAS). *Brain*. 2006;**129**(Pt 1):243-55.
201. Todd PK, Oh SY, Krans A, He F, Sellier C, Frazer M, et al. CGG repeat-associated translation mediates neurodegeneration in fragile X tremor ataxia syndrome. *Neuron*. 2013;**78**(3):440-55.
202. Ogle JM, Brodersen DE, Clemons WM, Jr., Tarry MJ, Carter AP, Ramakrishnan V. Recognition of cognate transfer RNA by the 30S ribosomal subunit. *Science*. 2001;**292**(5518):897-902.
203. Demeshkina N, Jenner L, Westhof E, Yusupov M, Yusupova G. A new understanding of the decoding principle on the ribosome. *Nature*. 2012;**484**(7393):256-9.
204. Jalkanen AL, Coleman SJ, Wilusz J. Determinants and implications of mRNA poly(A) tail size--does this protein make my tail look big? *Semin Cell Dev Biol*. 2014;**34**:24-32.
205. Eckmann CR, Rammelt C, Wahle E. Control of poly(A) tail length. *Wiley Interdiscip Rev RNA*. 2011;**2**(3):348-61.
206. Webster MW, Chen YH, Stowell JAW, Alhusaini N, Sweet T, Graveley BR, et al. mRNA Deadenylation Is Coupled to Translation Rates by the Differential Activities of Ccr4-Not Nucleases. *Mol Cell*. 2018;**70**(6):1089-100 e8.
207. Tucker M, Valencia-Sanchez MA, Staples RR, Chen J, Denis CL, Parker R. The transcription factor associated Ccr4 and Caf1 proteins are components of the major cytoplasmic mRNA deadenylase in Saccharomyces cerevisiae. *Cell*. 2001;**104**(3):377-86.
208. Wahle E, Winkler GS. RNA decay machines: deadenylation by the Ccr4-not and Pan2-Pan3 complexes. *Biochim Biophys Acta*. 2013;**1829**(6-7):561-70.
209. Nousch M, Techritz N, Hampel D, Millonigg S, Eckmann CR. The Ccr4-Not deadenylase complex constitutes the main poly(A) removal activity in C. elegans. *J Cell Sci*. 2013;**126**(Pt 18):4274-85.
210. Temme C, Zaessinger S, Meyer S, Simonelig M, Wahle E. A complex containing the CCR4 and CAF1 proteins is involved in mRNA deadenylation in Drosophila. *EMBO J*. 2004;**23**(14):2862-71.
211. Yamashita A, Chang TC, Yamashita Y, Zhu W, Zhong Z, Chen CY, et al. Concerted action of poly(A) nucleases and decapping enzyme in mammalian mRNA turnover. *Nat Struct Mol Biol*. 2005;**12**(12):1054-63.
212. Jonas S, Christie M, Peter D, Bhandari D, Loh B, Huntzinger E, et al. An asymmetric PAN3 dimer recruits a single PAN2 exonuclease to mediate mRNA deadenylation and decay. *Nat Struct Mol Biol*. 2014;**21**(7):599-608.
213. Wolf J, Valkov E, Allen MD, Meineke B, Gordiyenko Y, McLaughlin SH, et al. Structural basis for Pan3 binding to Pan2 and its function in mRNA recruitment and deadenylation. *EMBO J*. 2014;**33**(14):1514-26.
214. Boeck R, Tarun S, Jr., Rieger M, Deardorff JA, Muller-Auer S, Sachs AB. The yeast Pan2 protein is required for poly(A)-binding protein-stimulated poly(A)-nuclease activity. *J Biol Chem*. 1996;**271**(1):432-8.

215. Zuo Y, Deutscher MP. Exoribonuclease superfamilies: structural analysis and phylogenetic distribution. *Nucleic Acids Res*. 2001;**29**(5):1017-26.
216. Siddiqui N, Mangus DA, Chang TC, Palermino JM, Shyu AB, Gehring K. Poly(A) nuclease interacts with the C-terminal domain of polyadenylate-binding protein domain from poly(A)-binding protein. *J Biol Chem*. 2007;**282**(34):25067-75.
217. Sachs AB, Deardorff JA. Translation initiation requires the PAB-dependent poly(A) ribonuclease in yeast. *Cell*. 1992;**70**(6):961-73.
218. Uchida N, Hoshino S, Katada T. Identification of a human cytoplasmic poly(A) nuclease complex stimulated by poly(A)-binding protein. *J Biol Chem*. 2004;**279**(2):1383-91.
219. Braun JE, Huntzinger E, Fauser M, Izaurralde E. GW182 proteins directly recruit cytoplasmic deadenylase complexes to miRNA targets. *Mol Cell*. 2011;**44**(1):120-33.
220. Andersen KR, Jonstrup AT, Van LB, Brodersen DE. The activity and selectivity of fission yeast Pop2p are affected by a high affinity for Zn2+ and Mn2+ in the active site. *RNA*. 2009;**15**(5):850-61.
221. Dlakic M. Functionally unrelated signalling proteins contain a fold similar to Mg2+-dependent endonucleases. *Trends Biochem Sci*. 2000;**25**(6):272-3.
222. Suzuki T, Kikuguchi C, Sharma S, Sasaki T, Tokumasu M, Adachi S, et al. CNOT3 suppression promotes necroptosis by stabilizing mRNAs for cell death-inducing proteins. *Sci Rep*. 2015;**5**:14779.
223. Shirai YT, Suzuki T, Morita M, Takahashi A, Yamamoto T. Multifunctional roles of the mammalian CCR4-NOT complex in physiological phenomena. *Front Genet*. 2014;**5**:286.
224. Vissers L, Kalvakuri S, de Boer E, Geuer S, Oud M, van Outersterp I, et al. De Novo Variants in CNOT1, a Central Component of the CCR4-NOT Complex Involved in Gene Expression and RNA and Protein Stability, Cause Neurodevelopmental Delay. *Am J Hum Genet*. 2020;**107**(1):164-72.
225. Basquin J, Roudko VV, Rode M, Basquin C, Seraphin B, Conti E. Architecture of the nuclease module of the yeast Ccr4-not complex: the Not1-Caf1-Ccr4 interaction. *Mol Cell*. 2012;**48**(2):207-18.
226. Ito K, Takahashi A, Morita M, Suzuki T, Yamamoto T. The role of the CNOT1 subunit of the CCR4-NOT complex in mRNA deadenylation and cell viability. *Protein Cell*. 2011;**2**(9):755-63.
227. Miyasaka T, Morita M, Ito K, Suzuki T, Fukuda H, Takeda S, et al. Interaction of antiproliferative protein Tob with the CCR4-NOT deadenylase complex. *Cancer Sci*. 2008;**99**(4):755-61.
228. Fabian MR, Cieplak MK, Frank F, Morita M, Green J, Srikumar T, et al. miRNA-mediated deadenylation is orchestrated by GW182 through two conserved motifs that interact with CCR4-NOT. *Nat Struct Mol Biol*. 2011;**18**(11):1211-7.
229. Enwerem, III, Elrod ND, Chang CT, Lin A, Ji P, Bohn JA, et al. Human Pumilio proteins directly bind the CCR4-NOT deadenylase complex to regulate the transcriptome. *RNA*. 2021;**27**(4):445-64.
230. Lykke-Andersen J, Wagner E. Recruitment and activation of mRNA decay enzymes by two ARE-mediated decay activation domains in the proteins TTP and BRF-1. *Genes Dev*. 2005;**19**(3):351-61.
231. Wang X, McLachlan J, Zamore PD, Hall TM. Modular recognition of RNA by a human pumilio-homology domain. *Cell*. 2002;**110**(4):501-12.

232. Zamore PD, Williamson JR, Lehmann R. The Pumilio protein binds RNA through a conserved domain that defines a new class of RNA-binding proteins. *RNA*. 1997;**3**(12):1421-33.
233. Ezzeddine N, Chang TC, Zhu W, Yamashita A, Chen CY, Zhong Z, et al. Human TOB, an antiproliferative transcription factor, is a poly(A)-binding protein-dependent positive regulator of cytoplasmic mRNA deadenylation. *Mol Cell Biol*. 2007;**27**(22):7791-801.
234. Ogami K, Hosoda N, Funakoshi Y, Hoshino S. Antiproliferative protein Tob directly regulates c-myc proto-oncogene expression through cytoplasmic polyadenylation element-binding protein CPEB. *Oncogene*. 2014;**33**(1):55-64.
235. Hosoda N, Funakoshi Y, Hirasawa M, Yamagishi R, Asano Y, Miyagawa R, et al. Anti-proliferative protein Tob negatively regulates CPEB3 target by recruiting Caf1 deadenylase. *EMBO J*. 2011;**30**(7):1311-23.
236. Mathys H, Basquin J, Ozgur S, Czarnocki-Cieciura M, Bonneau F, Aartse A, et al. Structural and biochemical insights to the role of the CCR4-NOT complex and DDX6 ATPase in microRNA repression. *Mol Cell*. 2014;**54**(5):751-65.
237. Decker CJ, Parker R. A turnover pathway for both stable and unstable mRNAs in yeast: evidence for a requirement for deadenylation. *Genes Dev*. 1993;**7**(8):1632-43.
238. Song MG, Kiledjian M. 3' Terminal oligo U-tract-mediated stimulation of decapping. *RNA*. 2007;**13**(12):2356-65.
239. Shen B, Goodman HM. Uridine addition after microRNA-directed cleavage. *Science*. 2004;**306**(5698):997.
240. Mullen TE, Marzluff WF. Degradation of histone mRNA requires oligouridylation followed by decapping and simultaneous degradation of the mRNA both 5' to 3' and 3' to 5'. *Genes Dev*. 2008;**22**(1):50-65.
241. Lim J, Ha M, Chang H, Kwon SC, Simanshu DK, Patel DJ, et al. Uridylation by TUT4 and TUT7 marks mRNA for degradation. *Cell*. 2014;**159**(6):1365-76.
242. Baer BW, Kornberg RD. The protein responsible for the repeating structure of cytoplasmic poly(A)-ribonucleoprotein. *J Cell Biol*. 1983;**96**(3):717-21.
243. Kuhn U, Pieler T. Xenopus poly(A) binding protein: functional domains in RNA binding and protein-protein interaction. *J Mol Biol*. 1996;**256**(1):20-30.
244. Wilusz CJ, Wilusz J. New ways to meet your (3') end oligouridylation as a step on the path to destruction. *Genes Dev*. 2008;**22**(1):1-7.
245. Chowdhury A, Mukhopadhyay J, Tharun S. The decapping activator Lsm1p-7p-Pat1p complex has the intrinsic ability to distinguish between oligoadenylated and polyadenylated RNAs. *RNA*. 2007;**13**(7):998-1016.
246. Garre E, Pelechano V, Sanchez Del Pino M, Alepuz P, Sunnerhagen P. The Lsm1-7/Pat1 complex binds to stress-activated mRNAs and modulates the response to hyperosmotic shock. *PLoS Genet*. 2018;**14**(7):e1007563.
247. Mitchell SF, Jain S, She M, Parker R. Global analysis of yeast mRNPs. *Nat Struct Mol Biol*. 2013;**20**(1):127-33.
248. Wilusz CJ, Wilusz J. Eukaryotic Lsm proteins: lessons from bacteria. *Nat Struct Mol Biol*. 2005;**12**(12):1031-6.
249. Achsel T, Stark H, Luhrmann R. The Sm domain is an ancient RNA-binding motif with oligo(U) specificity. *Proc Natl Acad Sci U S A*. 2001;**98**(7):3685-9.

250. Ozgur S, Chekulaeva M, Stoecklin G. Human Pat1b connects deadenylation with mRNA decapping and controls the assembly of processing bodies. *Mol Cell Biol*. 2010;**30**(17):4308-23.
251. Sharif H, Conti E. Architecture of the Lsm1-7-Pat1 complex: a conserved assembly in eukaryotic mRNA turnover. *Cell Rep*. 2013;**5**(2):283-91.
252. Braun JE, Tritschler F, Haas G, Igreja C, Truffault V, Weichenrieder O, et al. The C-terminal alpha-alpha superhelix of Pat is required for mRNA decapping in metazoa. *EMBO J*. 2010;**29**(14):2368-80.
253. Coller JM, Tucker M, Sheth U, Valencia-Sanchez MA, Parker R. The DEAD box helicase, Dhh1p, functions in mRNA decapping and interacts with both the decapping and deadenylase complexes. *RNA*. 2001;**7**(12):1717-27.
254. Muhlrad D, Decker CJ, Parker R. Deadenylation of the unstable mRNA encoded by the yeast MFA2 gene leads to decapping followed by 5'-->3' digestion of the transcript. *Genes Dev*. 1994;**8**(7):855-66.
255. Bruderer T, Tu LC, Lee MG. The 5' end structure of transcripts derived from the rRNA gene and the RNA polymerase I transcribed protein coding genes in Trypanosoma brucei. *Mol Biochem Parasitol*. 2003;**129**(1):69-77.
256. Kessler AC, Maraia RJ. The nuclear and cytoplasmic activities of RNA polymerase III, and an evolving transcriptome for surveillance. *Nucleic Acids Res*. 2021;**49**(21):12017-34.
257. Schmid M, Jensen TH. The exosome: a multipurpose RNA-decay machine. *Trends Biochem Sci*. 2008;**33**(10):501-10.
258. Fabian MR, Sonenberg N. The mechanics of miRNA-mediated gene silencing: a look under the hood of miRISC. *Nat Struct Mol Biol*. 2012;**19**(6):586-93.
259. Bartel DP. MicroRNAs: target recognition and regulatory functions. *Cell*. 2009;**136**(2):215-33.
260. Fabian MR, Sonenberg N, Filipowicz W. Regulation of mRNA translation and stability by microRNAs. *Annu Rev Biochem*. 2010;**79**:351-79.
261. Eulalio A, Huntzinger E, Izaurralde E. Getting to the root of miRNA-mediated gene silencing. *Cell*. 2008;**132**(1):9-14.
262. Lewis BP, Shih IH, Jones-Rhoades MW, Bartel DP, Burge CB. Prediction of mammalian microRNA targets. *Cell*. 2003;**115**(7):787-98.
263. Brennecke J, Stark A, Russell RB, Cohen SM. Principles of microRNA-target recognition. *PLoS Biol*. 2005;**3**(3):e85.
264. Hausser J, Syed AP, Bilen B, Zavolan M. Analysis of CDS-located miRNA target sites suggests that they can effectively inhibit translation. *Genome Res*. 2013;**23**(4):604-15.
265. Takimoto K, Wakiyama M, Yokoyama S. Mammalian GW182 contains multiple Argonaute-binding sites and functions in microRNA-mediated translational repression. *RNA*. 2009;**15**(6):1078-89.
266. Wightman B, Ha I, Ruvkun G. Posttranscriptional regulation of the heterochronic gene lin-14 by lin-4 mediates temporal pattern formation in C. elegans. *Cell*. 1993;**75**(5):855-62.
267. Lee RC, Feinbaum RL, Ambros V. The C. elegans heterochronic gene lin-4 encodes small RNAs with antisense complementarity to lin-14. *Cell*. 1993;**75**(5):843-54.
268. Reinhart BJ, Slack FJ, Basson M, Pasquinelli AE, Bettinger JC, Rougvie AE, et al. The 21-nucleotide let-7 RNA regulates developmental timing in Caenorhabditis elegans. *Nature*. 2000;**403**(6772):901-6.

269. Huntzinger E, Kuzuoglu-Ozturk D, Braun JE, Eulalio A, Wohlbold L, Izaurralde E. The interactions of GW182 proteins with PABP and deadenylases are required for both translational repression and degradation of miRNA targets. *Nucleic Acids Res*. 2013;**41**(2):978-94.
270. Jinek M, Fabian MR, Coyle SM, Sonenberg N, Doudna JA. Structural insights into the human GW182-PABC interaction in microRNA-mediated deadenylation. *Nat Struct Mol Biol*. 2010;**17**(2):238-40.
271. Losson R, Lacroute F. Interference of nonsense mutations with eukaryotic messenger RNA stability. *Proc Natl Acad Sci U S A*. 1979;**76**(10):5134-7.
272. Maquat LE, Kinniburgh AJ, Rachmilewitz EA, Ross J. Unstable beta-globin mRNA in mRNA-deficient beta o thalassemia. *Cell*. 1981;**27**(3 Pt 2):543-53.
273. Behm-Ansmant I, Kashima I, Rehwinkel J, Sauliere J, Wittkopp N, Izaurralde E. mRNA quality control: an ancient machinery recognizes and degrades mRNAs with nonsense codons. *FEBS Lett*. 2007;**581**(15):2845-53.
274. McIlwain DR, Pan Q, Reilly PT, Elia AJ, McCracken S, Wakeham AC, et al. Smg1 is required for embryogenesis and regulates diverse genes via alternative splicing coupled to nonsense-mediated mRNA decay. *Proc Natl Acad Sci U S A*. 2010;**107**(27):12186-91.
275. Weischenfeldt J, Waage J, Tian G, Zhao J, Damgaard I, Jakobsen JS, et al. Mammalian tissues defective in nonsense-mediated mRNA decay display highly aberrant splicing patterns. *Genome Biol*. 2012;**13**(5):R35.
276. Lykke-Andersen S, Jensen TH. Nonsense-mediated mRNA decay: an intricate machinery that shapes transcriptomes. *Nat Rev Mol Cell Biol*. 2015;**16**(11):665-77.
277. Kim YK, Maquat LE. UPFront and center in RNA decay: UPF1 in nonsense-mediated mRNA decay and beyond. *RNA*. 2019;**25**(4):407-22.
278. Kervestin S, Jacobson A. NMD: a multifaceted response to premature translational termination. *Nat Rev Mol Cell Biol*. 2012;**13**(11):700-12.
279. Franks TM, Singh G, Lykke-Andersen J. Upf1 ATPase-dependent mRNP disassembly is required for completion of nonsense- mediated mRNA decay. *Cell*. 2010;**143**(6):938-50.
280. Singh G, Rebbapragada I, Lykke-Andersen J. A competition between stimulators and antagonists of Upf complex recruitment governs human nonsense-mediated mRNA decay. *PLoS Biol*. 2008;**6**(4):e111.
281. Kozlov G, Gehring K. Molecular basis of eRF3 recognition by the MLLE domain of poly(A)-binding protein. *PLoS One*. 2010;**5**(4):e10169.
282. Conti E, Izaurralde E. Nonsense-mediated mRNA decay: molecular insights and mechanistic variations across species. *Curr Opin Cell Biol*. 2005;**17**(3):316-25.
283. Rufener SC, Muhlemann O. eIF4E-bound mRNPs are substrates for nonsense-mediated mRNA decay in mammalian cells. *Nat Struct Mol Biol*. 2013;**20**(6):710-7.
284. Lejeune F. Nonsense-Mediated mRNA Decay, a Finely Regulated Mechanism. *Biomedicines*. 2022;**10**(1).
285. Mendell JT, Sharifi NA, Meyers JL, Martinez-Murillo F, Dietz HC. Nonsense surveillance regulates expression of diverse classes of mammalian transcripts and mutes genomic noise. *Nat Genet*. 2004;**36**(10):1073-8.
286. Giorgi C, Yeo GW, Stone ME, Katz DB, Burge C, Turrigiano G, et al. The EJC factor eIF4AIII modulates synaptic strength and neuronal protein expression. *Cell*. 2007;**130**(1):179-91.

287. Le Hir H, Gatfield D, Izaurralde E, Moore MJ. The exon-exon junction complex provides a binding platform for factors involved in mRNA export and nonsense-mediated mRNA decay. *EMBO J*. 2001;**20**(17):4987-97.
288. Kim VN, Kataoka N, Dreyfuss G. Role of the nonsense-mediated decay factor hUpf3 in the splicing-dependent exon-exon junction complex. *Science*. 2001;**293**(5536):1832-6.
289. Hug N, Caceres JF. The RNA helicase DHX34 activates NMD by promoting a transition from the surveillance to the decay-inducing complex. *Cell Rep*. 2014;**8**(6):1845-56.
290. Kashima I, Yamashita A, Izumi N, Kataoka N, Morishita R, Hoshino S, et al. Binding of a novel SMG-1-Upf1-eRF1-eRF3 complex (SURF) to the exon junction complex triggers Upf1 phosphorylation and nonsense-mediated mRNA decay. *Genes Dev*. 2006;**20**(3):355-67.
291. Loh B, Jonas S, Izaurralde E. The SMG5-SMG7 heterodimer directly recruits the CCR4-NOT deadenylase complex to mRNAs containing nonsense codons via interaction with POP2. *Genes Dev*. 2013;**27**(19):2125-38.
292. Boehm V, Kueckelmann S, Gerbracht JV, Kallabis S, Britto-Borges T, Altmuller J, et al. SMG5-SMG7 authorize nonsense-mediated mRNA decay by enabling SMG6 endonucleolytic activity. *Nat Commun*. 2021;**12**(1):3965.
293. Muhlrad D, Parker R. Aberrant mRNAs with extended 3' UTRs are substrates for rapid degradation by mRNA surveillance. *RNA*. 1999;**5**(10):1299-307.
294. Wittkopp N, Huntzinger E, Weiler C, Sauliere J, Schmidt S, Sonawane M, et al. Nonsense-mediated mRNA decay effectors are essential for zebrafish embryonic development and survival. *Mol Cell Biol*. 2009;**29**(13):3517-28.
295. Medghalchi SM, Frischmeyer PA, Mendell JT, Kelly AG, Lawler AM, Dietz HC. Rent1, a trans-effector of nonsense-mediated mRNA decay, is essential for mammalian embryonic viability. *Hum Mol Genet*. 2001;**10**(2):99-105.
296. Weischenfeldt J, Damgaard I, Bryder D, Theilgaard-Monch K, Thoren LA, Nielsen FC, et al. NMD is essential for hematopoietic stem and progenitor cells and for eliminating by-products of programmed DNA rearrangements. *Genes Dev*. 2008;**22**(10):1381-96.
297. Li T, Shi Y, Wang P, Guachalla LM, Sun B, Joerss T, et al. Smg6/Est1 licenses embryonic stem cell differentiation via nonsense-mediated mRNA decay. *EMBO J*. 2015;**34**(12):1630-47.
298. Han X, Wei Y, Wang H, Wang F, Ju Z, Li T. Nonsense-mediated mRNA decay: a 'nonsense' pathway makes sense in stem cell biology. *Nucleic Acids Res*. 2018;**46**(3):1038-51.
299. Sartor F, Anderson J, McCaig C, Miedzybrodzka Z, Muller B. Mutation of genes controlling mRNA metabolism and protein synthesis predisposes to neurodevelopmental disorders. *Biochem Soc Trans*. 2015;**43**(6):1259-65.
300. Sachs AB, Davis RW, Kornberg RD. A single domain of yeast poly(A)-binding protein is necessary and sufficient for RNA binding and cell viability. *Mol Cell Biol*. 1987;**7**(9):3268-76.
301. Sachs AB, Bond MW, Kornberg RD. A single gene from yeast for both nuclear and cytoplasmic polyadenylate-binding proteins: domain structure and expression. *Cell*. 1986;**45**(6):827-35.
302. Gorgoni B, Gray NK. The roles of cytoplasmic poly(A)-binding proteins in regulating gene expression: a developmental perspective. *Brief Funct Genomic Proteomic*. 2004;**3**(2):125-41.

303. Flamand MN, Wu E, Vashisht A, Jannot G, Keiper BD, Simard MJ, et al. Poly(A)-binding proteins are required for microRNA-mediated silencing and to promote target deadenylation in C. elegans. *Nucleic Acids Res*. 2016;**44**(12):5924-35.
304. Chorghade S, Seimetz J, Emmons R, Yang J, Bresson SM, Lisio M, et al. Poly(A) tail length regulates PABPC1 expression to tune translation in the heart. *Elife*. 2017;**6**.
305. Feral C, Guellaen G, Pawlak A. Human testis expresses a specific poly(A)-binding protein. *Nucleic Acids Res*. 2001;**29**(9):1872-83.
306. Yang H, Duckett CS, Lindsten T. iPABP, an inducible poly(A)-binding protein detected in activated human T cells. *Mol Cell Biol*. 1995;**15**(12):6770-6.
307. Blanco P, Sargent CA, Boucher CA, Howell G, Ross M, Affara NA. A novel poly(A)-binding protein gene (PABPC5) maps to an X-specific subinterval in the Xq21.3/Yp11.2 homology block of the human sex chromosomes. *Genomics*. 2001;**74**(1):1-11.
308. Khanam T, Muddashetty RS, Kahvejian A, Sonenberg N, Brosius J. Poly(A)-binding protein binds to A-rich sequences via RNA-binding domains 1+2 and 3+4. *RNA Biol*. 2006;**3**(4):170-7.
309. Sawazaki R, Imai S, Yokogawa M, Hosoda N, Hoshino SI, Mio M, et al. Characterization of the multimeric structure of poly(A)-binding protein on a poly(A) tail. *Sci Rep*. 2018;**8**(1):1455.
310. Baer BW, Kornberg RD. Repeating structure of cytoplasmic poly(A)-ribonucleoprotein. *Proc Natl Acad Sci U S A*. 1980;**77**(4):1890-2.
311. Deo RC, Bonanno JB, Sonenberg N, Burley SK. Recognition of polyadenylate RNA by the poly(A)-binding protein. *Cell*. 1999;**98**(6):835-45.
312. Imataka H, Gradi A, Sonenberg N. A newly identified N-terminal amino acid sequence of human eIF4G binds poly(A)-binding protein and functions in poly(A)-dependent translation. *EMBO J*. 1998;**17**(24):7480-9.
313. Kozlov G, Menade M, Rosenauer A, Nguyen L, Gehring K. Molecular determinants of PAM2 recognition by the MLLE domain of poly(A)-binding protein. *J Mol Biol*. 2010;**397**(2):397-407.
314. Roy G, De Crescenzo G, Khaleghpour K, Kahvejian A, O'Connor-McCourt M, Sonenberg N. Paip1 interacts with poly(A) binding protein through two independent binding motifs. *Mol Cell Biol*. 2002;**22**(11):3769-82.
315. Khaleghpour K, Kahvejian A, De Crescenzo G, Roy G, Svitkin YV, Imataka H, et al. Dual interactions of the translational repressor Paip2 with poly(A) binding protein. *Mol Cell Biol*. 2001;**21**(15):5200-13.
316. Hoshino S, Imai M, Kobayashi T, Uchida N, Katada T. The eukaryotic polypeptide chain releasing factor (eRF3/GSPT) carrying the translation termination signal to the 3'-Poly(A) tail of mRNA. Direct association of erf3/GSPT with polyadenylate-binding protein. *J Biol Chem*. 1999;**274**(24):16677-80.
317. Kozlov G, Trempe JF, Khaleghpour K, Kahvejian A, Ekiel I, Gehring K. Structure and function of the C-terminal PABC domain of human poly(A)-binding protein. *Proc Natl Acad Sci U S A*. 2001;**98**(8):4409-13.
318. Yoshida M, Yoshida K, Kozlov G, Lim NS, De Crescenzo G, Pang Z, et al. Poly(A) binding protein (PABP) homeostasis is mediated by the stability of its inhibitor, Paip2. *EMBO J*. 2006;**25**(9):1934-44.

319. Gu W, Kwon Y, Oko R, Hermo L, Hecht NB. Poly (A) binding protein is bound to both stored and polysomal mRNAs in the mammalian testis. *Mol Reprod Dev*. 1995;**40**(3):273-85.
320. Kleene KC, Wang MY, Cutler M, Hall C, Shih D. Developmental expression of poly(A) binding protein mRNAs during spermatogenesis in the mouse. *Mol Reprod Dev*. 1994;**39**(4):355-64.
321. Ren X, Chen X, Wang Z, Wang D. Is transcription in sperm stationary or dynamic? *J Reprod Dev*. 2017;**63**(5):439-43.
322. Zhao Y, Li Q, Yao C, Wang Z, Zhou Y, Wang Y, et al. Characterization and quantification of mRNA transcripts in ejaculated spermatozoa of fertile men by serial analysis of gene expression. *Hum Reprod*. 2006;**21**(6):1583-90.
323. Fischer BE, Wasbrough E, Meadows LA, Randlet O, Dorus S, Karr TL, et al. Conserved properties of Drosophila and human spermatozoal mRNA repertoires. *Proc Biol Sci*. 2012;**279**(1738):2636-44.
324. Chalmel F, Rolland AD, Niederhauser-Wiederkehr C, Chung SS, Demougin P, Gattiker A, et al. The conserved transcriptome in human and rodent male gametogenesis. *Proc Natl Acad Sci U S A*. 2007;**104**(20):8346-51.
325. Schafer M, Nayernia K, Engel W, Schafer U. Translational control in spermatogenesis. *Dev Biol*. 1995;**172**(2):344-52.
326. Mangus DA, Evans MC, Jacobson A. Poly(A)-binding proteins: multifunctional scaffolds for the post-transcriptional control of gene expression. *Genome Biol*. 2003;**4**(7):223.
327. Kini HK, Kong J, Liebhaber SA. Cytoplasmic poly(A) binding protein C4 serves a critical role in erythroid differentiation. *Mol Cell Biol*. 2014;**34**(7):1300-9.
328. Hein MY, Hubner NC, Poser I, Cox J, Nagaraj N, Toyoda Y, et al. A human interactome in three quantitative dimensions organized by stoichiometries and abundances. *Cell*. 2015;**163**(3):712-23.
329. Oliveira AG, Oliveira LD, Cruz MV, Guimaraes D, Lima TI, Santos-Favero BC, et al. Interaction between poly(A)-binding protein PABPC4 and nuclear receptor corepressor NCoR1 modulates a metabolic stress response. *J Biol Chem*. 2023;**299**(6):104702.
330. Li P, Fan W, Xu J, Lu M, Yamamoto H, Auwerx J, et al. Adipocyte NCoR knockout decreases PPARgamma phosphorylation and enhances PPARgamma activity and insulin sensitivity. *Cell*. 2011;**147**(4):815-26.
331. Wilkie GS, Gautier P, Lawson D, Gray NK. Embryonic poly(A)-binding protein stimulates translation in germ cells. *Mol Cell Biol*. 2005;**25**(5):2060-71.
332. Cosson B, Couturier A, Le Guellec R, Moreau J, Chabelskaya S, Zhouravleva G, et al. Characterization of the poly(A) binding proteins expressed during oogenesis and early development of Xenopus laevis. *Biol Cell*. 2002;**94**(4-5):217-31.
333. Tadros W, Lipshitz HD. The maternal-to-zygotic transition: a play in two acts. *Development*. 2009;**136**(18):3033-42.
334. Barkoff A, Ballantyne S, Wickens M. Meiotic maturation in Xenopus requires polyadenylation of multiple mRNAs. *EMBO J*. 1998;**17**(11):3168-75.
335. Ozturk S, Sozen B, Demir N. Epab and Pabpc1 are differentially expressed in the postnatal mouse ovaries. *J Assist Reprod Genet*. 2015;**32**(1):137-46.
336. Guzeloglu-Kayisli O, Pauli S, Demir H, Lalioti MD, Sakkas D, Seli E. Identification and characterization of human embryonic poly(A) binding protein (EPAB). *Mol Hum Reprod*. 2008;**14**(10):581-8.

337. Bentivoglio M, Cotrufo T, Ferrari S, Tesoriero C, Mariotto S, Bertini G, et al. The Original Histological Slides of Camillo Golgi and His Discoveries on Neuronal Structure. *Front Neuroanat*. 2019;**13**:3.
338. Mazzarello P. From images to physiology: A strange paradox at the origin of modern neuroscience. *Prog Brain Res*. 2018;**243**:233-56.
339. Glickstein M. Golgi and Cajal: The neuron doctrine and the 100th anniversary of the 1906 Nobel Prize. *Curr Biol*. 2006;**16**(5):R147-51.
340. Saceleanu VM, Mohan AG, Covache-Busuioc RA, Costin HP, Ciurea AV. Wilhelm von Waldeyer: Important Steps in Neural Theory, Anatomy and Citology. *Brain Sci*. 2022;**12**(2).
341. Gotz M, Huttner WB. The cell biology of neurogenesis. *Nat Rev Mol Cell Biol*. 2005;**6**(10):777-88.
342. Rakic P. A small step for the cell, a giant leap for mankind: a hypothesis of neocortical expansion during evolution. *Trends Neurosci*. 1995;**18**(9):383-8.
343. McConnell SK. Constructing the cerebral cortex: neurogenesis and fate determination. *Neuron*. 1995;**15**(4):761-8.
344. Luskin MB, Pearlman AL, Sanes JR. Cell lineage in the cerebral cortex of the mouse studied in vivo and in vitro with a recombinant retrovirus. *Neuron*. 1988;**1**(8):635-47.
345. Kriegstein A, Alvarez-Buylla A. The glial nature of embryonic and adult neural stem cells. *Annu Rev Neurosci*. 2009;**32**:149-84.
346. Campbell K, Gotz M. Radial glia: multi-purpose cells for vertebrate brain development. *Trends Neurosci*. 2002;**25**(5):235-8.
347. Malatesta P, Hartfuss E, Gotz M. Isolation of radial glial cells by fluorescent-activated cell sorting reveals a neuronal lineage. *Development*. 2000;**127**(24):5253-63.
348. Williams BP, Price J. Evidence for multiple precursor cell types in the embryonic rat cerebral cortex. *Neuron*. 1995;**14**(6):1181-8.
349. Gressens P. Mechanisms and disturbances of neuronal migration. *Pediatr Res*. 2000;**48**(6):725-30.
350. Cooper JA. A mechanism for inside-out lamination in the neocortex. *Trends Neurosci*. 2008;**31**(3):113-9.
351. Kessaris N, Pringle N, Richardson WD. Specification of CNS glia from neural stem cells in the embryonic neuroepithelium. *Philos Trans R Soc Lond B Biol Sci*. 2008;**363**(1489):71-85.
352. Robinson SR, Dreher B. The visual pathways of eutherian mammals and marsupials develop according to a common timetable. *Brain Behav Evol*. 1990;**36**(4):177-95.
353. Chen VS, Morrison JP, Southwell MF, Foley JF, Bolon B, Elmore SA. Histology Atlas of the Developing Prenatal and Postnatal Mouse Central Nervous System, with Emphasis on Prenatal Days E7.5 to E18.5. *Toxicol Pathol*. 2017;**45**(6):705-44.
354. Reemst K, Noctor SC, Lucassen PJ, Hol EM. The Indispensable Roles of Microglia and Astrocytes during Brain Development. *Front Hum Neurosci*. 2016;**10**:566.
355. Altman J, Das GD. Autoradiographic and histological evidence of postnatal hippocampal neurogenesis in rats. *J Comp Neurol*. 1965;**124**(3):319-35.
356. Ghosh HS. Adult Neurogenesis and the Promise of Adult Neural Stem Cells. *J Exp Neurosci*. 2019;**13**:1179069519856876.
357. Reynolds BA, Weiss S. Generation of neurons and astrocytes from isolated cells of the adult mammalian central nervous system. *Science*. 1992;**255**(5052):1707-10.

358. Richards LJ, Kilpatrick TJ, Bartlett PF. De novo generation of neuronal cells from the adult mouse brain. *Proc Natl Acad Sci U S A*. 1992;**89**(18):8591-5.
359. Stanfield BB, Trice JE. Evidence that granule cells generated in the dentate gyrus of adult rats extend axonal projections. *Exp Brain Res*. 1988;**72**(2):399-406.
360. Alvarez-Buylla A, Garcia-Verdugo JM. Neurogenesis in adult subventricular zone. *J Neurosci*. 2002;**22**(3):629-34.
361. Eriksson PS, Perfilieva E, Bjork-Eriksson T, Alborn AM, Nordborg C, Peterson DA, et al. Neurogenesis in the adult human hippocampus. *Nat Med*. 1998;**4**(11):1313-7.
362. Garcia-Lopez P, Garcia-Marin V, Freire M. The histological slides and drawings of cajal. *Front Neuroanat*. 2010;**4**:9.
363. Sudhof TC. The cell biology of synapse formation. *J Cell Biol*. 2021;**220**(7).
364. Thomson AM, Deuchars J. Temporal and spatial properties of local circuits in neocortex. *Trends Neurosci*. 1994;**17**(3):119-26.
365. The principles of nerve cell communication. *Alcohol Health Res World*. 1997;**21**(2):107-8.
366. Ludwig PE, Reddy V, Varacallo M. Neuroanatomy, Neurons. StatPearls. Treasure Island (FL)2023.
367. Vogel Z, Daniels MP, Nirenberg M. Synapse and acetylcholine receptor synthesis by neurons dissociated from retina. *Proc Natl Acad Sci U S A*. 1976;**73**(7):2370-4.
368. Muller KJ, Scott SA. Transmission at a 'direct' electrical connexion mediated by an interneurone in the leech. *J Physiol*. 1981;**311**:565-83.
369. Baylor DA, Nicholls JG. Chemical and electrical synaptic connexions between cutaneous mechanoreceptor neurones in the central nervous system of the leech. *J Physiol*. 1969;**203**(3):591-609.
370. Bai F, Witzmann FA. Synaptosome proteomics. *Subcell Biochem*. 2007;**43**:77-98.
371. Capetian P, Muller L, Volkmann J, Heckmann M, Ergun S, Wagner N. Visualizing the Synaptic and Cellular Ultrastructure in Neurons Differentiated from Human Induced Neural Stem Cells-An Optimized Protocol. *Int J Mol Sci*. 2020;**21**(5).
372. Sudhof TC, Rizo J. Synaptic vesicle exocytosis. *Cold Spring Harb Perspect Biol*. 2011;**3**(12).
373. Augustin I, Rosenmund C, Sudhof TC, Brose N. Munc13-1 is essential for fusion competence of glutamatergic synaptic vesicles. *Nature*. 1999;**400**(6743):457-61.
374. Fon EA, Edwards RH. Molecular mechanisms of neurotransmitter release. *Muscle Nerve*. 2001;**24**(5):581-601.
375. Heuser JE, Reese TS. Evidence for recycling of synaptic vesicle membrane during transmitter release at the frog neuromuscular junction. *J Cell Biol*. 1973;**57**(2):315-44.
376. Schratt GM, Nigh EA, Chen WG, Hu L, Greenberg ME. BDNF regulates the translation of a select group of mRNAs by a mammalian target of rapamycin-phosphatidylinositol 3-kinase-dependent pathway during neuronal development. *J Neurosci*. 2004;**24**(33):7366-77.
377. Kang H, Schuman EM. A requirement for local protein synthesis in neurotrophin-induced hippocampal synaptic plasticity. *Science*. 1996;**273**(5280):1402-6.
378. Biever A, Glock C, Tushev G, Ciirdaeva E, Dalmay T, Langer JD, et al. Monosomes actively translate synaptic mRNAs in neuronal processes. *Science*. 2020;**367**(6477).
379. Landis DM, Reese TS. Cytoplasmic organization in cerebellar dendritic spines. *J Cell Biol*. 1983;**97**(4):1169-78.

380. Igarashi M. Molecular basis of the functions of the mammalian neuronal growth cone revealed using new methods. *Proc Jpn Acad Ser B Phys Biol Sci*. 2019;**95**(7):358-77.
381. Lowery LA, Van Vactor D. The trip of the tip: understanding the growth cone machinery. *Nat Rev Mol Cell Biol*. 2009;**10**(5):332-43.
382. Liu G, Dwyer T. Microtubule dynamics in axon guidance. *Neurosci Bull*. 2014;**30**(4):569-83.
383. Pereda AE. Electrical synapses and their functional interactions with chemical synapses. *Nat Rev Neurosci*. 2014;**15**(4):250-63.
384. Sudhof TC, Malenka RC. Understanding synapses: past, present, and future. *Neuron*. 2008;**60**(3):469-76.
385. Sotelo C. The History of the Synapse. *Anat Rec (Hoboken)*. 2020;**303**(5):1252-79.
386. Fischbach GD. Synapse formation between dissociated nerve and muscle cells in low density cell cultures. *Dev Biol*. 1972;**28**(2):407-29.
387. Martin EA, Lasseigne AM, Miller AC. Understanding the Molecular and Cell Biological Mechanisms of Electrical Synapse Formation. *Front Neuroanat*. 2020;**14**:12.
388. Marin-Burgin A, Eisenhart FJ, Kristan WB, Jr., French KA. Embryonic electrical connections appear to pre-figure a behavioral circuit in the leech CNS. *J Comp Physiol A Neuroethol Sens Neural Behav Physiol*. 2006;**192**(2):123-33.
389. Saint-Amant L, Drapeau P. Motoneuron activity patterns related to the earliest behavior of the zebrafish embryo. *J Neurosci*. 2000;**20**(11):3964-72.
390. Han Y, Massey SC. Electrical synapses in retinal ON cone bipolar cells: subtype-specific expression of connexins. *Proc Natl Acad Sci U S A*. 2005;**102**(37):13313-8.
391. Wu SM. Synaptic organization of the vertebrate retina: general principles and species-specific variations: the Friedenwald lecture. *Invest Ophthalmol Vis Sci*. 2010;**51**(3):1263-74.
392. Anderson JR, Jones BW, Watt CB, Shaw MV, Yang JH, Demill D, et al. Exploring the retinal connectome. *Mol Vis*. 2011;**17**:355-79.
393. Melli G, Hoke A. Dorsal Root Ganglia Sensory Neuronal Cultures: a tool for drug discovery for peripheral neuropathies. *Expert Opin Drug Discov*. 2009;**4**(10):1035-45.
394. Goaillard JM, Moubarak E, Tapia M, Tell F. Diversity of Axonal and Dendritic Contributions to Neuronal Output. *Front Cell Neurosci*. 2019;**13**:570.
395. Didier A, Carleton A, Bjaalie JG, Vincent JD, Ottersen OP, Storm-Mathisen J, et al. A dendrodendritic reciprocal synapse provides a recurrent excitatory connection in the olfactory bulb. *Proc Natl Acad Sci U S A*. 2001;**98**(11):6441-6.
396. Huttenlocher PR, Dabholkar AS. Regional differences in synaptogenesis in human cerebral cortex. *J Comp Neurol*. 1997;**387**(2):167-78.
397. Huttenlocher PR. Synaptic density in human frontal cortex - developmental changes and effects of aging. *Brain Res*. 1979;**163**(2):195-205.
398. Riccomagno MM, Kolodkin AL. Sculpting neural circuits by axon and dendrite pruning. *Annu Rev Cell Dev Biol*. 2015;**31**:779-805.
399. Schuldiner O, Yaron A. Mechanisms of developmental neurite pruning. *Cell Mol Life Sci*. 2015;**72**(1):101-19.
400. Luo L, O'Leary DD. Axon retraction and degeneration in development and disease. *Annu Rev Neurosci*. 2005;**28**:127-56.
401. Erturk A, Wang Y, Sheng M. Local pruning of dendrites and spines by caspase-3-dependent and proteasome-limited mechanisms. *J Neurosci*. 2014;**34**(5):1672-88.

402. Li Z, Jo J, Jia JM, Lo SC, Whitcomb DJ, Jiao S, et al. Caspase-3 activation via mitochondria is required for long-term depression and AMPA receptor internalization. *Cell*. 2010;**141**(5):859-71.
403. Xu ZX, Tan JW, Xu H, Hill CJ, Ostrovskaya O, Martemyanov KA, et al. Caspase-2 promotes AMPA receptor internalization and cognitive flexibility via mTORC2-AKT-GSK3beta signaling. *Nat Commun*. 2019;**10**(1):3622.
404. Tang G, Gudsnuk K, Kuo SH, Cotrina ML, Rosoklija G, Sosunov A, et al. Loss of mTOR-dependent macroautophagy causes autistic-like synaptic pruning deficits. *Neuron*. 2014;**83**(5):1131-43.
405. Germann M, Brederoo SG, Sommer IEC. Abnormal synaptic pruning during adolescence underlying the development of psychotic disorders. *Curr Opin Psychiatry*. 2021;**34**(3):222-7.
406. Sakai J. Core Concept: How synaptic pruning shapes neural wiring during development and, possibly, in disease. *Proc Natl Acad Sci U S A*. 2020;**117**(28):16096-9.
407. Kristiansen M, Ham J. Programmed cell death during neuronal development: the sympathetic neuron model. *Cell Death Differ*. 2014;**21**(7):1025-35.
408. Cavallaro S. Cracking the code of neuronal apoptosis and survival. *Cell Death Dis*. 2015;**6**(11):e1963.
409. Merry DE, Korsmeyer SJ. Bcl-2 gene family in the nervous system. *Annu Rev Neurosci*. 1997;**20**:245-67.
410. Dlugosz PJ, Billen LP, Annis MG, Zhu W, Zhang Z, Lin J, et al. Bcl-2 changes conformation to inhibit Bax oligomerization. *EMBO J*. 2006;**25**(11):2287-96.
411. Deckwerth TL, Elliott JL, Knudson CM, Johnson EM, Jr., Snider WD, Korsmeyer SJ. BAX is required for neuronal death after trophic factor deprivation and during development. *Neuron*. 1996;**17**(3):401-11.
412. Aakalu G, Smith WB, Nguyen N, Jiang C, Schuman EM. Dynamic visualization of local protein synthesis in hippocampal neurons. *Neuron*. 2001;**30**(2):489-502.
413. Rangaraju V, Tom Dieck S, Schuman EM. Local translation in neuronal compartments: how local is local? *EMBO Rep*. 2017;**18**(5):693-711.
414. Sasaki Y, Welshhans K, Wen Z, Yao J, Xu M, Goshima Y, et al. Phosphorylation of zipcode binding protein 1 is required for brain-derived neurotrophic factor signaling of local beta-actin synthesis and growth cone turning. *J Neurosci*. 2010;**30**(28):9349-58.
415. Huttelmaier S, Zenklusen D, Lederer M, Dictenberg J, Lorenz M, Meng X, et al. Spatial regulation of beta-actin translation by Src-dependent phosphorylation of ZBP1. *Nature*. 2005;**438**(7067):512-5.
416. Krichevsky AM, Kosik KS. Neuronal RNA granules: a link between RNA localization and stimulation-dependent translation. *Neuron*. 2001;**32**(4):683-96.
417. Martin KC, Ephrussi A. mRNA localization: gene expression in the spatial dimension. *Cell*. 2009;**136**(4):719-30.
418. Doyle M, Kiebler MA. Mechanisms of dendritic mRNA transport and its role in synaptic tagging. *EMBO J*. 2011;**30**(17):3540-52.
419. Fusco CM, Desch K, Dorrbaum AR, Wang M, Staab A, Chan ICW, et al. Neuronal ribosomes exhibit dynamic and context-dependent exchange of ribosomal proteins. *Nat Commun*. 2021;**12**(1):6127.

420. Gumy LF, Yeo GS, Tung YC, Zivraj KH, Willis D, Coppola G, et al. Transcriptome analysis of embryonic and adult sensory axons reveals changes in mRNA repertoire localization. *RNA*. 2011;**17**(1):85-98.
421. Middleton SA, Eberwine J, Kim J. Comprehensive catalog of dendritically localized mRNA isoforms from sub-cellular sequencing of single mouse neurons. *BMC Biol*. 2019;**17**(1):5.
422. Perez JD, Dieck ST, Alvarez-Castelao B, Tushev G, Chan IC, Schuman EM. Subcellular sequencing of single neurons reveals the dendritic transcriptome of GABAergic interneurons. *Elife*. 2021;**10**.
423. Ross AF, Oleynikov Y, Kislauskis EH, Taneja KL, Singer RH. Characterization of a beta-actin mRNA zipcode-binding protein. *Mol Cell Biol*. 1997;**17**(4):2158-65.
424. Farina KL, Huttelmaier S, Musunuru K, Darnell R, Singer RH. Two ZBP1 KH domains facilitate beta-actin mRNA localization, granule formation, and cytoskeletal attachment. *J Cell Biol*. 2003;**160**(1):77-87.
425. Tiruchinapalli DM, Oleynikov Y, Kelic S, Shenoy SM, Hartley A, Stanton PK, et al. Activity-dependent trafficking and dynamic localization of zipcode binding protein 1 and beta-actin mRNA in dendrites and spines of hippocampal neurons. *J Neurosci*. 2003;**23**(8):3251-61.
426. Garner CC, Tucker RP, Matus A. Selective localization of messenger RNA for cytoskeletal protein MAP2 in dendrites. *Nature*. 1988;**336**(6200):674-7.
427. Rook MS, Lu M, Kosik KS. CaMKIIalpha 3' untranslated region-directed mRNA translocation in living neurons: visualization by GFP linkage. *J Neurosci*. 2000;**20**(17):6385-93.
428. Kobayashi H, Yamamoto S, Maruo T, Murakami F. Identification of a cis-acting element required for dendritic targeting of activity-regulated cytoskeleton-associated protein mRNA. *Eur J Neurosci*. 2005;**22**(12):2977-84.
429. Huang YS, Carson JH, Barbarese E, Richter JD. Facilitation of dendritic mRNA transport by CPEB. *Genes Dev*. 2003;**17**(5):638-53.
430. Kislauskis EH, Zhu X, Singer RH. Sequences responsible for intracellular localization of beta-actin messenger RNA also affect cell phenotype. *J Cell Biol*. 1994;**127**(2):441-51.
431. Patel VL, Mitra S, Harris R, Buxbaum AR, Lionnet T, Brenowitz M, et al. Spatial arrangement of an RNA zipcode identifies mRNAs under post-transcriptional control. *Genes Dev*. 2012;**26**(1):43-53.
432. Ma B, Savas JN, Yu MS, Culver BP, Chao MV, Tanese N. Huntingtin mediates dendritic transport of beta-actin mRNA in rat neurons. *Sci Rep*. 2011;**1**:140.
433. Darnell JC, Jensen KB, Jin P, Brown V, Warren ST, Darnell RB. Fragile X mental retardation protein targets G quartet mRNAs important for neuronal function. *Cell*. 2001;**107**(4):489-99.
434. Puig Lombardi E, Londono-Vallejo A. A guide to computational methods for G-quadruplex prediction. *Nucleic Acids Res*. 2020;**48**(1):1-15.
435. Lu R, Wang H, Liang Z, Ku L, O'Donnell W T, Li W, et al. The fragile X protein controls microtubule-associated protein 1B translation and microtubule stability in brain neuron development. *Proc Natl Acad Sci U S A*. 2004;**101**(42):15201-6.
436. Todd PK, Mack KJ, Malter JS. The fragile X mental retardation protein is required for type-I metabotropic glutamate receptor-dependent translation of PSD-95. *Proc Natl Acad Sci U S A*. 2003;**100**(24):14374-8.

437. Zalfa F, Eleuteri B, Dickson KS, Mercaldo V, De Rubeis S, di Penta A, et al. A new function for the fragile X mental retardation protein in regulation of PSD-95 mRNA stability. *Nat Neurosci*. 2007;**10**(5):578-87.
438. Castets M, Schaeffer C, Bechara E, Schenck A, Khandjian EW, Luche S, et al. FMRP interferes with the Rac1 pathway and controls actin cytoskeleton dynamics in murine fibroblasts. *Hum Mol Genet*. 2005;**14**(6):835-44.
439. Westmark CJ, Malter JS. FMRP mediates mGluR5-dependent translation of amyloid precursor protein. *PLoS Biol*. 2007;**5**(3):e52.
440. Didiot MC, Tian Z, Schaeffer C, Subramanian M, Mandel JL, Moine H. The G-quartet containing FMRP binding site in FMR1 mRNA is a potent exonic splicing enhancer. *Nucleic Acids Res*. 2008;**36**(15):4902-12.
441. Goering R, Hudish LI, Guzman BB, Raj N, Bassell GJ, Russ HA, et al. FMRP promotes RNA localization to neuronal projections through interactions between its RGG domain and G-quadruplex RNA sequences. *Elife*. 2020;**9**.
442. Darnell JC, Van Driesche SJ, Zhang C, Hung KY, Mele A, Fraser CE, et al. FMRP stalls ribosomal translocation on mRNAs linked to synaptic function and autism. *Cell*. 2011;**146**(2):247-61.
443. Davidovic L, Jaglin XH, Lepagnol-Bestel AM, Tremblay S, Simonneau M, Bardoni B, et al. The fragile X mental retardation protein is a molecular adaptor between the neurospecific KIF3C kinesin and dendritic RNA granules. *Hum Mol Genet*. 2007;**16**(24):3047-58.
444. Oe S, Yoneda Y. Cytoplasmic polyadenylation element-like sequences are involved in dendritic targeting of BDNF mRNA in hippocampal neurons. *FEBS Lett*. 2010;**584**(15):3424-30.
445. Steward O, Wallace CS, Lyford GL, Worley PF. Synaptic activation causes the mRNA for the IEG Arc to localize selectively near activated postsynaptic sites on dendrites. *Neuron*. 1998;**21**(4):741-51.
446. Tongiorgi E, Righi M, Cattaneo A. Activity-dependent dendritic targeting of BDNF and TrkB mRNAs in hippocampal neurons. *J Neurosci*. 1997;**17**(24):9492-505.
447. Wu L, Wells D, Tay J, Mendis D, Abbott MA, Barnitt A, et al. CPEB-mediated cytoplasmic polyadenylation and the regulation of experience-dependent translation of alpha-CaMKII mRNA at synapses. *Neuron*. 1998;**21**(5):1129-39.
448. Chao HW, Tsai LY, Lu YL, Lin PY, Huang WH, Chou HJ, et al. Deletion of CPEB3 enhances hippocampus-dependent memory via increasing expressions of PSD95 and NMDA receptors. *J Neurosci*. 2013;**33**(43):17008-22.
449. Sutcliffe JG, Milner RJ, Bloom FE, Lerner RA. Common 82-nucleotide sequence unique to brain RNA. *Proc Natl Acad Sci U S A*. 1982;**79**(16):4942-6.
450. Watson JB, Sutcliffe JG. Primate brain-specific cytoplasmic transcript of the Alu repeat family. *Mol Cell Biol*. 1987;**7**(9):3324-7.
451. Sutcliffe JG, Milner RJ, Gottesfeld JM, Lerner RA. Identifier sequences are transcribed specifically in brain. *Nature*. 1984;**308**(5956):237-41.
452. Robeck T, Skryabin BV, Rozhdestvensky TS, Skryabin AB, Brosius J. BC1 RNA motifs required for dendritic transport in vivo. *Sci Rep*. 2016;**6**:28300.
453. Muslimov IA, Banker G, Brosius J, Tiedge H. Activity-dependent regulation of dendritic BC1 RNA in hippocampal neurons in culture. *J Cell Biol*. 1998;**141**(7):1601-11.

454. Tiedge H, Fremeau RT, Jr., Weinstock PH, Arancio O, Brosius J. Dendritic location of neural BC1 RNA. *Proc Natl Acad Sci U S A*. 1991;**88**(6):2093-7.
455. Martignetti JA, Brosius J. Neural BC1 RNA as an evolutionary marker: guinea pig remains a rodent. *Proc Natl Acad Sci U S A*. 1993;**90**(20):9698-702.
456. Martignetti JA, Brosius J. BC200 RNA: a neural RNA polymerase III product encoded by a monomeric Alu element. *Proc Natl Acad Sci U S A*. 1993;**90**(24):11563-7.
457. Tiedge H, Chen W, Brosius J. Primary structure, neural-specific expression, and dendritic location of human BC200 RNA. *J Neurosci*. 1993;**13**(6):2382-90.
458. Mus E, Hof PR, Tiedge H. Dendritic BC200 RNA in aging and in Alzheimer's disease. *Proc Natl Acad Sci U S A*. 2007;**104**(25):10679-84.
459. Lee Y, Lee HS, Kim M, Shin H. Brain Cytoplasmic RNAs in Neurons: From Biosynthesis to Function. *Biomolecules*. 2020;**10**(2).
460. DeChiara TM, Brosius J. Neural BC1 RNA: cDNA clones reveal nonrepetitive sequence content. *Proc Natl Acad Sci U S A*. 1987;**84**(9):2624-8.
461. Rozhdestvensky TS, Kopylov AM, Brosius J, Huttenhofer A. Neuronal BC1 RNA structure: evolutionary conversion of a tRNA(Ala) domain into an extended stem-loop structure. *RNA*. 2001;**7**(5):722-30.
462. Martignetti JA, Brosius J. BC1 RNA: transcriptional analysis of a neural cell-specific RNA polymerase III transcript. *Mol Cell Biol*. 1995;**15**(3):1642-50.
463. Muslimov IA, Iacoangeli A, Brosius J, Tiedge H. Spatial codes in dendritic BC1 RNA. *J Cell Biol*. 2006;**175**(3):427-39.
464. Cristofanilli M, Iacoangeli A, Muslimov IA, Tiedge H. Neuronal BC1 RNA: microtubule-dependent dendritic delivery. *J Mol Biol*. 2006;**356**(5):1118-23.
465. Zalfa F, Adinolfi S, Napoli I, Kuhn-Holsken E, Urlaub H, Achsel T, et al. Fragile X mental retardation protein (FMRP) binds specifically to the brain cytoplasmic RNAs BC1/BC200 via a novel RNA-binding motif. *J Biol Chem*. 2005;**280**(39):33403-10.
466. Zalfa F, Giorgi M, Primerano B, Moro A, Di Penta A, Reis S, et al. The fragile X syndrome protein FMRP associates with BC1 RNA and regulates the translation of specific mRNAs at synapses. *Cell*. 2003;**112**(3):317-27.
467. Gruber AR, Lorenz R, Bernhart SH, Neubock R, Hofacker IL. The Vienna RNA websuite. *Nucleic Acids Res*. 2008;**36**(Web Server issue):W70-4.
468. Iacoangeli A, Rozhdestvensky TS, Dolzhanskaya N, Tournier B, Schutt J, Brosius J, et al. On BC1 RNA and the fragile X mental retardation protein. *Proc Natl Acad Sci U S A*. 2008;**105**(2):734-9.
469. Mallardo M, Deitinghoff A, Muller J, Goetze B, Macchi P, Peters C, et al. Isolation and characterization of Staufen-containing ribonucleoprotein particles from rat brain. *Proc Natl Acad Sci U S A*. 2003;**100**(4):2100-5.
470. Jeong JH, Nam YJ, Kim SY, Kim EG, Jeong J, Kim HK. The transport of Staufen2-containing ribonucleoprotein complexes involves kinesin motor protein and is modulated by mitogen-activated protein kinase pathway. *J Neurochem*. 2007;**102**(6):2073-84.
471. Duning K, Buck F, Barnekow A, Kremerskothen J. SYNCRIP, a component of dendritically localized mRNPs, binds to the translation regulator BC200 RNA. *J Neurochem*. 2008;**105**(2):351-9.
472. Wang H, Iacoangeli A, Popp S, Muslimov IA, Imataka H, Sonenberg N, et al. Dendritic BC1 RNA: functional role in regulation of translation initiation. *J Neurosci*. 2002;**22**(23):10232-41.

473. Briz V, Restivo L, Pasciuto E, Juczewski K, Mercaldo V, Lo AC, et al. The non-coding RNA BC1 regulates experience-dependent structural plasticity and learning. *Nat Commun*. 2017;**8**(1):293.
474. Zhong J, Chuang SC, Bianchi R, Zhao W, Lee H, Fenton AA, et al. BC1 regulation of metabotropic glutamate receptor-mediated neuronal excitability. *J Neurosci*. 2009;**29**(32):9977-86.
475. Ainger K, Avossa D, Morgan F, Hill SJ, Barry C, Barbarese E, et al. Transport and localization of exogenous myelin basic protein mRNA microinjected into oligodendrocytes. *J Cell Biol*. 1993;**123**(2):431-41.
476. Kloc M, Etkin LD. Two distinct pathways for the localization of RNAs at the vegetal cortex in Xenopus oocytes. *Development*. 1995;**121**(2):287-97.
477. Knowles RB, Sabry JH, Martone ME, Deerinck TJ, Ellisman MH, Bassell GJ, et al. Translocation of RNA granules in living neurons. *J Neurosci*. 1996;**16**(24):7812-20.
478. Kipper K, Mansour A, Pulk A. Neuronal RNA granules are ribosome complexes stalled at the pre-translocation state. *J Mol Biol*. 2022;**434**(20):167801.
479. Anadolu MN, Sun J, Kailasam S, Chalkiadaki K, Krimbacher K, Li JT, et al. Ribosomes in RNA Granules Are Stalled on mRNA Sequences That Are Consensus Sites for FMRP Association. *J Neurosci*. 2023;**43**(14):2440-59.
480. El Fatimy R, Davidovic L, Tremblay S, Jaglin X, Dury A, Robert C, et al. Tracking the Fragile X Mental Retardation Protein in a Highly Ordered Neuronal RiboNucleoParticles Population: A Link between Stalled Polyribosomes and RNA Granules. *PLoS Genet*. 2016;**12**(7):e1006192.
481. Bauer KE, Bargenda N, Schieweck R, Illig C, Segura I, Harner M, et al. RNA supply drives physiological granule assembly in neurons. *Nat Commun*. 2022;**13**(1):2781.
482. Lai A, Valdez-Sinon AN, Bassell GJ. Regulation of RNA granules by FMRP and implications for neurological diseases. *Traffic*. 2020;**21**(7):454-62.
483. Chen E, Sharma MR, Shi X, Agrawal RK, Joseph S. Fragile X mental retardation protein regulates translation by binding directly to the ribosome. *Mol Cell*. 2014;**54**(3):407-17.
484. Ishizuka A, Siomi MC, Siomi H. A Drosophila fragile X protein interacts with components of RNAi and ribosomal proteins. *Genes Dev*. 2002;**16**(19):2497-508.
485. Maher-Laporte M, Berthiaume F, Moreau M, Julien LA, Lapointe G, Mourez M, et al. Molecular composition of staufen2-containing ribonucleoproteins in embryonic rat brain. *PLoS One*. 2010;**5**(6):e11350.
486. Goetze B, Tuebing F, Xie Y, Dorostkar MM, Thomas S, Pehl U, et al. The brain-specific double-stranded RNA-binding protein Staufen2 is required for dendritic spine morphogenesis. *J Cell Biol*. 2006;**172**(2):221-31.
487. Heber S, Gaspar I, Tants JN, Gunther J, Moya SMF, Janowski R, et al. Staufen2-mediated RNA recognition and localization requires combinatorial action of multiple domains. *Nat Commun*. 2019;**10**(1):1659.
488. Heraud-Farlow JE, Sharangdhar T, Li X, Pfeifer P, Tauber S, Orozco D, et al. Staufen2 regulates neuronal target RNAs. *Cell Rep*. 2013;**5**(6):1511-8.
489. Kobayashi S, Goto S, Anzai K. Brain-specific small RNA transcript of the identifier sequences is present as a 10 S ribonucleoprotein particle. *J Biol Chem*. 1991;**266**(8):4726-30.

490. Villace P, Marion RM, Ortin J. The composition of Staufen-containing RNA granules from human cells indicates their role in the regulated transport and translation of messenger RNAs. *Nucleic Acids Res*. 2004;**32**(8):2411-20.
491. Kurosaki T, Mitsutomi S, Hewko A, Akimitsu N, Maquat LE. Integrative omics indicate FMRP sequesters mRNA from translation and deadenylation in human neuronal cells. *Mol Cell*. 2022;**82**(23):4564-81 e11.
492. Bannai H, Fukatsu K, Mizutani A, Natsume T, Iemura S, Ikegami T, et al. An RNA-interacting protein, SYNCRIP (heterogeneous nuclear ribonuclear protein Q1/NSAP1) is a component of mRNA granule transported with inositol 1,4,5-trisphosphate receptor type 1 mRNA in neuronal dendrites. *J Biol Chem*. 2004;**279**(51):53427-34.
493. Khudayberdiev S, Soutschek M, Ammann I, Heinze A, Rust MB, Baumeister S, et al. The cytoplasmic SYNCRIP mRNA interactome of mammalian neurons. *RNA Biol*. 2021;**18**(9):1252-64.
494. Williams KR, McAninch DS, Stefanovic S, Xing L, Allen M, Li W, et al. hnRNP-Q1 represses nascent axon growth in cortical neurons by inhibiting Gap-43 mRNA translation. *Mol Biol Cell*. 2016;**27**(3):518-34.
495. Bergemann AD, Johnson EM. The HeLa Pur factor binds single-stranded DNA at a specific element conserved in gene flanking regions and origins of DNA replication. *Mol Cell Biol*. 1992;**12**(3):1257-65.
496. Bergemann AD, Ma ZW, Johnson EM. Sequence of cDNA comprising the human pur gene and sequence-specific single-stranded-DNA-binding properties of the encoded protein. *Mol Cell Biol*. 1992;**12**(12):5673-82.
497. Johnson EM, Kinoshita Y, Weinreb DB, Wortman MJ, Simon R, Khalili K, et al. Role of Pur alpha in targeting mRNA to sites of translation in hippocampal neuronal dendrites. *J Neurosci Res*. 2006;**83**(6):929-43.
498. Kanai Y, Dohmae N, Hirokawa N. Kinesin transports RNA: isolation and characterization of an RNA-transporting granule. *Neuron*. 2004;**43**(4):513-25.
499. Mitsumori K, Takei Y, Hirokawa N. Components of RNA granules affect their localization and dynamics in neuronal dendrites. *Mol Biol Cell*. 2017;**28**(11):1412-7.
500. Ohashi S, Koike K, Omori A, Ichinose S, Ohara S, Kobayashi S, et al. Identification of mRNA/protein (mRNP) complexes containing Puralpha, mStaufen, fragile X protein, and myosin Va and their association with rough endoplasmic reticulum equipped with a kinesin motor. *J Biol Chem*. 2002;**277**(40):37804-10.
501. Barbee SA, Estes PS, Cziko AM, Hillebrand J, Luedeman RA, Coller JM, et al. Staufen- and FMRP-containing neuronal RNPs are structurally and functionally related to somatic P bodies. *Neuron*. 2006;**52**(6):997-1009.
502. Furic L, Maher-Laporte M, DesGroseillers L. A genome-wide approach identifies distinct but overlapping subsets of cellular mRNAs associated with Staufen1- and Staufen2-containing ribonucleoprotein complexes. *RNA*. 2008;**14**(2):324-35.
503. Kao DI, Aldridge GM, Weiler IJ, Greenough WT. Altered mRNA transport, docking, and protein translation in neurons lacking fragile X mental retardation protein. *Proc Natl Acad Sci U S A*. 2010;**107**(35):15601-6.
504. Bauer KE, Segura I, Gaspar I, Scheuss V, Illig C, Ammer G, et al. Live cell imaging reveals 3'-UTR dependent mRNA sorting to synapses. *Nat Commun*. 2019;**10**(1):3178.
505. Kumar A. Long-Term Potentiation at CA3-CA1 Hippocampal Synapses with Special Emphasis on Aging, Disease, and Stress. *Front Aging Neurosci*. 2011;**3**:7.

506. Bodian D. A Suggestive Relationship of Nerve Cell Rna with Specific Synaptic Sites. *Proc Natl Acad Sci U S A*. 1965;**53**(2):418-25.
507. Tennyson VM. The fine structure of the axon and growth cone of the dorsal root neuroblast of the rabbit embryo. *J Cell Biol*. 1970;**44**(1):62-79.
508. Gindina S, Botsford B, Cowansage K, LeDoux J, Klann E, Hoeffer C, et al. Upregulation of eIF4E, but not other translation initiation factors, in dendritic spines during memory formation. *J Comp Neurol*. 2021;**529**(11):3112-26.
509. Tang SJ, Reis G, Kang H, Gingras AC, Sonenberg N, Schuman EM. A rapamycin-sensitive signaling pathway contributes to long-term synaptic plasticity in the hippocampus. *Proc Natl Acad Sci U S A*. 2002;**99**(1):467-72.
510. Steward O, Levy WB. Preferential localization of polyribosomes under the base of dendritic spines in granule cells of the dentate gyrus. *J Neurosci*. 1982;**2**(3):284-91.
511. Ostroff LE, Botsford B, Gindina S, Cowansage KK, LeDoux JE, Klann E, et al. Accumulation of Polyribosomes in Dendritic Spine Heads, But Not Bases and Necks, during Memory Consolidation Depends on Cap-Dependent Translation Initiation. *J Neurosci*. 2017;**37**(7):1862-72.
512. Rosenberg T, Gal-Ben-Ari S, Dieterich DC, Kreutz MR, Ziv NE, Gundelfinger ED, et al. The roles of protein expression in synaptic plasticity and memory consolidation. *Front Mol Neurosci*. 2014;**7**:86.
513. Chin D, Means AR. Calmodulin: a prototypical calcium sensor. *Trends Cell Biol*. 2000;**10**(8):322-8.
514. Shifman JM, Choi MH, Mihalas S, Mayo SL, Kennedy MB. Ca2+/calmodulin-dependent protein kinase II (CaMKII) is activated by calmodulin with two bound calciums. *Proc Natl Acad Sci U S A*. 2006;**103**(38):13968-73.
515. Hanson PI, Schulman H. Neuronal Ca2+/calmodulin-dependent protein kinases. *Annu Rev Biochem*. 1992;**61**:559-601.
516. Fong YL, Taylor WL, Means AR, Soderling TR. Studies of the regulatory mechanism of Ca2+/calmodulin-dependent protein kinase II. Mutation of threonine 286 to alanine and aspartate. *J Biol Chem*. 1989;**264**(28):16759-63.
517. Hanson PI, Kapiloff MS, Lou LL, Rosenfeld MG, Schulman H. Expression of a multifunctional Ca2+/calmodulin-dependent protein kinase and mutational analysis of its autoregulation. *Neuron*. 1989;**3**(1):59-70.
518. Waxham MN, Aronowski J, Westgate SA, Kelly PT. Mutagenesis of Thr-286 in monomeric Ca2+/calmodulin-dependent protein kinase II eliminates Ca2+/calmodulin-independent activity. *Proc Natl Acad Sci U S A*. 1990;**87**(4):1273-7.
519. Erondu NE, Kennedy MB. Regional distribution of type II Ca2+/calmodulin-dependent protein kinase in rat brain. *J Neurosci*. 1985;**5**(12):3270-7.
520. Colbran RJ. Targeting of calcium/calmodulin-dependent protein kinase II. *Biochem J*. 2004;**378**(Pt 1):1-16.
521. Kennedy MB, Bennett MK, Erondu NE. Biochemical and immunochemical evidence that the "major postsynaptic density protein" is a subunit of a calmodulin-dependent protein kinase. *Proc Natl Acad Sci U S A*. 1983;**80**(23):7357-61.
522. Kelly PT, McGuinness TL, Greengard P. Evidence that the major postsynaptic density protein is a component of a Ca2+/calmodulin-dependent protein kinase. *Proc Natl Acad Sci U S A*. 1984;**81**(3):945-9.

523. Goldenring JR, McGuire JS, Jr., DeLorenzo RJ. Identification of the major postsynaptic density protein as homologous with the major calmodulin-binding subunit of a calmodulin-dependent protein kinase. *J Neurochem*. 1984;**42**(4):1077-84.
524. Chen S, Xu Y, Xu B, Guo M, Zhang Z, Liu L, et al. CaMKII is involved in cadmium activation of MAPK and mTOR pathways leading to neuronal cell death. *J Neurochem*. 2011;**119**(5):1108-18.
525. Dong X, Qin J, Ma J, Zeng Q, Zhang H, Zhang R, et al. BAFF inhibits autophagy promoting cell proliferation and survival by activating Ca(2+)-CaMKII-dependent Akt/mTOR signaling pathway in normal and neoplastic B-lymphoid cells. *Cell Signal*. 2019;**53**:68-79.
526. Dan HC, Ebbs A, Pasparakis M, Van Dyke T, Basseres DS, Baldwin AS. Akt-dependent activation of mTORC1 complex involves phosphorylation of mTOR (mammalian target of rapamycin) by IkappaB kinase alpha (IKKalpha). *J Biol Chem*. 2014;**289**(36):25227-40.
527. Crino PB. The mTOR signalling cascade: paving new roads to cure neurological disease. *Nat Rev Neurol*. 2016;**12**(7):379-92.
528. Kim DH, Sarbassov DD, Ali SM, King JE, Latek RR, Erdjument-Bromage H, et al. mTOR interacts with raptor to form a nutrient-sensitive complex that signals to the cell growth machinery. *Cell*. 2002;**110**(2):163-75.
529. Ostroff LE, Watson DJ, Cao G, Parker PH, Smith H, Harris KM. Shifting patterns of polyribosome accumulation at synapses over the course of hippocampal long-term potentiation. *Hippocampus*. 2018;**28**(6):416-30.
530. Hoeffer CA, Cowansage KK, Arnold EC, Banko JL, Moerke NJ, Rodriguez R, et al. Inhibition of the interactions between eukaryotic initiation factors 4E and 4G impairs long-term associative memory consolidation but not reconsolidation. *Proc Natl Acad Sci U S A*. 2011;**108**(8):3383-8.
531. Bohlen J, Roiuk M, Teleman AA. Phosphorylation of ribosomal protein S6 differentially affects mRNA translation based on ORF length. *Nucleic Acids Res*. 2021;**49**(22):13062-74.
532. Knight ZA, Tan K, Birsoy K, Schmidt S, Garrison JL, Wysocki RW, et al. Molecular profiling of activated neurons by phosphorylated ribosome capture. *Cell*. 2012;**151**(5):1126-37.
533. Graber TE, Hebert-Seropian S, Khoutorsky A, David A, Yewdell JW, Lacaille JC, et al. Reactivation of stalled polyribosomes in synaptic plasticity. *Proc Natl Acad Sci U S A*. 2013;**110**(40):16205-10.
534. Montanaro L, Sperti S, Testoni G, Mattioli A. Effect of elongation factor 2 and of adenosine diphosphate-ribosylated elongation factor 2 on translocation. *Biochem J*. 1976;**156**(1):15-23.
535. Taha E, Gildish I, Gal-Ben-Ari S, Rosenblum K. The role of eEF2 pathway in learning and synaptic plasticity. *Neurobiol Learn Mem*. 2013;**105**:100-6.
536. Sutton MA, Taylor AM, Ito HT, Pham A, Schuman EM. Postsynaptic decoding of neural activity: eEF2 as a biochemical sensor coupling miniature synaptic transmission to local protein synthesis. *Neuron*. 2007;**55**(4):648-61.
537. Kavalali ET. The mechanisms and functions of spontaneous neurotransmitter release. *Nat Rev Neurosci*. 2015;**16**(1):5-16.
538. Sharma G, Vijayaraghavan S. Modulation of presynaptic store calcium induces release of glutamate and postsynaptic firing. *Neuron*. 2003;**38**(6):929-39.

539. Nairn AC, Palfrey HC. Identification of the major Mr 100,000 substrate for calmodulin-dependent protein kinase III in mammalian cells as elongation factor-2. *J Biol Chem*. 1987;**262**(36):17299-303.
540. Scheetz AJ, Nairn AC, Constantine-Paton M. NMDA receptor-mediated control of protein synthesis at developing synapses. *Nat Neurosci*. 2000;**3**(3):211-6.
541. Chotiner JK, Khorasani H, Nairn AC, O'Dell TJ, Watson JB. Adenylyl cyclase-dependent form of chemical long-term potentiation triggers translational regulation at the elongation step. *Neuroscience*. 2003;**116**(3):743-52.
542. Davidkova G, Carroll RC. Characterization of the role of microtubule-associated protein 1B in metabotropic glutamate receptor-mediated endocytosis of AMPA receptors in hippocampus. *J Neurosci*. 2007;**27**(48):13273-8.
543. Autry AE, Adachi M, Nosyreva E, Na ES, Los MF, Cheng PF, et al. NMDA receptor blockade at rest triggers rapid behavioural antidepressant responses. *Nature*. 2011;**475**(7354):91-5.
544. Park S, Park JM, Kim S, Kim JA, Shepherd JD, Smith-Hicks CL, et al. Elongation factor 2 and fragile X mental retardation protein control the dynamic translation of Arc/Arg3.1 essential for mGluR-LTD. *Neuron*. 2008;**59**(1):70-83.
545. Negrutskii BS, El'skaya AV. Eukaryotic translation elongation factor 1 alpha: structure, expression, functions, and possible role in aminoacyl-tRNA channeling. *Prog Nucleic Acid Res Mol Biol*. 1998;**60**:47-78.
546. Bunai F, Ando K, Ueno H, Numata O. Tetrahymena eukaryotic translation elongation factor 1A (eEF1A) bundles filamentous actin through dimer formation. *J Biochem*. 2006;**140**(3):393-9.
547. Gross SR, Kinzy TG. Translation elongation factor 1A is essential for regulation of the actin cytoskeleton and cell morphology. *Nat Struct Mol Biol*. 2005;**12**(9):772-8.
548. Liu G, Tang J, Edmonds BT, Murray J, Levin S, Condeelis J. F-actin sequesters elongation factor 1alpha from interaction with aminoacyl-tRNA in a pH-dependent reaction. *J Cell Biol*. 1996;**135**(4):953-63.
549. Mendoza MB, Gutierrez S, Ortiz R, Moreno DF, Dermit M, Dodel M, et al. The elongation factor eEF1A2 controls translation and actin dynamics in dendritic spines. *Sci Signal*. 2021;**14**(691).
550. Gandin V, Gutierrez GJ, Brill LM, Varsano T, Feng Y, Aza-Blanc P, et al. Degradation of newly synthesized polypeptides by ribosome-associated RACK1/c-Jun N-terminal kinase/eukaryotic elongation factor 1A2 complex. *Mol Cell Biol*. 2013;**33**(13):2510-26.
551. Du L, Richter JD. Activity-dependent polyadenylation in neurons. *RNA*. 2005;**11**(9):1340-7.
552. Atkins CM, Nozaki N, Shigeri Y, Soderling TR. Cytoplasmic polyadenylation element binding protein-dependent protein synthesis is regulated by calcium/calmodulin-dependent protein kinase II. *J Neurosci*. 2004;**24**(22):5193-201.
553. Bliss TV, Lomo T. Long-lasting potentiation of synaptic transmission in the dentate area of the anaesthetized rabbit following stimulation of the perforant path. *J Physiol*. 1973;**232**(2):331-56.
554. Gustafsson B, Wigstrom H, Abraham WC, Huang YY. Long-term potentiation in the hippocampus using depolarizing current pulses as the conditioning stimulus to single volley synaptic potentials. *J Neurosci*. 1987;**7**(3):774-80.

555. Lomo T. The discovery of long-term potentiation. *Philos Trans R Soc Lond B Biol Sci*. 2003;**358**(1432):617-20.
556. Schulz PE. Long-term potentiation involves increases in the probability of neurotransmitter release. *Proc Natl Acad Sci U S A*. 1997;**94**(11):5888-93.
557. Malenka RC. The role of postsynaptic calcium in the induction of long-term potentiation. *Mol Neurobiol*. 1991;**5**(2-4):289-95.
558. Cracco JB, Serrano P, Moskowitz SI, Bergold PJ, Sacktor TC. Protein synthesis-dependent LTP in isolated dendrites of CA1 pyramidal cells. *Hippocampus*. 2005;**15**(5):551-6.
559. Schuman EM, Dynes JL, Steward O. Synaptic regulation of translation of dendritic mRNAs. *J Neurosci*. 2006;**26**(27):7143-6.
560. Fukazawa Y, Saitoh Y, Ozawa F, Ohta Y, Mizuno K, Inokuchi K. Hippocampal LTP is accompanied by enhanced F-actin content within the dendritic spine that is essential for late LTP maintenance in vivo. *Neuron*. 2003;**38**(3):447-60.
561. Schwechter B, Tolias KF. Cytoskeletal mechanisms for synaptic potentiation. *Commun Integr Biol*. 2013;**6**(6):e27343.
562. Sheng M, Lee SH. AMPA receptor trafficking and the control of synaptic transmission. *Cell*. 2001;**105**(7):825-8.
563. Shinoda Y, Ahmed S, Ramachandran B, Bharat V, Brockelt D, Altas B, et al. BDNF enhances spontaneous and activity-dependent neurotransmitter release at excitatory terminals but not at inhibitory terminals in hippocampal neurons. *Front Synaptic Neurosci*. 2014;**6**:27.
564. Sacktor TC. PKMzeta, LTP maintenance, and the dynamic molecular biology of memory storage. *Prog Brain Res*. 2008;**169**:27-40.
565. Park M. AMPA Receptor Trafficking for Postsynaptic Potentiation. *Front Cell Neurosci*. 2018;**12**:361.
566. Amaral MD, Pozzo-Miller L. Intracellular Ca2+ stores and Ca2+ influx are both required for BDNF to rapidly increase quantal vesicular transmitter release. *Neural Plast*. 2012;**2012**:203536.
567. Lohof AM, Ip NY, Poo MM. Potentiation of developing neuromuscular synapses by the neurotrophins NT-3 and BDNF. *Nature*. 1993;**363**(6427):350-3.
568. Li YX, Zhang Y, Lester HA, Schuman EM, Davidson N. Enhancement of neurotransmitter release induced by brain-derived neurotrophic factor in cultured hippocampal neurons. *J Neurosci*. 1998;**18**(24):10231-40.
569. Levine ES, Dreyfus CF, Black IB, Plummer MR. Brain-derived neurotrophic factor rapidly enhances synaptic transmission in hippocampal neurons via postsynaptic tyrosine kinase receptors. *Proc Natl Acad Sci U S A*. 1995;**92**(17):8074-7.
570. Tyler WJ, Zhang XL, Hartman K, Winterer J, Muller W, Stanton PK, et al. BDNF increases release probability and the size of a rapidly recycling vesicle pool within rat hippocampal excitatory synapses. *J Physiol*. 2006;**574**(Pt 3):787-803.
571. Nicoll RA, Schmitz D. Synaptic plasticity at hippocampal mossy fibre synapses. *Nat Rev Neurosci*. 2005;**6**(11):863-76.
572. Nicoll RA, Malenka RC. Contrasting properties of two forms of long-term potentiation in the hippocampus. *Nature*. 1995;**377**(6545):115-8.
573. Harris EW, Cotman CW. Long-term potentiation of guinea pig mossy fiber responses is not blocked by N-methyl D-aspartate antagonists. *Neurosci Lett*. 1986;**70**(1):132-7.

574. Staubli U. A peculiar form of potentiation in mossy fiber synapses. *Epilepsy Res Suppl*. 1992;**7**:151-7.
575. Castillo PE, Weisskopf MG, Nicoll RA. The role of Ca2+ channels in hippocampal mossy fiber synaptic transmission and long-term potentiation. *Neuron*. 1994;**12**(2):261-9.
576. Bear MF, Kirkwood A. Neocortical long-term potentiation. *Curr Opin Neurobiol*. 1993;**3**(2):197-202.
577. Kirkwood A, Dudek SM, Gold JT, Aizenman CD, Bear MF. Common forms of synaptic plasticity in the hippocampus and neocortex in vitro. *Science*. 1993;**260**(5113):1518-21.
578. Abraham WC. How long will long-term potentiation last? *Philos Trans R Soc Lond B Biol Sci*. 2003;**358**(1432):735-44.
579. Abraham WC, Logan B, Greenwood JM, Dragunow M. Induction and experience-dependent consolidation of stable long-term potentiation lasting months in the hippocampus. *J Neurosci*. 2002;**22**(21):9626-34.
580. Wu D, Bacaj T, Morishita W, Goswami D, Arendt KL, Xu W, et al. Postsynaptic synaptotagmins mediate AMPA receptor exocytosis during LTP. *Nature*. 2017;**544**(7650):316-21.
581. Cho E, Kim DH, Hur YN, Whitcomb DJ, Regan P, Hong JH, et al. Cyclin Y inhibits plasticity-induced AMPA receptor exocytosis and LTP. *Sci Rep*. 2015;**5**:12624.
582. Jurado S, Goswami D, Zhang Y, Molina AJ, Sudhof TC, Malenka RC. LTP requires a unique postsynaptic SNARE fusion machinery. *Neuron*. 2013;**77**(3):542-58.
583. Anggono V, Huganir RL. Regulation of AMPA receptor trafficking and synaptic plasticity. *Curr Opin Neurobiol*. 2012;**22**(3):461-9.
584. Malinow R, Malenka RC. AMPA receptor trafficking and synaptic plasticity. *Annu Rev Neurosci*. 2002;**25**:103-26.
585. Bredt DS, Nicoll RA. AMPA receptor trafficking at excitatory synapses. *Neuron*. 2003;**40**(2):361-79.
586. Wang Z, Edwards JG, Riley N, Provance DW, Jr., Karcher R, Li XD, et al. Myosin Vb mobilizes recycling endosomes and AMPA receptors for postsynaptic plasticity. *Cell*. 2008;**135**(3):535-48.
587. Kennedy MJ, Davison IG, Robinson CG, Ehlers MD. Syntaxin-4 defines a domain for activity-dependent exocytosis in dendritic spines. *Cell*. 2010;**141**(3):524-35.
588. Patterson MA, Szatmari EM, Yasuda R. AMPA receptors are exocytosed in stimulated spines and adjacent dendrites in a Ras-ERK-dependent manner during long-term potentiation. *Proc Natl Acad Sci U S A*. 2010;**107**(36):15951-6.
589. Zhu JJ, Qin Y, Zhao M, Van Aelst L, Malinow R. Ras and Rap control AMPA receptor trafficking during synaptic plasticity. *Cell*. 2002;**110**(4):443-55.
590. Parsons RG, Gafford GM, Helmstetter FJ. Translational control via the mammalian target of rapamycin pathway is critical for the formation and stability of long-term fear memory in amygdala neurons. *J Neurosci*. 2006;**26**(50):12977-83.
591. Otani S, Marshall CJ, Tate WP, Goddard GV, Abraham WC. Maintenance of long-term potentiation in rat dentate gyrus requires protein synthesis but not messenger RNA synthesis immediately post-tetanization. *Neuroscience*. 1989;**28**(3):519-26.
592. Frey U, Krug M, Reymann KG, Matthies H. Anisomycin, an inhibitor of protein synthesis, blocks late phases of LTP phenomena in the hippocampal CA1 region in vitro. *Brain Res*. 1988;**452**(1-2):57-65.

593. Jarome TJ, Helmstetter FJ. Protein degradation and protein synthesis in long-term memory formation. *Front Mol Neurosci*. 2014;**7**:61.
594. Gafford GM, Parsons RG, Helmstetter FJ. Consolidation and reconsolidation of contextual fear memory requires mammalian target of rapamycin-dependent translation in the dorsal hippocampus. *Neuroscience*. 2011;**182**:98-104.
595. Jobim PF, Pedroso TR, Christoff RR, Werenicz A, Maurmann N, Reolon GK, et al. Inhibition of mTOR by rapamycin in the amygdala or hippocampus impairs formation and reconsolidation of inhibitory avoidance memory. *Neurobiol Learn Mem*. 2012;**97**(1):105-12.
596. Dudek SM, Bear MF. Homosynaptic long-term depression in area CA1 of hippocampus and effects of N-methyl-D-aspartate receptor blockade. *Proc Natl Acad Sci U S A*. 1992;**89**(10):4363-7.
597. Dunwiddie T, Lynch G. Long-term potentiation and depression of synaptic responses in the rat hippocampus: localization and frequency dependency. *J Physiol*. 1978;**276**:353-67.
598. Nabavi S, Kessels HW, Alfonso S, Aow J, Fox R, Malinow R. Metabotropic NMDA receptor function is required for NMDA receptor-dependent long-term depression. *Proc Natl Acad Sci U S A*. 2013;**110**(10):4027-32.
599. Konnerth A, Dreessen J, Augustine GJ. Brief dendritic calcium signals initiate long-lasting synaptic depression in cerebellar Purkinje cells. *Proc Natl Acad Sci U S A*. 1992;**89**(15):7051-5.
600. Tanaka K, Khiroug L, Santamaria F, Doi T, Ogasawara H, Ellis-Davies GC, et al. Ca2+ requirements for cerebellar long-term synaptic depression: role for a postsynaptic leaky integrator. *Neuron*. 2007;**54**(5):787-800.
601. Hansel C, de Jeu M, Belmeguenai A, Houtman SH, Buitendijk GH, Andreev D, et al. alphaCaMKII Is essential for cerebellar LTD and motor learning. *Neuron*. 2006;**51**(6):835-43.
602. Carroll RC, Beattie EC, von Zastrow M, Malenka RC. Role of AMPA receptor endocytosis in synaptic plasticity. *Nat Rev Neurosci*. 2001;**2**(5):315-24.
603. Luscher C, Xia H, Beattie EC, Carroll RC, von Zastrow M, Malenka RC, et al. Role of AMPA receptor cycling in synaptic transmission and plasticity. *Neuron*. 1999;**24**(3):649-58.
604. Wiegert JS, Oertner TG. Long-term depression triggers the selective elimination of weakly integrated synapses. *Proc Natl Acad Sci U S A*. 2013;**110**(47):E4510-9.
605. Beattie EC, Carroll RC, Yu X, Morishita W, Yasuda H, von Zastrow M, et al. Regulation of AMPA receptor endocytosis by a signaling mechanism shared with LTD. *Nat Neurosci*. 2000;**3**(12):1291-300.
606. Lelivelt MJ, Culbertson MR. Yeast Upf proteins required for RNA surveillance affect global expression of the yeast transcriptome. *Mol Cell Biol*. 1999;**19**(10):6710-9.
607. Ge Y, Porse BT. The functional consequences of intron retention: alternative splicing coupled to NMD as a regulator of gene expression. *Bioessays*. 2014;**36**(3):236-43.
608. Boehm V, Gehring NH. Exon Junction Complexes: Supervising the Gene Expression Assembly Line. *Trends Genet*. 2016;**32**(11):724-35.
609. Woodward LA, Mabin JW, Gangras P, Singh G. The exon junction complex: a lifelong guardian of mRNA fate. *Wiley Interdiscip Rev RNA*. 2017;**8**(3).

610. Chen Z, Gore BB, Long H, Ma L, Tessier-Lavigne M. Alternative splicing of the Robo3 axon guidance receptor governs the midline switch from attraction to repulsion. *Neuron*. 2008;**58**(3):325-32.
611. Jaffrey SR, Wilkinson MF. Nonsense-mediated RNA decay in the brain: emerging modulator of neural development and disease. *Nat Rev Neurosci*. 2018;**19**(12):715-28.
612. Farris S, Lewandowski G, Cox CD, Steward O. Selective localization of arc mRNA in dendrites involves activity- and translation-dependent mRNA degradation. *J Neurosci*. 2014;**34**(13):4481-93.
613. Paolantoni C, Ricciardi S, De Paolis V, Okenwa C, Catalanotto C, Ciotti MT, et al. Arc 3' UTR Splicing Leads to Dual and Antagonistic Effects in Fine-Tuning Arc Expression Upon BDNF Signaling. *Front Mol Neurosci*. 2018;**11**:145.
614. Notaras M, Allen M, Longo F, Volk N, Toth M, Li Jeon N, et al. UPF2 leads to degradation of dendritically targeted mRNAs to regulate synaptic plasticity and cognitive function. *Mol Psychiatry*. 2020;**25**(12):3360-79.
615. Hale CR, Sawicka K, Mora K, Fak JJ, Kang JJ, Cutrim P, et al. FMRP regulates mRNAs encoding distinct functions in the cell body and dendrites of CA1 pyramidal neurons. *Elife*. 2021;**10**.
616. Jaagura M, Taal K, Koppel I, Tuvikene J, Timmusk T, Tamme R. Rat NEURL1 3'UTR is alternatively spliced and targets mRNA to dendrites. *Neurosci Lett*. 2016;**635**:71-6.
617. Ouwenga R, Lake AM, O'Brien D, Mogha A, Dani A, Dougherty JD. Transcriptomic Analysis of Ribosome-Bound mRNA in Cortical Neurites In Vivo. *J Neurosci*. 2017;**37**(36):8688-705.
618. Andreassi C, Riccio A. To localize or not to localize: mRNA fate is in 3'UTR ends. *Trends Cell Biol*. 2009;**19**(9):465-74.
619. Schratt G. microRNAs at the synapse. *Nat Rev Neurosci*. 2009;**10**(12):842-9.
620. Krol J, Busskamp V, Markiewicz I, Stadler MB, Ribi S, Richter J, et al. Characterizing light-regulated retinal microRNAs reveals rapid turnover as a common property of neuronal microRNAs. *Cell*. 2010;**141**(4):618-31.
621. Schratt GM, Tuebing F, Nigh EA, Kane CG, Sabatini ME, Kiebler M, et al. A brain-specific microRNA regulates dendritic spine development. *Nature*. 2006;**439**(7074):283-9.
622. Cougot N, Bhattacharyya SN, Tapia-Arancibia L, Bordonne R, Filipowicz W, Bertrand E, et al. Dendrites of mammalian neurons contain specialized P-body-like structures that respond to neuronal activation. *J Neurosci*. 2008;**28**(51):13793-804.
623. Kye MJ, Liu T, Levy SF, Xu NL, Groves BB, Bonneau R, et al. Somatodendritic microRNAs identified by laser capture and multiplex RT-PCR. *RNA*. 2007;**13**(8):1224-34.
624. McNeill E, Van Vactor D. MicroRNAs shape the neuronal landscape. *Neuron*. 2012;**75**(3):363-79.
625. Corradi E, Baudet ML. In the Right Place at the Right Time: miRNAs as Key Regulators in Developing Axons. *Int J Mol Sci*. 2020;**21**(22).
626. Bhattacharyya SN, Habermacher R, Martine U, Closs EI, Filipowicz W. Relief of microRNA-mediated translational repression in human cells subjected to stress. *Cell*. 2006;**125**(6):1111-24.
627. Vasudevan S, Tong Y, Steitz JA. Switching from repression to activation: microRNAs can up-regulate translation. *Science*. 2007;**318**(5858):1931-4.

628. Mueller JL, Mahadevaiah SK, Park PJ, Warburton PE, Page DC, Turner JM. The mouse X chromosome is enriched for multicopy testis genes showing postmeiotic expression. *Nat Genet*. 2008;**40**(6):794-9.
629. Mueller JL, Skaletsky H, Brown LG, Zaghlul S, Rock S, Graves T, et al. Independent specialization of the human and mouse X chromosomes for the male germ line. *Nat Genet*. 2013;**45**(9):1083-7.
630. Consortium GT. The Genotype-Tissue Expression (GTEx) project. *Nat Genet*. 2013;**45**(6):580-5.
631. Boeck R, Kolakofsky D. Positions +5 and +6 can be major determinants of the efficiency of non-AUG initiation codons for protein synthesis. *EMBO J*. 1994;**13**(15):3608-17.
632. Grunert S, Jackson RJ. The immediate downstream codon strongly influences the efficiency of utilization of eukaryotic translation initiation codons. *EMBO J*. 1994;**13**(15):3618-30.
633. Ray D, Kazan H, Cook KB, Weirauch MT, Najafabadi HS, Li X, et al. A compendium of RNA-binding motifs for decoding gene regulation. *Nature*. 2013;**499**(7457):172-7.
634. Li M, Cui Z, Niu Y, Liu B, Fan W, Yu D, et al. Synaptogenesis in the developing mouse visual cortex. *Brain Res Bull*. 2010;**81**(1):107-13.
635. Hesse R, Hurtado ML, Jackson RJ, Eaton SL, Herrmann AG, Colom-Cadena M, et al. Comparative profiling of the synaptic proteome from Alzheimer's disease patients with focus on the APOE genotype. *Acta Neuropathol Commun*. 2019;**7**(1):214.
636. Focking M, Dicker P, Lopez LM, Hryniewiecka M, Wynne K, English JA, et al. Proteomic analysis of the postsynaptic density implicates synaptic function and energy pathways in bipolar disorder. *Transl Psychiatry*. 2016;**6**(11):e959.
637. Fonseca BD, Zakaria C, Jia JJ, Graber TE, Svitkin Y, Tahmasebi S, et al. La-related Protein 1 (LARP1) Represses Terminal Oligopyrimidine (TOP) mRNA Translation Downstream of mTOR Complex 1 (mTORC1). *J Biol Chem*. 2015;**290**(26):15996-6020.
638. Tcherkezian J, Cargnello M, Romeo Y, Huttlin EL, Lavoie G, Gygi SP, et al. Proteomic analysis of cap-dependent translation identifies LARP1 as a key regulator of 5'TOP mRNA translation. *Genes Dev*. 2014;**28**(4):357-71.
639. Shin H, Lee J, Kim Y, Jang S, Lee Y, Kim S, et al. Knockdown of BC200 RNA expression reduces cell migration and invasion by destabilizing mRNA for calcium-binding protein S100A11. *RNA Biol*. 2017;**14**(10):1418-30.
640. Khoutorsky A, Yanagiya A, Gkogkas CG, Fabian MR, Prager-Khoutorsky M, Cao R, et al. Control of synaptic plasticity and memory via suppression of poly(A)-binding protein. *Neuron*. 2013;**78**(2):298-311.
641. Muddashetty R, Khanam T, Kondrashov A, Bundman M, Iacoangeli A, Kremerskothen J, et al. Poly(A)-binding protein is associated with neuronal BC1 and BC200 ribonucleoprotein particles. *J Mol Biol*. 2002;**321**(3):433-45.
642. Kiebler MA, Bassell GJ. Neuronal RNA granules: movers and makers. *Neuron*. 2006;**51**(6):685-90.
643. Dynes JL, Steward O. Arc mRNA docks precisely at the base of individual dendritic spines indicating the existence of a specialized microdomain for synapse-specific mRNA translation. *J Comp Neurol*. 2012;**520**(14):3105-19.
644. Tang SJ, Meulemans D, Vazquez L, Colaco N, Schuman E. A role for a rat homolog of staufen in the transport of RNA to neuronal dendrites. *Neuron*. 2001;**32**(3):463-75.

645. Kedersha N, Chen S, Gilks N, Li W, Miller IJ, Stahl J, et al. Evidence that ternary complex (eIF2-GTP-tRNA(i)(Met))-deficient preinitiation complexes are core constituents of mammalian stress granules. *Mol Biol Cell*. 2002;**13**(1):195-210.
646. Fallini C, Donlin-Asp PG, Rouanet JP, Bassell GJ, Rossoll W. Deficiency of the Survival of Motor Neuron Protein Impairs mRNA Localization and Local Translation in the Growth Cone of Motor Neurons. *J Neurosci*. 2016;**36**(13):3811-20.
647. Feuge J, Scharkowski F, Michaelsen-Preusse K, Korte M. FMRP Modulates Activity-Dependent Spine Plasticity by Binding Cofilin1 mRNA and Regulating Localization and Local Translation. *Cereb Cortex*. 2019;**29**(12):5204-16.
648. Antar LN, Afroz R, Dictenberg JB, Carroll RC, Bassell GJ. Metabotropic glutamate receptor activation regulates fragile x mental retardation protein and FMR1 mRNA localization differentially in dendrites and at synapses. *J Neurosci*. 2004;**24**(11):2648-55.
649. Fujii R, Okabe S, Urushido T, Inoue K, Yoshimura A, Tachibana T, et al. The RNA binding protein TLS is translocated to dendritic spines by mGluR5 activation and regulates spine morphology. *Curr Biol*. 2005;**15**(6):587-93.
650. Zhang G, Neubert TA, Jordan BA. RNA binding proteins accumulate at the postsynaptic density with synaptic activity. *J Neurosci*. 2012;**32**(2):599-609.
651. Sevigny M, Bourdeau Julien I, Venkatasubramani JP, Hui JB, Dutchak PA, Sephton CF. FUS contributes to mTOR-dependent inhibition of translation. *J Biol Chem*. 2020;**295**(52):18459-73.
652. Richter JD, Zhao X. The molecular biology of FMRP: new insights into fragile X syndrome. *Nat Rev Neurosci*. 2021;**22**(4):209-22.
653. Till SM, Asiminas A, Jackson AD, Katsanevaki D, Barnes SA, Osterweil EK, et al. Conserved hippocampal cellular pathophysiology but distinct behavioural deficits in a new rat model of FXS. *Hum Mol Genet*. 2015;**24**(21):5977-84.
654. Till SM, Wijetunge LS, Seidel VG, Harlow E, Wright AK, Bagni C, et al. Altered maturation of the primary somatosensory cortex in a mouse model of fragile X syndrome. *Hum Mol Genet*. 2012;**21**(10):2143-56.
655. Sephton CF, Good SK, Atkin S, Dewey CM, Mayer P, 3rd, Herz J, et al. TDP-43 is a developmentally regulated protein essential for early embryonic development. *J Biol Chem*. 2010;**285**(9):6826-34.
656. Khalili K, Del Valle L, Muralidharan V, Gault WJ, Darbinian N, Otte J, et al. Puralpha is essential for postnatal brain development and developmentally coupled cellular proliferation as revealed by genetic inactivation in the mouse. *Mol Cell Biol*. 2003;**23**(19):6857-75.
657. Hazelett DJ, Chang JC, Lakeland DL, Morton DB. Comparison of parallel high-throughput RNA sequencing between knockout of TDP-43 and its overexpression reveals primarily nonreciprocal and nonoverlapping gene expression changes in the central nervous system of Drosophila. *G3 (Bethesda)*. 2012;**2**(7):789-802.
658. Bolduc FV, Bell K, Cox H, Broadie KS, Tully T. Excess protein synthesis in Drosophila fragile X mutants impairs long-term memory. *Nat Neurosci*. 2008;**11**(10):1143-5.
659. Aumiller V, Graebsch A, Kremmer E, Niessing D, Forstemann K. Drosophila Pur-alpha binds to trinucleotide-repeat containing cellular RNAs and translocates to the early oocyte. *RNA Biol*. 2012;**9**(5):633-43.

660. Bellott DW, Skaletsky H, Pyntikova T, Mardis ER, Graves T, Kremitzki C, et al. Convergent evolution of chicken Z and human X chromosomes by expansion and gene acquisition. *Nature*. 2010;**466**(7306):612-6.
661. Macha J, Teichmanova R, Sater AK, Wells DE, Tlapakova T, Zimmerman LB, et al. Deep ancestry of mammalian X chromosome revealed by comparison with the basal tetrapod Xenopus tropicalis. *BMC Genomics*. 2012;**13**:315.
662. Jackson EK, Bellott DW, Cho TJ, Skaletsky H, Hughes JF, Pyntikova T, et al. Large palindromes on the primate X Chromosome are preserved by natural selection. *Genome Res*. 2021;**31**(8):1337-52.
663. Raefski AS, O'Neill MJ. Identification of a cluster of X-linked imprinted genes in mice. *Nat Genet*. 2005;**37**(6):620-4.
664. Zechner U, Wilda M, Kehrer-Sawatzki H, Vogel W, Fundele R, Hameister H. A high density of X-linked genes for general cognitive ability: a run-away process shaping human evolution? *Trends Genet*. 2001;**17**(12):697-701.
665. Skuse DH. X-linked genes and mental functioning. *Hum Mol Genet*. 2005;**14 Spec No 1**:R27-32.
666. Davis EJ, Solsberg CW, White CC, Minones-Moyano E, Sirota M, Chibnik L, et al. Sex-Specific Association of the X Chromosome With Cognitive Change and Tau Pathology in Aging and Alzheimer Disease. *JAMA Neurol*. 2021;**78**(10):1249-54.
667. Laumonnier F, Cuthbert PC, Grant SG. The role of neuronal complexes in human X-linked brain diseases. *Am J Hum Genet*. 2007;**80**(2):205-20.
668. Fatemi SH, Folsom TD. The role of fragile X mental retardation protein in major mental disorders. *Neuropharmacology*. 2011;**60**(7-8):1221-6.
669. Steinberg J, Webber C. The roles of FMRP-regulated genes in autism spectrum disorder: single- and multiple-hit genetic etiologies. *Am J Hum Genet*. 2013;**93**(5):825-39.
670. Uchigashima M, Cheung A, Futai K. Neuroligin-3: A Circuit-Specific Synapse Organizer That Shapes Normal Function and Autism Spectrum Disorder-Associated Dysfunction. *Front Mol Neurosci*. 2021;**14**:749164.
671. Sephton CF, Yu G. The function of RNA-binding proteins at the synapse: implications for neurodegeneration. *Cell Mol Life Sci*. 2015;**72**(19):3621-35.
672. Blair IP, Williams KL, Warraich ST, Durnall JC, Thoeng AD, Manavis J, et al. FUS mutations in amyotrophic lateral sclerosis: clinical, pathological, neurophysiological and genetic analysis. *J Neurol Neurosurg Psychiatry*. 2010;**81**(6):639-45.
673. Katisko K, Huber N, Kokkola T, Hartikainen P, Kruger J, Heikkinen AL, et al. Serum total TDP-43 levels are decreased in frontotemporal dementia patients with C9orf72 repeat expansion or concomitant motoneuron disease phenotype. *Alzheimers Res Ther*. 2022;**14**(1):151.
674. Sitzmann AF, Hagelstrom RT, Tassone F, Hagerman RJ, Butler MG. Rare FMR1 gene mutations causing fragile X syndrome: A review. *Am J Med Genet A*. 2018;**176**(1):11-8.
675. Bassell GJ, Warren ST. Fragile X syndrome: loss of local mRNA regulation alters synaptic development and function. *Neuron*. 2008;**60**(2):201-14.
676. Alami NH, Smith RB, Carrasco MA, Williams LA, Winborn CS, Han SSW, et al. Axonal transport of TDP-43 mRNA granules is impaired by ALS-causing mutations. *Neuron*. 2014;**81**(3):536-43.
677. Gagnon JA, Mowry KL. Molecular motors: directing traffic during RNA localization. *Crit Rev Biochem Mol Biol*. 2011;**46**(3):229-39.

678. Sweeney HL, Holzbaur ELF. Motor Proteins. *Cold Spring Harb Perspect Biol*. 2018;**10**(5).
679. Glock C, Biever A, Tushev G, Nassim-Assir B, Kao A, Bartnik I, et al. The translatome of neuronal cell bodies, dendrites, and axons. *Proc Natl Acad Sci U S A*. 2021;**118**(43).
680. Moraleva AA, Deryabin AS, Rubtsov YP, Rubtsova MP, Dontsova OA. Eukaryotic Ribosome Biogenesis: The 60S Subunit. *Acta Naturae*. 2022;**14**(2):39-49.
681. Slomnicki LP, Pietrzak M, Vashishta A, Jones J, Lynch N, Elliot S, et al. Requirement of Neuronal Ribosome Synthesis for Growth and Maintenance of the Dendritic Tree. *J Biol Chem*. 2016;**291**(11):5721-39.
682. Kaplan BB, Gioio AE, Hillefors M, Aschrafi A. Axonal protein synthesis and the regulation of local mitochondrial function. *Results Probl Cell Differ*. 2009;**48**:225-42.
683. Muddashetty RS, Kelic S, Gross C, Xu M, Bassell GJ. Dysregulated metabotropic glutamate receptor-dependent translation of AMPA receptor and postsynaptic density-95 mRNAs at synapses in a mouse model of fragile X syndrome. *J Neurosci*. 2007;**27**(20):5338-48.
684. Nicholson-Shaw AL, Kofman ER, Yeo GW, Pasquinelli AE. Nuclear and cytoplasmic poly(A) binding proteins (PABPs) favor distinct transcripts and isoforms. *Nucleic Acids Res*. 2022;**50**(8):4685-702.
685. Kimball SR, Horetsky RL, Ron D, Jefferson LS, Harding HP. Mammalian stress granules represent sites of accumulation of stalled translation initiation complexes. *Am J Physiol Cell Physiol*. 2003;**284**(2):C273-84.
686. Anderson P, Kedersha N. RNA granules. *J Cell Biol*. 2006;**172**(6):803-8.
687. Costa-Mattioli M, Gobert D, Harding H, Herdy B, Azzi M, Bruno M, et al. Translational control of hippocampal synaptic plasticity and memory by the eIF2alpha kinase GCN2. *Nature*. 2005;**436**(7054):1166-73.
688. Takei N, Kawamura M, Hara K, Yonezawa K, Nawa H. Brain-derived neurotrophic factor enhances neuronal translation by activating multiple initiation processes: comparison with the effects of insulin. *J Biol Chem*. 2001;**276**(46):42818-25.
689. Costa-Mattioli M, Gobert D, Stern E, Gamache K, Colina R, Cuello C, et al. eIF2alpha phosphorylation bidirectionally regulates the switch from short- to long-term synaptic plasticity and memory. *Cell*. 2007;**129**(1):195-206.
690. Costa-Mattioli M, Sossin WS, Klann E, Sonenberg N. Translational control of long-lasting synaptic plasticity and memory. *Neuron*. 2009;**61**(1):10-26.
691. Li Z, Zhang Y, Ku L, Wilkinson KD, Warren ST, Feng Y. The fragile X mental retardation protein inhibits translation via interacting with mRNA. *Nucleic Acids Res*. 2001;**29**(11):2276-83.
692. Tiruchinapalli DM, Ehlers MD, Keene JD. Activity-dependent expression of RNA binding protein HuD and its association with mRNAs in neurons. *RNA Biol*. 2008;**5**(3):157-68.
693. Khaleghpour K, Svitkin YV, Craig AW, DeMaria CT, Deo RC, Burley SK, et al. Translational repression by a novel partner of human poly(A) binding protein, Paip2. *Mol Cell*. 2001;**7**(1):205-16.
694. Lee SH, Oh J, Park J, Paek KY, Rho S, Jang SK, et al. Poly(A) RNA and Paip2 act as allosteric regulators of poly(A)-binding protein. *Nucleic Acids Res*. 2014;**42**(4):2697-707.
695. von Der Haar T, Ball PD, McCarthy JE. Stabilization of eukaryotic initiation factor 4E binding to the mRNA 5'-Cap by domains of eIF4G. *J Biol Chem*. 2000;**275**(39):30551-5.

696. Wei CC, Balasta ML, Ren J, Goss DJ. Wheat germ poly(A) binding protein enhances the binding affinity of eukaryotic initiation factor 4F and (iso)4F for cap analogues. *Biochemistry*. 1998;**37**(7):1910-6.
697. Gallie DR. The cap and poly(A) tail function synergistically to regulate mRNA translational efficiency. *Genes Dev*. 1991;**5**(11):2108-16.
698. Laggerbauer B, Ostareck D, Keidel EM, Ostareck-Lederer A, Fischer U. Evidence that fragile X mental retardation protein is a negative regulator of translation. *Hum Mol Genet*. 2001;**10**(4):329-38.
699. Takei N, Inamura N, Kawamura M, Namba H, Hara K, Yonezawa K, et al. Brain-derived neurotrophic factor induces mammalian target of rapamycin-dependent local activation of translation machinery and protein synthesis in neuronal dendrites. *J Neurosci*. 2004;**24**(44):9760-9.
700. tom Dieck S, Kochen L, Hanus C, Heumuller M, Bartnik I, Nassim-Assir B, et al. Direct visualization of newly synthesized target proteins in situ. *Nat Methods*. 2015;**12**(5):411-4.
701. Muslimov IA, Titmus M, Koenig E, Tiedge H. Transport of Neuronal BC1 RNA in Mauthner Axons. *J Neurosci*. 2002;**22**(11):4293-301.
702. Wang H, Iacoangeli A, Lin D, Williams K, Denman RB, Hellen CU, et al. Dendritic BC1 RNA in translational control mechanisms. *J Cell Biol*. 2005;**171**(5):811-21.
703. Aleshkina D, Iyyappan R, Lin CJ, Masek T, Pospisek M, Susor A. ncRNA BC1 influences translation in the oocyte. *RNA Biol*. 2021;**18**(11):1893-904.
704. Hochstoeger T, Chao JA. Towards a molecular understanding of the 5'TOP motif in regulating translation of ribosomal mRNAs. *Semin Cell Dev Biol*. 2023.
705. Okochi K, Suzuki T, Inoue J, Matsuda S, Yamamoto T. Interaction of anti-proliferative protein Tob with poly(A)-binding protein and inducible poly(A)-binding protein: implication of Tob in translational control. *Genes Cells*. 2005;**10**(2):151-63.
706. Chen CA, Strouz K, Huang KL, Shyu AB. Tob2 phosphorylation regulates global mRNA turnover to reshape transcriptome and impact cell proliferation. *RNA*. 2020;**26**(9):1143-59.
707. Jonas S, Izaurralde E. Towards a molecular understanding of microRNA-mediated gene silencing. *Nat Rev Genet*. 2015;**16**(7):421-33.
708. Yao G, Chiang YC, Zhang C, Lee DJ, Laue TM, Denis CL. PAB1 self-association precludes its binding to poly(A), thereby accelerating CCR4 deadenylation in vivo. *Mol Cell Biol*. 2007;**27**(17):6243-53.
709. Jinek M, Coyle SM, Doudna JA. Coupled 5' nucleotide recognition and processivity in Xrn1-mediated mRNA decay. *Mol Cell*. 2011;**41**(5):600-8.
710. Ray D, Ha KCH, Nie K, Zheng H, Hughes TR, Morris QD. RNAcompete methodology and application to determine sequence preferences of unconventional RNA-binding proteins. *Methods*. 2017;**118-119**:3-15.
711. Ray D, Kazan H, Chan ET, Pena Castillo L, Chaudhry S, Talukder S, et al. Rapid and systematic analysis of the RNA recognition specificities of RNA-binding proteins. *Nat Biotechnol*. 2009;**27**(7):667-70.
712. Svitkin YV, Agol VI. Complete translation of encephalomyocarditis virus RNA and faithful cleavage of virus-specific proteins in a cell-free system from Krebs-2 cells. *FEBS Lett*. 1978;**87**(1):7-11.
713. Svitkin YV, Sonenberg N. An efficient system for cap- and poly(A)-dependent translation in vitro. *Methods Mol Biol*. 2004;**257**:155-70.

714. Khazaei S, Chen CCL, Andrade AF, Kabir N, Azarafshar P, Morcos SM, et al. Single substitution in H3.3G34 alters DNMT3A recruitment to cause progressive neurodegeneration. *Cell*. 2023;**186**(6):1162-78 e20.
715. Stuart T, Srivastava A, Madad S, Lareau CA, Satija R. Single-cell chromatin state analysis with Signac. *Nat Methods*. 2021;**18**(11):1333-41.
716. Hao Y, Hao S, Andersen-Nissen E, Mauck WM, 3rd, Zheng S, Butler A, et al. Integrated analysis of multimodal single-cell data. *Cell*. 2021;**184**(13):3573-87 e29.
717. Germain PL, Lun A, Garcia Meixide C, Macnair W, Robinson MD. Doublet identification in single-cell sequencing data using scDblFinder. *F1000Res*. 2021;**10**:979.
718. Li C, Liu B, Kang B, Liu Z, Liu Y, Chen C, et al. SciBet as a portable and fast single cell type identifier. *Nat Commun*. 2020;**11**(1):1818.
719. Tan Y, Cahan P. SingleCellNet: A Computational Tool to Classify Single Cell RNA-Seq Data Across Platforms and Across Species. *Cell Syst*. 2019;**9**(2):207-13 e2.
720. Aran D, Looney AP, Liu L, Wu E, Fong V, Hsu A, et al. Reference-based analysis of lung single-cell sequencing reveals a transitional profibrotic macrophage. *Nat Immunol*. 2019;**20**(2):163-72.
721. Jessa S, Blanchet-Cohen A, Krug B, Vladoiu M, Coutelier M, Faury D, et al. Stalled developmental programs at the root of pediatric brain tumors. *Nat Genet*. 2019;**51**(12):1702-13.
722. Yao Z, Liu H, Xie F, Fischer S, Adkins RS, Aldridge AI, et al. A transcriptomic and epigenomic cell atlas of the mouse primary motor cortex. *Nature*. 2021;**598**(7879):103-10.
723. Suzuki K, Bose P, Leong-Quong RY, Fujita DJ, Riabowol K. REAP: A two minute cell fractionation method. *BMC Res Notes*. 2010;**3**:294.
724. Wang J, Lv X, Wu Y, Xu T, Jiao M, Yang R, et al. Postsynaptic RIM1 modulates synaptic function by facilitating membrane delivery of recycling NMDARs in hippocampal neurons. *Nat Commun*. 2018;**9**(1):2267.
725. Qiu S, Chen T, Koga K, Guo YY, Xu H, Song Q, et al. An increase in synaptic NMDA receptors in the insular cortex contributes to neuropathic pain. *Sci Signal*. 2013;**6**(275):ra34.
726. Gandin V, Sikstrom K, Alain T, Morita M, McLaughlan S, Larsson O, et al. Polysome fractionation and analysis of mammalian translatomes on a genome-wide scale. *J Vis Exp*. 2014(87).
727. Bolger AM, Lohse M, Usadel B. Trimmomatic: a flexible trimmer for Illumina sequence data. *Bioinformatics*. 2014;**30**(15):2114-20.
728. Wang T, Liu J, Shen L, Tonti-Filippini J, Zhu Y, Jia H, et al. STAR: an integrated solution to management and visualization of sequencing data. *Bioinformatics*. 2013;**29**(24):3204-10.
729. Li B, Dewey CN. RSEM: accurate transcript quantification from RNA-Seq data with or without a reference genome. *BMC Bioinformatics*. 2011;**12**:323.
730. Love MI, Huber W, Anders S. Moderated estimation of fold change and dispersion for RNA-seq data with DESeq2. *Genome Biol*. 2014;**15**(12):550.
731. Raudvere U, Kolberg L, Kuzmin I, Arak T, Adler P, Peterson H, et al. g:Profiler: a web server for functional enrichment analysis and conversions of gene lists (2019 update). *Nucleic Acids Res*. 2019;**47**(W1):W191-W8.